

STRUCTURAL FRAMEWORK OF  
THE SUNDA SHELF AND VICINITY

by

ZVI BEN-AVRAHAM

B.Sc. The Hebrew University of Jerusalem  
(1969)

SUBMITTED IN PARTIAL FULFILLMENT OF THE  
REQUIREMENTS FOR THE DEGREE OF  
DOCTOR OF PHILOSOPHY

at the

MASSACHUSETTS INSTITUTE OF TECHNOLOGY

and the

WOODS HOLE OCEANOGRAPHIC INSTITUTION

January, 1973

Signature of Author.....

Joint Program in Oceanography, Massachusetts  
Institute of Technology - Woods Hole Oceano-  
graphic Institution, and Department of Earth  
and Planetary Sciences, and Department of  
Meteorology, Massachusetts Institute of  
Technology, January 1973

Certified by.....

Thesis Supervisor

Accepted by.....

Chairman, Joint Oceanography Committee in  
the Earth Sciences, Massachusetts Institute  
of Technology - Woods Hole Oceanographic  
Institution

Lindgren  
WITHDRAWN  
MASS. INST. TECH.  
FEB 24 1973  
MIT LIBRARIES

STRUCTURAL FRAMEWORK OF  
THE SUNDA SHELF AND VICINITY

Zvi Ben-Avraham

Submitted to the Massachusetts Institute of Technology - Woods Hole Oceanographic Institution Joint Program in Oceanography on December 26, 1972 in partial fulfillment of the requirements for the degree of Doctor of Philosophy.

ABSTRACT

The Sunda Shelf is one of the most extensive coherent shelves in the world. A geophysical survey was conducted over the southern Sunda Shelf (Java Sea). Water depth, sediment thickness, and the gravity and magnetic fields were continuously measured. Expendable radiosonobuoys were used for seismic refraction measurements. These geophysical data supplemented by earlier studies over the northern Sunda Shelf and geological data from land areas provide a comprehensive picture of the structural framework of the entire Sunda Shelf. In addition, structural studies over some of the deep-sea floors surrounding the Sunda Shelf are combined with those over the Sunda Shelf to develop an evolutionary scheme of the Sunda Shelf and adjacent deep seas.

Seismic reflection profiles show that the Sunda Shelf consists of three major units: the northern Sunda Shelf basinal area, the Singapore Platform, and the Java Sea basinal area. In the northern Sunda Shelf are two large sedimentary basins, the Brunei and Gulf of Thailand basins, which are separated by the Natuna Ridge. In the Java Sea are several other basins separated by uplifts. The basins in the eastern Java Sea are narrow and long and seem to result from compressional forces, while those in the western Java Sea are more circular and seem to result from tensional forces. Radiosonobuoys revealed small basement features and resolved many strata having different velocities.

Faults are abundant throughout the Sunda Shelf and clearly control the distribution and shapes of the basins. The faults strike north-south in the western Java Sea and northeast-southwest in the eastern Java Sea. A major discontinuity trending north-south (termed here the Natuna Rift in the northern Sunda Shelf and the Billiton Depression in the central Sunda Shelf) cuts the structures of the entire Sunda Shelf. The discontinuity continues south across Central Java to the deep ocean floor.

Analysis of magnetic anomalies shows that the area can be divided into several distinct magnetic provinces that do not always follow the major structural units mapped by the seismic reflection data. These magnetic provinces coincide with corresponding provinces of lithic units. The gravity field over the central and southern Sunda Shelf averages around +30 mgal. Local gravity anomalies having relative amplitude of 10-25 mgal are superimposed on the regional background level. Although the local gravity anomalies were helpful in resolving the upper crustal structures, the cause for the relatively high regional gravity is unknown.

The structural elements on the Sunda Shelf are interpreted as the result of past interaction between the Indian Ocean-Australian, Pacific, and Asian plates. The evolution of the Sunda Shelf during the Mesozoic resulted from horizontal differential movement in a north-south direction as both the Indian Ocean and Pacific plates were moving to the north. In Eocene time two major events affected the evolution of the Sunda Shelf: the direction of movement of the Pacific plate changed from north to west-northwest producing north-east-southwest trending structural elements in the eastern Java Sea, and a spreading ridge that previously existed in the deep sea south of the shelf (Wharton Basin) was subducted along the Java Trench.

Thesis Supervisor: Dr. K. O. Emery  
Title: Senior Scientist

## ACKNOWLEDGEMENTS

4

I thank K. O. Emery for introducing me to the problem of the Far East geology, and serving as my thesis supervisor through the course of this thesis research. His guidance and firm support were essential for the successful completion of the study. The continuing support of C. O. Bowin and N. M. Toksoz who served as members of my thesis committee is greatly appreciated. Discussions with J. D. Phillips, S. Uyeda, E. T. Bunce, W. Hamilton, J. R. Heirtzler, E. Uchupi, S. T. Knott, W. B. Bryan, B. P. Luyendyk, H. Hoskins, J. A. Grow, and J. C. MacIlvaine have also stimulated various aspects of this study. J. G. Sclater has discussed some of his unpublished data from the Wharton Basin. H. Hoskins helped with the analysis of sonobuoy records, K. E. Prada with the processing of the seismic reflection data, and T. Todd with velocity measurements on basement rock samples.

The writer is indebted to the officers, crew and scientific staff on the cruise of R/V CHAIN to the Java Sea. W. C. Pitman, M. Talwani, and W. R. Raitt provided unpublished geophysical data from this region. W. Hamilton provided the basement samples used in the study with the permission of Atlantic Richfield Indonesia, Inc., and Cities Service Oil Company, and also an unpublished tectonic map of Indonesia.

Shell Internationale Petroleum Maatschappij N.V., The Hague, Netherlands provided gravity maps (through C. O. Bowin ) from land areas. The work has benefitted from some proprietary data from oil companies and from discussion with many oil company geologists.

This study was made possible by National Science Foundation Grant GA-27449. The writer was supported by the Woods Hole Oceanographic Institution in part through a grant from Mobil Foundation Incorporated. Transportation to the Japanese R/V HAKUHO MARU cruise in the Philippine and Sulu seas was made possible by Contract N0014-66-C-0241 with the Office of Naval Research.

K. O. Emery, N. M. Toksoz, C. O. Bowin, E. T. Bunce, J. D. Phillips, W. B. Bryan, R. P. Von Herzen, J. G. Sclater, B. P. Luyendyk and J. C. MacIlvaine reviewed various portions of this thesis and made valuable suggestions. G. Mosier typed the manuscript.

Finally I thank my wife, Rachel, for her patience and continuous encouragement during the course of this study.

## TABLE OF CONTENTS

	Page
ABSTRACT.....	2
ACKNOWLEDGEMENTS.....	4
LIST OF FIGURES.....	8
LIST OF TABLES.....	13
CHAPTER I INTRODUCTION.....	14
Statement of the problem.....	14
Previous work.....	19
Present work.....	21
CHAPTER II GEOLOGICAL SETTING.....	23
Physiography and bottom material.....	23
Stratigraphy and igneous activity.....	31
CHAPTER III THE SEAS SURROUNDING THE SUNDA SHELF.....	37
Andaman Sea.....	38
China Basin.....	40
Western Philippine Basin.....	51
Sulu Sea.....	55
Small Ocean basins of Eastern Indonesia.....	56
Java Trench.....	58
CHAPTER IV GEOPHYSICAL STUDIES OF THE SUNDA SHELF....	65
Seismic Refraction, oblique reflection and stratigraphy.....	65
Introduction.....	65
Results.....	68
Java Sea.....	68
Northern Sunda Shelf.....	76
Velocity cross-sections.....	81
Seismic Reflection over the Java Sea...	86
Introduction.....	86
Results.....	88
Seismic reflection over the northern Sunda Shelf.....	116
Magnetics.....	123
Introduction.....	123
Interpretation.....	123
The nature of the magnetic anomalies.....	127

	Page
Gravity.....	140
Introduction.....	140
Regional gravity.....	146
Gravity anomalies of Java Sea....	148
Gravity anomalies over land areas.....	153
Crustal model.....	157
Basement Petrology.....	164
 CHAPTER V STRUCTURAL ELEMENTS OF THE SUNDA SHELF....	 169
Faults.....	174
Structural highs.....	176
a. Ridges.....	177
b. Platforms.....	185
Basins.....	188
 CHAPTER VI TECTONIC EVOLUTION OF THE SUNDA SHELF....	 192
Previous theories.....	192
Proposed Evolution of the Sunda Shelf.	194
Early-middle Cretaceous.....	196
Late Cretaceous-early Eocene.....	200
Middle Miocene.....	203
Late Pliocene.....	205
Recent.....	207
Remarks.....	207
 REFERENCES.....	 209
 APPENDIX I SEISMIC REFRACTION STUDIES.....	 227
Analysis of sonobuoys.....	227
Sonobuoy profiles.....	229
 APPENDIX II PETROLOGY OF BASEMENT ROCK SAMPLES.....	 259
Thin section descriptions.....	259
Density measurements.....	265
Compressional wave velocity measurements.....	267
 BIOGRAPHY.....	 268

## LIST OF FIGURES

Figure	Page
1. Bathymetry of the Indonesian Archipelago.	16
2. Epicenters of recent earthquakes in the Indonesian Archipelago.	25
3. Bathymetry and topography of the Sunda Shelf and vicinity.	28
4. Diagramatic map of the Sunda Shelf and vicinity.	30
5. Pattern of ridges in the China Basin.	42
6. Magnetic anomalies in the China Basin.	45
7. Geophysical profiles in the China Basin.	47
8. Tectonic map and paleogeographic reconstruction of the China Basin.	50
9. A geophysical profile across the Philippine Ridge.	53
10. Gravity anomaly belts, active volcanoes, surface trace of underthrusting, limits of belt of epicenters and topographic axes in the Indonesian Archipelago.	61
11. Location map showing the position of geophysical traverses and sonobuoy stations over the Sunda Shelf.	67



Figure	Page
12. Average velocity profiles from wells and from sonobuoy stations.	71
13. Histograms of sonobuoy refraction data over the Java Sea.	73
14. Comparison of velocity structure of the northern Sunda Shelf with those of continents and ocean basins.	79
15. A north-south seismic structure section across the Java Sea and the deep-sea to the south.	83
16. A northeast-southwest seismic structure section across the Sunda Shelf.	85
17. Analog and processed seismic reflection profile.	90
18. Interpretative geophysical profiles 1, 3, and 5 across the northern Java Sea.	92
19. Interpretive geophysical profiles 6, 7, and 8 across the western Java Sea.	95
20. Interpretive geophysical profiles 10, 12, and 14 across the western and central Java Sea.	97
21. Interpretive geophysical profiles 16, 17 and 18 across the central and eastern Java Sea.	102

Figure	Page
22. Interpretive geophysical profiles 20, 21, and 22 across the eastern Java Sea.	104
23. Schematic north-south cross section across the East Java Basin, the Java Sea, and the Barito Basin.	107
24. Interpretive geophysical profile 22 across the westernmost Flores Sea.	110
25. Sections of original recording in the Java Sea.	113
26. Section of original recording in the westernmost Flores Sea.	115
27. Geophysical profiles across the Natuna Rift and the Billiton Depression.	120
28. Three-dimensional cardboard model of continuous seismic profiles in the northern Sunda Shelf.	122
29. Magnetic anomalies in the Sunda Shelf and vicinity.	125
30. Magnetic provinces over the Sunda Shelf.	129
31. Observed and simulated magnetic profiles across the Natuna Ridge.	131

Figure	Page
32. Magnetic anomaly contours over the Java Sea and the deep-sea to the south.	138
33. Free-air anomaly map of the East Indies.	143
34. Bouguer anomaly map of Sunda Shelf and vicinity.	145
35. Bouguer anomaly map of the South Sumatra Basin.	156
36. Structural model across the Indonesian Island Arc.	159
37. Basement rock types.	168
38. Structural map on top of basement	171
39. Tectonic elements over the Sunda Shelf and vicinity.	173
40. Schematic evolutionary stages in the development of the Sunda Shelf and vicinity	198
41. Sonobuoy station 3.	232
42. Sonobuoy station 4.	234
43. Sonobuoy station 5.	236
44. Sonobuoy station 7.	238
45. Sonobuoy station 8.	240
46. Sonobuoy station 10.	242

Figure	Page
47. Sonobuoy station 13.	244
48. Sonobuoy station 15.	246
49. Sonobuoy station 20.	248
50. Sonobuoy station 21.	250
51. Sonobuoy station 22.	252
52. Sonobuoy station 24.	254
53. Sonobuoy station 25.	256
54. Sonobuoy station 26.	258
55. Polished-sections of basement samples	261
56. Thin section photographs.	263

## LIST OF TABLES

	Page
1. Sonobuoy refraction data from the Java Sea.	69
2. Location of stations, seismic velocities and thickness of layers in the northern Sunda Shelf.	77
3. Density of basement rock samples.	266

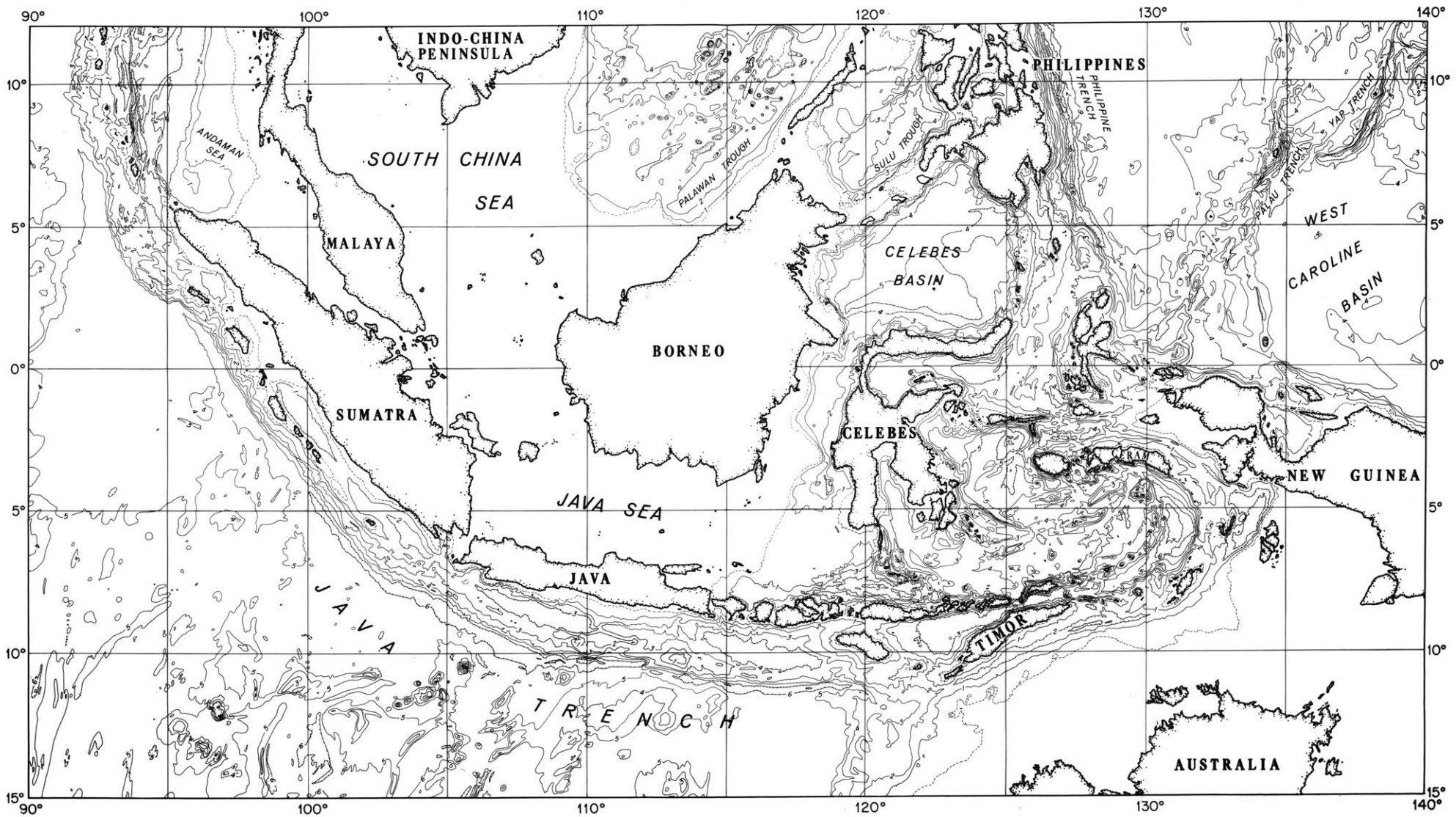
## CHAPTER I

## INTRODUCTION

## STATEMENT OF THE PROBLEM

The Sunda Shelf is situated on the western side of the Indonesian Archipelago, surrounded by the Malay Peninsula, the Indochina Peninsula and the islands of Borneo, Java and Sumatra. It comprises the Gulf of Thailand (between Indochina and Malaya), Malacca Strait (between Malaya and Sumatra), the southwestern part of the South China Sea, the Java Sea and the southwestern part of the Makassar Strait (between Borneo and Celebes) (Fig. 1). With an area of 1,850,000 square km, it is one of the most extensive coherent shelves in the world. The Indonesian Archipelago with its active volcanism, seismicity and orogenesis is among the most complex structural regions in the world. van Bemmelen (1954) stated that Indonesia is a most suitable region for the study of mountain building processes. Many other famous Dutch geologists such as Brouwer, Umbgrove, Kuenen, Vening Meinesz, Ritsema and others recognized that this area illustrates various stages in the evolution of orogenic belts. The impressive arcuate sweep of the Sunda Island and associated ocean trenches has been linked with the concept of geosynclines since the beginning of the century. In fact, critical

Figure 1. Bathymetry of the Indonesian Archipelago. Contour interval = 1 km, with the 150-m contour added as dashed line. Interpolated and re-drawn from Chase and Menard (1969) and from Fisher (1968).





observations from this region and especially from the Sunda Land (the Sunda Shelf and adjacent islands) have been used in most theories of orogenics and tectonics, and such fundamental concepts as the tectogene and idiogeosyncline were originally introduced in this area. Newly developed views concerning plate tectonics and sea-floor spreading (Hess, 1962; Dietz, 1961; Vine and Matthews, 1963; Isacks, et al., 1968; Le Pichon, 1968; and Morgan, 1968) indicate that classical theories of orogeny such as the "geosynclinal cycle" which were developed for the Sunda Land may be largely in error. One of the "advantages" of the previous tectonic theories was that most parts of the tectonic belts were hidden under the waters of the Sunda Shelf. In view of the fact that at that time nothing at all was known of the geology of the shelf and very little was known of the geology of adjacent land areas, these theories must be regarded as speculative.

According to the modern concept of plate tectonics the Indonesian area has been a major "triple junction" between three mega-plates throughout most of the Mesozoic and Cenozoic. These plates are the Indian Ocean-Australian plate, the Asian plate, and the Pacific plate. The geology of Sunda Land probably resulted from the accomodation of the

large motion between the three plates. Therefore, a proper understanding of Sunda Land is needed before one can deduce the complete evolution of the eastern Indian Ocean and the western Pacific Ocean. Nowhere else in the world are there so many tectonic elements within one area, including remnant spreading ridges, transform faults, subduction zones, magmatic arcs, and marginal seas. Therefore no place else holds so many clues to so many different parts of the over-all tectonic process. At the present, the Sunda Shelf is an inactive part of the Asian plate. However, the geology of the surrounding land areas provides evidence of intense activity in the past and indicates that the present subduction and magmatic arc pattern around the shelf has only recently reached its present position (Hamilton, 1970).

The plate tectonics theory has been quite successful in dealing with the evolution of deep ocean basins, largely because the oceanic crust is young and has had a much simpler tectonic history than the continental crust. Therefore, structural and tectonic study of the seas surrounding the Sunda Shelf (which are probably underlain by an oceanic crust) should help us better understand the evolution of the shelf itself.

The Indonesian Archipelago has been compared with the Caribbean Sea by many scientists (e.g., Daly, 1940; Vening Meinesz, 1937). This apparent similarity and the location of the Sunda Shelf in the midst of oceanic basins raises the question of whether this shelf originated as a marginal sea that filled up with sediments since its activity stopped or whether the shelf was part of the Asian continent for a long time and is thus underlain by a thick continental crust.

For these reasons it was decided to investigate the Sunda Shelf and vicinity. The aims of the study were: 1) to determine sub-bottom structure of the shelf, and 2) by combination of these results with data from the deep seas surrounding the shelf, to deduce the geologic history of Sunda Shelf and the surrounding ocean basins. It is hoped that the results of these studies will also lead to better understanding of the early evolution of the eastern Indian Ocean and the western Pacific Ocean.

#### PREVIOUS WORK

Some of the seas surrounding the Sunda Shelf have been studied before. The bathymetry, sediments and water of the deep sea depressions in eastern Indonesia were first investigated during the Snellius Expedition of 1929-1930 (Kuenen, 1935). Vening Meinesz made his classical gravimetric

survey of the entire Indonesian Archipelago in the 1920's and 1930's. All this marine work was prior to the development of modern techniques for seismic reflection and refraction, magnetics and gravity from surface ships. Modern geophysical studies of the Indonesian Archipelago were initiated during the International Indian Ocean Expedition 1960-1965. United States Coast and Geodetic Survey Ship PIONEER made a geophysical survey in the Andaman Sea (Peter, et al., 1966). Farther south R/V VITYAS (Marova, 1966) and R/V ARGO and R/V HORIZON (Fisher, 1964) made geophysical studies of the Java Trench. As yet only a few of the magnetic and heat flow measurements of the trench have been published (Vacquier and Taylor, 1966) but Raitt (1966) described two north-south seismic refraction profiles across the Java Trench.

Of the entire Sunda Shelf only the northern part has been studied by seismic reflection and magnetic techniques (data collected aboard R/V F.V. HUNT; Parke, et al., 1971). For the southern Sunda Shelf the only geophysical data available are a few gravity and magnetic traverses taken by ships crossing this area (R/V H.M.S. COOK, USCGS ship PIONEER, NOAA ship OCEANOGRAPHER and R/V VEMA and R/V ROBERT CONRAD). The geophysical data from all these ships

(including R/V F.V. HUNT) are incorporated in the present study. Many geophysical studies have been made in the Sunda Shelf by oil companies since about 1967 (Humphrey, 1970, 1971; Tanner and Kennett, 1972), but the results are proprietary and not available outside the companies for a synthesis of regional geology that is the object of this study.

#### PRESENT WORK

The present work is based primarily on data collected in the Java Sea by the Woods Hole Oceanographic Institution's R/V CHAIN during her global cruise (1970-1971). The shipboard measurements included seismic reflection and refraction (via radiosonobuoys) profiles, gravity, magnetics and bathymetry. The geophysical methods are described in Emery, et al., (1970, 1972). All ten Project MAGNET profiles in this area were analyzed and combined with the shipboard data. Land gravity measurements were obtained from Shell Internationale Petroleum Maatschappij and from some published reports. Also available were some data concerning basement rocks and seismic velocities provided by oil companies operating in this area.

Another aspect of the present study involved a structural synthesis of other studies of the seas surrounding the Sunda Shelf. They include the China Basin (Emery and

Ben-Avraham, 1972; Ben-Avraham and Phillips, 1972; Ben-Avraham and Uyeda, in press), the western Philippine Basin (Ben-Avraham, et al., 1972), the Sulu Sea (Ben-Avraham, Segawa and Bowin, unpublished data) and the Java Trench (Bowin and Ben-Avraham, 1972, and in preparation).

## CHAPTER II

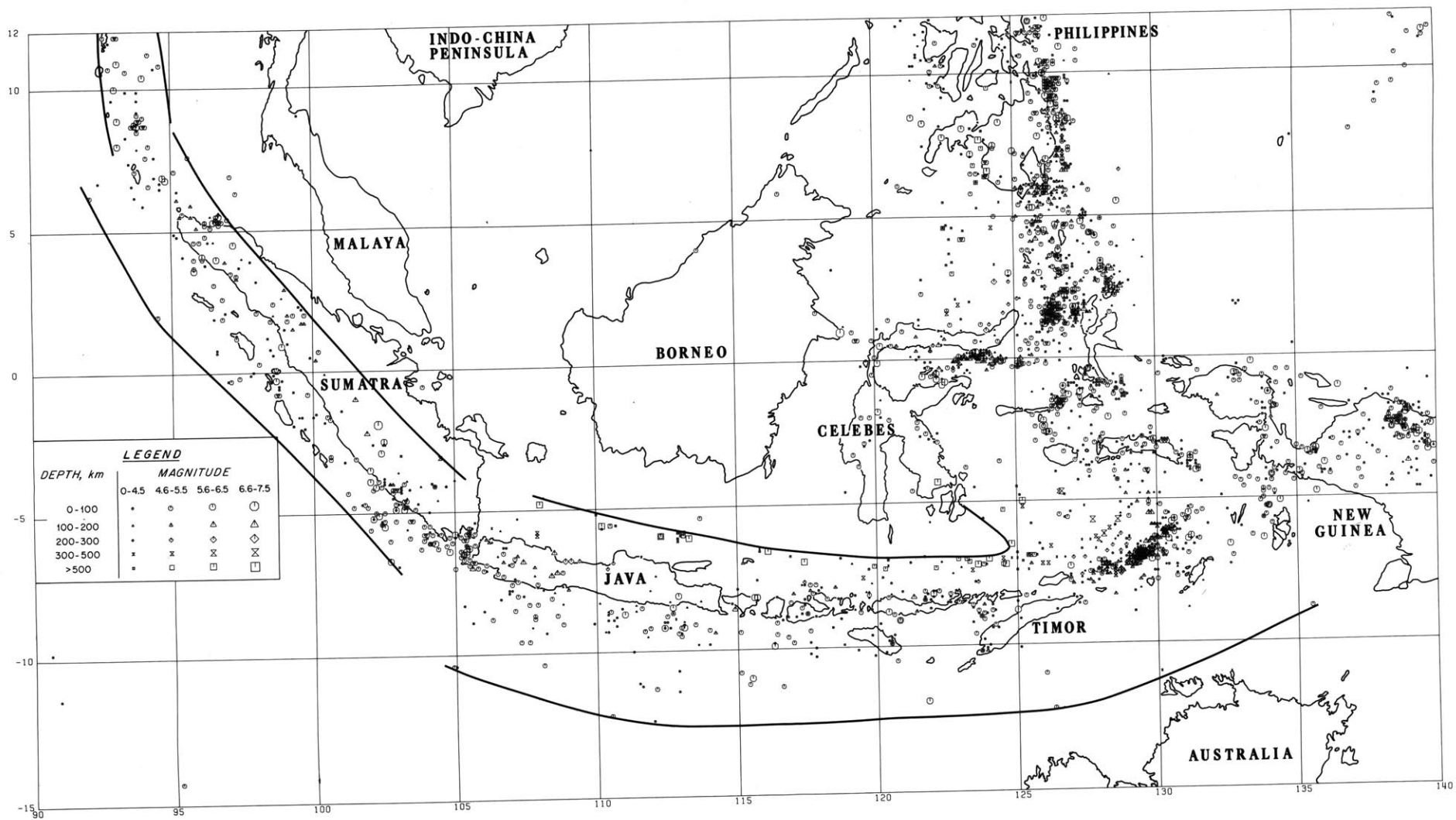
## GEOLOGICAL SETTING

## PHYSIOGRAPHY AND BOTTOM MATERIAL

The Indonesian Archipelago is bounded by the Asiatic continent to the northwest, Australia to the southeast, the Indian Ocean to the southwest and the Pacific Ocean to the northeast. On the basis of shallow earthquakes, Fitch (1970) divided the area into four corresponding major plates of lithosphere: Indian Ocean-Australian, Asian, Philippine Sea, and Pacific plates. In addition several small plates occur in the eastern part of the archipelago, but their boundaries are subject to considerable interpretation. The Sunda Shelf is part of the Asian Plate, which is separated from the other plates by a series of oceanic trenches associated with seismic activity (Fig. 2). As a result of a late Cenozoic interaction between the four major plates, two large and long orogenic belts meet in the Indonesian Archipelago. The Western Circum-Pacific Belt enters the area by way of the northern arm of Celebes, and the Alpine System extends from Burma into the arc of the Greater Sunda Islands (Sumatra and Java). The land areas around the shelf have considerable relief (as high as 4 km above sea level) associated with these two orogenic belts and with older

Figure 2. Epicenters of recent (1961-1968) earthquakes computed by the United States Coast and Geodetic Survey.





belts on Malay Peninsula and Borneo (Fig. 3).

The main structural elements of the Indonesian Archipelago are a double island arc and a broad shelf (the Sunda Shelf). The double island arc is composed of: (a) the non-volcanic Outer Banda Arc (Brouwer, 1925) running from Ceram via Timor and the submarine ridge south of Java to the islands west of Sumatra; and (b) the volcanic Inner Banda Arc running from Banda south of Ceram via Lesser Sunda Islands to the row of volcanoes on Java and Sumatra.

The Sunda Shelf is a shallow sea generally less than a hundred meters deep (Figs. 1, 3). The widely spaced contours of Figures 1 and 3 fail to reveal many of the topographic details of Figure 4, but the three figures supplement each other. They show the sharp contrast between the flat Sunda Shelf and the rather complex and irregular bathymetry of the deep seas surrounding it. Earle (1845) was first to report the extensive flat area of the Sunda Shelf. About 75 years later, after the results of the Siboga Expedition had become known, Molengraaff (1921) advanced Earle's concept and argued that the Sunda Shelf is a submerged peneplain, resulting from eustatic changes in sea level during the latest Pleistocene glaciation. Kuenen (1950, p. 482) and others suggested that the course of several submerged drainage systems can be

Figure 3. Bathymetry and topography of the Sunda Shelf and vicinity. Sunda Shelf: Contour interval = 20 m; deep sea: Contour interval = 1 km; land area: topographic contours of 100 m, 500 m and 2 km. Compiled from U.S. Navy Hydrographic Office navigational charts 1170 and 3001 plus acoustic soundings from R/V CHAIN over the shelf area; Chase and Menard (1969) and Fisher (1968) over the deep sea and the Times Atlas over the land area (Bartholomew, 1958).

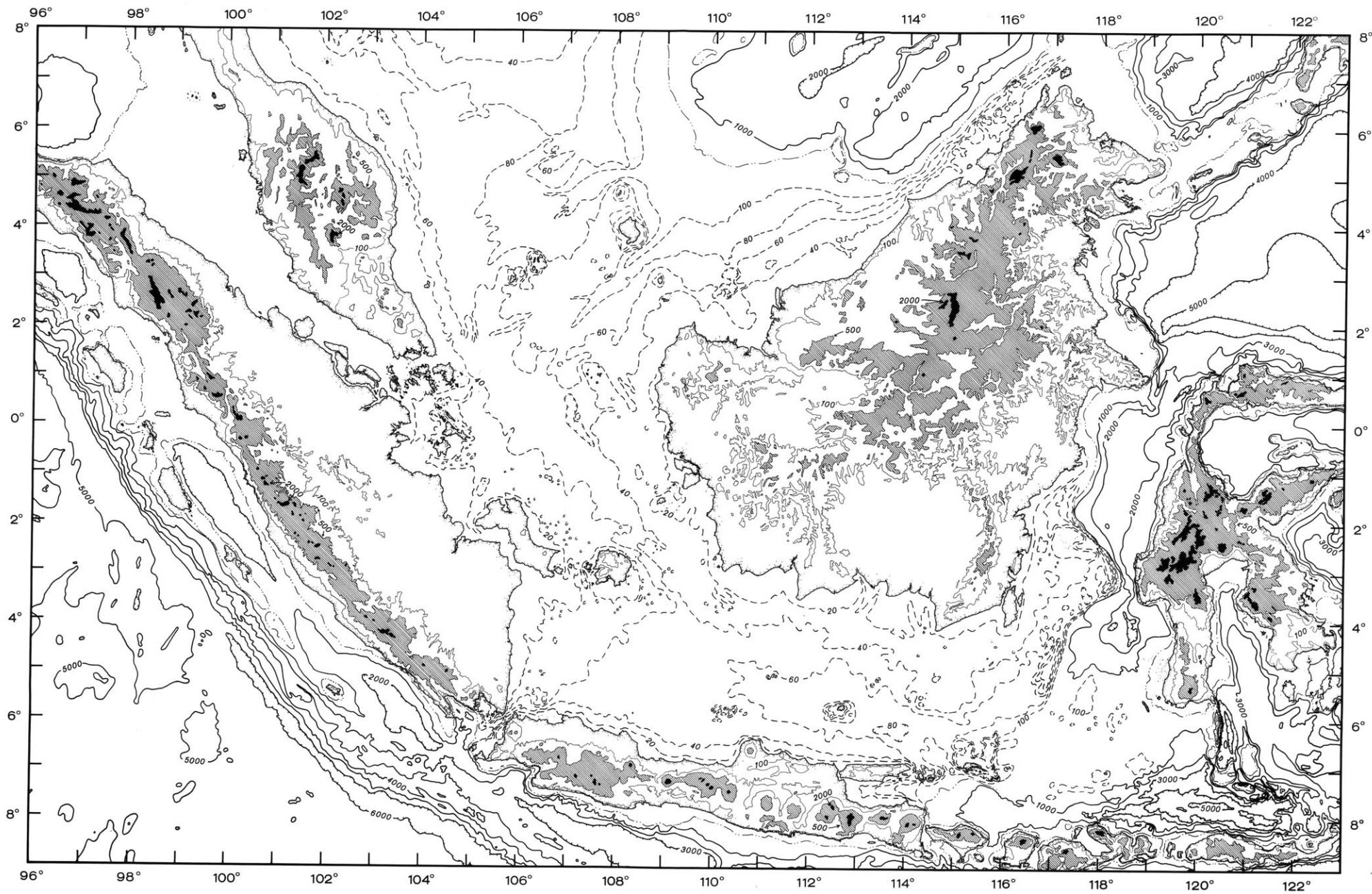


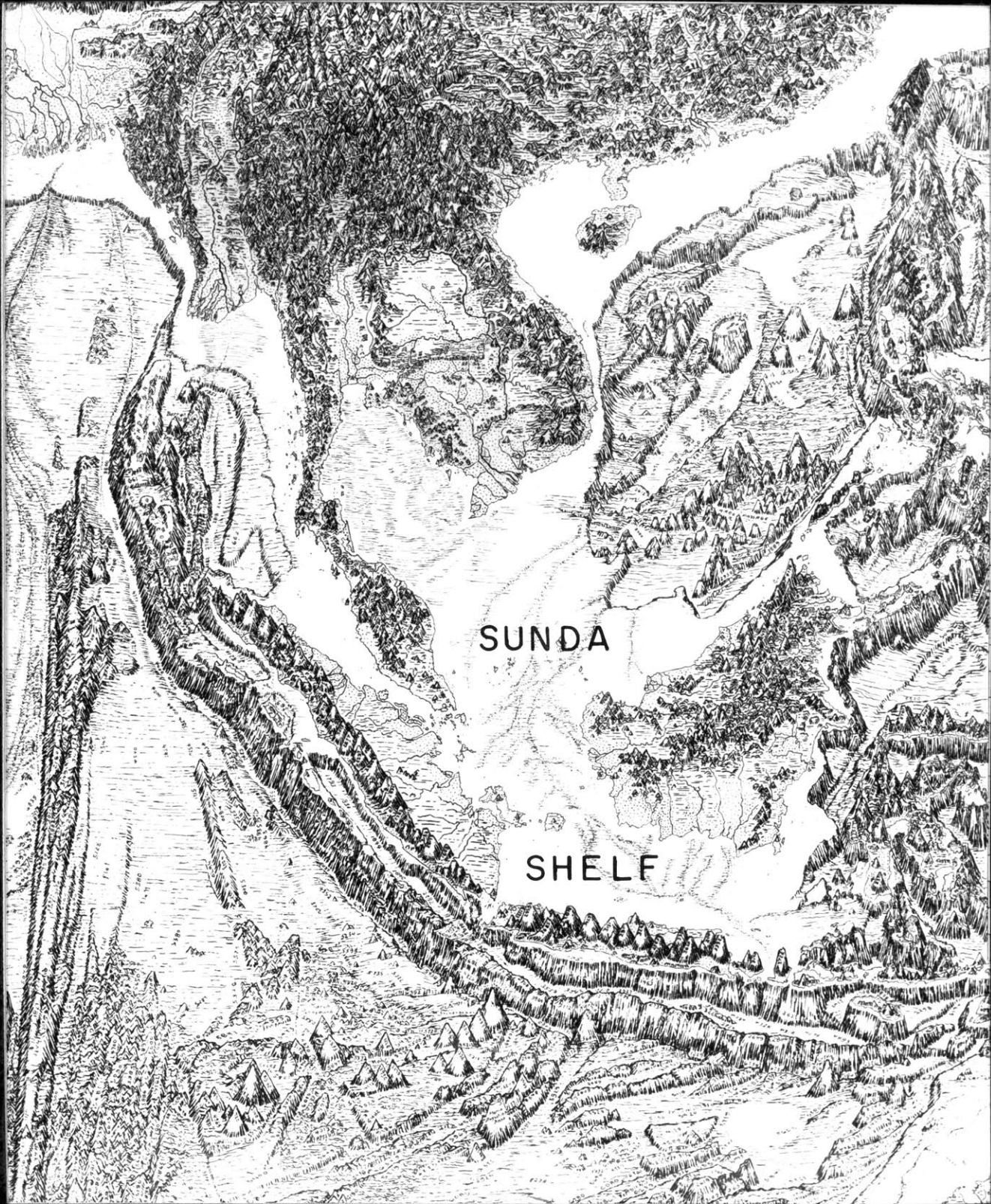
Figure 4. Diagrammatic map of Sunda Shelf and vicinity.  
From Heezen and Tharp (1971).

90°E

100°

110°

120°



SUNDA

SHELF

20° N

10°

0°

10° S

distinguished on the Sunda Shelf: the river systems in the Malacca Strait, in the South China Sea and in the Java Sea.

Bottom sediments over the shelf have been mapped by Emery and Niino (1963), Emery (1969, 1971), Keller and Richards (1967), van Baren and Kiel (1950) and by Mohr (1938). In general, the patterns show the presence of widespread modern silts and clays in the Gulf of Thailand and the axial part of the shelf between Sumatra, Java and Borneo, and modern ditrital sands along most of the shores except those of the northern Gulf of Thailand, eastern Sumatra and western Borneo. Most of the outer shelf is covered by coarse sands that probably are relict from the latest glacial period. Gravel bottom is common around the islands between Sumatra and Borneo, and in the entrance to Malacca Strait.

#### STRATIGRAPHY AND IGNEOUS ACTIVITY

The land geology of the areas surrounding the Sunda Shelf is still poorly known in spite of several thousand scientific papers that have been published as a result of nearly a century of work by many geologists (according to Umbgrove (1949) about 6000 publications on the geology of Indonesia already existed prior to the year 1937). It is impossible in the framework of this work to describe the

geology of Indonesia in great detail; for a summary of our geological knowledge of this area up to 1949 the reader is referred to van Bemmelen (1949). Since the work by van Bemmelen little has been added to the geological knowledge of this region as a unit. A review of the geology of Malay Peninsula is given by Alexander (1962) and Chung (1968). Leichti, et al., (1960) compiled the work of the Royal Dutch Shell Group in the British Territories in Borneo. Recently Hamilton (1972a) prepared a tectonic map of Indonesia utilizing the plate tectonic concept. In this section only the main highlights of the geology will be given.

The oldest stratigraphic unit is composed of crystalline schists of unknown age. van Bemmelen (1949, p. 60) stated that these crystalline schists are products of sedimentary deposits of various ages that were altered by regional metamorphism. The oldest fossiliferous deposits on Sunda Land are of middle and late Paleozoic age and have a very restricted distribution, mainly on Sumatra and Malay Peninsula. Not much is known about these deposits but Umbgrove (1938) suggested that in Indonesia they originated in a neritic to littoral environment. The Paleozoic of the Malay Peninsula is characterized by north-south parallel belts having sediments of widely different facies. Several



geologists described an extensive unconformity in upper Paleozoic strata associated with intense folding and volcanic activity (e.g. Umbgrove, 1938); however Klompé (1954) questioned the validity of such an unconformity.

During the Mesozoic sedimentary belts continued to be formed in the Malay Peninsula and new ones were formed in Indonesia. The fossils clearly indicate a Mesozoic sea connection (the Tethys Sea) between the present Indonesian Archipelago and the Mediterranean region (van Bemmelen, 1949, p. 63-79). The Paleozoic, Mesozoic, as well as the Cenozoic sedimentary belts in the Sunda Land region denote important differences in depth of deposition. In west Borneo, for example, the early Mesozoic occurs in littoral and neritic as well as deep sea facies (van Bemmelen, 1949, p. 225). Similar environments are represented also in Sumatra and the Malay Peninsula. These sedimentary belts may have resulted from a continuous interaction between lithospheric plates (Hamilton, 1972) during these periods. All of the Mesozoic and Cenozoic sediments on the Malay Peninsula are non-marine (Chung, 1968), indicating that since early Mesozoic time the peninsula has been above sea level. Of the larger islands, Java has the least Mesozoic sediments, consisting of only a few small localities in Central Java

(van Bemmelen, 1949, p. 603; Umbgrove, 1938) where pre-Tertiary sediments were recognized.

Orogenic movements in the Cenozoic Era gave the region its present physiography. About 75 percent of the surface of the islands consist of sediments and volcanic deposits of Cenozoic age. During the Tertiary enormous volcanic activity occurred in most parts of the Archipelago. Many of the deposits are mixed or intercalated tuffs, breccias and lava flows. The Tertiary sediments show evidence for isolated oblong basins with high rates of sedimentation on the islands of Sumatra, Java and Borneo. Umbgrove (1938) gave these basins a special name, "idiogeosynclines". According to van Bemmelen (1949), in part of south Sumatra the Neogene alone has a thickness of 11.5 km.

The stratigraphy of these Tertiary basins is of particular interest since they are similar to basins that occur on the Sunda Shelf. On land these basins were described by Umbgrove (1938), Schuppli (1946), van Bemmelen (1949), Schaub and Jackson (1958), Weeda (1958a, b), Wennekers (1958), Haile (1963), and Koesoemadinata (1969). Offshore basins were described by Todd and Pulunggono (1971), Koesoemadinata and Pulunggono (1971) and Cree (1972). The basins did not originate simultaneously, although some geologists argue that

the sedimentary sequences inside the various basins are similar. According to Koesoemadinata (1969), each basin underwent a mega-cycle of sedimentation, beginning with a transgression followed immediately by bathyal conditions and terminating with a regression.

Marine Eocene occurrences are restricted, with best development in the eastern Java Sea, eastern and northwestern Borneo and possible northern Sumatra. The Eocene in southern Sumatra and western Java Sea is represented by volcanics. During the Oligocene thick deltaic clastic deposits accumulated in the western Java Sea (Todd and Pulunggono, 1971), while marine conditions existed in east Java and southeast Borneo (Weeda, 1958a, b). Thick accumulation of carbonates occurred during the Oligocene in southeast Borneo.

The most widespread lithologic unit in the southern Sunda Shelf is a late Miocene reefoidal limestone. It seems that for the first time in the basin's history deposition became continuous throughout this area (Koesoemadinata and Pulunggono, 1971). Carbonate deposition was followed by a regressive phase in which shales were deposited in the deeper portions of the west Java Sea basins, and shale and carbonate in the eastern Java Sea. This regressive phase

in the eastern Java Sea was associated with folding and uplift. In the western Java Sea a shorter second marine transgression can be recognized at the end of the Miocene. Not much is known yet about the stratigraphy of the basins in the northern Sunda Shelf during mid-Tertiary.

During the Plio-Pleistocene marine sedimentation continued over the whole Sunda Shelf and gradually changed the floor to a relatively flat plane.

Igneous activity in the Indonesian Archipelago occurred almost throughout its history (van Bemmelen, 1949, 1954). This activity probably was associated with major tectonic events. Some of the most conspicuous magmatic features are the granitic belts which in areas (e.g. Malay Peninsula) are very long and continuous and clearly mark the position of old tectonic belts. Not all the granites and other igneous rocks are arranged in belts and in many places relationships to tectonic belts are not clear. Intrusive rocks range in type from large batholithic bodies to abundant smaller stocks, sheets and dikes. A wide range of compositions is present in the igneous rocks. The composition of a given rock probably reflects its relative position with respect to tectonic belts (Hatherton and Dickinson, 1969; Hamilton, 1972). Metamorphism, both regional and thermal (contact), is widespread and affected both sedimentary and igneous rocks.

## CHAPTER III

## THE SEAS SURROUNDING THE SUNDA SHELF

The Sunda Shelf is almost completely surrounded by deep sea basins, most of them probably are regions of oceanic crust. A number of theories have been advanced to explain the origin of these and other small ocean basins in the past 50 years. The major concepts published prior to 1935 have been reviewed by Kuenen (1935). More recent theories include those by Belousov, 1968; Menard, 1967; Vogt, et al., 1969; Karig, 1971; and Packham and Falvey, 1971. While Belousov (1969) has suggested that these ocean basins were originally continental areas that have become oceanic by a process of "oceanization", most other theories argue that these small ocean basins were formed by extensional rifting during the Tertiary. The basins around the Sunda Shelf are: the Andaman Sea, the China Basin, the Sulu Sea, the Celebes Sea, the Flores Sea (south of Celebes) and the northern Wharton Basin (northeastern Indian Ocean) (Fig. 1). Only the Andaman Sea and the China Basin have been studied, but the northern Wharton Basin, mainly the Java Trench, and the Sulu Sea are now being investigated.

## ANDAMAN SEA

Studies of the Andaman Sea were made mainly during the Indian Ocean Expedition, 1960-1965 aboard the U.S. Coast and Geodetic Survey ship PIONEER with reconnaissance magnetic, gravity, heat flow, and seismic profile surveys. Other American and Russian oceanographic ships made some additional studies. The results were published in a series of papers by Burns (1964), Peter, et al., (1966), Weeks, et al., (1967), Rodolfo (1969), and Frerichs (1971).

The Andaman Sea extends from the Irrawaddy Delta 1200 km southward to northern Sumatra and the Malacca Strait with an area of 800,000 km<sup>2</sup>. It consists of structural belts that trend southward from as far north as the eastern Himalayas and that curve eastward into Sumatra and the islands west of it. These belts from west to east are: a structural high including the Arakan Yoma range of Burma, the Andaman-Nicobar islands and the islands west of Sumatra; a topographic low including the Irrawaddy Valley of Burma, the deep western portion of the Andaman Sea and the Java Trough west of Sumatra; a volcanic arc including the Central Belt in Burma, the inner row of islands in the Andaman Sea and the Barisan Range in Sumatra.

With the exception of the double arc system, mentioned above, the trends in the Andaman Basin itself tend to strike north-northeast. The most prominent north-northeast trend is formed by continuity of magnetic and positive free-air gravity anomalies with the shelf break along the Malaysian peninsula (Peter, et al., 1966). The Malayan continental slope has been interpreted as a major normal fault, (Peter, et al., 1966; Rodolfo, 1969). A similar trend is displayed by a strong trend in the magnetic anomalies along the submarine slope at the northwestern end of the Malacca Strait. Projected to the northeast, this trend coincides with a major transcurrent fault across the angular elbow-like feature in the Malay Peninsula. Garson and Mitchell (1970) interpreted this fault as a left-lateral transform fault that was active in the late Jurassic to early Cretaceous.

Sediment accumulation and contemporaneous rates of sedimentation suggest that the Andaman Sea may not be older than the Miocene. On the basis of geological and geophysical studies Rodolfo (1969) concluded that the Andaman Sea is dominated by youthful structures that are tensional in origin. He suggested that the sea was formed by rifting to the southeast. Geomorphic (Weeks, et al., 1967) and seismic (Fitch, 1970, 1972) evidence shows that active extension along the central Andaman Trough is still in progress along a

WNW-NW direction.

#### CHINA BASIN

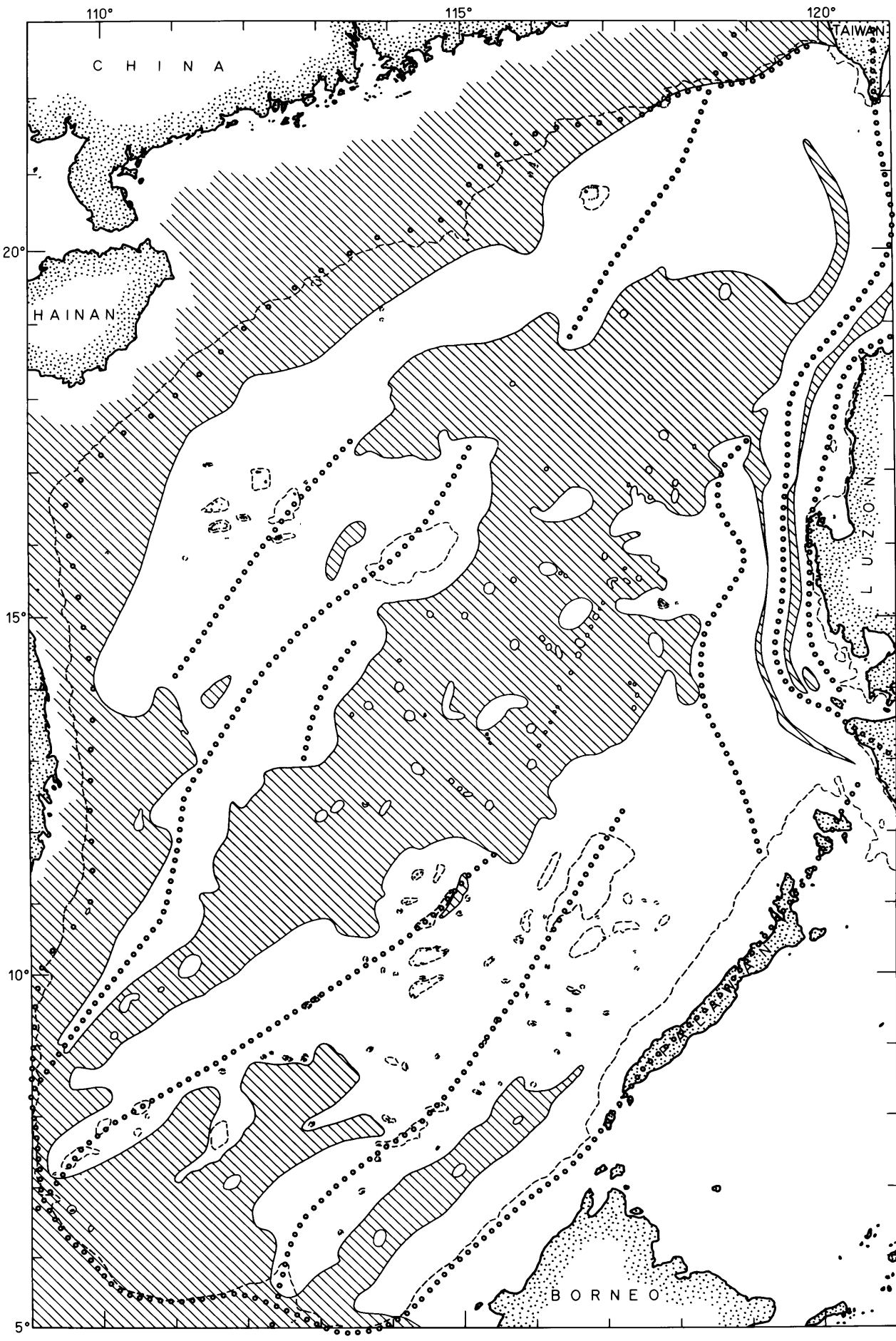
At the eastern side of the China Basin, the structure of the Manila Trench and West Luzon Trough was studied by Ludwig, (1970); Ludwig, et al., (1967); and Hayes and Ludwig, 1967. More recently Emery and Ben-Avraham (1972) investigated the structure of the entire China Basin from continuous seismic reflection and magnetic data collected by R/V F.V. HUNT, RUTH ANN and SANTA MARIA on contract to the U.S. Naval Oceanographic Office. Ben-Avraham and Phillips (1972) and Ben-Avraham and Uyeda (in press) proposed a model for the evolution of the China Basin to explain the structural elements in the basin and the surrounding land masses.

Emery and Ben-Avraham found that a series of ridges trends northeast-southwest in the center of the China Basin and another series trends north-south near its eastern margin (Fig. 5). Seismic reflection and refraction profiles and magnetic characteristics showed that these ridges consist of folded sediments.

The eastern part of the China Basin has a velocity-structure similar to that of normal oceanic crust (Ludwig, 1970), except that the average thickness of the main crustal



Figure 5. Pattern of ridges (dotted lines) in the China Basin. The hatching depicts the areas that are covered with undisturbed sediments (from Emery and Ben-Avraham, 1972).



layer (Layer 3) is only about half the normal thickness, and the M-discontinuity is shallower than normal by about 2-3 km.

Most of the basin has subdued magnetic anomalies except in a broad area west of Luzon Island that has very disturbed magnetic anomalies closely resembling oceanic ones (Fig. 6). In this disturbed zone the apparent wavelengths of the magnetic anomalies along east-west tracks are generally longer than those along north-south tracks, as noted by Hayes and Ludwig (1967). Thus, if any magnetic trends exist they probably extend east-west. The dashed lines in Figure 6 show possible correlations of the magnetic anomalies. The nature of the magnetic anomalies, the fact that they are not related to the basement relief (Fig. 7), the oceanic nature of the crustal structure, and the deep water of the area (4 km) lead to the conclusion that these anomalies may have originated when the crust of this portion of the China Basin formed by sea-floor spreading.

The east-west trend of the magnetic anomalies in the disturbed zone of the China Basin is almost perpendicular to the north-south trend of the structural ridges. Similarly, in southern Taiwan the Tertiary structural trends are generally north-south (Meng and Chang, 1971; Ho, 1971), whereas the deeper magnetic trends are east-west (Bosum, et al.,

Figure 6. Chart of magnetic anomalies plotted along tracks in the China Basin. The anomaly amplitude is plotted normal to the track direction. Data from Emery and Ben-Avraham (1972) and Hayes and Ludwig (1967). Airplane lines (Project MAGNET) are identified by three digit numbers. The areas of disturbed magnetic anomalies are enclosed by large dots. Dashed lines show possible correlations of the magnetic anomalies.

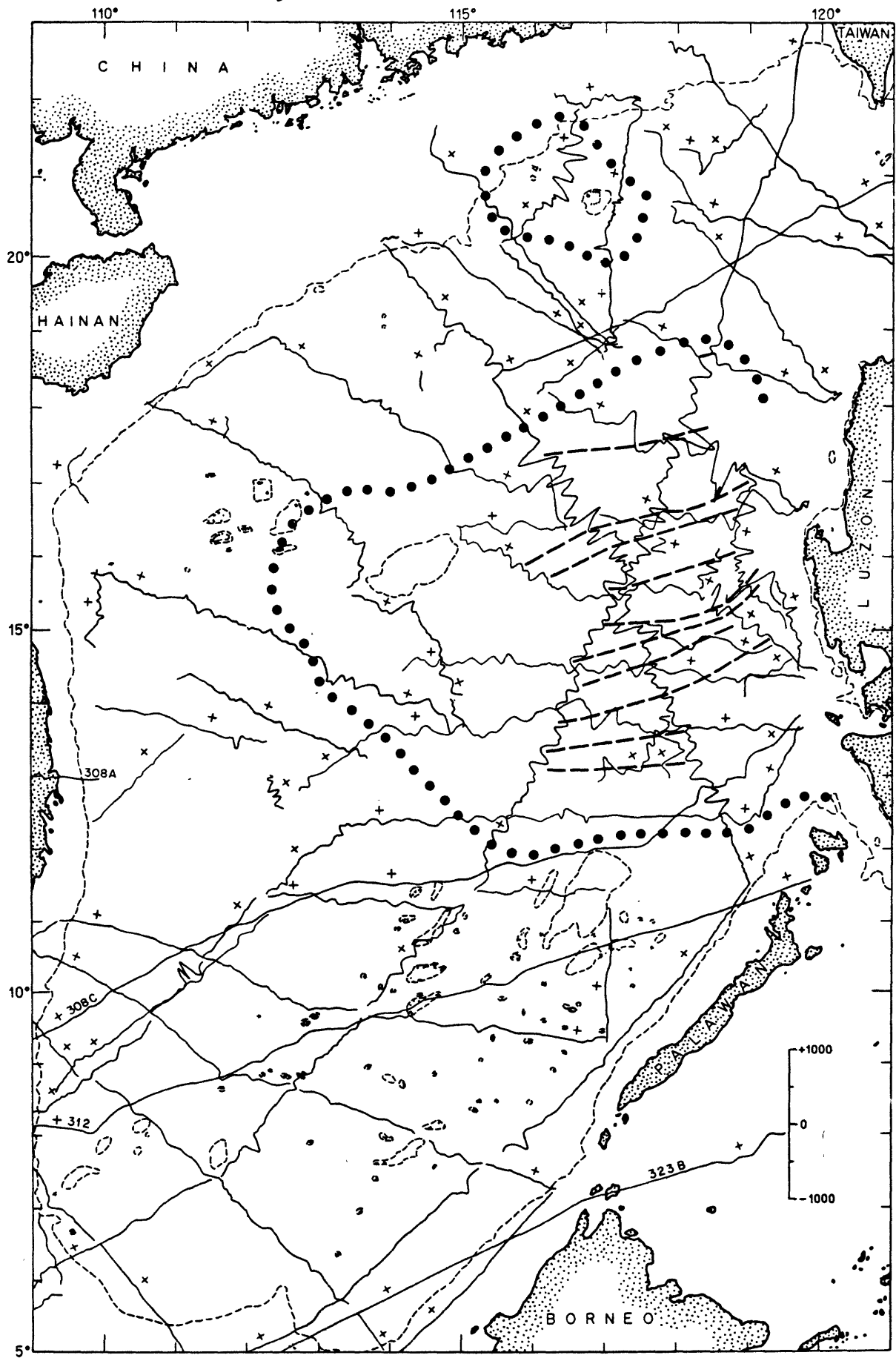
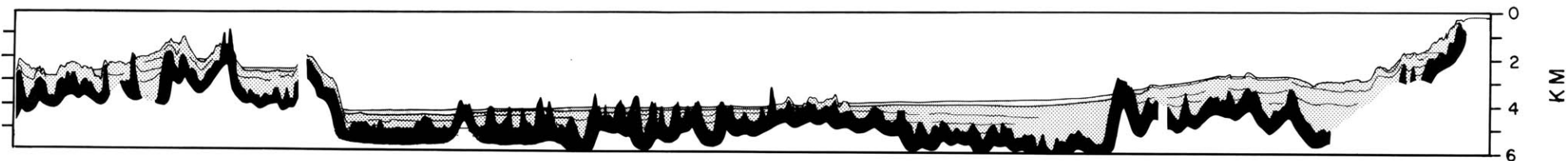
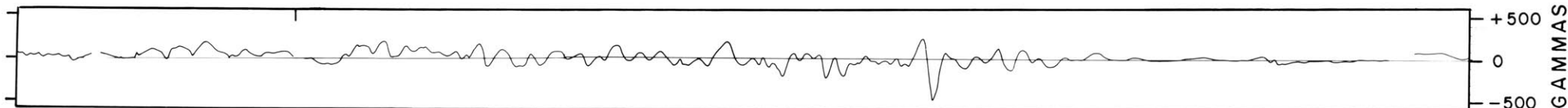


Figure 7. Interpretive seismic (bottom) and magnetic (top) profiles. Latitude and longitude of the edges are given on top of the profiles. The profiles are along the two long north-south lines in Figure 6.

11° 20' N  
115° 06' E

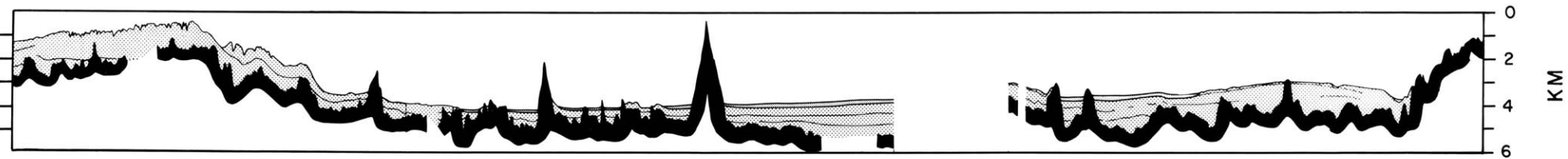
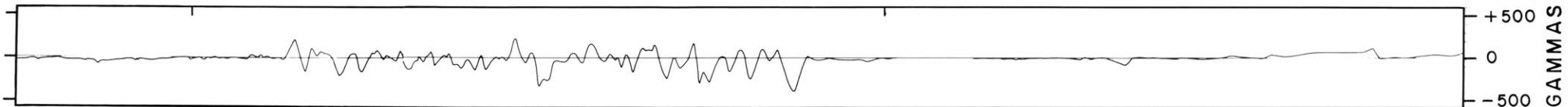
23° 00' N  
119° 50' E



11° 31' N  
118° 59' E

18° 20' N  
115° 27' E

20° 52' N  
121° 00' E



0 100 KM

1970). Gravity anomalies in the Philippines both on Luzon Island (Bureau of Mines, 1969) and offshore (Hayes and Ludwig, 1967) show very distinctive north-south lineation although the magnetic trends are probably east-west. This suggests that the more recent north-south and northeast-southwest tectonic trends are superimposed over older east-west trends throughout this area.

At least three stages in the development of the China Basin may be inferred from this evidence. The first stage was a north-south extension associated with the formation of the oceanic crust beneath the China Basin. A simple paleogeographic reconstruction for the early Mesozoic era requires Borneo to have been adjacent to mainland China and Hainan (Ben-Avraham and Phillips, 1972) (Fig. 8) as suggested previously by Carey (1958, p. 287). Later stages of north-west-southeast and east-west compression are superimposed on the first one and are associated with the closing of the China Basin.

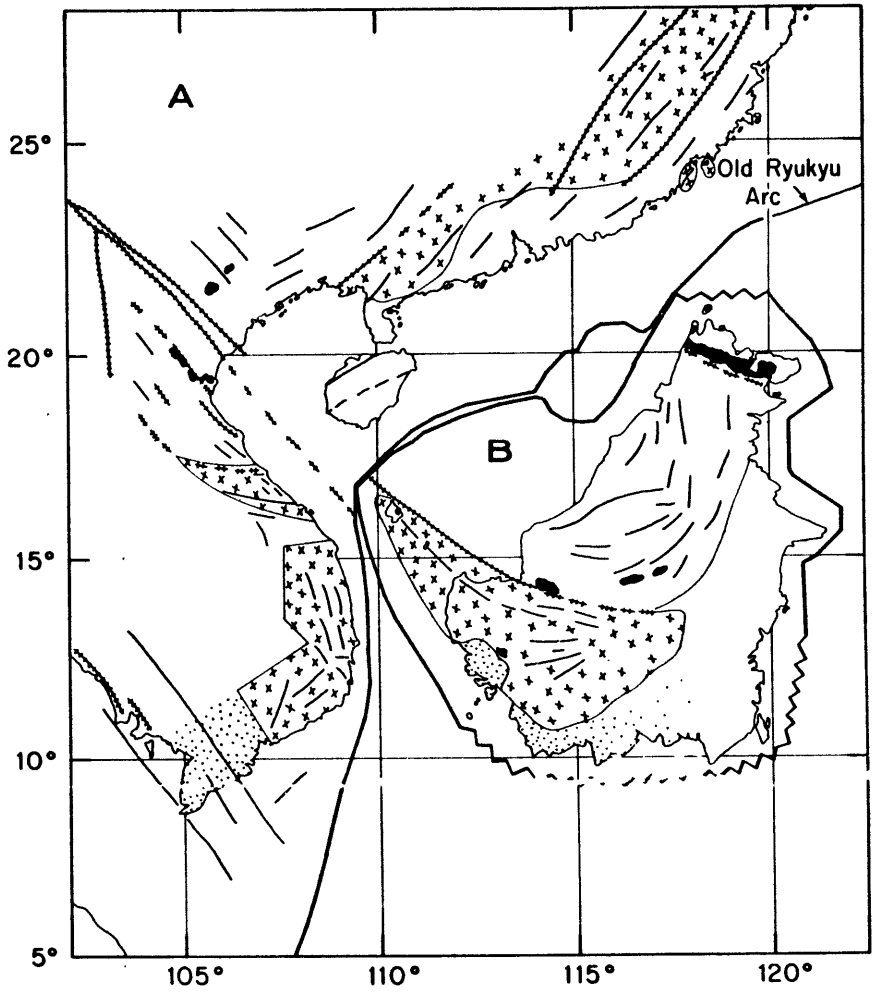
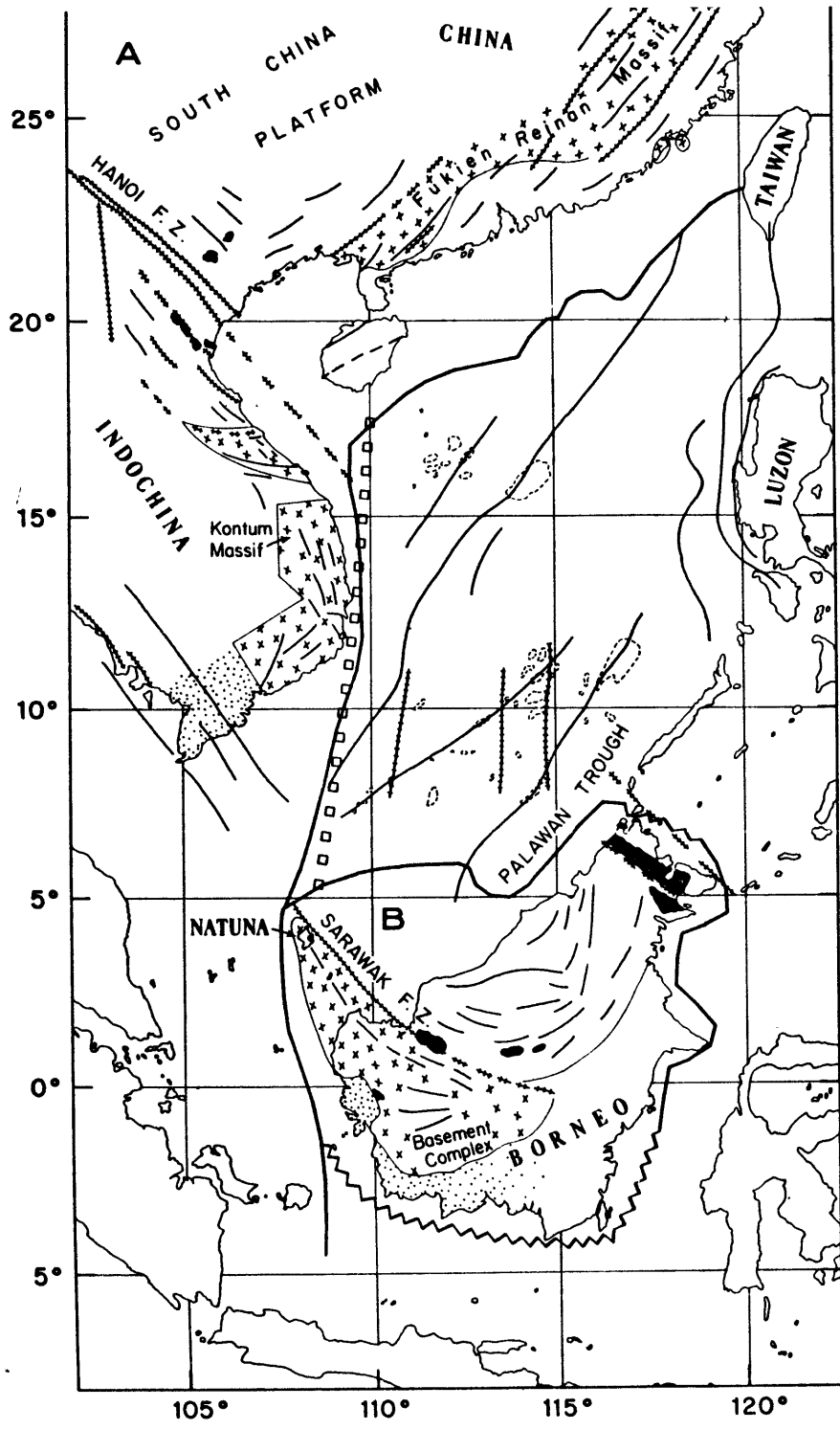
The tectonic evolution of the China Basin (Ben-Avraham and Uyeda, in press) may be summarized as follows:


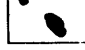

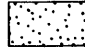



In mid-Mesozoic north-south extension formed the oceanic crust of the China basin by a clockwise rotation of  $14.2^\circ$  of a small plate that included Borneo and Natuna Islands away from mainland China around the pole of rotation,



Figure 8. Left: Simplified tectonic map showing the major tectonic elements in the China Basin and its margins. Sources of information are: Yanshin (1966), the Geological Institute USSR (1970); Li and Meng (1970); Klompé and Sigit (1965); Mainguy (1968, 1970, 1971); van Bemmelen (1949); and this study. Also shown are the boundaries of plate A (Asia) and plate B (Borneo), and a small circle (marked by small squares) about the pole, Latitude  $13.0^{\circ}\text{N}$ , Longitude  $44.0^{\circ}\text{E}$ .

Right: Paleogeographic reconstruction of the China Basin area for the early Mesozoic. The tectonic elements are the same as in the figure on the left. The reconstruction was obtained by rotation of plate B  $14.2^{\circ}$  about a pole at Latitude  $13.0^{\circ}\text{N}$ , Longitude  $44.0^{\circ}\text{E}$ .



- |   |                                   |   |                   |
|---|-----------------------------------|---|-------------------|
|  | Plate Boundary                    |  | Ophiolite Body    |
|  | Inferred Plate Boundary           |  | Sedimentary Cover |
|  | Fault                             |  | Basement          |
|  | Fold Axes & Other Geologic Trends |   |                   |

Latitude  $13.0^{\circ}\text{N}$ , Longitude  $44.0^{\circ}\text{E}$  (Fig. 8). The opening of the basin probably was associated with the formation of the faulted margin of the Indochina Peninsula and the faults in the center of the basin.

During early and middle Tertiary times underthrusting along the Palawan Trough and movement along sinistral wrench faults resulted in northwestward movement of Borneo relative to Asia. This minor narrowing of the China Basin caused a compression which formed some of the northeasterly trending ridges along the length of the China Basin. Since late Tertiary time, activity along the modern system of trenches in the Philippine region has formed three northerly trending ridges west of Luzon Island and has truncated the mid-Tertiary trench system along northwestern Borneo and Palawan.

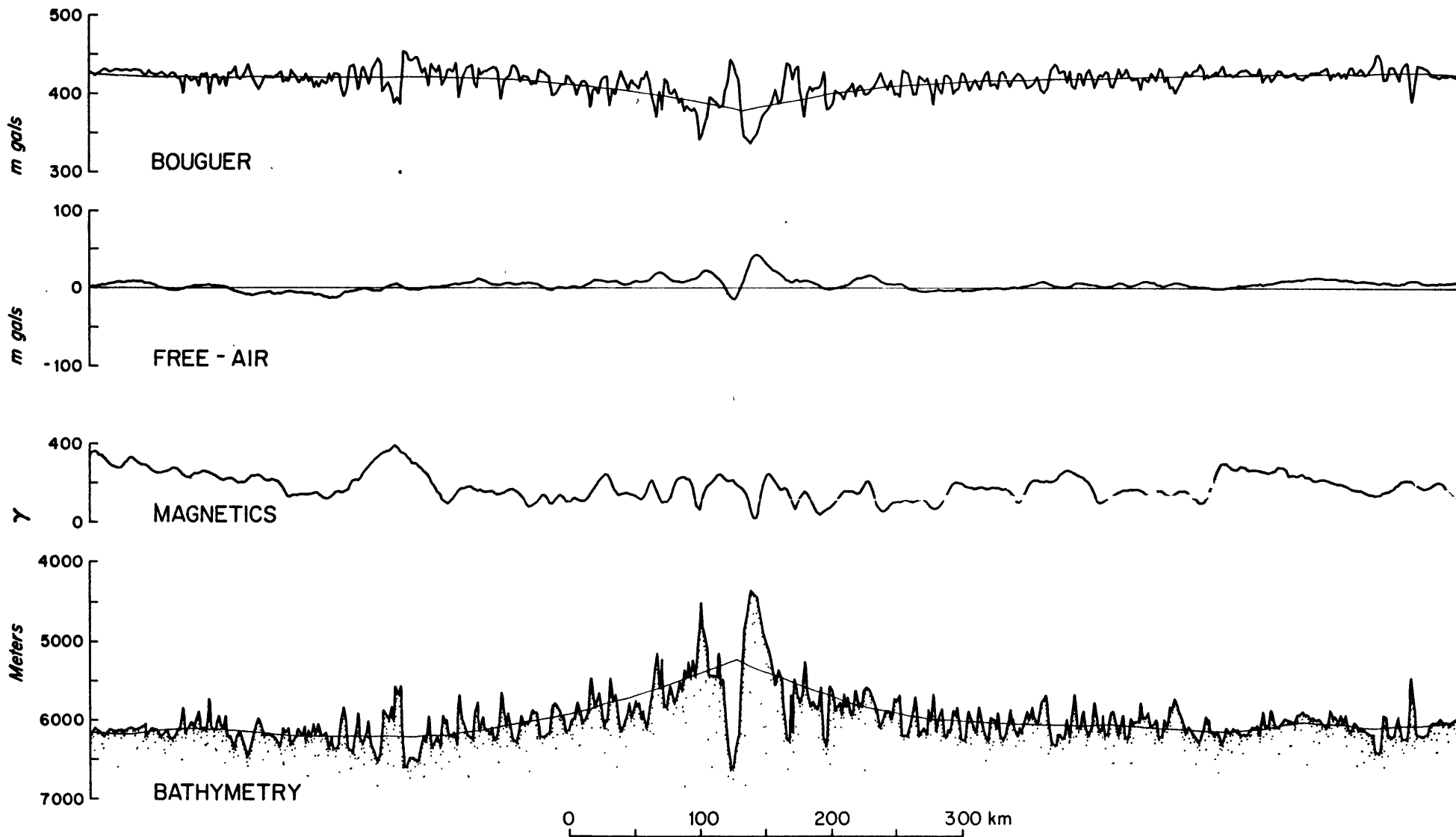
#### WESTERN PHILIPPINE BASIN

Recent study of the western Philippine Basin (Ben-Avraham, et al., 1972) shows the presence of an extinct spreading center in the middle of the basin (Fig. 9). The ridge, which was named the Philippine Ridge, extends 1500 km from the Palau-Kyushu Ridge towards the southern edge of the Ryukyu Trench along a strike of  $\text{N } 50^{\circ}\text{W}$ . Ben-Avraham, et al., (1972) concluded that the Philippine Ridge was active during the Mesozoic at least  $7^{\circ}$  south of its present location and that it has moved to its present position by under-

Figure 9. Gravity, magnetic, and bathymetry profiles over the Philippine Ridge. The profile strikes north-south. Location of the ridge crest where crossed by the profile is at Latitude  $15^{\circ}00'N$ , Longitude  $132^{\circ}00'E$ .

N

S



thrusting along the Ryukyu Trench after sea-floor spreading was stopped.

The Philippine Islands did not exist during the early Mesozoic. Major differences exist in the nature of basement rocks from early Mesozoic and older periods as compared to those of later Mesozoic to Cenozoic (Gervasio, 1968, 1971). The older sequence consists of ultrabasic, basic and/or intermediate volcanic flows with a closer affinity to oceanic crustal material than to continental-type rocks (Ludwig, 1970). The younger sequence commenced during the Cretaceous period and consists of a series of sedimentation cycles and volcanic activity. This sequence was interpreted by Hamilton (1972) as a subduction melange. The sequence probably started in the late Cretaceous, when the Philippine Archipelago was elevated to separate the China Basin from the Philippine Sea. This conclusion is supported somewhat by Krause' (1966) conclusion that no land existed prior to Cretaceous time in the Celebes and Sulu archipelagoes.

Although the exact period in which spreading occurred in the China Basin and the western Philippine Basin is yet to be proved by deep-sea drilling, it may have occurred in both places during mid-Mesozoic. The area occupied at present by the Philippine Islands probably was a transform fault (Fig. 40, below). At present the active Philippine fault

(Allen, 1962; Fitch, 1970) probably is at or very near the location of the Mesozoic transform fault.

#### SULU SEA

The Sulu Sea is a small ocean basin bounded by Palawan Island, Philippine Islands, Sulu Archipelago and Borneo. It is divided by a submarine ridge into a deep (more than 4 km) eastern part, the Sulu Trough, and a shallow (less than 2 km) western part. The only geophysical data from this sea are three heat flow measurements (Nagasaka, et al., 1971) and a recent geophysical survey by the Japanese R/V HAKUHO MARU (Ben-Avraham, Segawa, and Bowin, unpublished data). The mean of the heat flow value ( $2.4 \mu\text{cal}/\text{cm}^2 \text{ sec}$ ) is about double the over-all mean oceanic heat flow value and is close to the mean value for marginal seas. Gravity measurements made aboard the HAKUHO MARU across the sea show that the area between the median ridge and Palawan Island is a trough containing several km of low density sediments. It seems likely therefore, that this area contains three major ridges separated by deep troughs. Large ( $200-450 \gamma$ ) negative magnetic anomalies were recorded over the two eastern ridges by the HAKUHO MARU. This supports the idea that the ridges are composed of basic rocks and can

be remnant arcs as inferred also by Hamilton (1972) and Karig (1972). The three arcs come ashore at the southern Philippines and northern Borneo. To the north the eastern arc comes ashore as the Zamboanga Peninsula of Mindanao; the median arc as western Panay Island and the western arc (Palawan) as Mindoro Island. To the south all three arcs crop out on northern Borneo as a large melange terrain including large masses of ophiolites (Fig. 8), for which Hamilton (1972) proposed a Miocene age. A fault zone may exist between Palawan Island and northern Borneo in the Balabac Strait (Mainguy, 1970, 1972). Fitch (1963) argued that Palawan had moved along a northwest-trending sinistral fault. The eastern arc is still seismicly active (Fig. 2) and it probably is the youngest arc in the Sulu Sea.

#### SMALL OCEAN BASINS OF EASTERN INDONESIA

East of the Sunda Shelf are several deep basins inside the Banda Arcs. The largest are the Flores, Banda and Celebes Seas. Except for bathymetry that was recorded mainly during the Snellius Expedition (Kuenen, 1935) and data compiled by Krause (1966), the only geophysical data from these seas available so far are the results of gravity surveys (Fig. 33, below) and a few seismic refraction



measurements (Raitt, 1967). Raitt concluded that the crust beneath the Banda Sea is remarkably thin, less than 6 km.

The exact structure of these seas is still unknown. Geologic evidence from the adjacent islands indicate a late Tertiary or younger origin (Kuenen, 1950). A model for the evolution of eastern Indonesia in terms of plate-tectonics has been proposed recently by Audley-Charles, et al., (1972). In general, these authors conclude that the Outer Banda Arc formed part of the Australian continental margin from at least the Permian, but that Ceram, Buru and eastern Celebes became detached after the breakup of Gondwanaland. The subsequent history of the area is then described in terms of a series of collisions between the northward-drifting Australian continent and a series of northward-dipping subduction zones. The first collision took place between the late Cretaceous and the Eocene after which renewed subduction began further north to allow the continuing northward motion of Australia. The second collision (with the new subduction zone) took place during the middle Miocene. Another subduction zone developed still further north, with which the Australian continent collided (the third collision) during the late Pliocene. The northward motion of Australia occurred between two north-south transform faults,

the western one postulated to be an extension of the Fossa Sarasina in Central Celebes. On land this fault is known to be left-lateral (Katili, 1970). It is possible that during the Mesozoic this transform fault was part of an even larger fault system which included the Philippine transform fault.

#### JAVA TRENCH

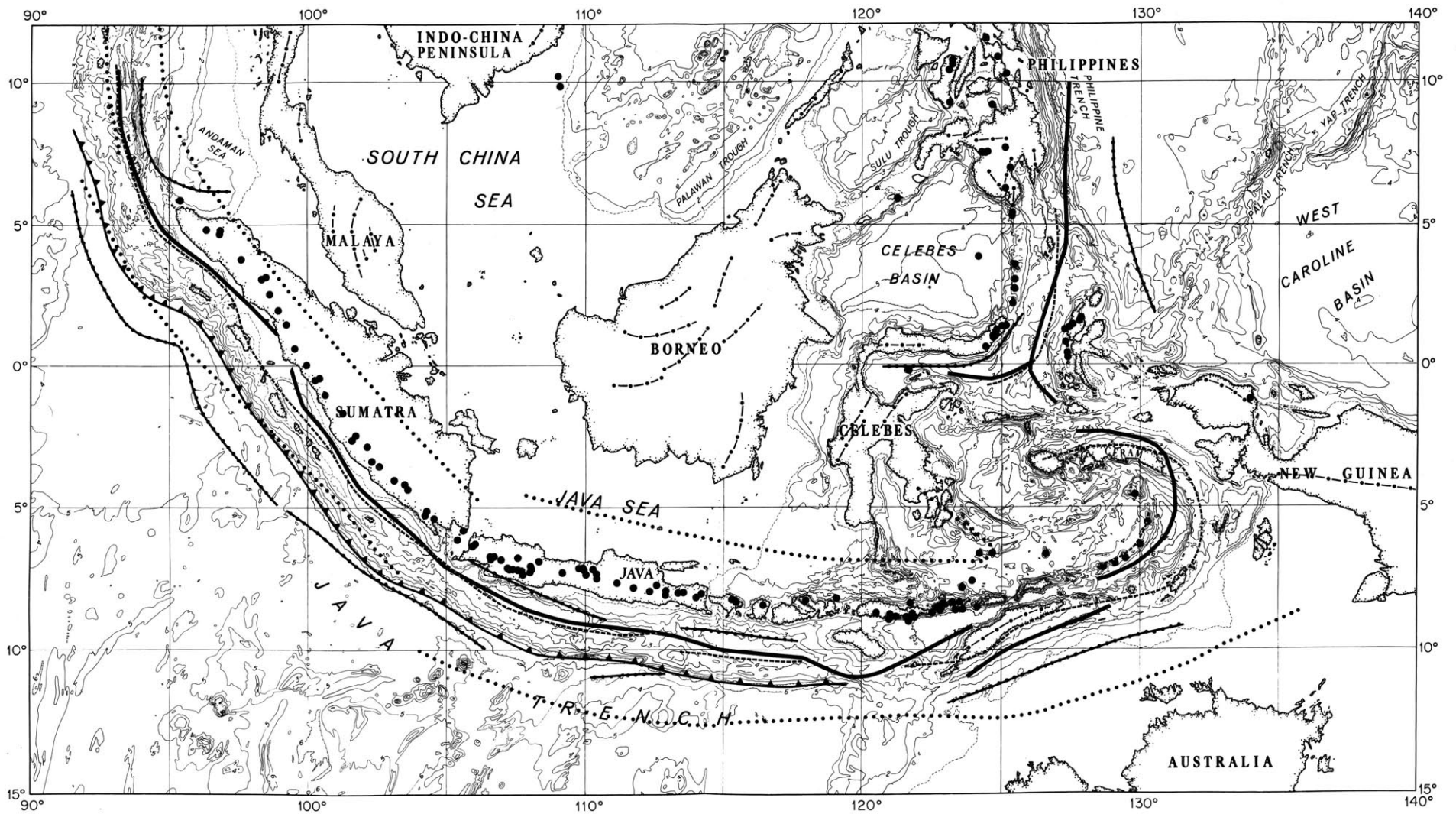
The Java Trench off Sumatra, Java and the Lesser Sunda Islands is 4000 km long. South of Java it is well defined and narrow (Fig. 1); the maximum depth is 7500 m, and the top of its seaward slope is 3000 m shoaler than the trench axis. West of Sumatra it is poorly defined and much shallower. North of the equator its western part is only slightly deeper than 5000 m and the trench axis is less than 500 m deeper than the adjacent sea floor on the south. The Java Trench does not extend beyond latitude 5°N in the Andaman Sea region.








Besides the differences in the topographic expression of the trench other changes in structures occur along the western Sunda Arc. The outer arc starts as the Andaman-Nicobar ridge in the north. It continues as the Mentawai Islands southwest of Sumatra and the submarine ridge south

of Java. The Andaman-Nicobar Islands and the Mentawai Islands contain ophiolites, radiolarian cherts and other evidence of underthrusting. Most of the Andaman-Nicobar Arc is below sea level, and there is no known evidence for the time at which the lithosphere started to descent beneath the zone now occupied by these islands. Garson and Mitchell (1970) suggested that the underthrusting beneath this zone started in late Jurassic, about the same time as the lateral displacement along faults in Malay Peninsula. The Andaman-Nicobar Ridge with its serpentinitized peridotites was uplifted in late Cretaceous time (Rodolfo, 1969), and its activity then stopped. By the late Cretaceous to early Eocene an oceanic lithosphere began to descend beneath the zone now occupied by the Mentawai Islands, resulting in volcanic activity in the Gumai and Garba ranges of southern Sumatra (the "old andesites" of van Bemmelen, 1949, p. 117). The Mentawai Islands with their ophiolite complexes were uplifted during the middle Miocene (van Bemmelen, 1949, p. 703), after which the area south of Java has been a zone of underthrusting (Audley-Charles, et al., 1972).

Gravity anomaly belts and volcanoes parallel the topography in the Indonesian Archipelago (Fig. 10). The distance between the axis of the free-air gravity minimum and

Figure 10. Gravity anomaly belts, active volcanoes, surface trace of underthrusting, approximate limits of belt of epicenters and topographic axes in the Indonesian Archipelago.



- |   |                               |  |                                 |   |                |
|---|-------------------------------|--|---------------------------------|---|----------------|
|  | FREE-AIR ANOMALY MINIMUM AXIS |  | TOPOGRAPHIC AXIS                |  | ACTIVE VOLCANO |
|  | BOUGUER ANOMALY MINIMUM AXIS  |  | SURFACE TRACE OF UNDERTHRUSTING |   |                |
|  | BOUGUER ANOMALY MAXIMUM AXIS  |  | LIMITS OF EPICENTER BELT        |   |                |

the active volcanoes decreases along the arc from southeast to northwest. Another feature shown in Figure 10 is a slight displacement of the volcanic belt on Java between Longitudes  $108^{\circ}30'E$  and  $110^{\circ}00'E$ . Discontinuities in the bathymetry (Fig. 1) and gravity (Fig. 33, below) contours over the deep sea off Java are apparent south of this displacement. A minor displacement in the volcanoes also exists in north Sumatra along Longitude  $97^{\circ}E$ .

The spatial distribution of earthquake epicenters changes dramatically along the arc (Fig. 2). The Sunda Strait (between Sumatra and Java) marks a limit for deep-focus earthquakes; to the west the activity does not extend below 200 km, but to the east events are common between 500 and 650 km. Another sharp change occurs between Sumatra and the Nicobar Islands; northwest of Sumatra no events below 70 km were recorded. Accordingly, a good correlation exists between maximum water depth and the depth of seismic activity along the Sunda Arc (Fitch, 1970).

The variations of geophysical and geological characteristics along the Sunda Arc, which are discussed in more detail by Bowin and Ben-Avraham (in preparation), suggest different kinds of tectonism along different segments of the arc. Along Java the major mode of deformation is under-

thrusting. The very active volcanoes of the island show the northward increase in potassium - silicon ratios expected from their position over a northward-dipping Benioff zone (Hatherton and Dickinson, 1969). Along Sumatra two basic modes of deformation were derived from analysis of focal mechanisms of earthquakes (Fitch, 1970, 1972; Fitch and Molnar, 1970). One is consistent with shallow underthrusting of the oceanic lithosphere beneath the arc. Earthquakes with this mechanism are shallow and concentrated between Sumatra and the non-volcanic arc. Paralleling this zone of underthrusting is the Semangko fault system in Sumatra and its submarine continuation along the eastern side of the Andaman-Nicobar Ridge. This segment is very seismic and shows evidence of a right-lateral transcurrent movement. Active or recently active andesitic volcanism in Sumatra lies directly over or very close to faults belonging to this system. Posavec, et al., (1972) pointed out that the active volcanoes lie at the intersections of these transcurrent faults and older east-west lineaments which can be seen in aeromagnetic maps; they suggested that the volcanism in Sumatra is controlled mainly by these intersections. In the Andaman Sea region most shallow seismic activity is concentrated along a submarine continuation of the Semangko

fault in Sumatra. Focal mechanism solutions (Fitch, 1972) confirmed a right-lateral motion along the fault. The major mode of deformation in the Andaman Sea is transcurrent motion along the arc and extension inside the basin, where mechanism solutions are consistent with normal faulting. Only one active volcano, the Barren Island, exists in the Andaman Sea (Rodolfo, 1969). It last erupted in 1803. All other volcanic seamounts are extinct today.

The internal deformation along the western Sunda Arc can be explained by the directions of relative motion between the Asian and Indian Ocean Plates. According to Le Pichon (1968) this direction is roughly north-northeast. Therefore, at Java the convergence of the Indian Ocean Plate is normal, along Sumatra there is an oblique convergence, and along Andaman and Nicobar Island the motion between the two plates is transcurrent.



## CHAPTER IV

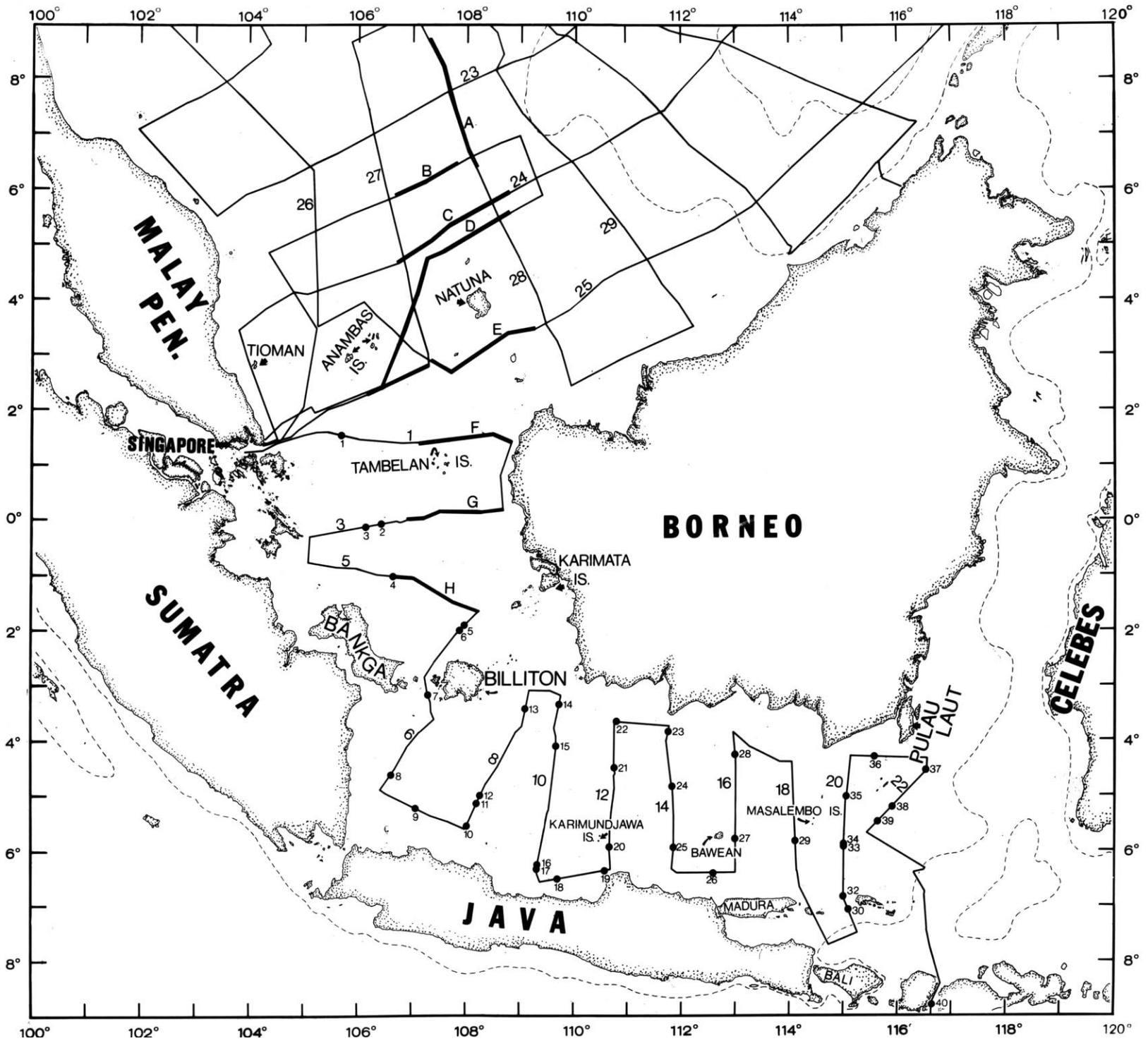
## GEOPHYSICAL STUDIES OF THE SUNDA SHELF

## SEISMIC REFRACTION, OBLIQUE REFLECTION AND STRATIGRAPHY

Introduction

Forty oblique reflection-refraction profiles made with expendable AN/SSQ41 radiosonobuoys in the Java Sea (Fig. 11) provided information on the depth to acoustic basement, the velocity of sound within it, and the velocity of sound at various depths within the overlying sediments. Because of the small depth of water (40-60 m), the sonobuoy hydrophone was very close to the bottom. This proximity to the sea-floor and the 10-second source repetition rate allowed the resolution of relatively small features in the basement and the overlying sediments and the distinguishing of relatively many strata having different velocities. Examples of sonobuoy profiles are shown and discussed in Appendix I, where the analysis technique is also described. These results are combined with previously obtained two-ship seismic refraction data from the deep sea area south and east of the Java Sea (Raitt, 1967) and from the northern Sunda Shelf (Dash, 1970, 1971) to study the relation of the shelf to the deep sea.

Figure 11. Position of traverses along with geophysical measurements. The large numbers 1-22 identify traverses that are shown in Figures 18-24; numbers 23-29 identify traverses (from Parke, et al., 1971) used to construct the three-dimensional model of Figure 28. Other lines are from Parke, et al., (1971). The small numbers indicate the positions of radiosonobuoys. Wide lines marked A-H identify positions of seismic and magnetic profiles shown in Figure 27.



## Results

Java Sea. Seven groups of refraction velocities have been identified in the Java Sea (Table 1), although the complete succession of velocities was detected in no single location. The computations show some layers to be very thin, probably the result of discontinuous sedimentation, folding, and faulting. Because the source pulse length was 50-75 ms, the minimum resolution of layer thickness is about 40 meters.

A comparison between velocity logs of some wells in the sedimentary basins of the west Java Sea with sonobuoy profiles over these basins (Fig. 12), shows a reasonable correlation. Possibly the main reason the refraction profiles do not show as many velocity discontinuities as the well logs is the existence of two limestone layers having relatively high velocities which cause velocity inversion. Such inversions cannot be detected by the seismic refraction process.

Sonobuoy refraction velocities listed in Table 1 appear as histograms in Figure 13. Velocities of the order 1.8 - 2.3 km/sec were the most frequently observed over the entire area with higher velocities tending to be confined to certain geographic locations. Refraction velocities of 2.5 - 4.2 km/sec are almost absent in the area between

Table 1. Sonobuoy Refraction Data from the Java Sea

Station	Lat.	Long.	Water Depth (m)	Velocity, km/sec									Thickness, km								
				v <sub>2</sub>	v <sub>3</sub>	v <sub>4</sub>	v <sub>5</sub>	v <sub>6</sub>	v <sub>7</sub>	v <sub>8</sub>	v <sub>9</sub>	h <sub>2</sub>	h <sub>3</sub>	h <sub>4</sub>	h <sub>5</sub>	h <sub>6</sub>	h <sub>7</sub>	h <sub>8</sub>			
1	1.56°	105.75°	62	1.60*						4.44	4.93	5.27	.09					.64	.74		
2	-0.04°	106.47°	41	1.60*	1.84					4.28		(6.57)	.04	.30				.75			
3	-0.09°	106.12°	47	1.60*	1.82					3.82		6.96	.09	.17				.86			
4	-0.99°	106.70°	35	1.60*	2.00						5.22		.05	.54							
5	-1.84°	108.04°	41	1.60*		2.28				4.87	5.71	6.87	.14		.36			.56	.46		
6	-1.98°	107.90°	38	1.60*	1.73	2.05				4.26	4.59	6.26	.15	.05	.15			.45	.37		
7	-3.13°	107.32°	54							4.70											
8	-4.57°	106.65°	21	1.60*	2.04	2.15						(5.84)	.26	.61	.13						
9	-5.20°	107.08°	24	1.60*	1.67	2.06		(3.16)		5.39	(7.07)	.09	.08	.84			.11		1.43		
10	-5.56°	108.01°	47	1.60*	1.98	2.04		(3.05)		5.08		.13	.58	.09			.21				
11	-5.12°	108.22°	41	1.60*		2.05				4.82			.29		.48						
12	-4.97°	108.28°	39	1.60*		2.19					6.47	.32		.66							
13	-3.38°	109.12°	38	1.60*	1.77	2.38				3.79	4.85		.26	.12	.20			.32			
14	-3.29°	109.75°	26	1.60*	1.76	2.14				4.36			.19	.05	.22						
15	-4.08°	109.70°	41	1.60*		2.35				4.37		(6.04)	.33		.72			1.07			
16	-6.19°	109.35°	51	1.60*	(1.99)	(2.37)							.11	.19							
17	-6.29°	109.34°	45		1.71						4.72	(5.57)		.25					2.03		
18	-6.49°	109.71°	45	1.60*	2.10					4.26			.14	.16							
19	-6.32°	110.57°	47	1.60*	1.93	2.12	2.66			(4.75)			.11	.09	.18	.27					
20	-5.93°	110.69°	49	1.60*							4.83	(5.95)	.09						.12		
21	-4.52°	110.78°	51		1.78	2.18	2.26				5.32			.19	.10	.62					
22	-3.64°	110.83°	38	1.60*	1.90		2.65	2.76	3.98	4.69			.09	.48		.16	.40	.46			
23	-3.81°	111.78°	30	1.60*	1.94		2.58		(4.35)				.19	.17		.36					
24	-4.76°	111.84°	56	1.60*					4.19	2.56 <sup>s</sup>			.11								
25	-5.95°	111.88°	66	1.60*		2.18	2.47	3.18			5.35			.23		.09	.56	1.27			
26	-6.38°	112.63°	60	1.60*	1.99	2.37	2.55		3.78				.07	.06	.17	.74					
27	-5.81°	113.02°	71	1.60*	2.03	2.17		3.26	3.59	(5.30)			.15	.08	.33		.54	.70			
28	-4.24°	113.01°	32	1.60*	1.73	1.77	2.46	2.79		4.85			.05	.16	.17	.34	.36				
29	-5.69°	114.13°	66	1.60*	1.66	2.14	2.53	3.03	(4.12)				.10	.06	.31	.33					
30	-7.00°	115.08°	105	1.60*		2.19			3.90				.10		.41						
32	-6.82°	115.02°	73		2.14	2.45	2.88	3.12	3.29					.17	.06	.09	.37				
33	-5.99°	115.01°	50	1.60*	1.95	2.26				(5.40)			.04	.14	1.4						
34	-5.88°	115.03°	53	1.60*	1.89	2.36							.05	.29							
35	-4.99°	115.07°	30	1.60*					3.64				.12								
36	-4.27°	115.57°	24	1.60*					3.44	4.73	(6.29)		.02					.69	.26		
37	-4.54°	116.56°	58		2.03	2.41								.25							
38	-5.20°	115.92°	62	1.60*	2.08	2.40			(4.10)				.15	.25	.66						
39	-5.44°	115.69°	58	1.60*	2.06			3.05	3.69				.13	.30			.52				
40	-8.70°	116.67°	84	1.60*			2.82						.15								
Average					1.90	2.21	2.59	3.04	4.09	5.02	6.27										
Standard deviations					.14	.16	.17	.17	.43	.33	.56										

\* assumed velocities.

( ) indicate doubtful refraction velocities.

<sup>s</sup> Shear wave velocity.

Figure 12. An average velocity and lithology log from some wells in the Java Sea basins. Also shown in dashed-line is an average result of the sonobuoys over sedimentary basins (sonobuoys 8, 9, 10, 15, 21, 22, 26, 29).

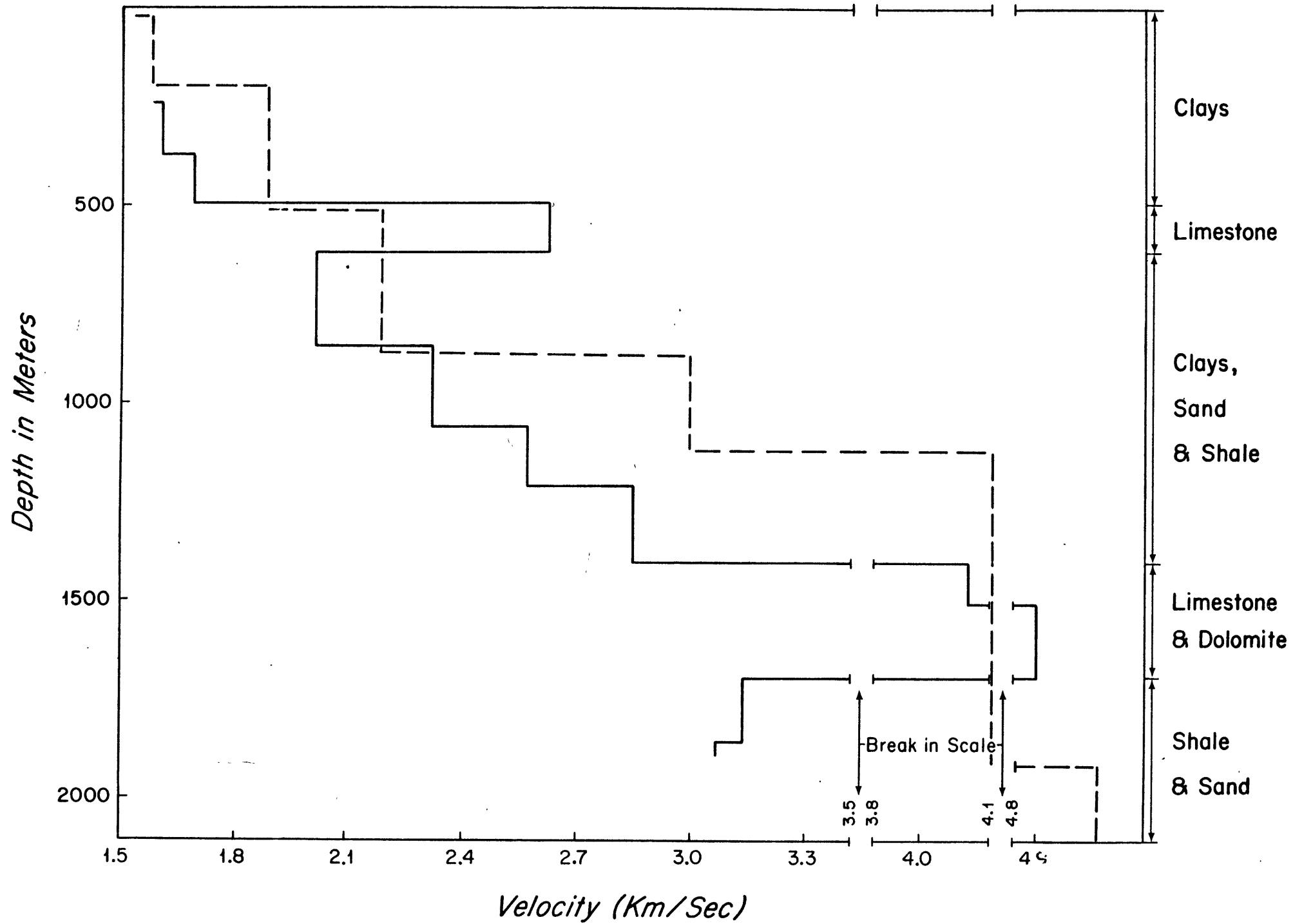
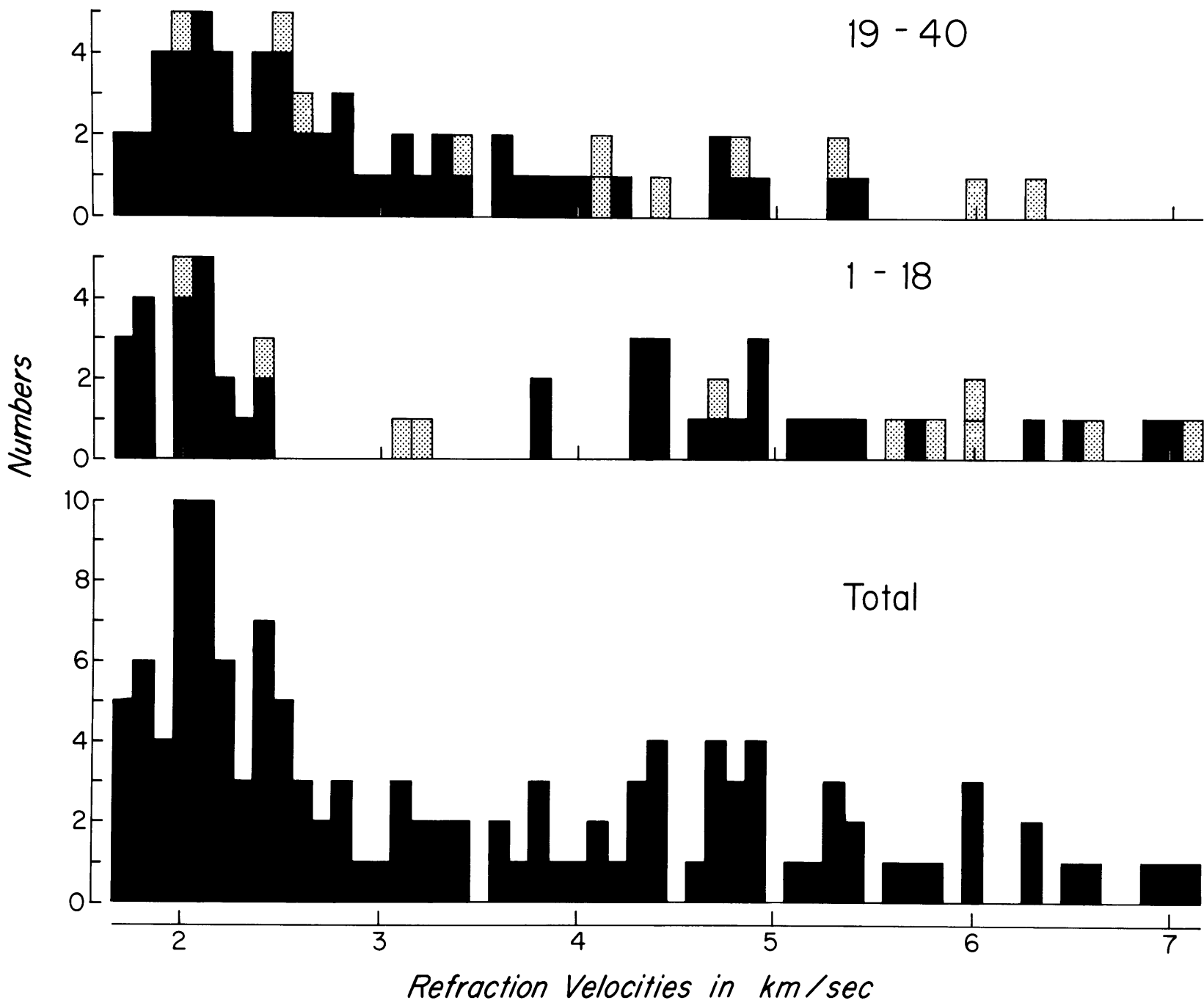


Figure 13. Histograms of sonobuoy refraction data from the Java Sea. The stippled entries represent velocities of doubtful accuracy. Top: eastern Java Sea (sonobuoys 19-40); Middle; west and north Java Sea (sonobuoys 1-18); Bottom: the entire Java Sea.





Sumatra and Borneo (Fig. 13) but they appear in the eastern Java Sea between Borneo and Java. On the other hand, velocities higher than 5 km/sec appear rarely in the eastern Java Sea, but they are more common in the north, between Borneo and Sumatra. The regional limits probably are due to the difference both in basement type and in the material of the sedimentary columns of the two areas.

The acoustic basement can be represented by  $V_7$ ,  $V_8$  or  $V_9$  (Table 1) depending on the area. The average refraction velocity of  $V_9$ , which is confined almost entirely to the area between Borneo and Sumatra, is 6.27 km/sec with a standard deviation of 0.56. According to Birch (1960) these velocities for rocks at pressure of 500 bars (appropriate to the depth of  $V_9$ ) are typical of a wide variety of igneous and metamorphic rock types; however, the highest velocities (as in sonobuoys 3 and 5) are most likely to be from basic, ultrabasic and metamorphic rocks rather than from granitic rocks.  $V_8$ , which averages 5.02 km/sec, probably is also characteristic of several rock types but is mainly representative of granite and a lower Miocene limestone and dolomite. Sonobuoy 7, between the two granitic islands of Bangka and Billiton, recorded a very prominent refraction arrival from the shallow basement. It has

a velocity of 4.70 km/sec (Appendix I), which should represent the granitic basement. This velocity is slightly lower than a typical velocity for granites. Similarly, sonobuoy 20, over the Karimundjawa Arch which is probably a granitic body (see page 180) has a basement velocity of 4.83 km/sec. In this station, however, the granite may have a velocity as high as 5.95 km/sec (Appendix I, Fig. 49). In the deep sedimentary basins  $V_8$  can belong to a lower Miocene limestone, the Batu Radja limestone (Todd and Pulunggono (1971)) in the western Java Sea, and to the upper Kudjung limestone (Cree, 1972) farther east. The average velocity value of the refraction arrivals from what appears on the normal incidence records to be the lower Miocene limestone is in good agreement with the velocities measured in wells for this horizon (Fig. 12).  $V_7$  with an average value of 4.09 km/sec, also is from the lower Miocene limestone. Figure 12 shows that two distinct units having velocities of 4.90 and 4.06 km/sec, respectively, belong to the lower Miocene limestone. It seems that  $V_7$  corresponds mainly to the lower velocity in this limestone.

$V_6$  and  $V_5$  refraction velocities of 3.04 and 2.59 km/sec respectively are observed mainly in the eastern Java Sea, whereas they are almost absent from its western and northern portion (Fig. 13, Table 1). These velocities may be due

to sedimentary layers that are either very thin or absent in the western and northern areas. The published stratigraphic sections from portions of the Java Sea (Todd and Pulunggono, 1971; Cree, 1972) suggest that  $V_6$  and  $V_5$  can be assigned to a series of shallow water glauconitic sands and clays of lower Miocene age.  $V_4$ ,  $V_3$  and  $V_2$  are abundant throughout the Java Sea and belong to sediments of Mio-Pliocene and Plio-Pleistocene age.

Northern Sunda Shelf. The preliminary results of some two-ship seismic refraction studies using explosives made by the Imperial College of London with the cooperation of various countries in the region (Dash, 1970, 1971, and Dash, et al., 1970) are summarized in Table 2. These profiles do not have the resolution of the sonobuoy profiles, but they give the gross structure of the crust in the northern Sunda Shelf. Three profiles around Natuna Island penetrated to the mantle at a depth of about 20 km. Comparison of the crustal structure of the northern Sunda Shelf with typical oceanic and continental structures shows it to be intermediate (Fig. 14). In fact, the crustal thickness there resembles that of some of the smaller ocean basins, such as the Gulf of Mexico (Ewing, et al., 1960) and the Columbia Basin in the Caribbean Sea. The main difference is in the

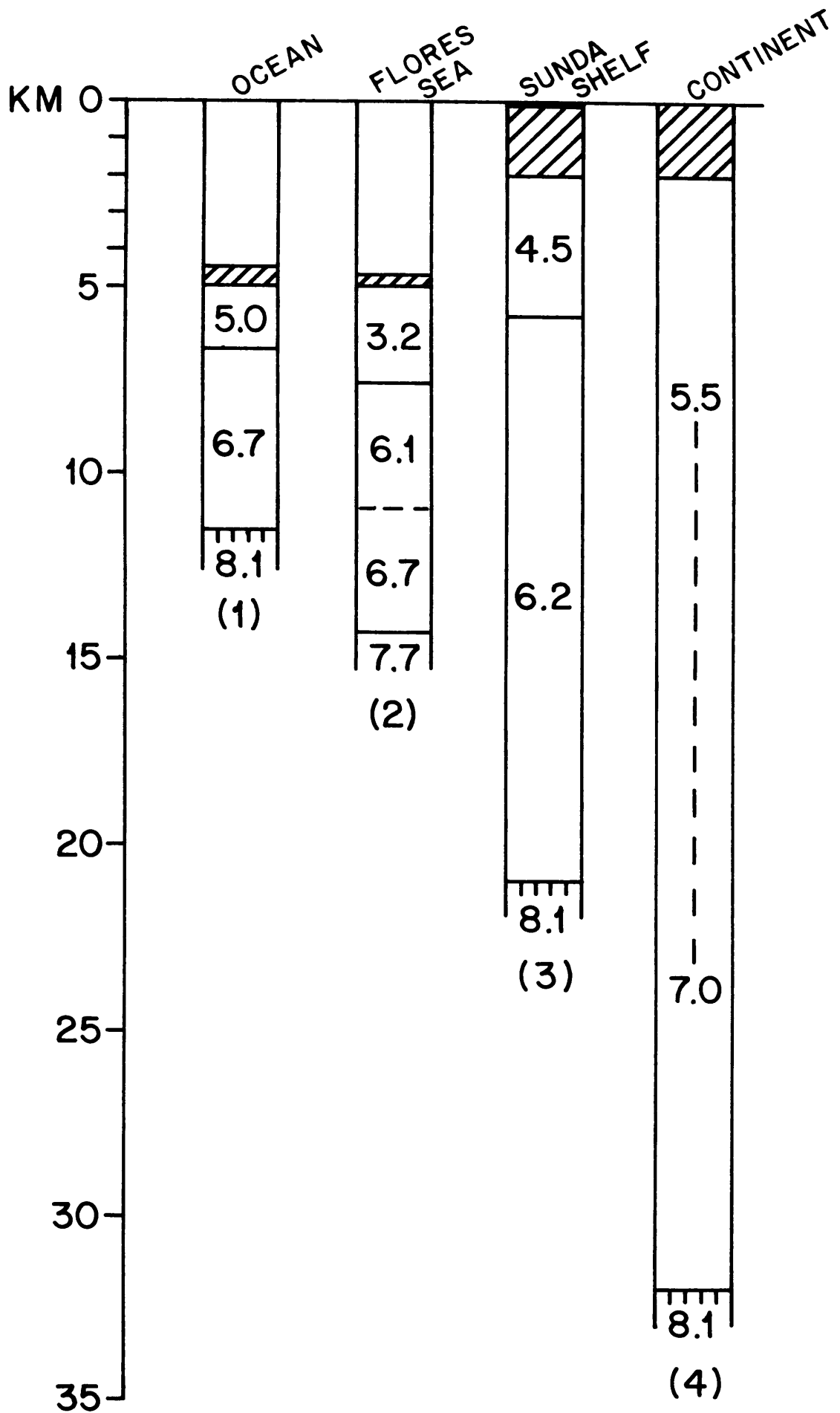
Table 2. Location of stations, seismic velocities and thicknesses of layers in the northern Sunda Shelf

Station	Lat. N	Long. E	Water Depth (m)	Velocity, km/sec					Thickness, km				Depth to Mantle (km)	
				V <sub>1</sub>	V <sub>2</sub>	V <sub>3</sub>	V <sub>4</sub>	V <sub>5</sub>	h <sub>1</sub>	h <sub>2</sub>	h <sub>3</sub>	h <sub>4</sub>		
Natuna 1	4.00°	108.42°*		3.0**	4.2					1.4				
Natuna 2	3.50°	108.60°	100	3.0	4.5		6.0	8.1	2.6	3.2		15.2	21	
Natuna 3	2.80°	109.10°			4.5		6.5			5.0				
Natuna 4	3.05°	108.25°	80	3.0	4.7		6.2	7.9					23.5	
Natuna 5	3.05°	109.50°	60	3.5	4.7		6.2	8.3					19.5	
Tioman 1	2.60°	104.50°	50	2.1	3.4		6.8		1.3	5.6				
Tioman 2	2.50°	104.20°	50	1.6	5.1				.02					
Vietnam 1	9.35°	103.62°	40	3.1	4.8	5.7	6.7		1.4	2.1	4.3			
Vietnam 2	9.15°	103.25°	40	3.1	4.8	5.7	6.7		.8	2.4	8.8			
Vietnam 3	9.00°	103.47	40	3.1	4.5	5.5	6.2		1.1	1.9	4.5			
Vietnam 4	9.42°	103.42°	40	3.1	4.5	5.5	6.2		.8	2.3	3.3			

\* All the locations are inaccurate.

\*\* All the data are from preliminary reports (Dash, 1970, 1971, and Dash, et al., 1970) and should be considered as such.

Figure 14. Comparison of velocity structure of the northern Sunda Shelf with those of continents and ocean basins. (1) Raitt, 1963; (2) Raitt, 1967; (3) Dash, 1971; (4) Edgar, et al., 1971.

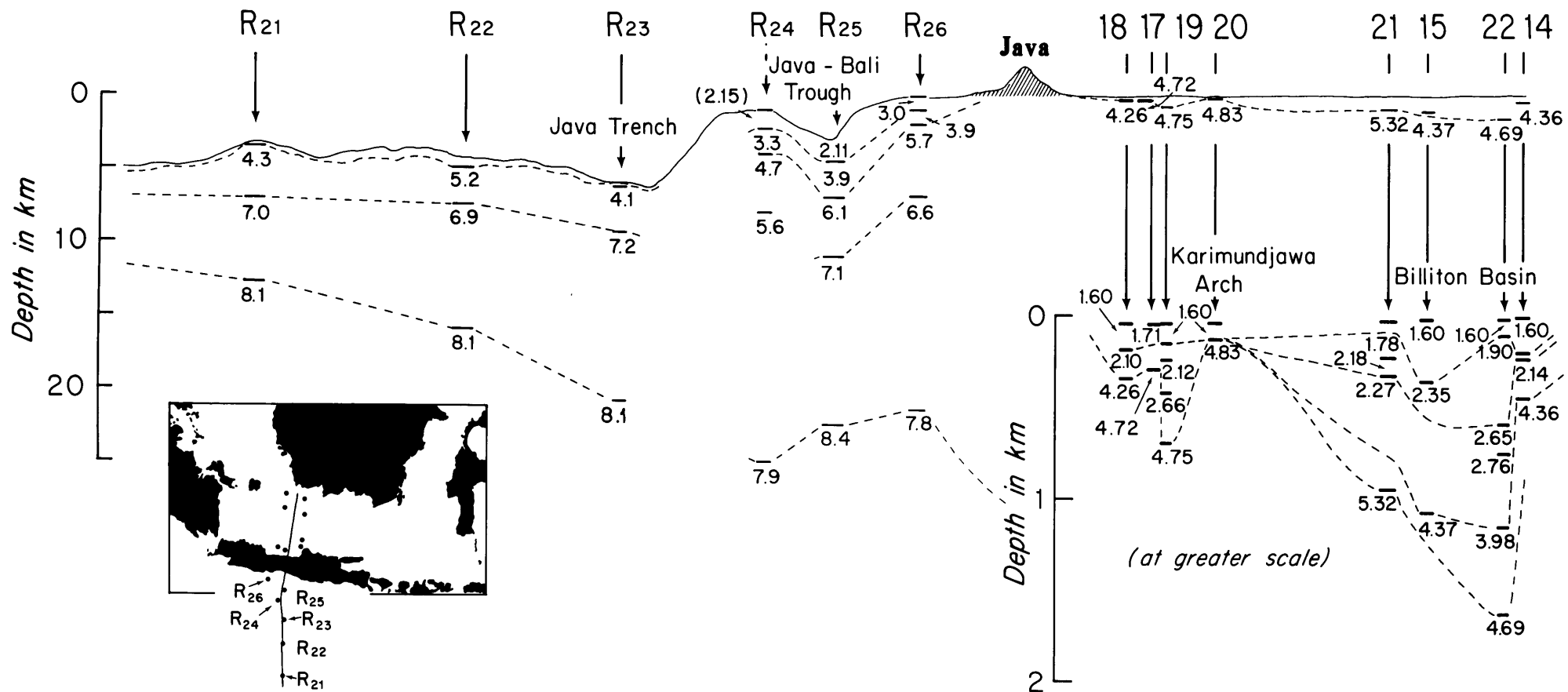


water depth, which is a few tens of meters on the shelf and several km in these ocean basins. The crustal structure in most marginal basins is closely related to that of the adjacent main ocean basin, except for the comparatively greater thickness of low-velocity sediments in the former. As Menard (1967) has pointed out, the essential characteristic of a normal oceanic crust is that it includes Layer 3 material with a velocity near 6.7 km/sec and a thickness of about 5 km. If this layer is so represented, the velocity and/or thickness of other layers would be considered modifications of an otherwise normal oceanic crust. Dash (Table 2) showed that crustal velocities of 6.7 and 6.8 km/sec occur in some profiles, whereas others have a lower value of about 6.2 km/sec. Since these are preliminary results, the crustal layer thickness is given only for one profile where a layer with 6.2 km/sec velocity is 15 km thick (Fig. 14). As a whole, Dash's data indicates the crustal structure to have characteristics intermediate between continental and oceanic crust: These data, however, are not sufficient to determine whether this crust originated as continental or oceanic crust.



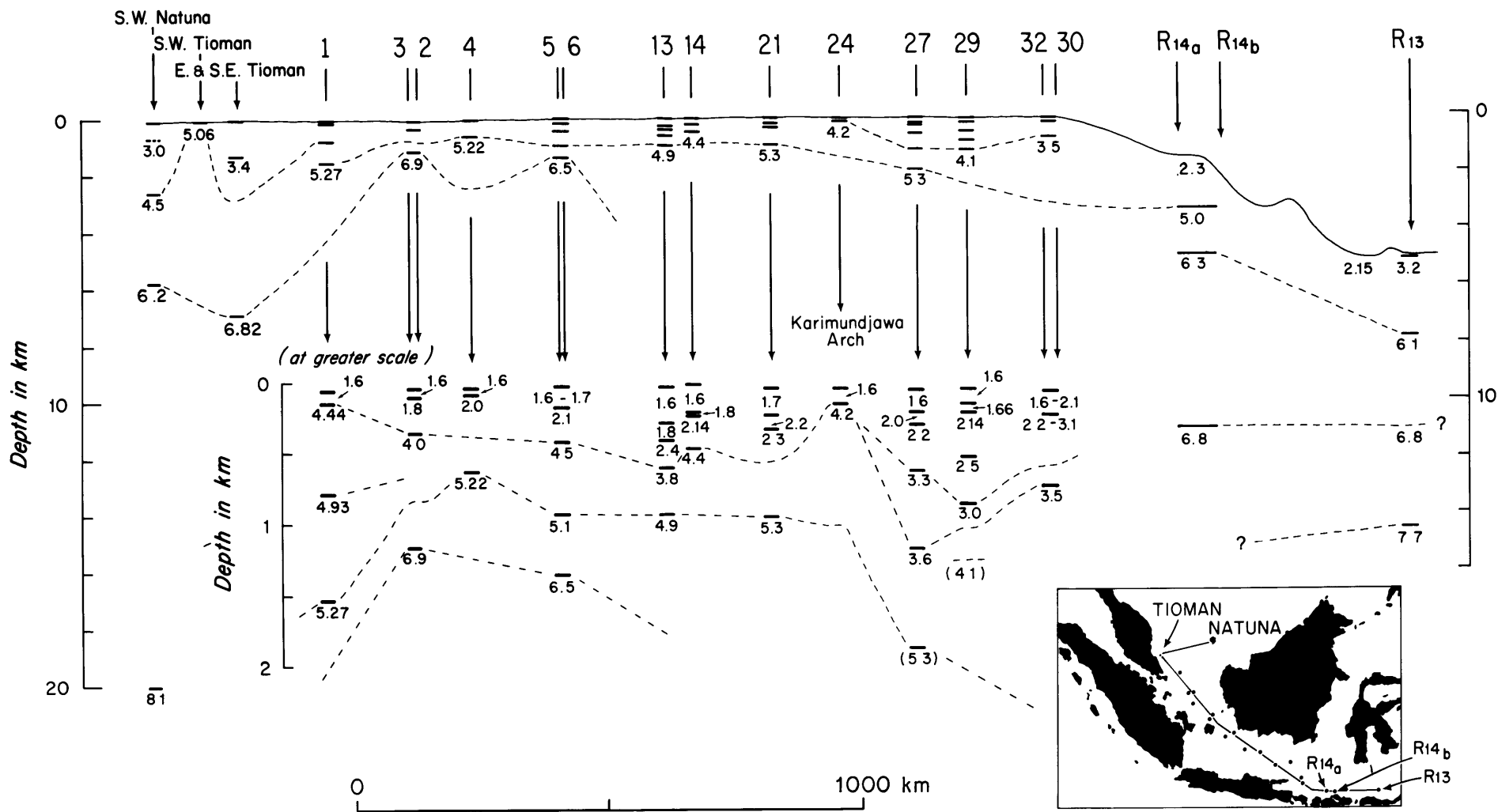
Velocity Cross Sections. Two structural sections based on seismic refraction information are shown in Figures 15 (north-south) and 16 (northwest-southeast). The data in the deep sea are from Raitt (1967) and on the shelf from the sonobuoy profiles and Dash (1971). The section of Figure 15 is normal to four "ridges"; one south of the trench, one separating the Java Trough from the Java Trench, Java Island, and the Karimundjawa Arch. In the oceanic section south of Java the two most conspicuous features are that the crust north of the Java Trench is much thicker than the crust south of it. North of the Java Trench the thickness of the unconsolidated and the semi-consolidated sediments is much greater than south of the trench. Secondly, the oceanic crustal layer, Layer 3 (with velocity 6.9 - 7.2 km/sec) extends across the trench to within 50 km of Java and seems to continue beneath the island of Java (Raitt, 1967). North of the island the sonobuoy information is limited to the upper crustal structure, to the lower Miocene limestone in the basins and to the postulated granitic layer over the Karimundjawa Arch. The section clearly demonstrates the differences in penetration capability and in resolution of two-ship refraction and sonobuoy techniques. While the latter can give detailed information

Figure 15. Seismic structure section across the Java Sea, Java Trough, Java Trench and the northern Wharton Basin. Dots represent sonobuoy stations and dots marked with R represent two-ship refraction stations from an unpublished report by Raitt (1967). The sonobuoy results are shown also at greater (expanded) scale.



0 500 km

Figure 16. Seismic structure section from the Flores Sea across the Java Sea to Tioman and Natuna islands. Symbols the same as in Figure 15. The stations at Tioman and Natuna islands are from Dash (1971).



of the sedimentary column, the former essentially averages the structure over the range of the profile and is necessarily insensitive to detailed structures; it does, however, penetrate much deeper.

The structural section from the Flores Sea along the Sunda Shelf to Natuna Island is shown in Figure 16. From a normal oceanic section in the Flores Sea (Station R<sub>13</sub>) the crustal thickness appears to increase rapidly westward on the evidence of the two-ship profiles (the sonobuoy data simply indicate uniformity of the upper crustal thickness). The structural transition from the oceanic basin to the shelf is unclear. In the Natuna Island area, the mantle is at a depth of 20 km. The main crustal layer in the Natuna area has a velocity of 6.2 km/sec and near Tioman Island a velocity of 6.8 km/sec, which is similar to that of Layer 3.

## SEISMIC REFLECTION OVER THE JAVA SEA

### Introduction

The seismic profiler system used in the Java Sea was a more sophisticated version of the system described by Knott and Bunce (1968). Two different sound sources were operated separately and together (fired simultaneously) at various

times during the cruise; one, an underwater spark discharging 85,000 to 95,000 joules of stored energy, the other an air gun of 40, 120, or 300 in<sup>3</sup> charged to 1,800 psi. The seismic signals were received on two 30-m linear arrays. The signals from the arrays were band-pass filtered between 20 and 50 Hz and recorded on three Precision Graphic Recorders operative at 5 and 2.5 second sweep rates. In addition, about two-thirds of the traverses were recorded unfiltered on magnetic tapes.

The analog profiles over the shelf are very noisy, therefore the normal incidence reflection data were processed at the laboratory by a simple spatial filter. The analog magnetic tape recordings were filtered at 18 3/4 - 250 Hz band-pass and digitized using the shot instant of each successive outgoing pulse to start a 10-bit digitizer driven by a stable 512 Hz oscillator. A running summation of four shots was made and displayed on an incremental x-y-z plotter. An average of four gave about a two-fold reduction in random background noise while adding the horizontally coherent returns. Sloping layers with dip up to 3° were added with less than 3 dB attenuation due to phase shift (at 30 Hz signal center frequency). These processed data were used to edit the shipboard interpretation and proved most useful

for detecting the basement and removing noise (Fig. 17).

### Results

The seismic profiles (Figs. 18-24) show that the Java Sea can be divided into the Singapore Platform (or Sunda Shield) in the northwest, and the basins and ridges in the south and east (Fig. 38).

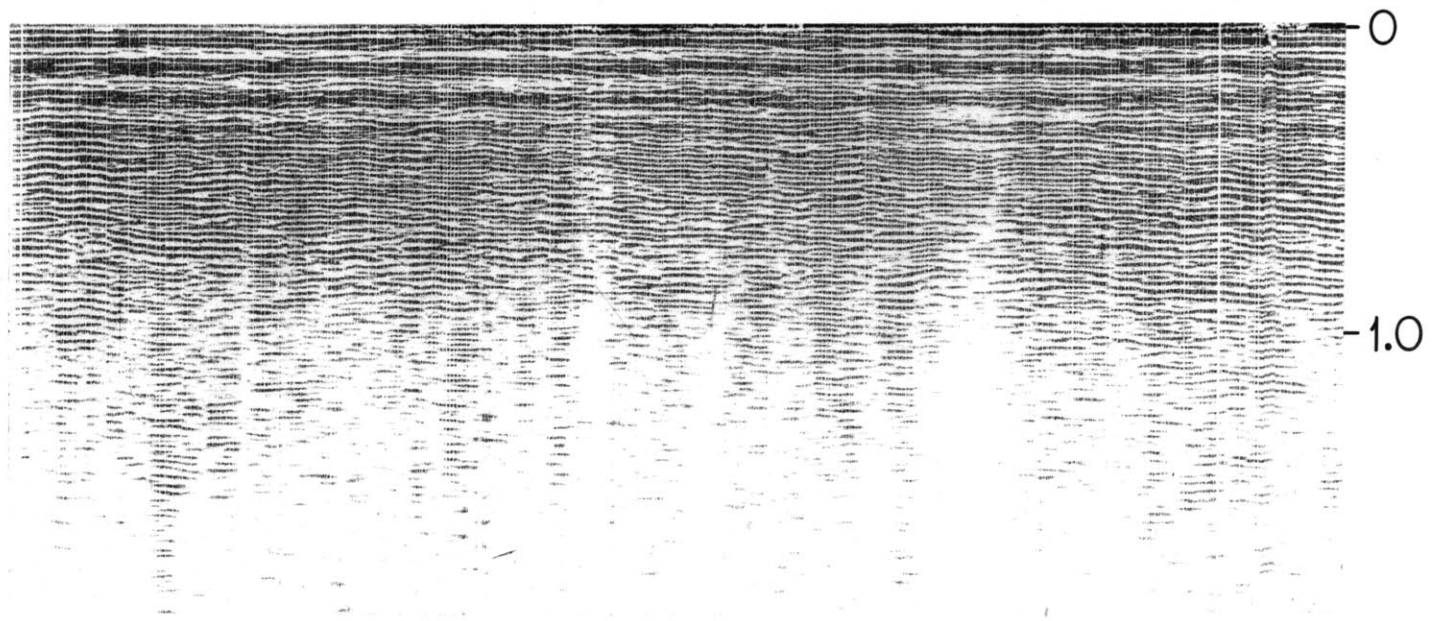
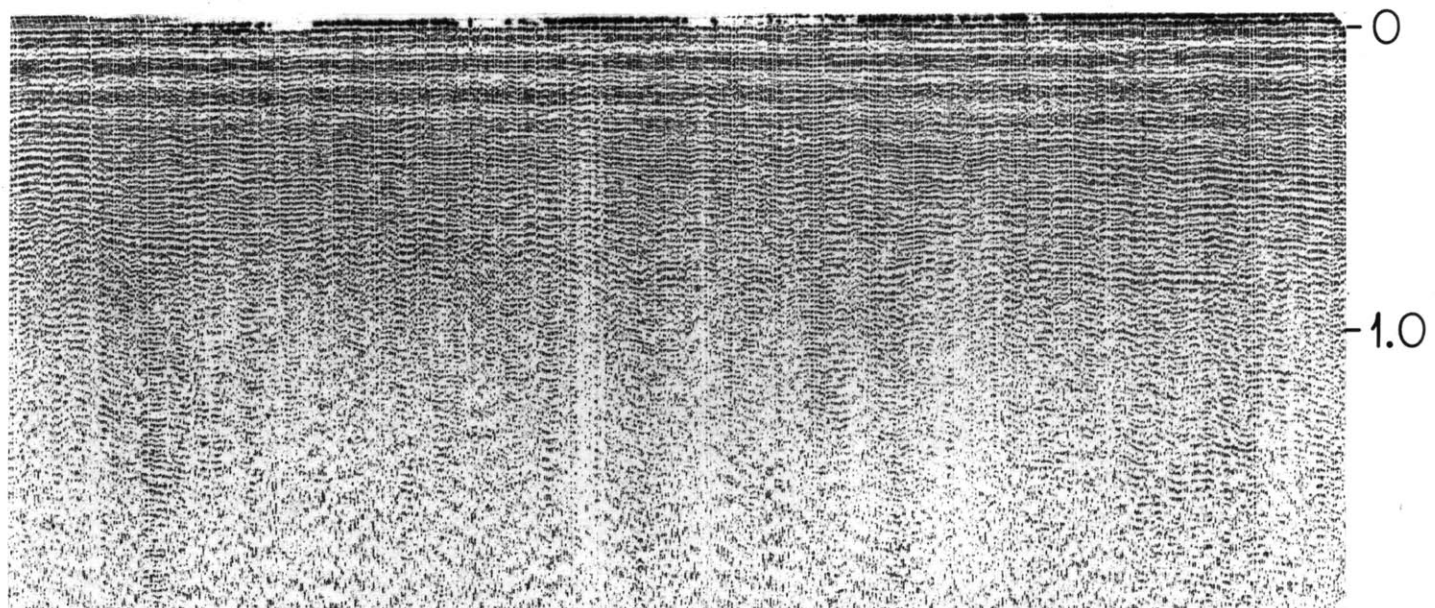
The Singapore platform has shallow basement and is overlain by a thin sedimentary cover (Fig. 18). The basement appears to consist of small "bodies". Sonobuoy 1 (Fig. 18) indicates that as much as 1.5 km of sediments can be present between the basement "bodies"; however, the basement could be continuous and composed of a rough surface (as shown by the preliminary interpretation aboard ship - Emery, et al., 1972). The line spacing of the profiles is not close enough to determine whether the basement "bodies" are equidimensional in plane or elongated. Two troughs containing more than 800 m of sediments are the most prominent features in this area; the Bangka Depression which strikes northwest-southeast parallel to the coast of Sumatra (Fig. 38, below) and the Billiton Depression (Figs. 18, 25) which runs north-south parallel to the west coast of Borneo.

South of the islands of Bangka and Billiton, in the western Java Sea, several deep basins with sediments



Figure 17. Analog (top) and processed (bottom) reflection profile from the Billiton Basin, profile 10 (Fig. 20). The method of processing is described in the text. Note that the apparent acoustic basement on the analog profile proved to be a sedimentary layer.

Reflection Time (Sec.)

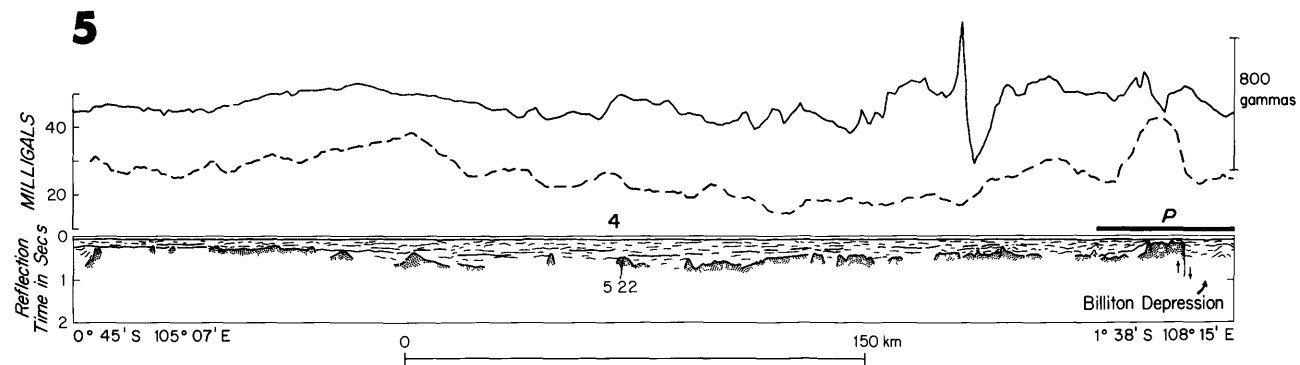
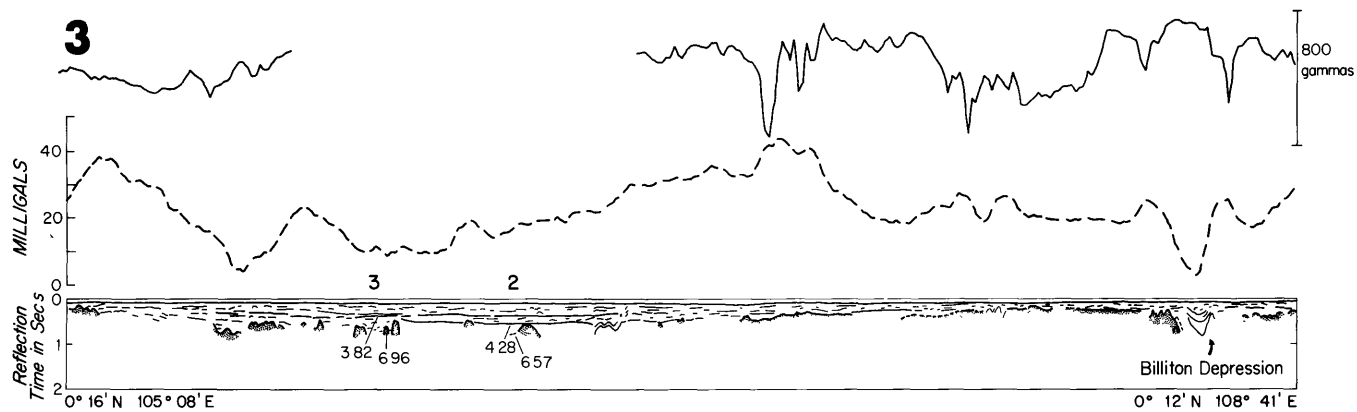
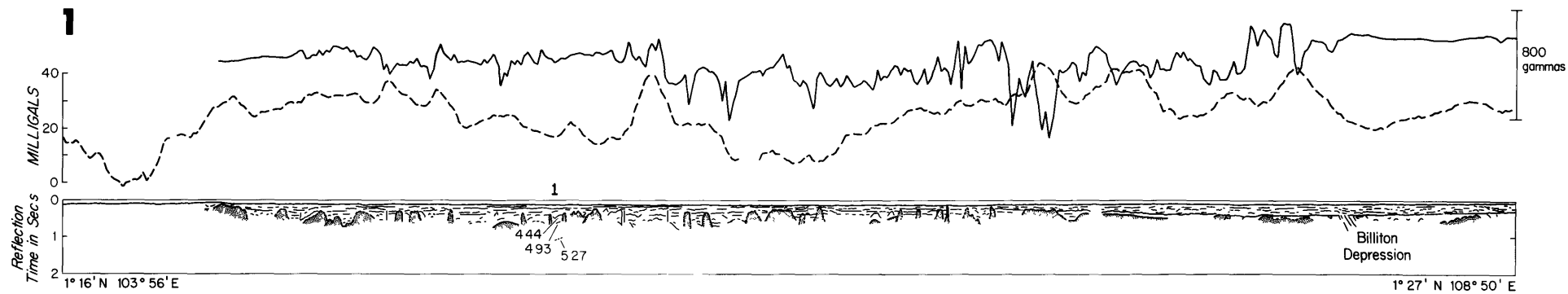


0 |-----| 120  
Km

Figure 18. Interpretative seismic magnetic and gravity profiles 1, 3, and 5 across the Singapore Platform between Singapore and Billiton Island.

Top: Total intensity magnetic anomaly (continuous line) and free-air gravity anomaly (dashed line). Gamma scale on right shows relative amplitude of magnetic anomalies; free-air gravity scale on left.

Bottom: Line-drawing interpretation of continuous seismic reflection records. Fine dotted pattern designates acoustic basement where we believe it to be igneous or metamorphic rock. Prominent reflectors are marked by wide lines. The velocities in km/sec derived from the radiosonobuoy stations are shown. Horizontal bar and P designate part of original recording for profile 5 reproduced in Figure 25.



exceeding 1 km in thickness can be recognized (Figs. 19 and 20): South Sumatra (on land), Sunda, West Java (partly on land), Billiton and Tjeribon (partly on land) (nomenclature after Todd and Pulunggono, 1971). The land basins have previously been described by Umbgrove (1938) as short lived marginal basins filled with a thick series of sediments that are weakly folded. Umbgrove named them "Idiogeosynclines". The basins are separated by high areas, the Lampung High (on land), the Seribu Platform and the Karimundjawa Arch. The Seribu Platform (profile 7) and part of the Karimundjawa Arch (profile 14) appear as fault blocks on the reflection profiler records.

Detailed seismic coverage of the area between Java, Sumatra, Bangka, Billiton and the Karimundjawa Arch (Todd and Pulunggono, 1971) shows that deep north-south faults separate the basins from the uplifts. The straight north-south coast of Sumatra between Bangka and Java, which strikes at  $45^\circ$  to the lineation of the island itself, may mark the position of a major fault which separates the Lampung High from the Sunda Basin. This area has been extensively drilled (Humphrey, 1971). Todd and Pulunggono (1971) presented some drill logs and cross sections that show the

Figure 19. Interpretive geophysical profiles 6, 7, and 8 across western Java Sea. L designates the Batu Radja, a lower Miocene limestone. The basement configuration on the left of profile 6 and in profile 7 was inferred from cross sections reported by Todd and Pulunggono (1971) and gravity anomalies. Other symbols are the same as for Figure 18.

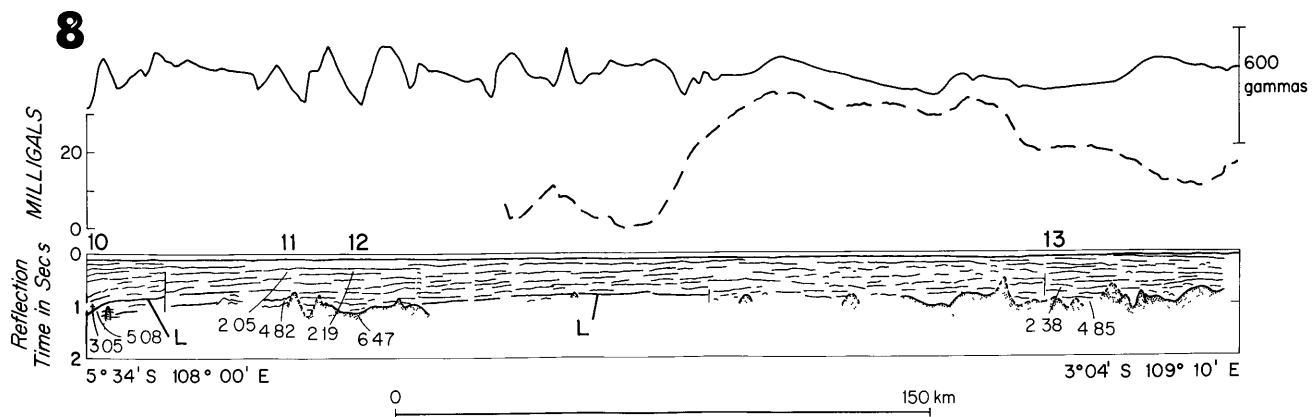
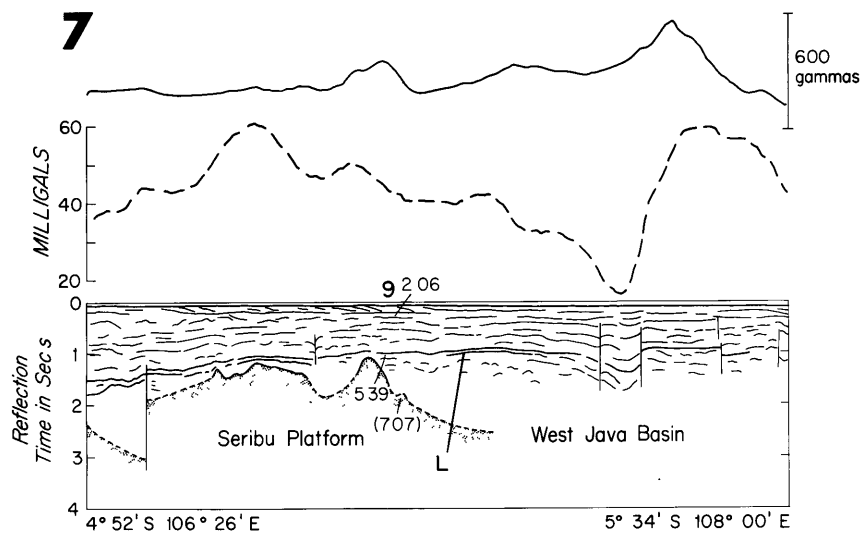
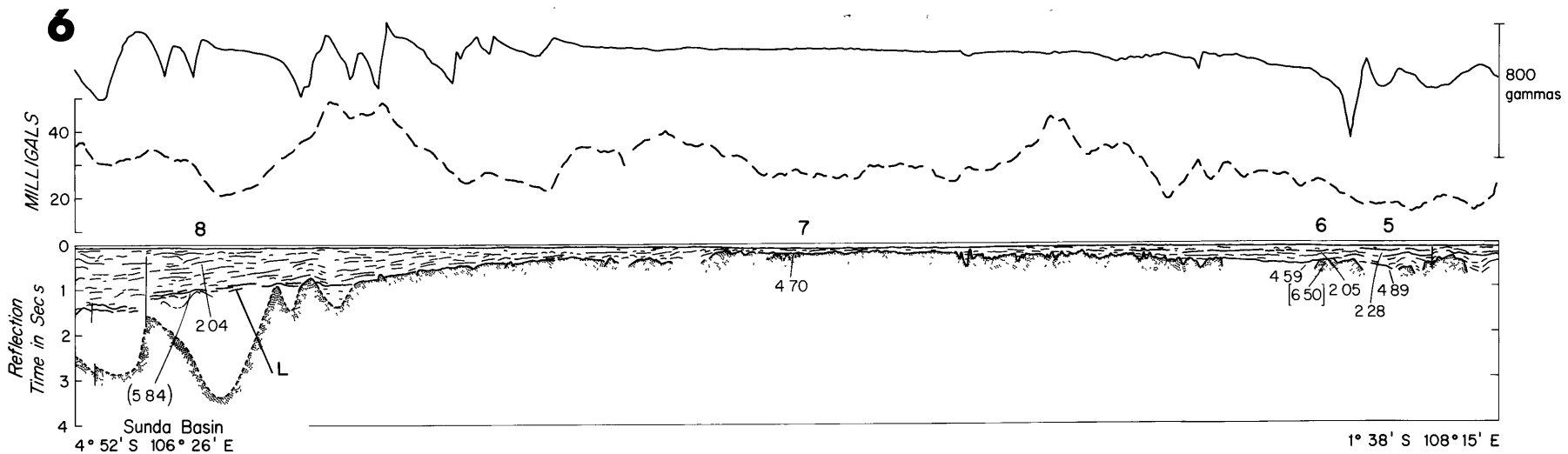
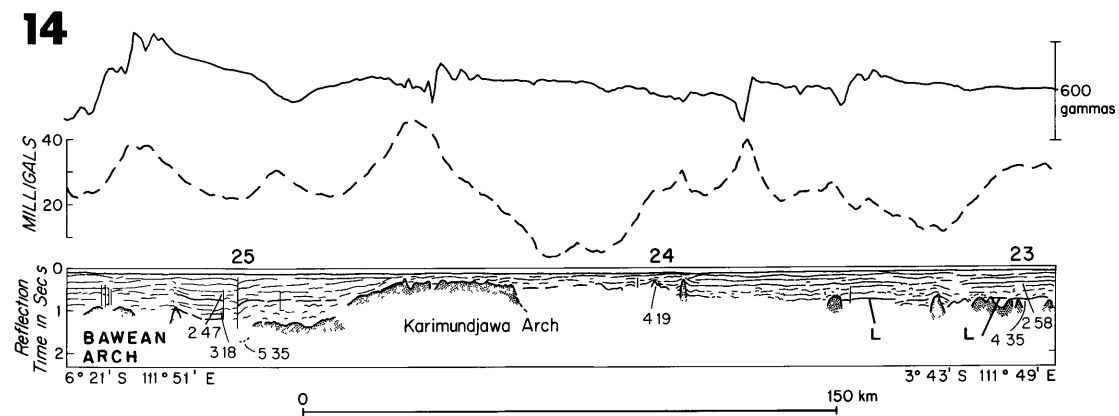
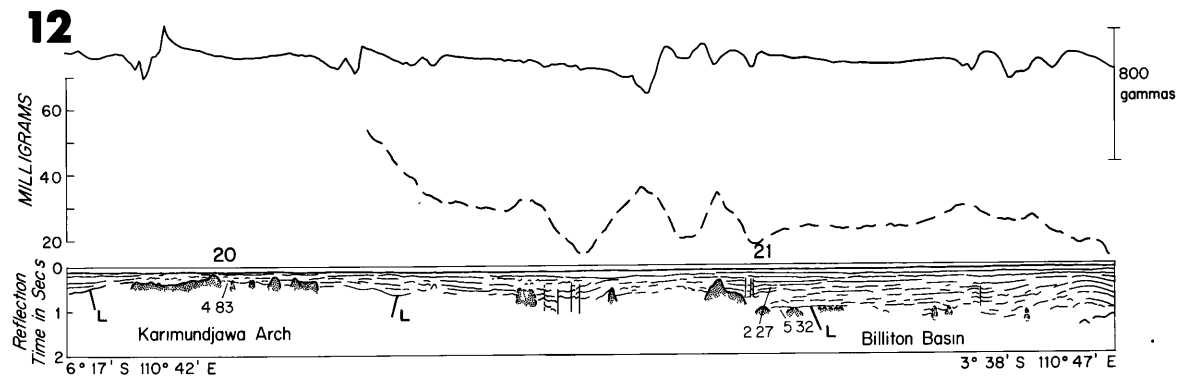
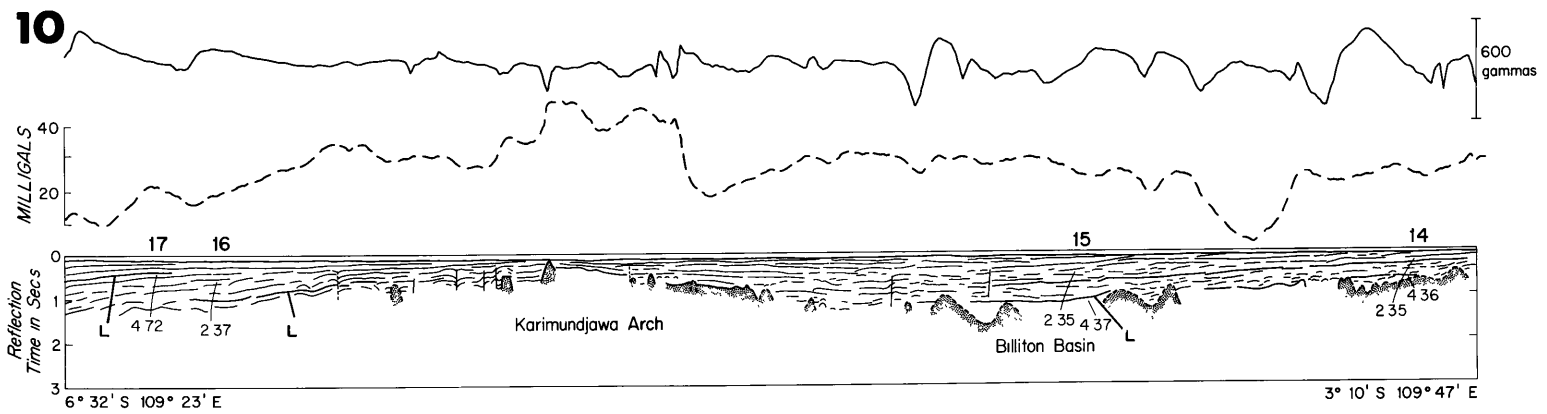


Figure 20. Interpretive geophysical profiles 10, 12, and 14 across the western and central Java Sea. Symbols are the same as for Figure 19.





metamorphic and igneous basement to be more than 3 km deep in the Sunda Basin and about 2.5 km deep in the West Java Basin. An important feature shown by the seismic profiles is a group of strong discrete reflectors that can be traced throughout most of the basins. This group is identified as the Batu-Radja, a lower Miocene reefoid limestone plus thin dolomite (Todd and Pulunggono, 1971). The group is known on south Sumatra and west Java (van Bemmelen, 1949, p. 116). Its average velocity determined by the sonobuoy profiles is 5.0 km/sec (Fig. 12). The importance of this horizon is its widespread distribution in the Java Sea and its value as a time marker, as it seems to be continuous through the various basins (Fig. 13) and over some of the highs. Note how this layer covers the Seribu Platform (Fig. 19, profile 7) and partly covers the Karimundjawa Arch (Fig. 20, profiles 10, 12). In large portions of the sedimentary basins this lower Miocene limestone is the acoustic basement (Figs. 19, 20). At the southern end of profile 6 (Fig. 19) drill hole data (Todd and Pulunggono, 1971) indicate the true basement to be more than 3 km deep, about double the penetration of the seismic profile.

A few other prominent reflectors are visible above the Batu Radja limestone in the sedimentary basins (e.g. on the

right hand side of profile 10, in the Billiton Basin) and over the Singapore Platform (e.g. at the Billiton Depression in profile 1). These reflectors are usually limited in area, and they cannot be correlated from one profile to another. They may represent different lithologies or changes in physical properties of the sediments.

Since basin fill-material above the lower Miocene limestone in general dips away from the high areas, the Singapore Platform, the Lampung High and the Karimundjawa Arch (Figs. 19, 20) these uplifts probably served in the past as sources of the sediments. Locally some of the strata dip in one direction and other strata in the same section dip in another direction. This can be seen in profile 7 (Fig. 19) where the Batu-Radja formation dips away from the Seribu Platform to east and west. In the upper part of the section the layers dip westward away from the Karimundjawa Arch, and at the very top the layers have strong eastward dip away from the Lampung High. This may indicate that some movements occurred along the faults bordering the highs during various periods of the basins' evolution. On the south side of the Karimundjawa Arch in profile 14 the relatively steep dips indicate continuous uplift during the period of basin filling. Many structural discontinuities such as small folds, faults

and angular unconformities exist in the basin fill. Except for the Batu Radja limestone, a single reflecting horizon can be followed for only a short distance.

In the eastern Java Sea (Figs. 21-24) basins and ridge-like features also exist, but their characteristics, dimension and orientations differ from those in the western Java Sea. Five dominant uplifts are: the Meratus and Pulau Laut ridges, which extend from the Meratus Mountains on Borneo and the Pulau Laut Island southwestward into the Java Sea; the Karimundjawa Arch, which extends eastward and northeastward from the western Java Sea into its eastern portion; the Bawean Arch; and the Madura Ridge, which extends eastward from Madura Island to Kangean Island and the Flores Sea. Except for the Madura Ridge which strikes east-west all the ridges strike northeast-southwest. The Karimundjawa Arch is transitional, as it strikes generally east-west in the western Java Sea but bends to the northeast in the eastern Java Sea. All of these uplifts are relatively long and narrow and look (except for the Karimundjawa Arch) like anticlines. The seismic profiles (Figs. 21, 22) clearly demonstrate that these structures are plunging; the Meratus, Pulau Laut and probably also the Bawean ridges plunge to the southwest and the Madura Ridge to the east. The Pulau Laut

Figure 21. Interpretive geophysical profiles 16, 17, and 18 across the central and eastern Java Sea. Fine dashed line shows the Bouguer gravity anomaly. Horizontal bar with P designate part of original recording for profile 18 reproduced in Figure 25. Other symbols are the same as for Figure 19.

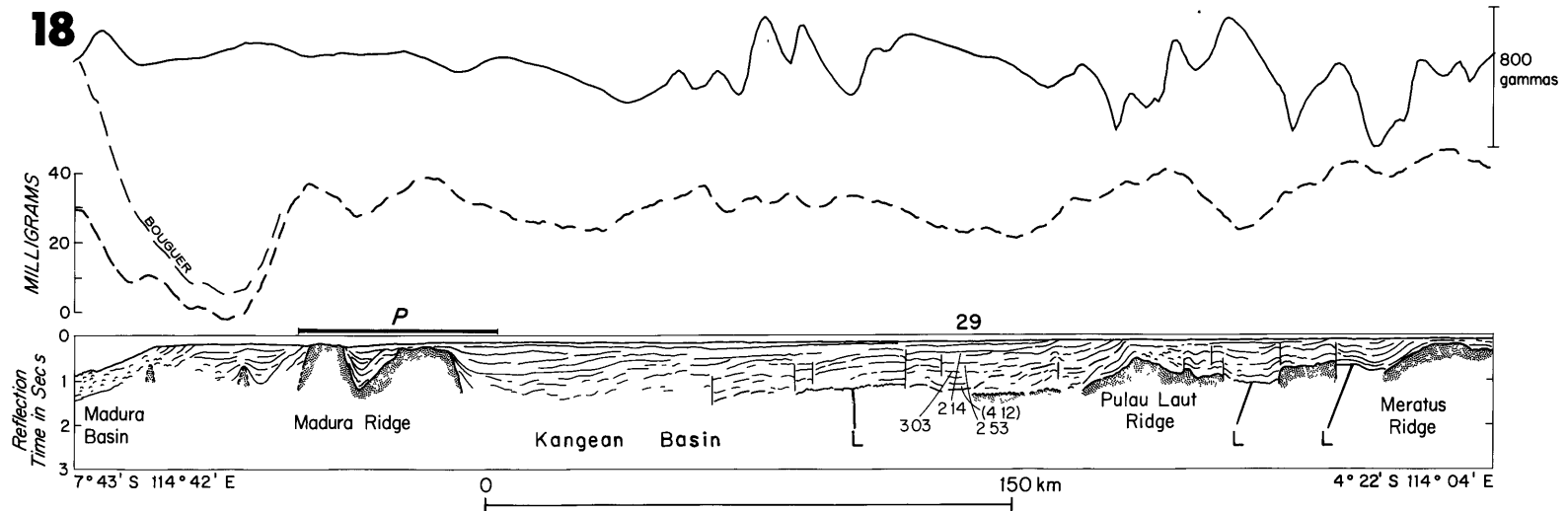
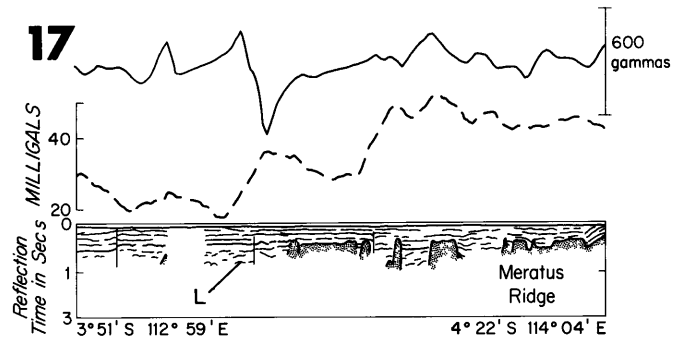
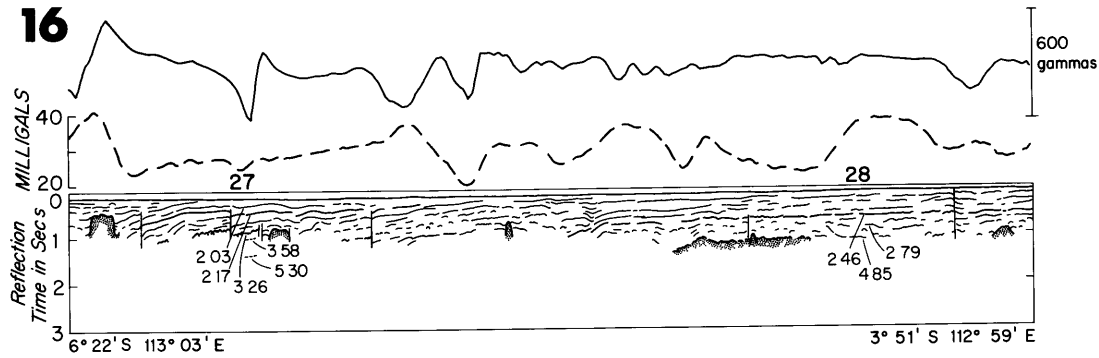
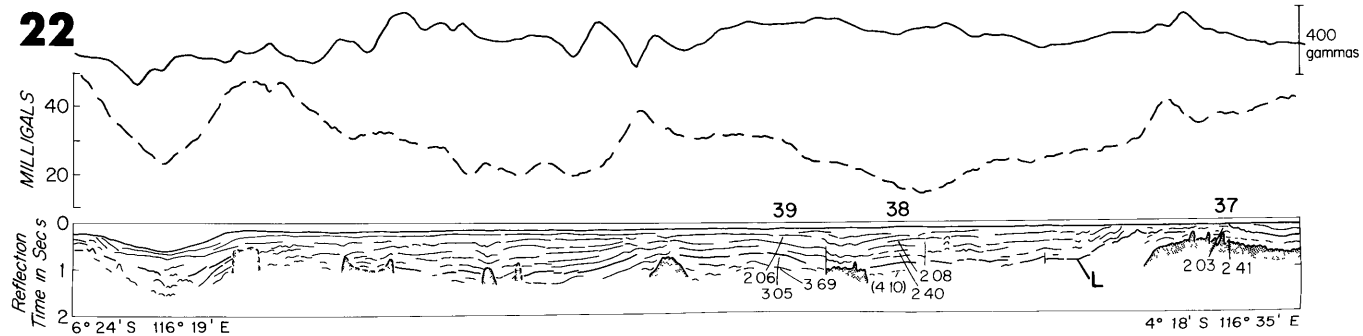
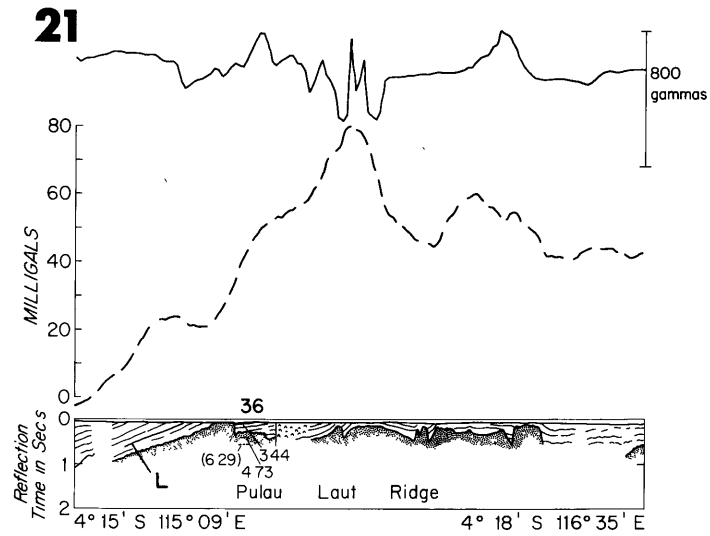
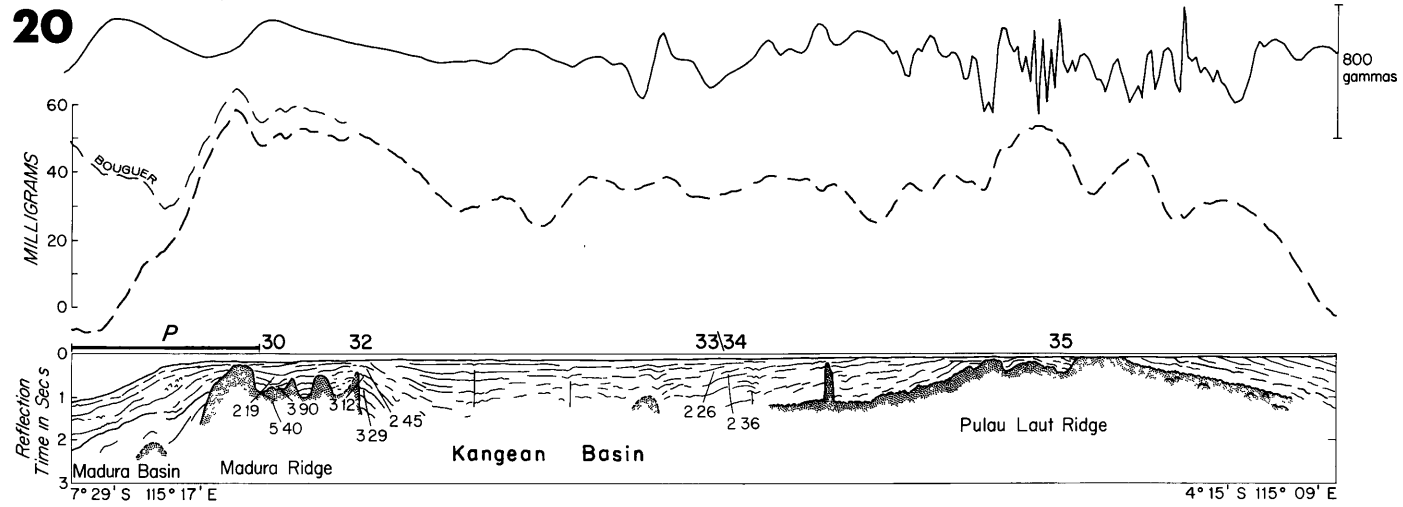


Figure 22. Interpretive geophysical profiles 20, 21, and 22 across the eastern Java Sea. Horizontal bar with P designate part of original recording for profile 20 reproduced in Figure 25. Symbols are the same as for Figure 21.



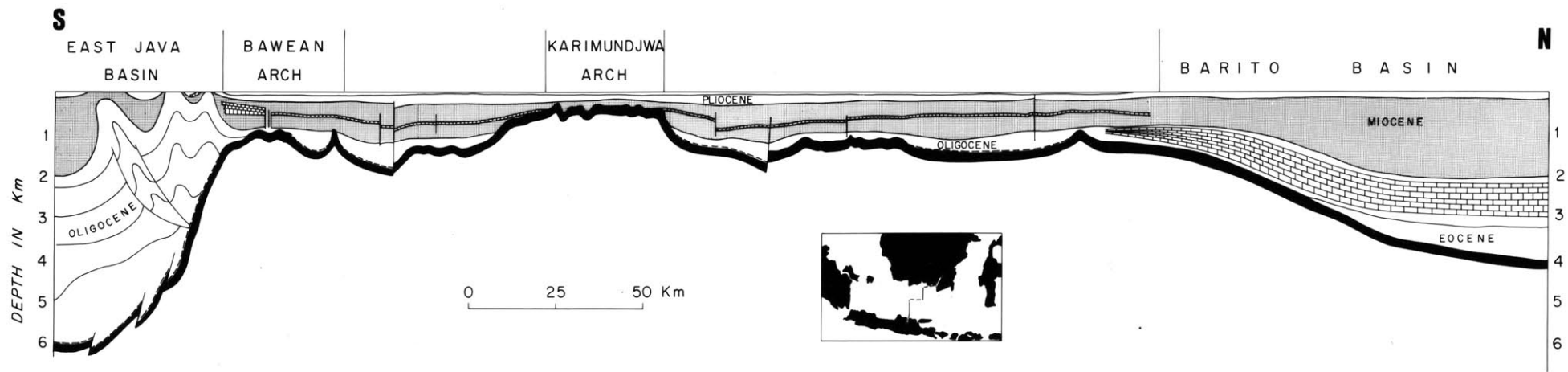
150 km



Ridge and the Bawean Arch may be parts of one continuous structure or two separate en-echelon structures. If these two uplifts join, their junction is east of Bawean Island near sonobuoy station 27 (profile 16). A detailed seismic survey of an area north of east Java and Madura (Cree, 1972) shows the existence of a few other structural highs parallel to the Pulau Laut Ridge, but they are short and could not be seen because of the wide spacing of our seismic reflection lines.

As in the western Java Sea, the uplifts in the east are separated by deep sedimentary basins: the Bawean Trough (or the Muriah Trough of Cree (1972)); the Kangean Basin and the Madura Basin. The basins in the eastern Java Sea differ from those in the west. Here the basins are narrow and long, whereas those in the west are wide and more circular in shape. The reflection and refraction profiles show the material interpreted to be lower Miocene limestone preserved in this area (Figs. 21, 22). As in the western Java Sea, it is a very strong reflector and locally is the acoustic basement (Fig. 23). Cree reports the prominent occurrence of a limestone horizon of probably lower Miocene age in some wells located north of eastern Java and Madura. This stratigraphic position correlates with that of the Batu-Radja

Figure 23. Schematic north-south cross section across the East Java Basin on Java, the Java Sea and the Barito Basin on Borneo. Based on seismic profiles 14 and 16 (Figs. 11, 20, 21), and on van Bemmelen (1949, Fig. 293), Weeda (1958, a, b) Koesoemadinata and Pulunggono (1971) and unpublished information from drill holes.

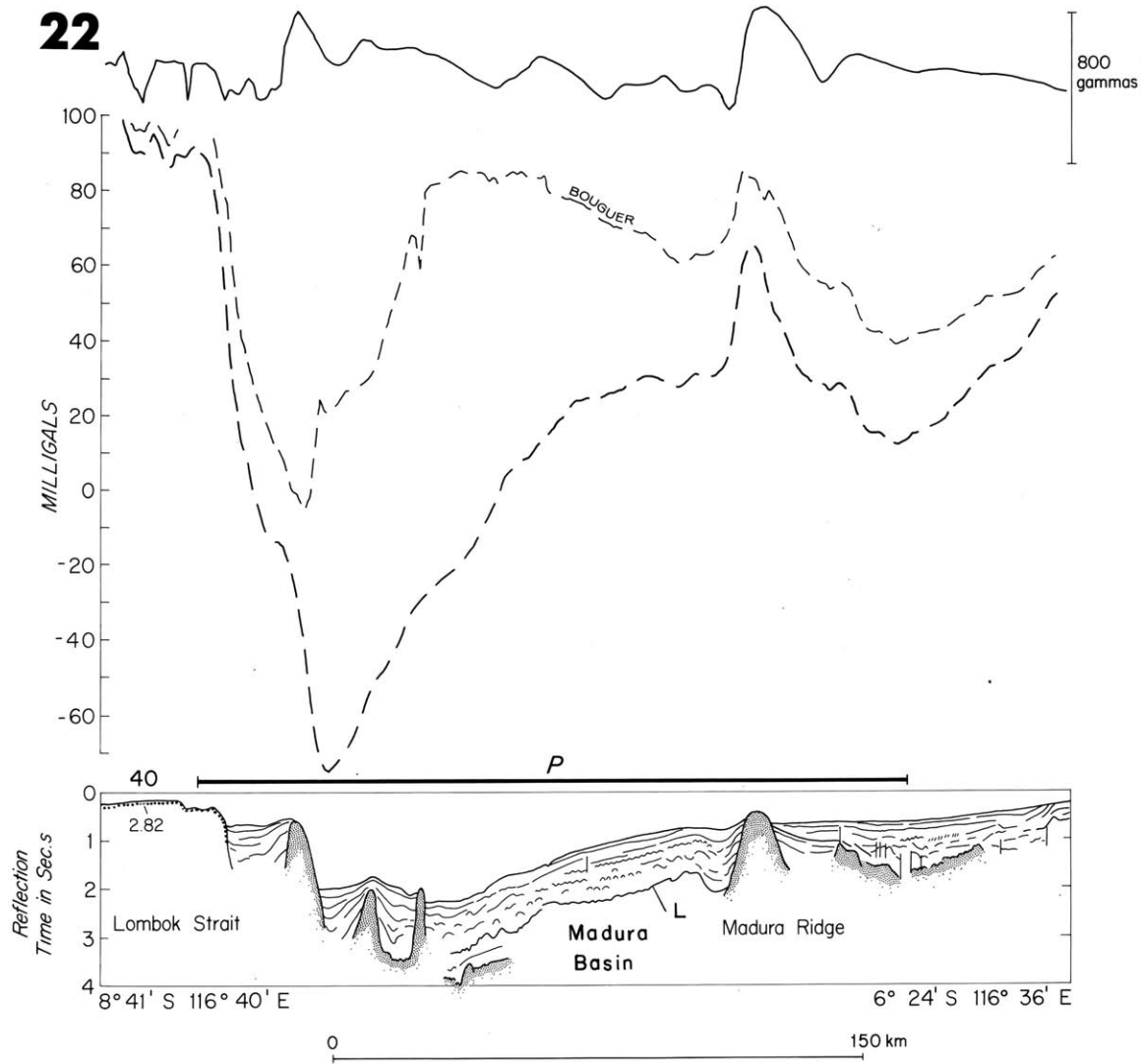


limestone in the western Java Sea. Cree terms this layer Upper Kudjung limestone, but we use the name Batu Radja to reduce confusion.

Strata in the eastern basins are more deformed than those in the basins of the western Java Sea. They contain broad folds with axes parallel to the trends of the main structural units. Many faults also are seen. Among the most important features in this area are the unconformities and dips of the sedimentary layers. On both sides of the Meratus and the Pulau Laut ridges the sedimentary layers dip parallel to the ridge flanks (profiles 18, 20, 21), and the up-dip ends of the strata as well as the ridges themselves are truncated by the sea floor. The spacing between the reflectors on the ridge flanks is uniform and does not increase away from the ridges crests. All of this indicates that these two ridges formed relatively recently, and subsequent to the horizontal deposition of the layers. The time of this event is difficult to date, but it must be post-lower Miocene, as the limestone layer (profile 21) was uplifted and tilted when the ridges were formed and subsequently truncated. The Bawean Arch may have a similar history but only one profile (14) provided data. In contrast the Madura Ridge has been continuously uplifted during the period

Figure 24. Interpretive geophysical profile 22 when it crosses deep water between the Java Sea and Lombok. Horizontal bar with P designates part of the original recording reproduced in Figure 26. Symbols are the same as for Figure 21.

**22**



of basin filling, as the sediments dip steeply and thicken away from the ridge (Fig. 25). The seismic profiles indicate that the Madura Ridge was uplifted very recently or that it is active still. Bordering the Madura Basin to the south are four basement ridges; the largest one is the present volcanic arc on which the islands of Bali, Lombok and Sumbawa are situated (Fig. 26). The other ridges probably trend east-west parallel to the island arc.

As a whole the tectonic pattern of the western Java Sea seems to result from tensional forces, whereas that of the eastern Java Sea from compressional forces.

One of the most interesting features of the eastern Java Sea is the relationship between the structures and the shelf break. While the Pulau Laut and the Meratus ridges trend more or less parallel to the shelf edge (Fig. 38), the Kangean Basin strikes obliquely to it, and the Madura Ridge and the Madura Basin cut the shelf break perpendicular to its trend and continue into the Flores Sea. The structural section (Fig. 16) shows that the crust beneath the Flores Sea is oceanic and that it thickens very rapidly westward. This suggests that the Madura Basin is underlain by oceanic crust with a thick sedimentary column over the Java Sea but with thinner sediments over the Flores Sea.

Figure 25. Sections of original recording in the Java Sea.

Top: Profile across the Billiton Depression (profile 5, Fig. 18) showing a fault on the western side of the depression.

Middle: Profile across the Madura Ridge (profile 18, Figure 21). Note how the sedimentary layers dip steeply away from the ridge, and that the ridge here is composed of two units.

Bottom: Profile across the shelf edge south of Madura (profile 20, Figure 22) showing the Madura Ridge on the right and the Madura Basin on the left. Note the structure that exists beneath the shelf break.



Reflection Time (Sec.)

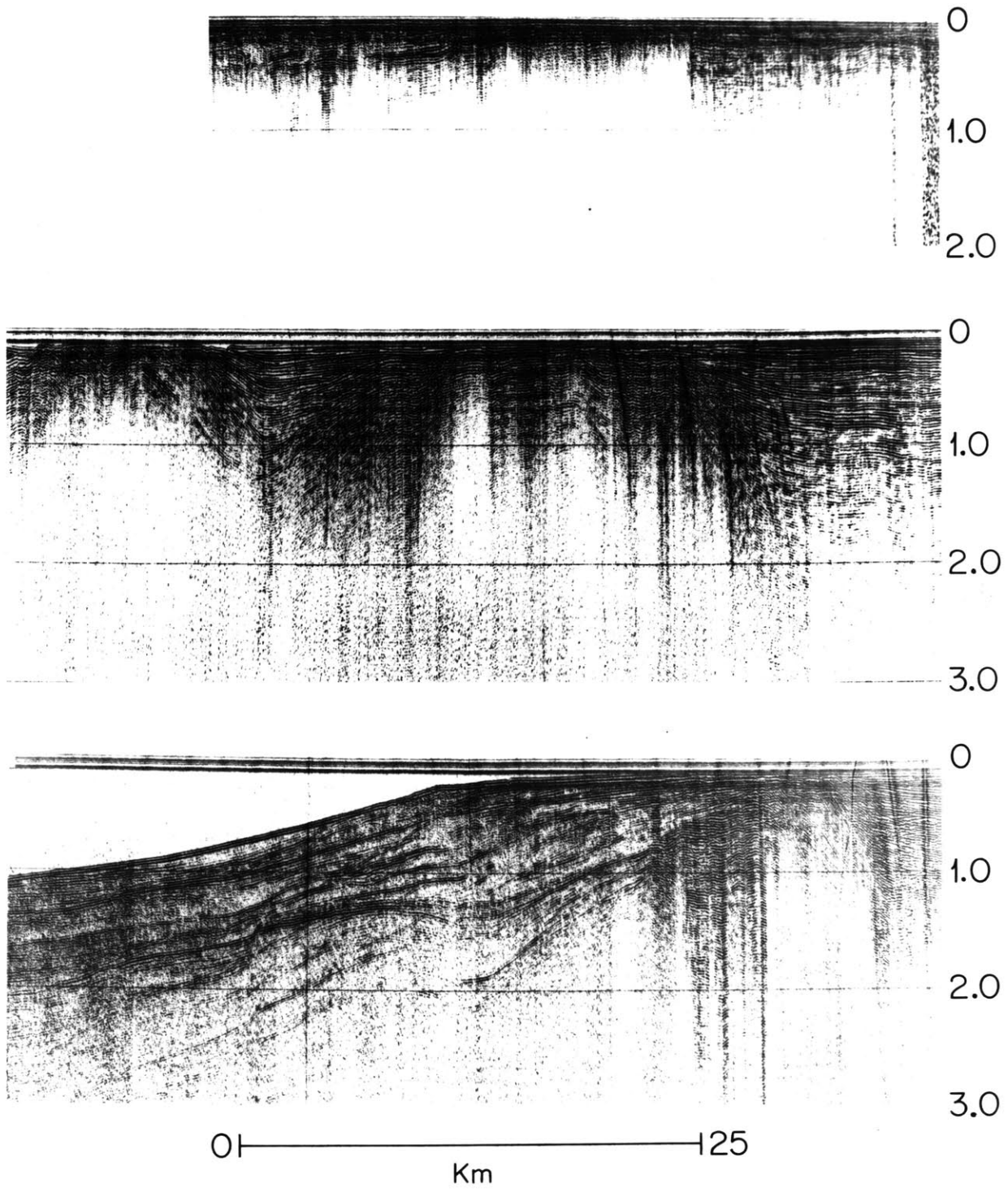
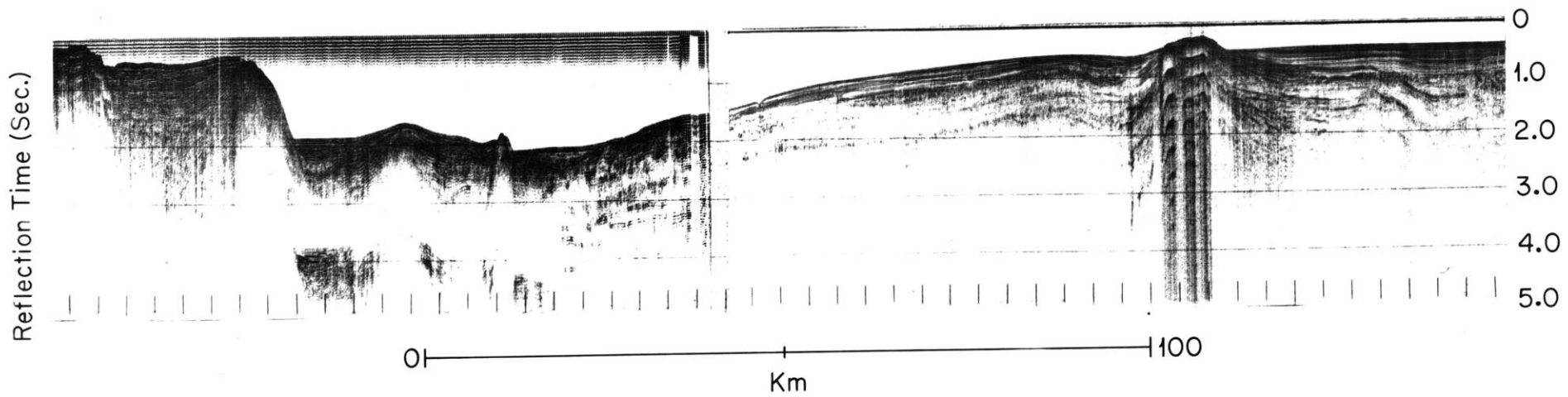


Figure 26. Section of original recording across the deep water between the Java Sea and Lombok (profile 22, Figure 24) showing the Madura Basin, the Madura Ridge on its northern side and the four basement ridges on its southern side.



## SEISMIC REFLECTION OVER THE NORTHERN SUNDA SHELF

The most extensive work in the northern Sunda Shelf was done by Parke, et al., (1971) with R/V F.V. HUNT. In the present study, two seismic profiles of R/V F.V. HUNT, not previously published were analyzed and incorporated along with the previously published results (Fig. 38). In addition, some small scale studies were reported by Dash (1970, 1971) and Dash, et al., (1970, 1972). Preliminary results of offshore exploration were discussed by Koesoemadinata and Pulunggono (1971). In this section the structural elements in this area will be summarized briefly.

A major ridge separates two large sediment-filled basins: the Brunei Basin in the east, and the Gulf of Thailand Basin in the west. The Gulf of Thailand Basin is about 1,100 km long and an average of 200 km wide at the 2-km isopach depth. In this basin large folds and faults have been recognized. In the widest portion of the basin between Latitudes 4°15' and 5°30'N a 300 km long zone of intensive folds trends east-west and appears to be due to tectonism. The folds have side dips of 5-10 degrees and are truncated by an unconformity that is 0.5 - 1.0 km below the sea floor. In some places these folds are associated with steep normal faults that cannot be mere slump planes, because they occur

beneath the flat shelf with no free slope toward which slumps or slides could move. Several folds in this zone have the characteristics of diapirs. These diapiric intrusions, if they exist, probably consist of shale, as indicated from some offshore drilling results (Koesoemadinata and Pulunggono, 1971). In the southern portion of the Gulf of Thailand Basin northeast-trending faults parallel the boundary between the basin and the Singapore Platform.

The Brunei Basin is even larger than the Gulf of Thailand Basin, with a total length of about 1,500 km and an average width of 200 km at the 2-km isopach depth. This basin appears to be part of the Northwest Borneo Geosyncline on Borneo. The part of the basin on land was described by Leichti, et al., (1960), Fitch (1961), Wilford (1961), Haile (1963) and others. The Brunei Basin has two major trends: the western portion trends to the northwest parallel to the Gulf of Thailand Basin, and the eastern portion trends to the northeast subparallel to the northwest coast of Borneo. As in the Gulf of Thailand Basin, folds and faults exist but here they probably trend to the northwest. Offshore drilling in this basin reached a basement of low grade metamorphic rocks, including phyllites of Cretaceous-Eocene age.

The Gulf of Thailand and Brunei basins are separated by the prominent Natuna Ridge. This ridge is a direct continuation of the Semitau zone in Borneo (van Bemmelen, 1949, p. 331) and it plunges to the northwest. Faults within the ridge probably trend parallel to its strike (Fig. 27). Along the northeastern flank of the Natuna Ridge a major fault (the Sarawak fault) extends the entire distance from central Borneo into the Sunda Shelf (Fig. 27) (Yanshin, 1966; Tjia, 1970; Dash, et al., 1972).

The southern and the northeastern boundaries of the Gulf of Thailand Basin abut platforms, one of which is the previously described Singapore Platform at the south. The Khorat-Con Son Platform at the north seems to be a direct continuation beneath the sea floor of the basement rocks on South Vietnam. It is characterized by a rough topography and becomes deeper to the south. The Khorat-Con Son Platform and the Natuna Ridge are separated by a major discontinuity termed the Natuna Rift (Figs. 27 and 28) that crosses the entire northern Sunda Shelf and becomes narrower southward. It seems to be connected with the Billiton Depression on the Singapore Platform.

Figure 27. Eight line drawings of seismic profiler and magnetic anomaly traverses across the Natuna Rift and Billiton Depression. Locations of the profiles are indicated in Figure 11. Stippled parts represent the acoustic basement. Note that the Natuna Rift becomes narrower towards the south. Profile D runs mainly along the strike of the Natuna Rift (see Figure 11) and the actual width of the rift is marked there by a small vertical bar.

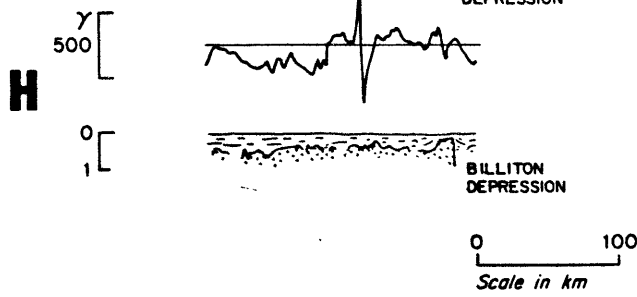
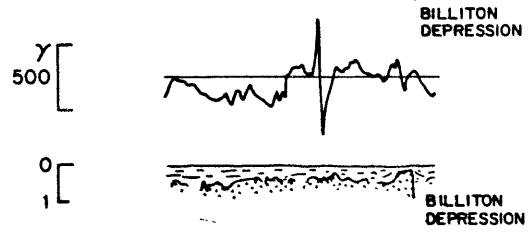
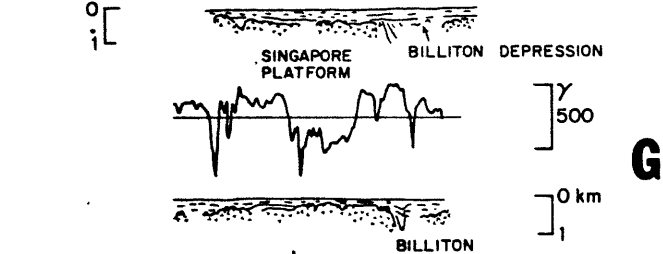
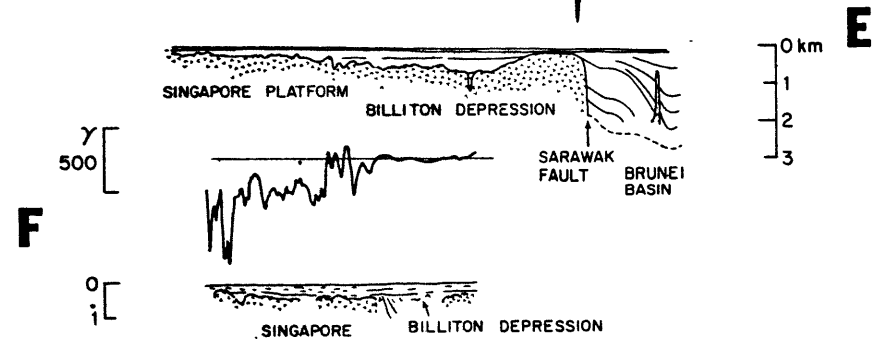
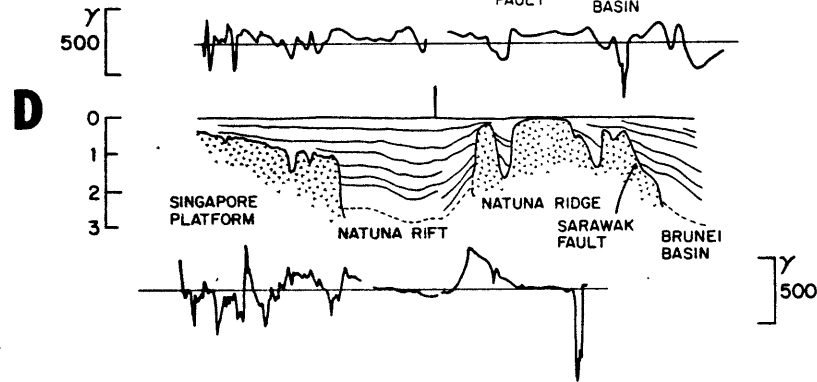
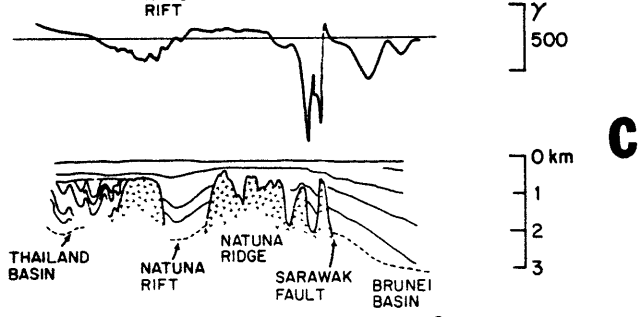
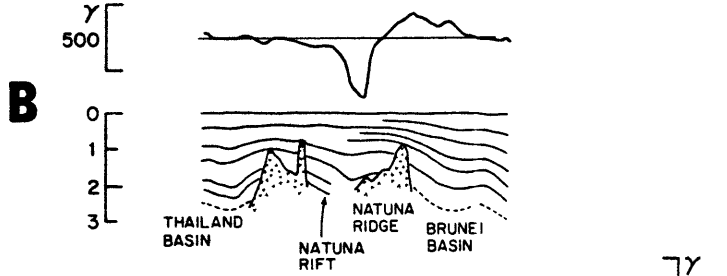
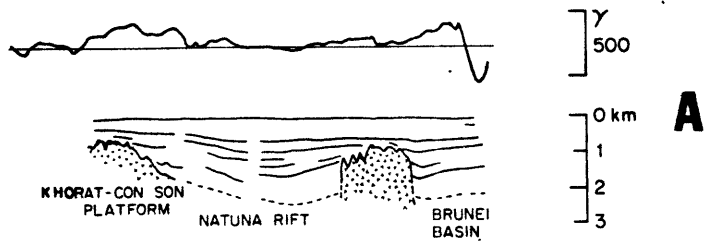
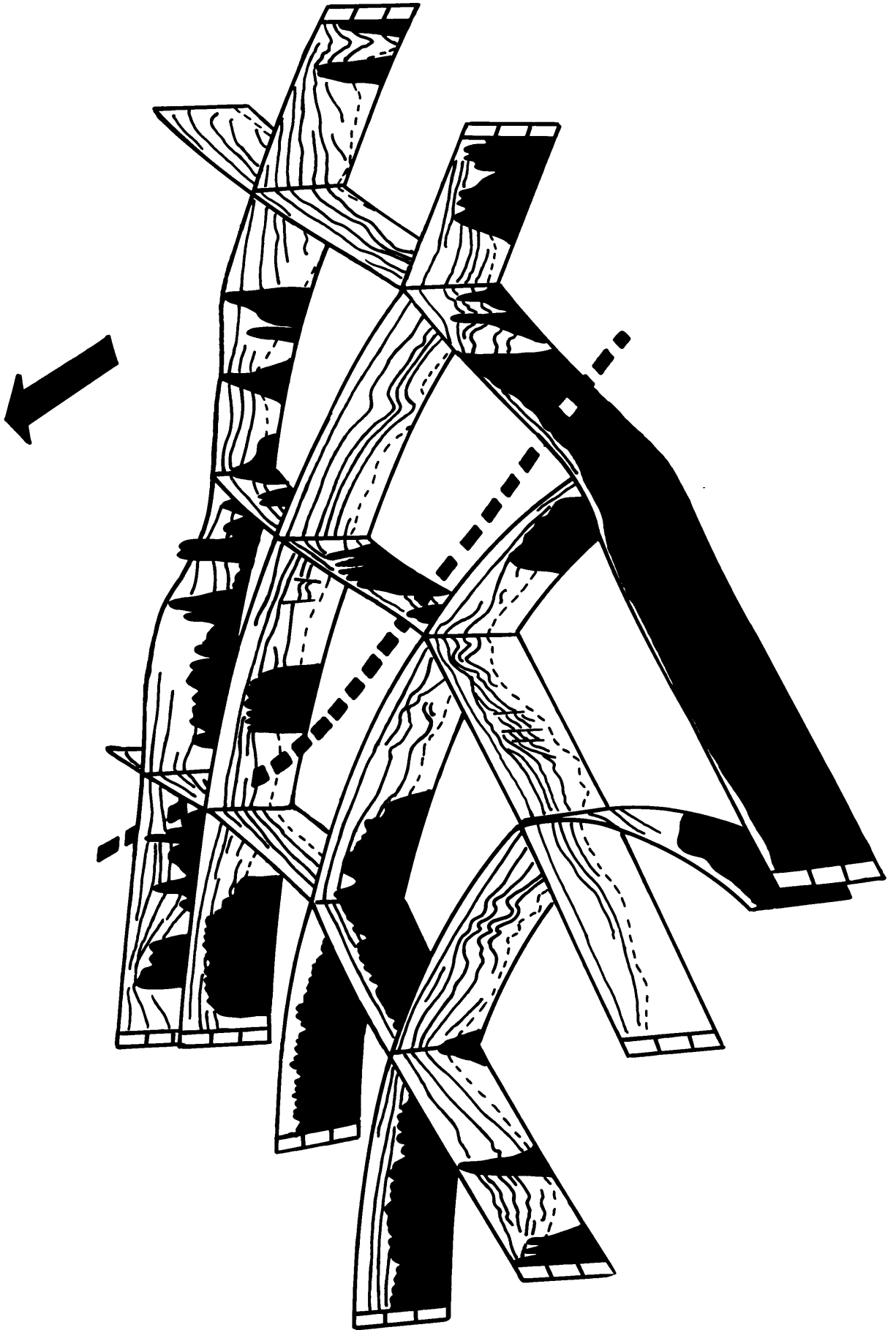




Figure 28. Photograph of three-dimensional cardboard model of continuous seismic reflection profiles taken in the northern Sunda Shelf (Parke, et al. 1971). Broad arrow at top indicates north. Heavy dashed lines indicate the position of the Natuna Rift. Profiles 23-29 of Figure 11.



## MAGNETICS

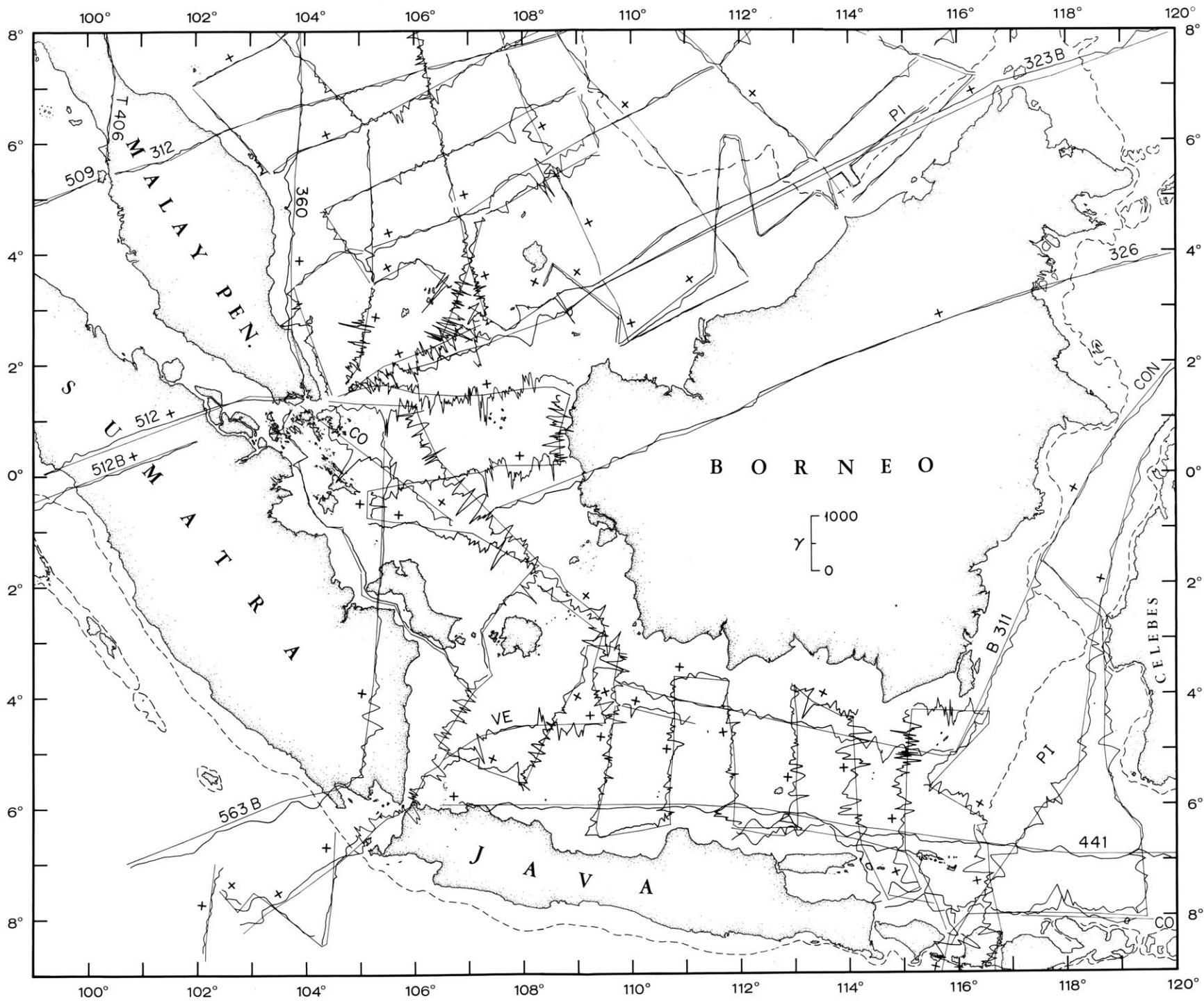
### Introduction

Magnetic data over the Sunda Shelf were recorded by various ships and by Project Magnet aircraft of the U.S. Naval Oceanographic Office (Fig. 29). Except for the data of R/V F.V. HUNT, all the magnetic data were digitized and the regional field based upon the reference field of Cain, et al., (1968) was removed. The data of R/V F.V. HUNT was reduced graphically as described by Parke, et al., (1971). In the construction of the magnetic anomaly map (Fig. 29), the regional field was reduced by 150 gammas to provide a better fit to the observed data. Temporal variations were considered in none of the anomaly computations.

### Interpretation

The Sunda Shelf is located near the magnetic equator. Under such conditions, where the magnetic field direction is at a low angle of inclination, the secondary field induced by a body of high susceptibility in the earth's field will mainly be opposed to the direction of the earth's field along a plane of observation above the body. Thus, the resulting total intensity anomaly must be negative. Another feature of magnetic bodies near the magnetic equator

Figure 29. Total magnetic anomaly profiles plotted along all traverses. Most of the data north of  $2^{\circ}\text{N}$  were taken by R/V. F.V. HUNT of the U.S. Naval Oceanographic Office (Parke, et al., 1971) and south of  $2^{\circ}\text{N}$  by R/V CHAIN of Woods Hole Oceanographic Institution (Emery, et al., 1972). Supplementary traverses from other ships (VE - R/V VEMA and CON - R/V CONRAD of Lamont-Doherty Geological Observatory; CO - H.M.S. COOK of Hydrographic Survey, England (Gray, 1959-1962); PI - PIONEER of U.S. Coast and Geodetic Survey) and from airplanes of Project MAGNET (three-digit numbers), were used.



concerns two-dimensionality. If a two-dimensional body strikes north-south, it should produce no anomalies because the component of magnetization along the body cannot affect the field outside the block as the lines of force never emerge from the sea floor. This is one reason why east-west sea-floor spreading near the equator produces low amplitude anomalies (McKenzie and Sclater, 1971).

Analysis of magnetic anomalies in terms of the shape and magnetic properties of the source is difficult, partly because of the complexity of the field arising from distribution of dipoles, and partly because both remnant and induced components may be present in the source. However, several model studies were based on the magnetic anomalies over the Sunda Shelf, and in general the magnetic data were found to be very helpful in the structural study (especially where the basement is shallow and its structure could not be resolved properly by the seismic reflection method), and in showing differences between basement types in various portions of the shelf. The magnetic anomalies provide little help in estimating the depth to the magnetic basement, because their wave lengths and amplitudes appear to be more a function of the varied lithology of basement rocks than their depth, unlike areas in which the basement is of

uniform lithology. Also it is not clear if the length/width ratio of the basement irregularities is sufficiently large to assume two-dimensionality. There are more magnetic lines than either seismic or gravity lines, and thus in some areas the magnetics serves as the only source of information about the basement structure.

#### The Nature of the Magnetic Anomalies

The magnetic anomaly profile map (Fig. 29) shows that this area can be divided into several distinct magnetic provinces (Fig. 30) that denote corresponding provinces of lithic units. Province 1 is characterized by large isolated anomalies with amplitudes of 400-700  $\gamma$  and wave-lengths of 40-70 km. Most of the anomalies are negative, although some are positive. This type of anomaly generally is associated with ridges and the use of two-dimensional models appears justified. Studies of one of these ridges, the Natuna Ridge, are shown in Figure 31. The models are generated by ridges parallel to the trend of the Natuna Ridge, and they show that the ridge is plunging to the northwest more rapidly than is indicated by the seismic reflection profiles (Fig. 27). At the southern part of the ridge, the configuration of the top of the model block generally

Figure 30. Magnetic provinces over the Sunda Shelf. A typical magnetic anomaly from each province is shown in the legend.



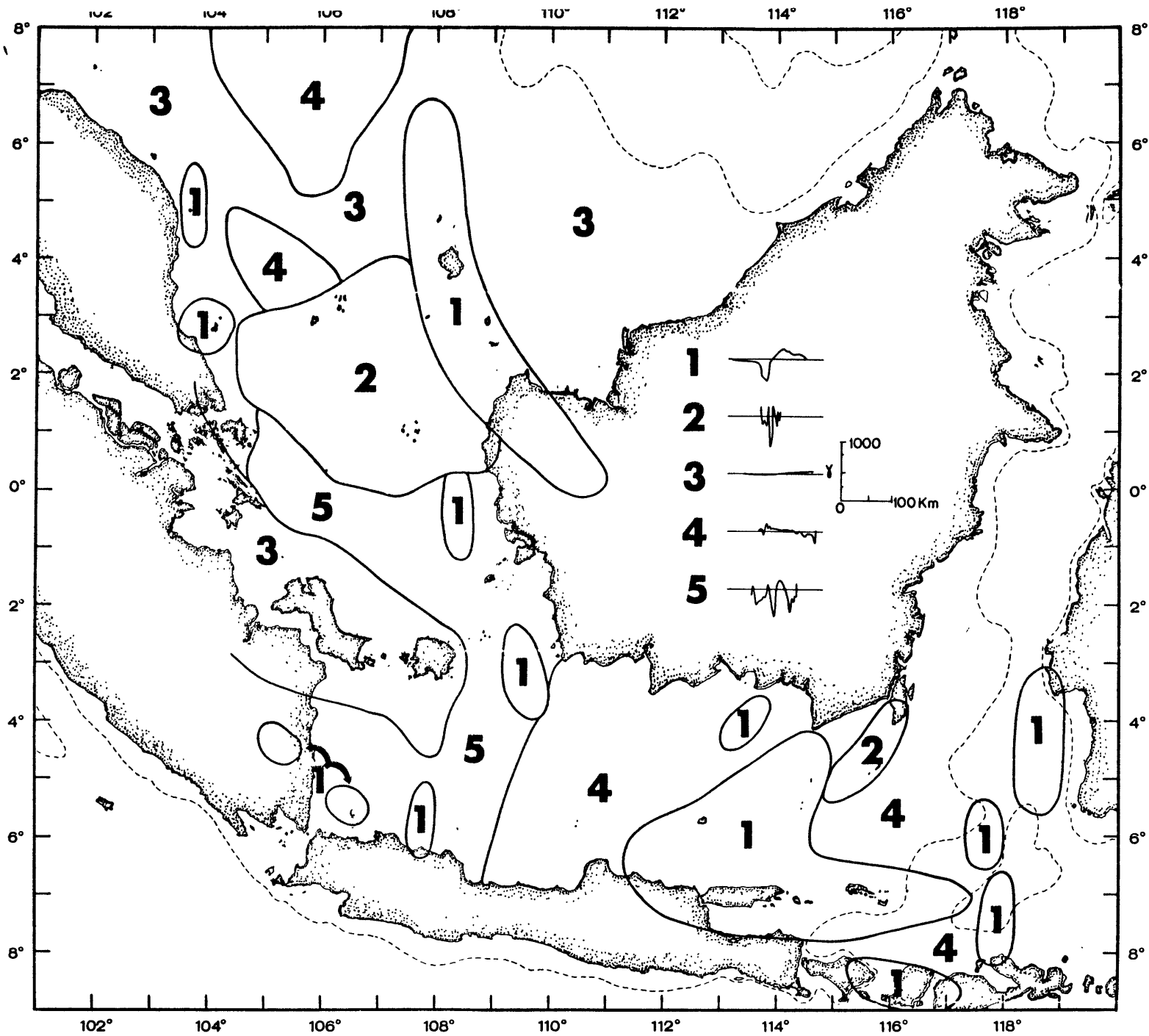
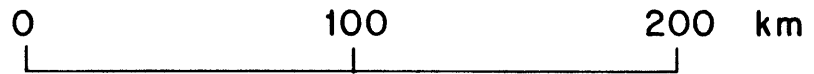
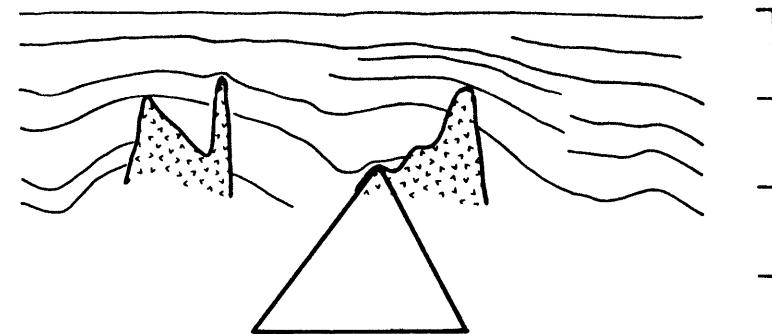
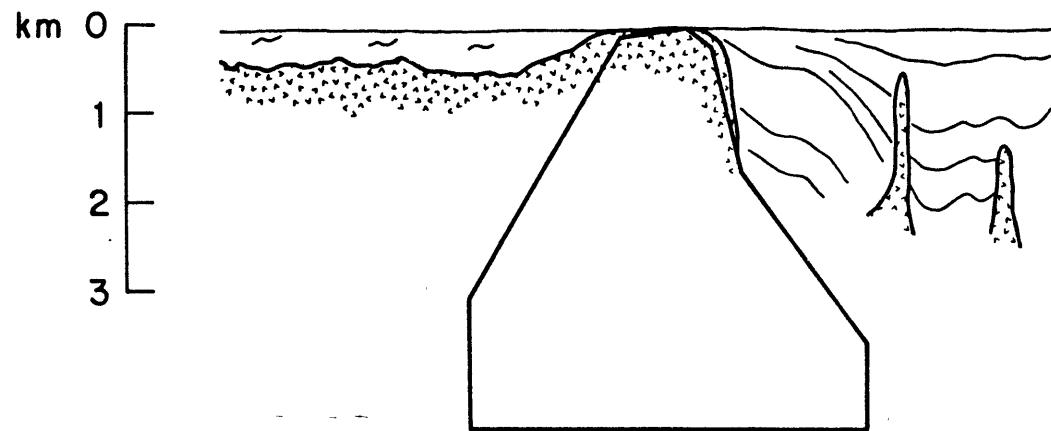
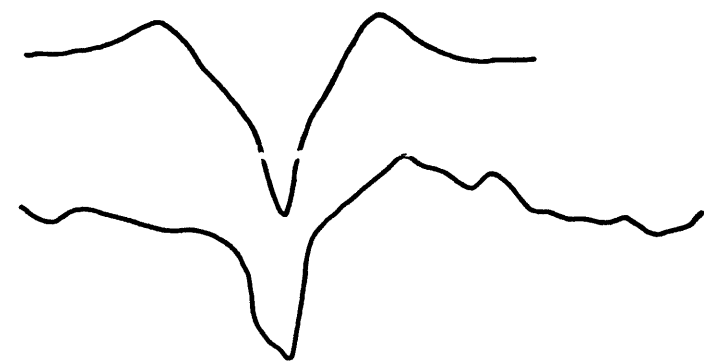
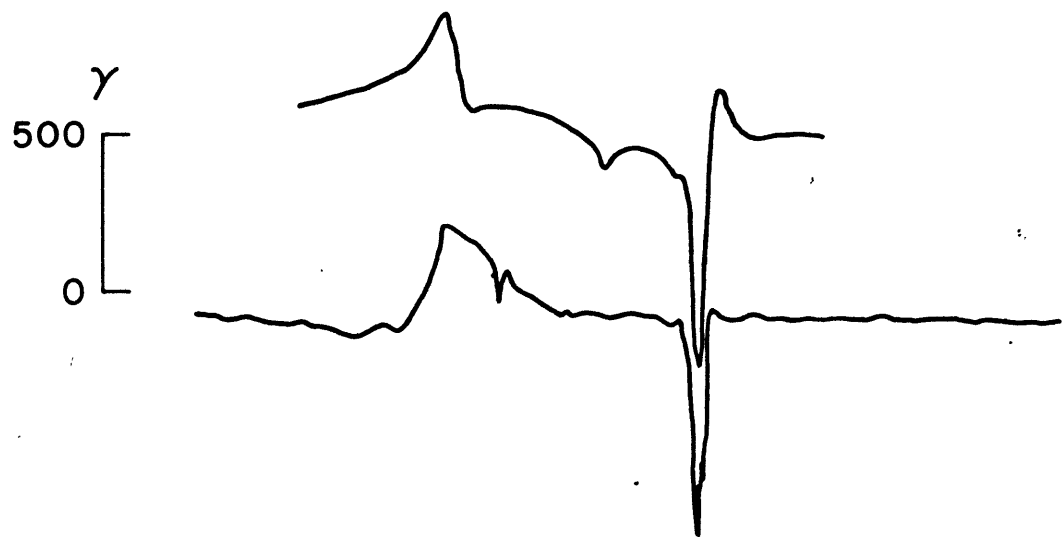


Figure 31. Natuna Ridge magnetic and reflection profiles (Profiles B and E of Figure 27). The top curve is a simulated profile generated by the block model at bottom, middle curve is observed profile, bottom is seismic profile. The simulated profiles were calculated using a modified version of a computer program described by Talwani and Heirtzler (1964). The strike of the model block is  $N60^{\circ}W$ , magnetic inclination  $0^{\circ}$ , the geomagnetic field is taken to be 40,000 gammas and the rock susceptibility is .03 for the left profile and .06 for the right profile.



reflects the acoustic basement topography, but at the north, the magnetic body must be deeper so that most of the acoustic basement may be a coral reef or other non-magnetized body. The model also explains the large negative anomalies of about  $-800 \gamma$  with very sharp gradients that are associated with the Sarawak Fault (Fig. 27, Profiles C, D, and E).

The Province 1 type of anomaly also occurs in the eastern Java Sea (Profiles 14-22) in association with the Bawean Arch, the Meratus, Pulau Laut, and the Madura ridges and the ridge on which the islands of Bali and Lombok are situated. Other examples of Province 1 anomalies are in the Flores Sea and in the western Java Sea along the Billiton Depression, along a major north-south fault and along the southeast portion of the Lampung High (Fig. 38, below). The high susceptibilities required by the models (Fig. 31) suggest that the structural elements accompanied by these anomalies are associated with basic or ultrabasic bodies.

Magnetic Province 2 is characterized by sharp anomalies with high amplitude and very short wave-lengths, indicating that the source of these anomalies is very close to the sea floor. Anomaly amplitudes are  $400-800 \gamma$ , but some reach  $1500 \gamma$ . These anomalies occur mainly in the northern part of the Singapore Platform, where they are probably associated

with small basement bodies (Profile 1, Fig. 18). Calculations by Peters' half-slope method (Peters, 1949) on some of the more elongate anomalies indicate a depth to magnetic basement of 200 m below sea-level, which is in good agreement with the seismic interpretation. A few wide negative anomalies similar to those in magnetic Province 1 also exist in this platform, but the sharp anomalies of Province 2 are superimposed upon them. These anomalies also occur above the Pulau Laut Ridge, where they may be associated with basalt flows on the ridge top.

Magnetic Province 3 is characterized by very broad low magnetic anomalies (less than 50  $\gamma$ ) or no magnetic anomalies. This province occupies a major portion of the northern Sunda Shelf and the China Basin at the north. It also occurs around the islands of Bangka and Billiton. This smooth magnetic province is the result of several different factors. In the northern Sunda Shelf, it may be due to the great depth of burial of magnetic basement or to a regional metamorphism which decreased the magnetization of the basement rocks. In the China Basin, which is underlain by an oceanic crust, the smooth province may reflect sea-floor spreading during a long period of constant geomagnetic field polarity. Around the islands of Bangka and Billiton, the smooth magnetic field is the result of the low susceptibility of

the widespread granitic basement.

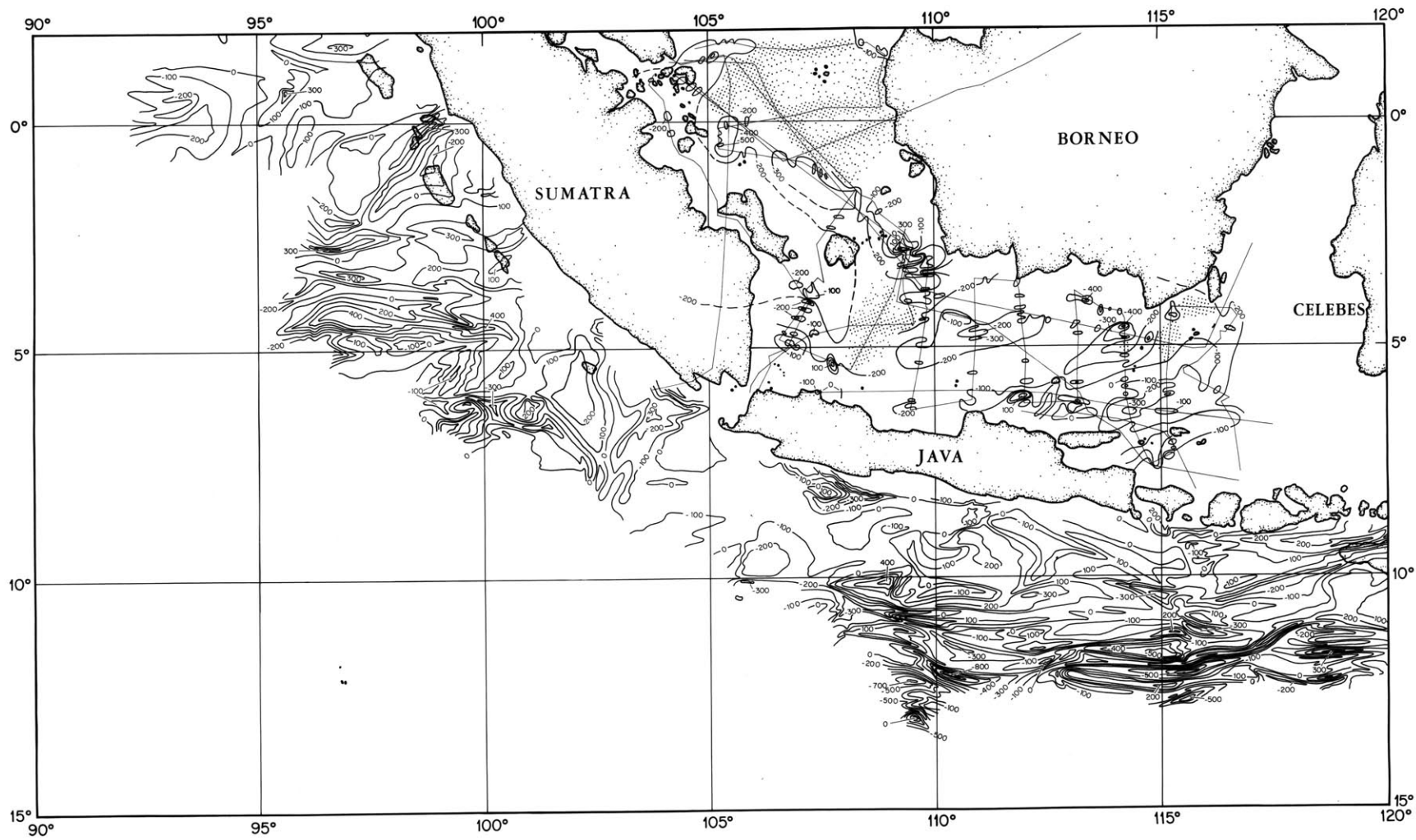
Magnetic provinces 4 and 5 are not so well defined as the other provinces. Province 4, which is located over the central and eastern Java Sea, the Khorat-Con Son Platform, and small portions of the northern Sunda Shelf is characterized by a low-level field with isolated magnetic anomalies having short wave-lengths, sharp gradients and varied amplitudes of less than 300  $\gamma$ . These small isolated anomalies are related to small near-surface magnetic bodies. In the central Java Sea, they occur on both sides of the Karimundjawa Arch (Profiles 10, 12) and probably indicate the presence of dikes along the faulted flanks of the arch. There is no major change in the overall magnetic characteristic between the Karimundjawa Arch and the Billiton Basin suggesting that the arch is composed of rocks with very low magnetic susceptibility, such as granite. The Khorat-Con Son Platform, with similar magnetic characteristics, probably also is composed of granite as indicated by the granitic islands situated on the platform (Hilde and Engle, 1967). The general low-level magnetic field of Province 4 over the sedimentary basins (mainly over the Billiton Basin) implies that igneous rocks are deep as is evident from the seismic profiles.

Province 5 is the most problematic one. The boundaries between this province and provinces 1, 2, and 4 are not abrupt as though this province may not be unique but also contains elements from provinces 1 and 4. The province occurs in the west and north Java Sea, in the area between Borneo, Sumatra, and Java, both over the Singapore Platform and the Sunda and West Java basins. The magnetic anomalies have rather large amplitudes (200-600  $\gamma$ ), but slightly smaller than those in provinces 1 and 2 and wavelengths (10-30 km) that are smaller than those in province 1, but larger than those in province 2. Their dimensions are similar to those reported by Emery, et al., (1970) in the Atlantic Ocean for oceanic magnetic anomalies, and are the only anomalies over the entire Sunda Shelf that resemble oceanic magnetic anomalies. The existence of this magnetic province indicates a possible difference between the basement material under the Sunda and West Java basins and that under the Billiton Basin. Contrasts in the character of the magnetic field over the Singapore Platform are apparent between the northern part (with magnetic province 2) and the southern part (with magnetic province 5), indicating corresponding contrasts between the lithic units underlying these areas.

A contour map of the magnetic anomalies in the Java Sea is shown in Figure 32. Only magnetic anomalies of provinces 1 and 4 have long enough wavelengths for contouring at this scale. The map shows a general northeast-southwest trend of the magnetic anomalies in the eastern Java Sea, which is approximately parallel to the major structural elements in this area. In the west and north Java Sea, anomaly wavelengths are too short for contouring and the trend of the magnetic anomalies, if any, is not known. A prominent magnetic feature exists between Billiton Island and Borneo in the southern portion of the Billiton Depression. Also shown in Figure 32 are contours of magnetic anomalies south of Java and Sumatra, in the Indian Ocean. The map demonstrates the difference between the nature of the oceanic magnetic anomalies and those over the shelf. While it is usually considered that magnetic anomaly lineations in the ocean originate from the upper, basaltic, part of the oceanic crust and represent strips of rocks which were formed at the center of mid-ocean ridges during periodically reversing magnetic fields of the earth (Vine and Matthews, 1963), the anomalies over the shelf mainly reflect the structural elements beneath it. The possibility still exists that a few areas of this large shelf were



Figure 32. Total magnetic intensity anomaly contoured with interval of 100  $\gamma$  over the southern Sunda Shelf and the northern Indian Ocean. The contours in the deep-sea are from Vacquier and Taylor (1966). Fine lines show the data-control on the shelf. Dotted pattern shows areas in which the anomaly wave-lengths are too short for contouring.



formed by a mechanism of sea-floor spreading, but the control of our data is insufficient for such structural analysis.

The magnetic anomalies south of the Java Trench trend mostly east-west and do not follow the curve of the Indonesian Island Arc. This supports the idea that they originated from an east-west mid-ocean ridge. A major discontinuity in the magnetic anomaly pattern exists between the area south of Java and that southwest of Sumatra. Also shown in the map (Fig. 32) is a zone, more than 500 km long, of large east-west magnetic anomalies at Latitude  $4^{\circ}30'S$ . This zone is associated with high heat-flow and was interpreted by Vacquier and Taylor (1966) to be a fracture zone. Project Magnet flight 563B shows a large magnetic anomaly at  $4^{\circ}30'S$  in southeast Sumatra (Fig. 29), some 500 km east of the anomaly mapped at sea. Perhaps a large east-west structure along this latitude is continuous from the deep-sea across southern Sumatra.

## GRAVITY

Introduction

Gravity observations in the Indonesian Archipelago started with the classical survey aboard submarines by Vening Meinesz in the 1920's and 1930's (Vening Meinesz, 1932). At that time about 30 gravity pendulum stations were made in the Java Sea showing that this area is characterized by "positive anomalies varying around 30 mgal" (Vening Meinesz, 1948, p. 36). The various gravity maps of the Indonesian Archipelago that were published over the years based on Vening Meinesz' data (e.g. Vening Meinesz, 1932; Daly, 1940; Woollard and Strange, 1962) contain no contours over the Java Sea since the contour interval was 50 mgal. The main source of later data is the survey by R/V CHAIN (Emery, et al., 1971) plus some lines made by other ships crossing this area.

The most important result of Vening Meinesz' work was the discovery of a belt 100 to 200 km wide of intense negative anomalies paralleling the tectonic arc over the inshore slope of the deep trench south of Java and Sumatra. This discovery led Vening Meinesz to the well-known theory of downbuckled tectogenes. Most tectonics theories to explain the structural elements in the Indonesian Archipelago

were engendered by this negative gravity anomaly zone. Today, the gravity minimum is explained as due to underthrusting of lithospheric plates in accordance with the plate tectonics theory (e.g., Bowin, 1972). Much more data over the Indonesian Trench were obtained during the International Indian Ocean Expedition, mainly by the Scripps Institution of Oceanography and by the United States Coast and Geodetic Survey (USCGS). A free-air gravity anomaly chart based on all available data is shown in Figure 33 that is generally concordant with the charts of Vening Meinesz. A detailed description of the gravity field over the Indonesian Archipelago and its explanation is given by Bowin and Ben-Avraham (in preparation).

On land the most extensive gravity survey so far was made by Shell Internationale Petroleum Maatschappij N.V. The Hague, Netherlands and affiliated companies. Recently, some local surveys were made by Japanese scientists on Java, Bali, and Krakatau islands (Yokoyama and Hadikusumo, 1969; Yokoyama, et al., 1970; Yokoyama and Suparto, 1970).

For the present study, a compilation was made of all the available gravity data over the Sunda Shelf and adjacent land areas (Fig. 34). The gravity measurements aboard R/V CHAIN were done with a vibrating-string gravity meter

Figure 33. Free-air anomaly map of the East Indies. Hatching designates areas with negative anomalies. Sources of information are from Lusiad and Monsoon Expeditions of Scripps Institution of Oceanography; USCGS ship PIONEER; NOAA ship OCEANOGRAPHER; VEMA 19 cruise of Lamont-Doherty Geological Observatory; Vening Meinesz pendulum data and R/V CHAIN of Woods Hole Oceanographic Institution. Data on land are from Japanese surveys (Yokoyama, et al., 1970; and Yokoyama and Suparto, 1970). Contour interval is 50 mgal.

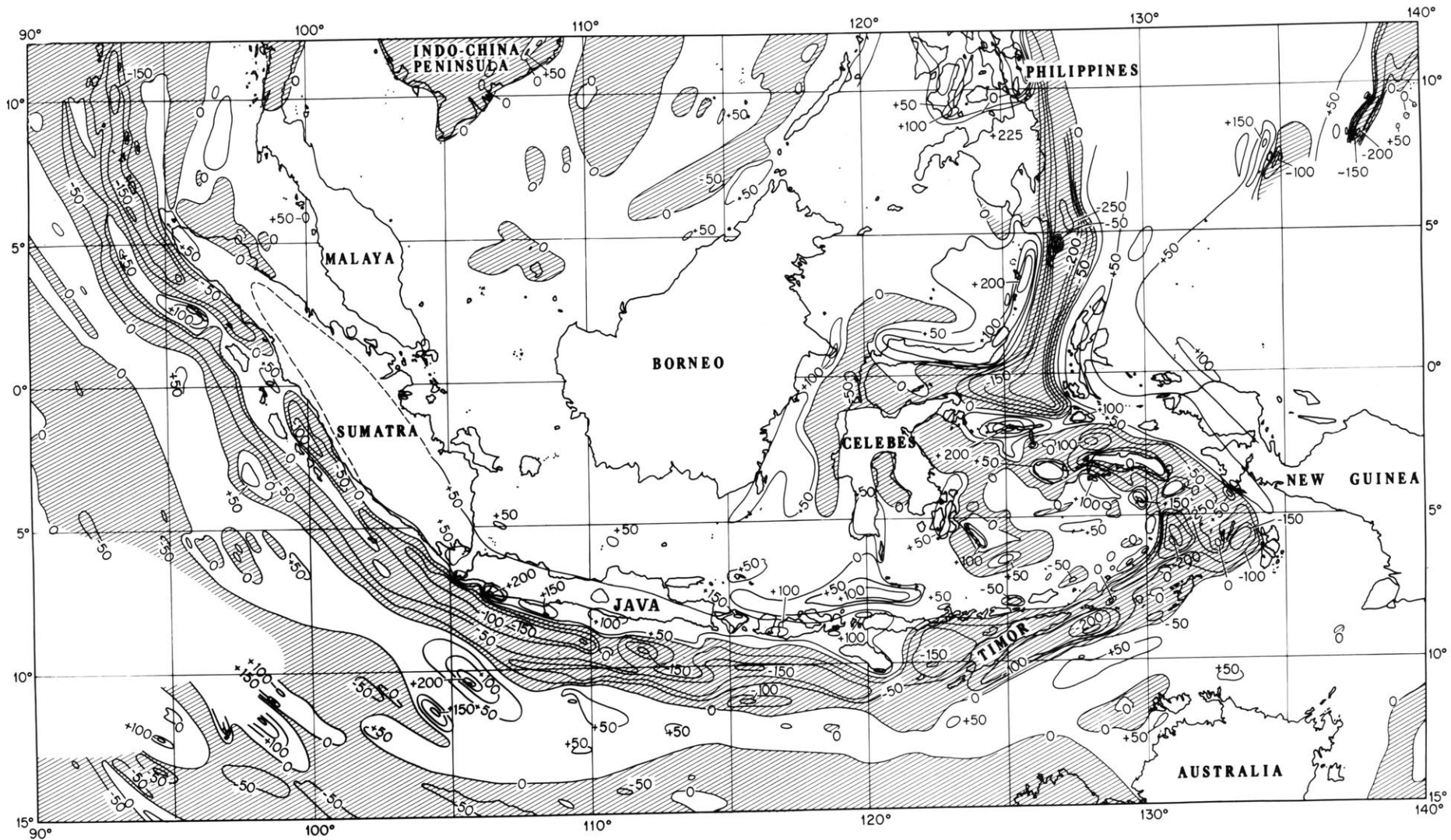
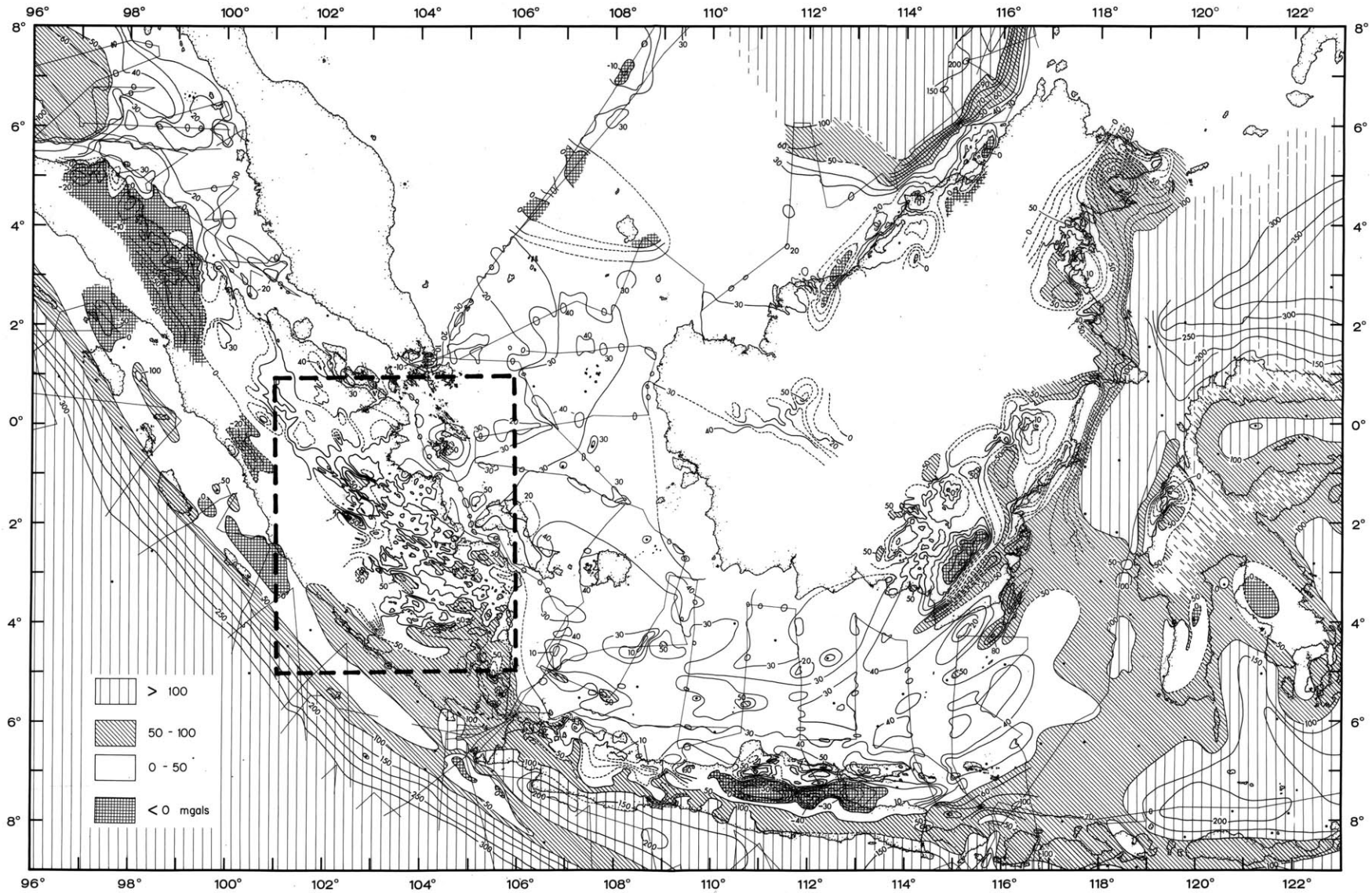


Figure 34. Bouguer anomaly map of the Sunda Shelf and adjacent land masses. Sources of information are the same as in Figure 33 except that most of the land data are from 27 different maps of Shell Internationale Petroleum Maatschappij N.V., The Hague, Netherlands. Control for contours at sea is indicated by fine lines for ship data and small solid circles for pendulum data. Contour interval is 10 mgal.





(Wing, 1969; Bowin, et al., 1972). The digital readout at five-minute intervals was adjusted for the Eötvös acceleration caused by the ship's east-west velocity and compared with the International Gravity Formula of 1930 to get free-air anomalies. Bouguer anomalies were calculated on an assumption of an infinite slab correction (density  $2.67 \text{ g/cm}^3$ ) and seawater density of  $1.03 \text{ g/cm}^3$ . The gravity profiles of Vema 19, obtained with an Askania-Graf stable platform meter, were supplied by M. Talwani of Lamont-Doherty Geological Observatory. The data reduction was done in a similar manner as for the R/V CHAIN data. Reduced data were obtained from all the other ship tracks. Over the shelf the Bouguer and free-air anomalies are quite similar, owing to the shallow water depths (40-60 m), so in this report only the profiles for free-air anomalies are presented with the reflection and magnetic profiles (Figs. 18-24). The Bouguer anomaly profiles are presented only when the water deepens and the Bouguer anomalies differ significantly from those of the free-air.

#### Regional Gravity

The gravity field over the Sunda Shelf averages about +30 mgal, in accordance with the original description of Vening Meinesz. This positive field is now recognized as

one of the main features of the earth's gravity field. A regional free-air map (Talwani, 1970) calculated from a spherical harmonic expansion of the earth's gravity field by Kaula (1966) shows a gravity high associated with the entire Pacific margin and especially with the island arc areas along the western margin. The field over the Sunda Shelf is among the highest in the western Pacific. Similar results were obtained with free-air anomaly averages over  $20^{\circ} \times 20^{\circ}$  squares from surface ship measurements (Le Pichon and Talwani, 1969). Talwani (1970) offered two possible explanations for this high gravity field in the western margin of the Pacific. One is that the island arcs themselves have large positive anomalies and, because the satellite-derived gravity anomalies have long wavelength, these large anomalies contribute to the entire region. This does not explain the high gravity field observed by ships over the Java Sea. Another explanation is that the gravity high might be caused by higher rock densities associated with a descending lithospheric plate in the mantle, an explanation that is supported by the long wavelength anomalies that must reflect deep sources. A structure model based on the broad gravity features will be discussed later in this chapter.

Gravity Anomalies of the Java Sea

Local gravity anomalies superimposed on the regional background level have relative amplitude of 20-30 mgal and varied gradient. The main potential of the gravity anomalies is in the information they can give about structures of the basement, in particular beneath a deep sedimentary basin. Analysis of gravity anomalies is quite different from that of magnetic. The theoretical background is considerably simpler. A body with a specific density contrast produces the same gravity anomaly no matter where it is on the earth's surface and, therefore, it is not subject to variation in its expression with latitude or orientation as is a magnetic anomaly. On the other hand, gravity interpretation lacks the great geological simplicity which the magnetic method has because of the definite contrast at the surface of the basement. The basement surface may or may not be the surface of density contrast from which gravity anomalies originate.

Over the eastern and central Java Sea the trends of the Bouguer anomalies (Fig. 34) are similar to the structural trends. In the western and northern Java Sea the trend of the anomalies, if any, is unclear. Although the area as a whole is slightly out of isostatic equilibrium, the various structural elements have relatively small gravity

anomalies and seem to be isostatically compensated. A possible reason for this is that most of the shelf has been inactive since early Tertiary. Since the activity stopped, sediments buried the tectonic relief, producing a flat shallow sea floor. Only a few of the structural highs (e.g. Pulau Laut Ridge) protrude through the sediment cover.

In most of the sedimentary basins of the Java Sea the seismic reflection profiles did not penetrate to basement. At the south end of profile 6 (Fig. 19) a steep drop in gravity of 15 mgals was observed near the northern margin of the Sunda Basin. Oil company drill holes (Todd and Pulunggono, 1971) indicate a difference in depth between acoustic and true basement of 1.5 km. With an infinite slab approximation this is consistent with a density difference of  $0.24 \text{ g/cm}^3$  between the true basement and the sediments. If one assumes a density of 2.48 for the acoustic basement (a lower Miocene limestone (Fig. 12)) the computation indicates that this anomaly is consistent with a density of 2.20 for the material below the acoustic basement and 2.50 for the true basement. On the basis of these density values, thicknesses of sediments in other basins were estimated and incorporated in the structural map (Fig. 38, below).

In most instances gravity lows are centered above lows in the acoustic basement. For instance, note how gravity lows mark the position of the Billiton Depression (Profiles 1, 2, and 3). On profiles 8, 10, and 14 large gravity lows indicate the existence of sedimentary basins although the seismic profiles did not. In some instances (Profiles 1, 3, and 6) gravity lows occur over large distances in areas where the acoustic basement is indicated by seismic reflection and refraction to be true basement. This can be explained by a low density basement, perhaps a felsic intrusive material. It is well established now that gravity lows are frequently caused by felsic plutons, mainly granites (Garland, 1965, p. 112) especially where the felsic pluton is surrounded by other igneous and metamorphic rocks. At least several of these gravity lows probably fit this explanation. The large gravity low on the left side of Profile 1 probably is associated with a granitic body that crops out on the islands south of Singapore. Similarly, the broad gravity low in the middle of Profile 6 (in the vicinity of Sonoguoy 7) between the two granitic islands Bangka and Billiton probably is caused by granitic basement (Untung, 1967).

Gravity highs are abundant throughout the area. The size and magnitude of these positive anomalies clearly indicate large high-density bodies. Various rules for estimating the maximum possible depth of a density interface from observed gravity anomalies have been derived over the years (Grant and West, 1965). In earlier works this depth was expressed by the "anomaly half-width relation" (Nettleton, 1940, p. 123). More recently, Bott and Smith (1958) generalized this concept for two and three-dimensional bodies, and Bancroft (1960) extended the generalization to a semi-infinite sheet. Bott and Smith stated that an upper limit for the depth of the body can be deduced from the formula:

$$D \text{ max} = \frac{kA}{S \text{ max}}$$

where,  $D \text{ max}$  is the maximum depth;  $A$  is anomaly amplitude,  $S \text{ max}$  is maximum gradient and  $k$  is a constant less than unity depending on the basic shape of the source. According to this computation most of the anomalies of the Sunda Shelf are of a shallow origin, less than 6 km below sea level.

In some instances the shape of the anomaly shows that it is caused directly by the basement. The Madura and

Pulau Laut ridges (Profiles 18, 20, 21, and 22) are clearly associated with high gravity anomalies that show the presence of dense material. A gravity high composed of a broad anomaly and local anomaly superimposed on it is associated with the Karimundjawa Arch (Profiles 10, 12, and 14). If the Karimundjawa Arch were a granitic body as suggested by the seismic refraction and magnetic data the broad anomaly over it would be explained by the presence of sedimentary basins surrounding it. The local anomaly is narrower than the arch itself. The fact that it is not centered over the arch and that it is associated with magnetic anomalies suggests that the anomaly probably is caused by basic intrusion on the flank of the arch. The same probably is true for the Seribu Platform, which was proved to be a granitic body by offshore drilling (see Fig. 37, below). In some instances the shape of the positive anomalies is not related in any direct way to the shape of the acoustic basement, probably indicating a deeper buried structure (Profile 1 and 3). The positive anomaly on the right-hand side of Profile 1 and the one in Profile 3 are located north and south of the Tambelan Islands respectively, and may indicate a north-south structure parallel to the Billiton Depression.



Over the eastern and central Java Sea (Profiles 10-22) a general agreement exists between the gravity anomalies and the structural units; the wavelengths of the anomalies are about the size of the various structural elements. In the western and northern Java Sea, and especially over the Singapore Platform (Profiles 1-5), the situation is different. While the seismic and magnetic data indicate that the basement is intruded by many small bodies with high susceptibility and seismic velocity, the gravity data with their few large anomalies probably reflects deeper structures. The lack of agreement between the basement bodies and the gravity anomalies suggests that these bodies are either too small to produce a significant anomaly or that they lack sufficient density contrast.

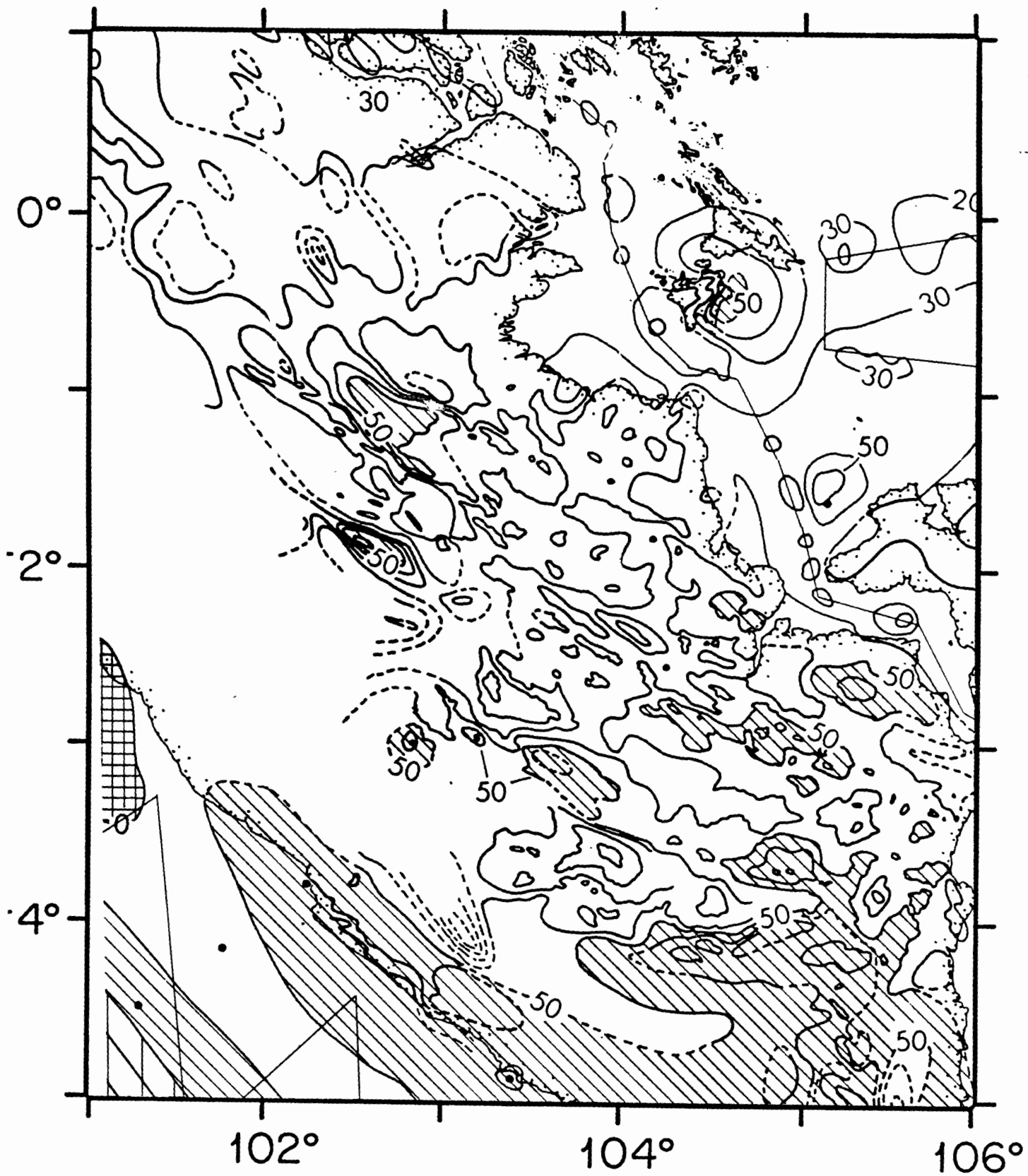
#### Gravity Anomalies over Land Areas.

Several prominent gravity features occur on land (Fig. 34). Large negative anomalies are centered over the East Java Basin (-60 mgal), the Barito Basin in Borneo (-30 mgal), and the North Sumatra Basin (-25 mgal). The only other site of such negative anomalies is between Sumatra and the outer non-volcanic arc (-65 mgal) where offshore exploration has confirmed the presence of sedimentary basins (Koesoemadinata and Pulunggono, 1971).

The negative anomalies are elongate parallel to the basins' axes. The anomaly over the Barito Basin is asymmetrical: to the west the contours are continuous and ellipsoidal, while to the east their trend is truncated against the belt of high gravity over the Meratus mountains. This suggests that a deep fault separates the Barito Basin from the Meratus mountain range. It is interesting that the South Sumatra Basin with about 4 km of sediment has no large negative anomalies. A very interesting feature shown in the South Sumatra Basin is a lineation of gravity anomalies that forms an angle of  $15^\circ$  with the elongation of Sumatra (Figs. 34 and 35). This lineation is associated with the Palembang Anticlinorium, the most prominent of three major anticlinoria that cross the South Sumatra Basin. The anticlinoria are the result of compression during the Plio-Pleistocene (Wennekers, 1958) that probably destroyed an original negative gravity anomaly over the basin.

Other interesting features are the belts of Bouguer gravity high above the Meratus mountain range and the Pulau Laut Ridge (Fig. 34 and Profile 21). These belts indicate that the crust does not thicken sufficiently under the ridges to make them isostatically compensated. A similar situation exists on Java, where the row of active

Figure 35. Bouguer anomaly map of the South Sumatra Basin and vicinity. This is an enlargement of the inset shown in Figure 34.

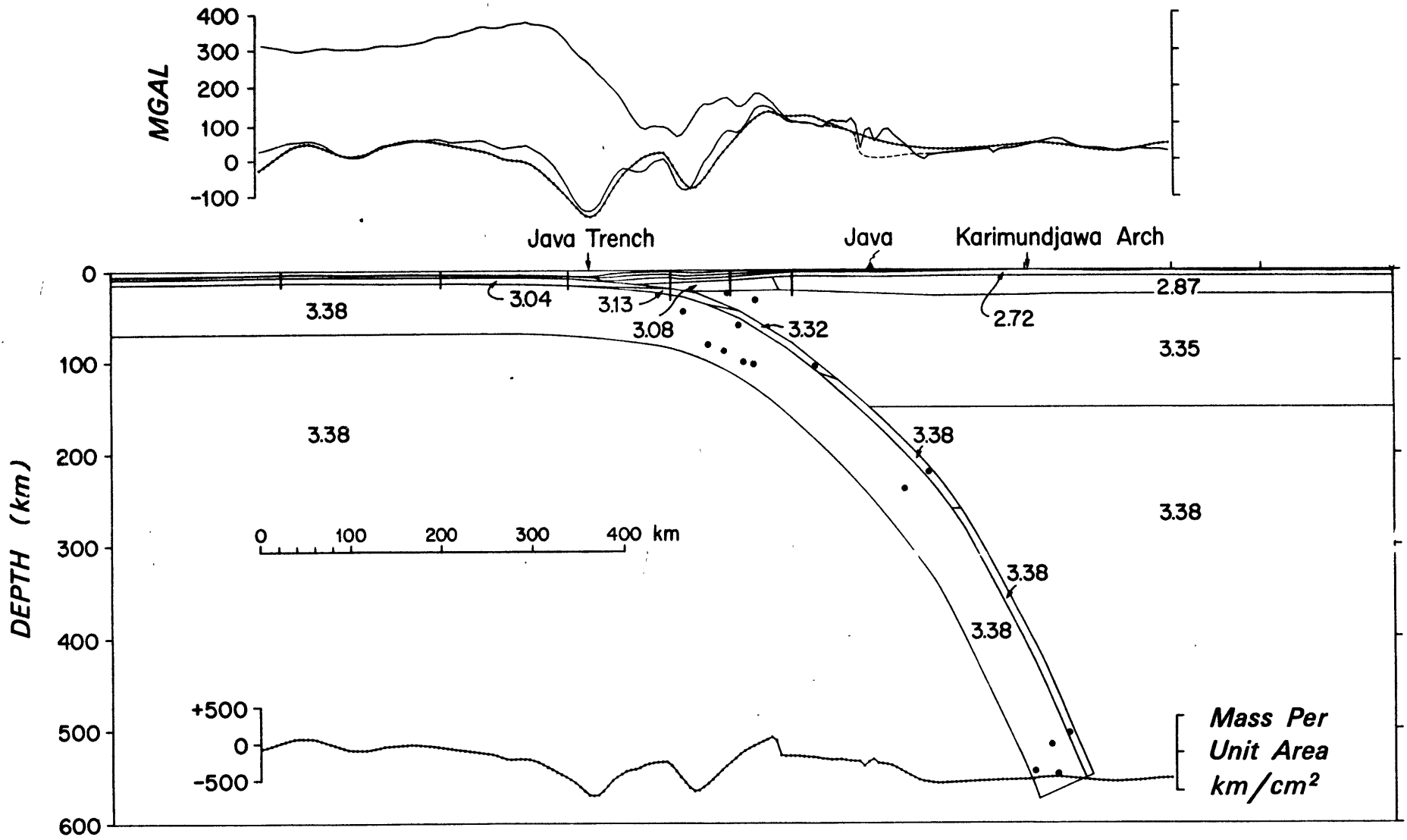


volcanoes does not coincide with the minimum Bouguer anomaly axis but lies south of it. The gravity minimum is approximately coincident with the axis of the greatest thickness of sediments in the East Java Basin. The free-air anomaly over the volcanoes in Java increases to +150 mgal, indicating a mass excess in this region. A large free-air anomaly is also shown on the south end of Profile 22 over the Lombok Strait (between the islands of Lombok and Sumbawa). On Sumatra at least part of the row of active volcanoes coincides with a belt of gravity minimum that is shown even more clearly on an isostatic anomaly map by De Bruyn (1951). Accordingly, the volcanoes on Sumatra may be in a different evolutionary stage than those on Java.

#### Crustal Model

A north-south structure model across the Java Trench, Java Island and Java Sea along longitude  $110^{\circ}45'E$  (Fig. 36) was constructed on the basis of seismic refraction, bathymetric and gravity measurements. It runs parallel to the seismic section shown in Figure 15. The model is based on the assumption that the Indian Ocean Plate is underthrusting the Asian Plate along the Java Trench, as indicated by a

Figure 36. Structural model across the Indonesian Island Arc. No vertical exaggeration. Numbers indicate the density of various portions of the model in grams per cubic centimeter. Vertical lines indicate the locations of seismic refraction profiles. Dots indicate the location of hypocenters for earthquakes in the period 1961-1968. Upper profile is the complete Bouguer gravity anomaly calculated assuming two-dimensionality of the bathymetry, dashed line is the simple Bouguer gravity anomaly above Java, lower solid line is the free-air gravity anomaly and the solid line with dots is the free-air anomaly calculated from the structure model and referenced to the observed free-air value at 180 km south of the trench axis. The mass per unit area profile at the bottom of the figure is calculated from the structural model.



dipping zone of earthquakes, the active volcanoes that show northward increase in the potassium-silicon ratios (Hather-ton and Dickinson, 1969), the increasing depth to the acoustic basement (Bowin and Ben-Avraham, 1972), and the large negative gravity anomalies over the trench. Earthquake hypocenters, seismic refraction stations south of Java (Raitt, 1967), and sonobuoy stations in the Java Sea within 100 km of the profile were projected to the location of the profile. The dip and extent of the underthrusting lithosphere were determined by the configuration of the earthquake zone, the crustal structure over the deep sea is from refraction data, and the shallow sediment structures above the basement in the Java Sea from the sonobuoy results. Figure 15 shows the shallow crustal structure. The gravitational attraction of the structural model was computed using the polygon technique described by Talwani, et al., (1959); the density of the polygons for which seismic velocities are available were obtained using Nafe-Drake empirical relationship (in Talwani, et al., 1959); the basement density over the Java Sea was determined from six basement samples (see Appendix II, Table 3). The calculated gravity anomaly is referenced to the observed free-air anomaly value 180 km south of the trench axis. Also shown are variations in the mass per unit area of the model.



Two major problems exist with the model. First, the location of the profile was controlled by the only published gravity profile across Java (Yokoyama, et al., 1970). It is, however, not an ideal place for a two-dimensional gravity model as the free-air anomalies between the Java Trench and Java, are much smaller than the sections at the east and west (Fig. 33). Secondly, the structure model shows a large mass deficiency under the shelf compared to the deep sea at the south. This seems to be unjustified in view of the fact that the average free-air gravity value over the shelf is +30 mgal. Therefore the model is probably poor and does not reveal the true structure. The mass deficiency does not result from the crust-mantle boundary as several different depths of this boundary with or without a layer with lithospheric density ( $3.35 \text{ g/cm}^3$ ) gave the same results. Increasing density of the oceanic lithosphere also could not resolve this mass deficiency. A low velocity (and density) zone beneath the lithosphere similar to the one used recently by Bowin (1972) and Grow (1972) in gravity models would tend to increase the mass deficiency. Deep structures in the mantle may cause this mass anomaly. As no information is available yet on deep structures in this area, the problem remains unsolved. The model does suggest

however, a few features concerning the structure of the upper 50 km.

The model shows that in order to be consistent with the seismic-refraction information the density of the oceanic crustal material ( $3.04 \text{ g/cm}^3$ ) must increase with depth during underthrusting. One other feature of the model is the existence of a layer with density of  $3.08 \text{ g/cm}^3$  between the crustal layer under the Java Sea and the descending oceanic crust. The thickness of this layer (about 12 km) was determined by seismic refraction (Fig. 15). The dimensions and density of this layer suggest that it may be a piece of oceanic crust. The distance between the Java Trench to the volcanoes is about the same (300 km) as the distance between the northern boundary of the  $3.08 \text{ g/cm}^3$  layer and the Karimundjawa Arch. This leads to the speculation that a previous site of underthrusting was situated along the northern boundary of the  $3.08 \text{ g/cm}^3$  layer, with the Karimundjawa Arch being a former magmatic arc. Later on, the subduction zone gradually shifted to its present position. This interpretation of the Karimundjawa Arch is in agreement with the geophysical measurements over it. The interpretation of the  $3.08 \text{ g/cm}^3$  layer as a piece of oceanic crust can also resolve the difficulty that Raitt (1967) noted: that Layer 3 seems to continue beneath the

island of Java (see p. 81). In the northern Sunda Shelf a crustal layer with a similar thickness and possibly similar velocities has been identified in one refraction profile (see p. 76). This layer may also be a piece of old oceanic crust, but not the same layer as shown by the model, as it does not extend beneath the central Java Sea. Evidently some portions of the Sunda Shelf may be underlain by pieces of oceanic crust. An extensive deep seismic refraction survey can help in understanding the nature of the crust beneath the Sunda Shelf and can check the validity of the hypothesis presented above.

One of the main uncertainties of the model is that the depth to mantle beneath the Java Sea is unknown. A possible fit with the observed data can be achieved by a crustal layer with density of  $2.87 \text{ g/cm}^3$  and depth to Moho of 35 km. If, however, one introduces a continental lithosphere, as in Figure 36, the depth to the Moho is smaller. The thickness of the crust under the Java Sea, then, is basically determined by the shape and density of the lithosphere. Since deep seismic refraction results in the northern Sunda Shelf show the Moho to be about 20 km deep, the second solution may be more realistic. In the solution presented in Figure 36 one possible configuration with a continental

lithosphere is shown. In Chapter VI below, the possibility is discussed that the central and eastern Java Sea and Java Island as well as some parts of the northern Sunda Shelf were built by accretion of the continental margin by the seaward migration of subduction zones. If this is correct, it may explain the intermediate crust found by the seismic refraction studies and presented in the structural model. The fact that the Java Sea is presently part of the Asian Plate (Fitch, 1970) and that it is surrounded by the old land masses of Borneo, Sumatra and Malay Peninsula may justify the presence of a continental lithosphere lighter than an oceanic lithosphere under Sunda Land. In Figure 36, the down-going lithospheric slab is shown as cutting across the bottom of the continental lithosphere directly below the site of active volcanism on Java. Bowin (1972) found somewhat similar situation in the Lesser Antilles and suggested that the low velocity zone (which lies immediately beneath the lithosphere) may be the principal source of magma for the surficial volcanism.

#### BASEMENT PETROLOGY

Offshore exploration in Indonesia in recent years has resulted in extensive drilling of the Sunda Shelf (Humphrey, 1971; Tanner and Kennett, 1972), but the results are

proprietary and not available, with the exception of the short report by Todd and Pulunggono (1971) on some drill holes in the western Java Sea. These authors state that the "basement in the basinal area consists primarily of low grade pre-Tertiary metamorphics and late Cretaceous igneous rocks", but they give no further details. The only other information about the basement rocks is from the islands on the Sunda Shelf (van Bemmelen, 1949, p. 303; and Haile, 1970).

For the present work six basement samples from oil company wells were available, plus some information on about thirty other basement samples from the southern Java Sea. The positions of the six basement samples are shown in Figure 37, and their thin-section descriptions are given in Appendix II. All the rock samples (except sample VI) reveal low grade metamorphism and seem to have originated as sedimentary rocks. They can be divided into two groups: the first, consisting of samples I, II, and IV have poor sorting indicating rapid deposition and relief in the environment of deposition. The relief may be tectonic and/or volcanic. They were taken from sedimentary basins and their metamorphism is probably the result of sedimentary load. The second group with samples III and V (Fig. 37)

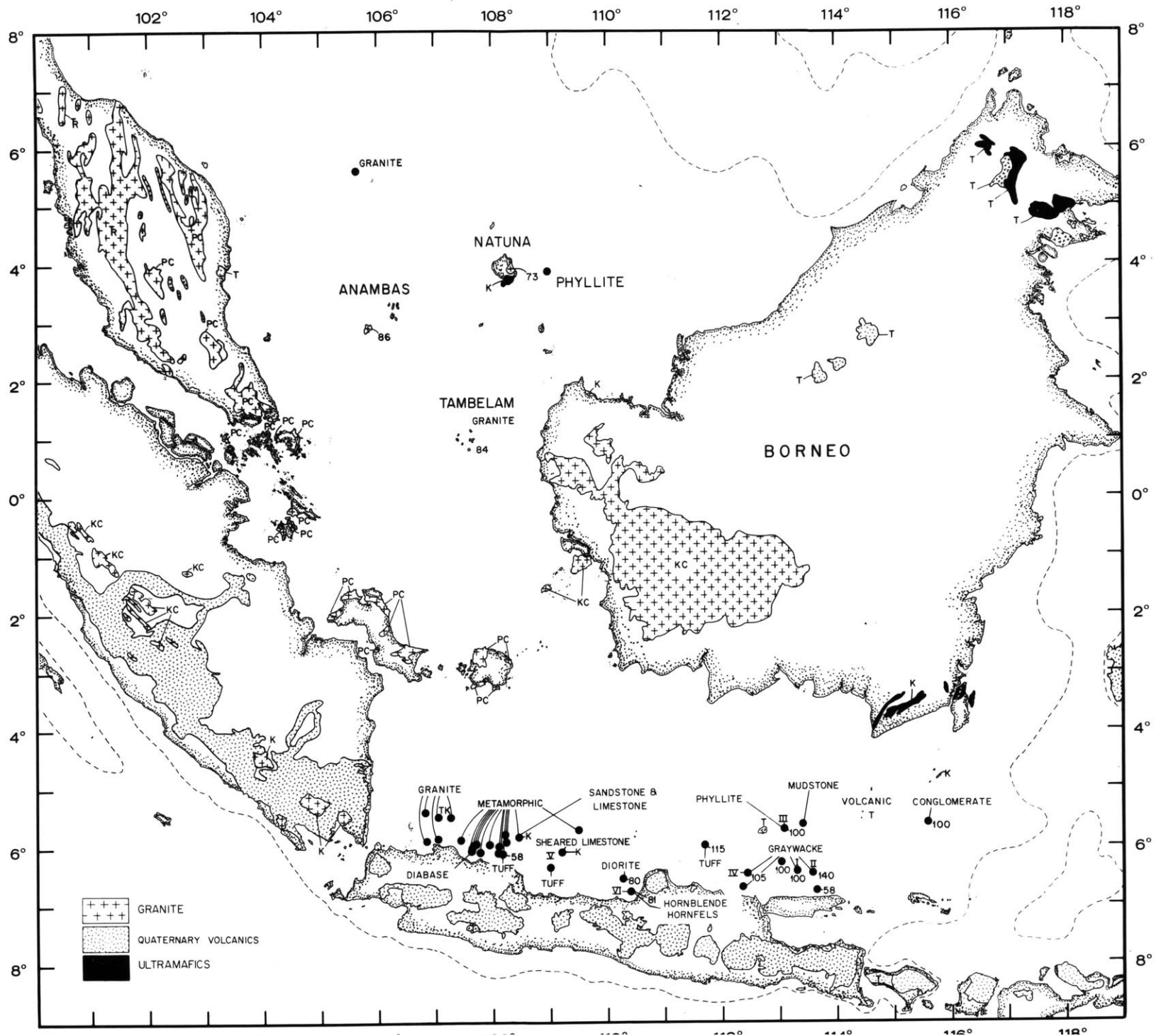
originated as shelf deposits and were subsequently deformed.

Sample III is from the southern flank of the Bawean Arch and contains evidence of compression. Sample V also shows evidence for directional deformation. This sheared sample comes from the southern flank of the Karimundjawa Arch.

Sample VI is somewhat ambiguous, it may have originated like III and V as a shelf deposit that later underwent thermal metamorphism, but it may also be of igneous origin.

These six rock samples are what one might term "continental rocks", unrelated to oceanic crust. Due to the nature of oil exploration the basement samples usually are from deep sedimentary basins and not from the ridges or from places where the basement is shallow. The nature of the basement is shown in Figure 37, which is based on available well data and outcrops on the islands. Various elements in this map will be discussed in the next chapter (V).

Figure 37. Basement information. Solid circles indicate position of offshore drill holes. Two-digit numbers indicate age in millions of years; T, Tertiary; TK, upper Cretaceous-Eocene; K, Cretaceous; KC, early Cretaceous through Carboniferous; R, Triassic; PC, Permian and Carboniferous. Roman letters I-VI identify the position of basement samples discussed in Chapter IV and in Appendix II. Igneous rock outcrops of land and the islands on the Sunda Shelf are from Klompé and Sigit (1965), Haile (1970) and Hamilton (1972a).





## CHAPTER V

## STRUCTURAL ELEMENTS OF THE SUNDA SHELF

The geophysical results discussed above, combined with geological data from outcrops on land and drill holes on the sea floor (Fig. 37) reveal the gross structure and lithology of the large Sunda Shelf. Although ambiguous relations exist between physical properties and certain rock types, some relationships between geophysical anomalies and specific lithic units have been established. For example, mafic or ultra-mafic masses have high density and high magnetic susceptibility, and thus they cause high gravity anomalies, high magnetic anomalies, and high seismic wave velocities.

The Sunda Shelf can be divided into three major units: the northern Sunda Shelf basinal area, the Singapore Platform and the Java Sea basinal area (Figs. 38, and 39). The subbottom structure of all three units contains major faults and uplifts that probably resulted from past interaction between lithospheric plates. In recent years considerable discussion of the impact of plate tectonics upon continental geology has been published (Coleman, 1971; Coney, 1970; Dewey and Bird, 1970, 1971; Dickinson, 1970, 1971; Ernst, 1970; Hamilton, 1969; Mitchell and Reading,

Figure 38. Structural map on top of basement. Based on the seismic reflection and gravity information of Figures 18-24; Todd and Pulunggono (1971); Cree (1972); Parke, et al., (1971) and other information in the northern Sunda Shelf described in the text. Contours are in kilometers, assuming sediment velocity of 2.0 km/sec.

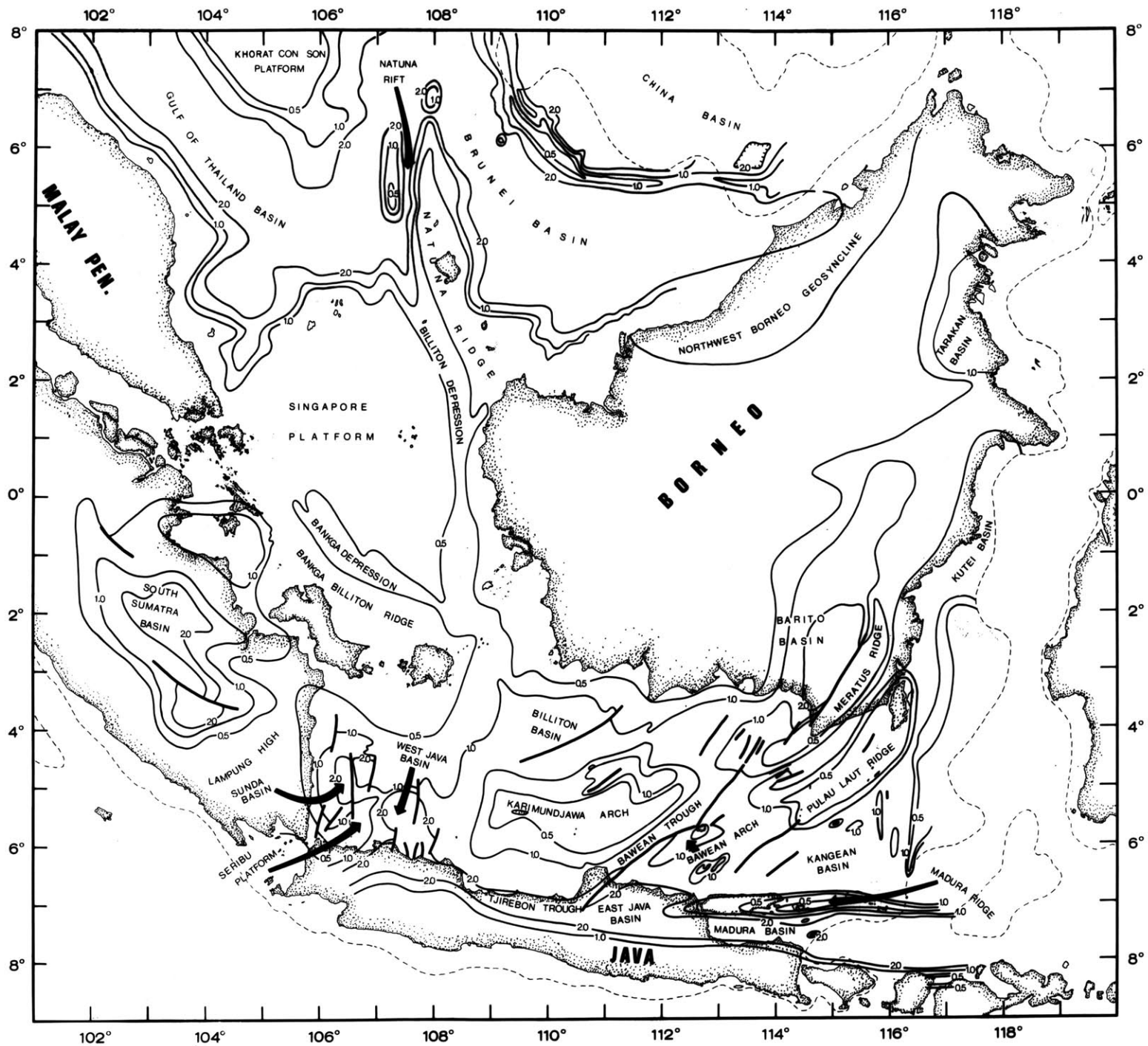
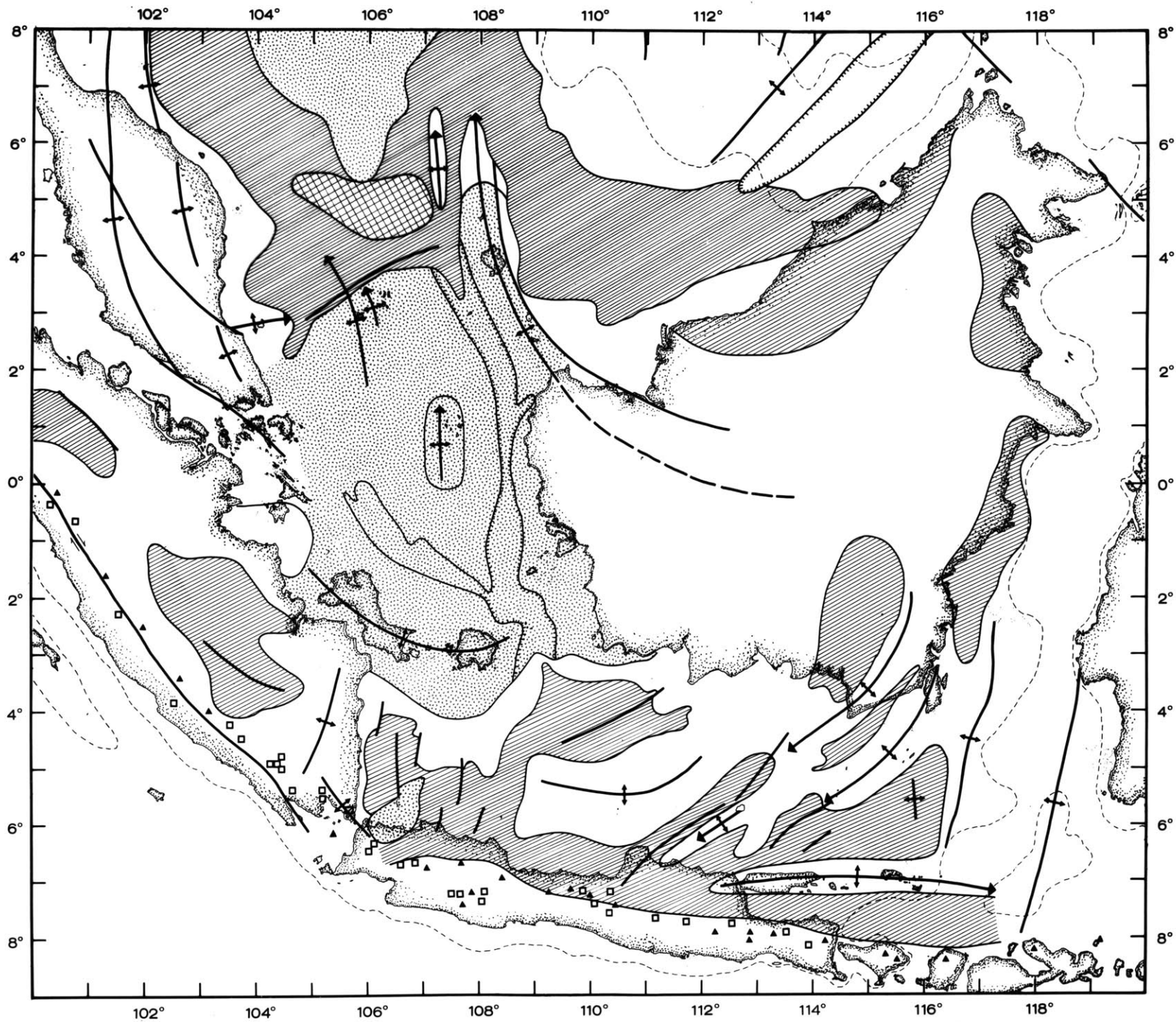


Figure 39. Tectonic elements over the Sunda Shelf and vicinity. Based on the structural map of Figure 38 plus data from Koesoemadinata (1969); Mainguy (1968, 1970, 1971); Alexander (1962); and Klompé and Sigit (1965). Quaternary (squares) and active (triangles) volcanoes from Hamilton (1972a). Single hatching designates basin areas contain more than 1 km of sediments, double crosshatching designates area of "diapir"-like structures in the Gulf of Thailand Basin and stippled areas denotes platforms.



1971; and others). In this section the various structural elements of this area will be discussed, and will be related, when possible, to the over-all process of plate tectonics.

#### FAULTS

The most prominent structural elements on the Sunda Shelf are faults which clearly control the basins' distribution. Most faults are inactive at the present; some may have originated as strike-slip faults, but others are definitely normal faults.

In the northern Sunda Shelf area, one of the most striking tectonic features is the Sarawak fault. It extends from central Borneo well into the Sunda Shelf along the northern flank of the Natuna Ridge (Yanshin, 1966; Tjia, 1970; Dash, 1971, and Figs. 8, 27, 39) and is associated with large negative magnetic anomalies having very sharp gradients. Field evidence led Tjia (1970) to conclude that left-lateral transcurrent movement along this zone may have started before late Jurassic times. The alignment of the Sarawak and Hanoi (along the Red River in North Vietnam) fracture zones in the reconstruction of Figure 8 suggests that they were once part of the same fault system.

In the western Java Sea large normal faults form a series of fault blocks. Tertiary fault movement occurred primarily during the Oligocene and very early Miocene and continued through the middle Miocene. Offshore drilling shows at least 1300 m of displacement during this period along the east flank of the Sunda Basin (Todd and Pulunggono, 1971). The tectonic pattern of the western Java Sea thus resulted from tensional forces during the Oligo-Miocene. The orientation of the faults and other structural axes in the western Java Sea is north-south, at right angles to the modern elements of the double arc.

In the Eastern Java Sea large faults trend to the northeast, paralleling the major structural elements in this area. These faults may have originated as strike-slip faults (Koesoemadinata and Pulunggono, 1971) but some differential vertical movement must also have occurred.

Other inactive transcurrent faults across the elbow-like feature in the Malay Peninsula and between Borneo and Palawan Island were discussed earlier (see p. 39, 56). In addition, a northwest-trending inactive left-lateral fault more than 1000 km long that bisects the southern Malay Peninsula (Fig. 39) has been recognized by Burton (1965).

Presently, several of the earth's most extensive zones of transcurrent faulting are located around the Sunda Shelf. The axis of the 1650 km long Semangko fault-zone (van Bemmelen, 1949, p. 685) lies along Sumatra. Katili (1970) demonstrated a right lateral movement along this fault starting in late Tertiary after earlier vertical movement along this zone. The median zone of central Celebes is cut obliquely by a north-northwest trending 200 km long fault zone known as the Fossa Sarasina (van Bemmelen, 1947, p. 407). Katili (1970) interpreted this fault as a left lateral transcurrent fault. It is unclear when the movement along this fault started (Katili, 1970). The fault is still active, as inferred from the focal mechanisms of shallow earthquakes along its length (Fitch, 1972). Another major transcurrent fault is the 1200 km long Philippine fault zone. This left-lateral fault is presently active (Allen, 1962), but faulting may have started as early as the Mesozoic (see discussion in Chapter III).

#### STRUCTURAL HIGHS

Two basic kinds of structural highs exist over the Sunda Shelf. Structural highs in which two-dimensionality can be recognized are termed "ridges". Highs having no two-dimensionality are termed "platforms".



a. Ridges: Natuna Ridge is the most prominent ridge in the Northern Sunda Shelf. The ridge is a direct continuation of the Semitau zone on Borneo (see p. 118). On Borneo, the association of radiolarian cherts and ophiolites of the Danau Formation along the Semitau zone was attributed by Molengraaff (1913) to deposition in "a narrow very deep sea". Coarse clastic sediments and ophiolites are present in what appears to be a deep-sea facies, suggesting that the Danau Formation may mark a former subduction zone. Natuna Islands show a close resemblance in geology to West Sarawak (the extreme west of Borneo). The Bunguran Formation of the Natuna Islands also contain radiolarian cherts and ophiolites and are correlated with the Danau Formation of Borneo (van Bemmelen, 1949, p. 225). The age of the Danau Formation is somewhat questionable, but there are some indications that it may be Jurassic or early Cretaceous (Kobayashi, 1944; Haile, 1970). According to Coleman (1971), ophiolite complexes may result from the initial stage of orogeny between oceanic and continental lithospheric plates. It seems therefore that the Natuna-Semitau Ridge was a subduction zone which became active in the late Jurassic to early Cretaceous. If one accepts a north-south opening of the China Basin (see p. 48), the most logical explanation for this subduction zone is that it was associated with the

sea floor spreading inside the China Basin.

The Natuna Ridge is associated with large magnetic anomalies (Figs. 27, 30, p. 127). The model studies of Figure 31 required susceptibilities of .03 - .06 cgs. These high values may be caused by the ophiolite complexes on the Natuna Ridge. Recent measurements of the susceptibility of pillow lavas (one of the major constituents of an ophiolite complex) from the Mid-Atlantic Ridge (de Boer, et al., 1969; Irving, et al., 1970) and from Cyprus (Moores and Vine, 1971) suggest that their susceptibility may be .05. In their study of the magnetic anomalies in the western Mediterranean, Vogt, et al., (1971) assumed a susceptibility of .03 for model studies of ophiolite belts. These values are comparable with the results of Figure 31.

The polarity of the subduction zone along the Natuna Ridge is unknown. However, the regional tectonics (see Chapter VI) suggest that the underthrusting was from the south. During late Cretaceous granites were emplaced in Natuna Island and in west Sarawak (westernmost Borneo) (Haile, 1970). Late Cretaceous granites are not confined to the Natuna-Semitau Ridge but also occur in the Tambelan and Anambas Islands on the Sunda Shelf (Haile, 1971). The emplacement of these granites may mark the last stage of activity of the subduction zone along the Natuna Ridge.

Bordering the Singapore Platform on the south is the Bangka-Billiton Ridge. Bangka and Billiton Islands are composed of tin-bearing upper Paleozoic-lower Mesozoic granites. A granitic basement between Bangka and Billiton (Untung, 1967) is consistent with the geophysical profile between these islands (center of profile 6, Fig. 19) that shows a very flat magnetic field, a relative gravity low and a basement velocity of 4.70 km/sec. The Bangka and Billiton granites are the southernmost extension of the so-called "tin belt" granites, which have their major development in the Malay Peninsula (Alexander, 1962). On the Malay Peninsula the granites (with tin) are arranged in two belts, the Eastern and Western Tin Belts. The age of the Bangka and Billiton granites is unclear, though it once was considered to be 180 m.y. and served as an important marker in the geological time scale to define the Jurassic/upper Triassic boundary (Holmes, 1959), and it has been listed as item 71 in the Phanerozoic Time Scale (Harland, et al., 1964). However, Edwards and McLaughlin (1965) and Hutchinson (1968) showed that the emplacement of the "tin belt" granite was much more complex and occurred over long periods from the Permian to the Cretaceous. More recently, Snelling, et al., (1968) and Hosking, (1972) showed that

that granites of the Eastern Belt on Malay Peninsula may be dominantly upper Carboniferous whereas those of the Western Belt appear to be mainly of Triassic age. The granite of Bangka and Billiton islands has a close affinity to that of the Eastern Belt and may also be mainly upper Carboniferous in age. Obviously the granitic masses owe their existence to more than one period of acid igneous activity. The Bangka-Billiton Ridge probably marks the southern edge of an old island arc (Katili, 1967) which extended along the "tin belt" granite. The tin belt does not continue into western Borneo or to the Karimata Islands (van Bemmelen, 1949, p. 325; W. Hamilton, personal communication).

The dominant ridge in the central Java Sea is the Karimundjawa Arch which strikes northeast-southwest in its eastern part and east-west in its western part. The Karimundjawa Islands on this ridge consist of pre-Tertiary metamorphic sediments (van Bemmelen, 1949, p. 321). Some similarities between geophysical parameters across the Bangka-Billiton granite and the Karimundjawa Arch (Figs. 19, 20) suggest the ridge may be a granitic batholith, though it could consist entirely of metamorphic sediments just as well. The flanks of the arch (Fig. 20) are associated with

local magnetic and positive gravity anomalies that may be caused by intrusion of basic dikes. This is consistent with the work of Kane (1970) who reported that felsic plutons in the Gulf of Maine are associated with magnetic aureoles.

The northwest trending ridges in the eastern Java Sea, the Meratus Ridge, the Pulau Laut Ridge and the Bawean Arch (Fig. 38) probably are part of a remnant arc system. The first two ridges continue north as the Meratus mountains in southeastern Borneo and the Pulau Laut Island. The Meratus mountains consist of ultrabasic rocks (serpentinized peridotites and gabbros) as well as radiolarian cherts (van Bemmelen, 1949, p. 339-353), that Hamilton (1970, 1972) interpreted as subduction melanges of late Cretaceous-Paleogene age. Pulau Laut Island has a similar composition except that it contains some volcanics in addition. On the Sunda Shelf, the Maselambo Islands (Fig. 11) that form the southern limit of the Pulau Laut Ridge, are composed of Tertiary volcanic rocks. Bawean Island atop the Bawean Arch consists of alkaline volcanics of Tertiary age. The Bawean Arch plunges to the southwest and seems to be continuous with the extinct Muria volcano on northern Java (approximately Latitude  $6^{\circ}30'S$ , Longitude  $110^{\circ}55'E$ ). On west-central Java

late Cretaceous-Paleogene subduction melanges are exposed in several areas (Hamilton, 1972; Tjia, 1966; van Bemmelen, 1949, p. 603; and others). Hamilton (1972) suggests that this subduction zone is the southern extension of the subduction zone along the Meratus mountains.

Geophysical profiles over the three northeast trending ridges in the eastern Java Sea (Fig. 20-22) show that the Meratus Ridge is characterized by magnetic anomalies of province 1 similar to those associated with the Natuna Ridge whereas the Pulau Laut Ridge and possibly the Bawean Arch are characterized by sharp magnetic anomalies of magnetic province 2 (see Chapter IV) that may indicate basalt flows on the ridge tops. A basement sample from the flank of the Bawean Arch (sample III, see discussion in Chapter IV) indicates that this structural element resulted from compression.

Geophysical data from the sea plus geological data from the islands and land discussed above suggest that the northeast trending tectonic elements in the eastern Java Sea may be part of an arc system which was active during the late Cretaceous-very early Tertiary. The proposed strike-slip faults in the eastern Java Sea (Fig. 38; p. 175) may thus be due to an oblique convergence similar to the one that causes the great Sumatran fault (Fitch, 1972).

The direction of subduction along this arc system is not revealed by local geological evidence. One possibility is that this was a double arc in which the Meratus mountains and the pre-Tertiary melanges on Java is the subduction zone and the Pulau Laut Ridge and the Bawean Arch are the volcanic arc. This would indicate subduction toward the southeast. The main difficulty with this interpretation is that no continuity exists between the Meratus mountains and the melanges on central Java. If, however, the Pulau Laut Ridge and the Meratus Ridge are subduction zones resulting from underthrusting to the northwest, then the Karimundjawa Arch may be part of the magmatic arc. Its proposed granitic composition may be due to emplacement during the last stage of underthrusting. This interpretation may be more correct because the subduction zone later migrated to Celebes (see below), a fact that would explain the volcanism on the Pulau Laut Ridge.

Superimposed on the old northeast ridges discussed above is the east-west trending Madura Ridge. On the west the ridge starts as the Rembang Anticlinorium on east Java and it extends eastward through the island of Madura and the Kangean Islands into the Flores Sea. The core of this ridge consists of marine Oligo-Miocene sediments of the

Rembang Beds (Schuppli, 1946) (Fig. 23), deformed and folded first during middle to upper Miocene, and later in the Pleistocene when the Madura Island and the Rembang Anticlinorium emerged from the sea. There is no evidence from the land geology that the Madura Ridge was either a subduction zone or a magnetic arc.

The three geophysical crossings over the Madura Ridge show variations in the geophysical characteristics from west to east. Overall the ridge is associated with a gravity high and variable magnetic anomalies; this may be consistent with folded sediments.

A similar origin may exist for the three basement ridges to the north of the present volcanic arc inside the Madura Basin (Profile 22, Figs. 24, 26). These ridges are associated with a large negative gravity anomaly and may be the eastward continuation of the Kendeng Anticlinorium in the east Java Basin which is also associated with a large negative gravity field (Fig. 34). According to van Bemmelen (1949, p. 571-584) the Kendeng Anticlinorium evolved in a way similar to the Rembang Anticlinorium except that the Kendeng Anticlinorium is situated above the deepest portion of the original sedimentary basin.



In the easternmost Java Sea are three parallel north-south structural highs. The easternmost of these is a barrier reef (U.S. Navy Hydrographic Office Chart 3001). The two small western structural highs have no major magnetic or gravity expression. Two sonobuoys close to these highs (38 and 39) gave basement velocities of 4.10 and 3.69 km/sec, indicating that they probably are old barrier reefs. They probably developed on the shelf break when it was farther to the west.

The magnetic data indicates a north-northwest trending ridge in the Flores Sea parallel to the southwestern arm of Celebes. This ridge is probably a subduction zone which migrated here from the Meratus mountains as indicated by the subduction melanges of the southwest arm of Celebes (Hamilton, 1972). This subduction zone may be associated with the rifting in the Makassar Strait and may be the cause of volcanism on the Pulau Laut Ridge.

b. Platforms: Platforms are structural highs without linear character. At the north, the Khorat-Con Son Platform is composed of granite, as indicated by the granitic islands situated on it (Hilde and Engle, 1967) and from drill hole data (Fig. 37). Hilde and Engle determined the age of this granite as late-Cretaceous (between 70 and 100

m.y.). This age implies a period of granite intrusion during the late Cretaceous over a large part of the northern Sunda Shelf (including the Natuna and Anambas Islands).

The Singapore Platform is the largest such feature and is situated in the middle of the Sunda Shelf, (Fig. 38). The platform is characterized by small basement "bodies" with high seismic velocities, by sharp magnetic anomalies, and by a rather smooth gravity field. Two deep north-south structures are postulated beneath the Singapore Platform (Fig. 39) associated with broad positive gravity anomalies and large negative magnetic anomalies (on which are superimposed shorter anomalies with sharp gradients). Geological studies of the Andaman and Tambelan Islands (Haile, 1970), which lie along these structural trends, show that they consist mostly of igneous rocks. A distinction can be made between an older (Mesozoic?) group of gabbros, diabases and andesites and a younger group of biotite granites which have been dated as late Cretaceous (84-86 m.y. by the potassium/argon method, Haile, 1971). The granites themselves are intruded by basaltic and andesitic dikes possibly of very early Tertiary age (Haile, 1970). These last events may explain the presence of the rough magnetic field over the northern Singapore Platform.

The Singapore Platform can be divided into two parts on the basis of the magnetic field (Fig. 30). Over the southern part the sharp magnetic anomalies of magnetic province 2 are absent. The reflection profiles confirm this difference between the northern and southern areas. Whereas in the north the basement is composed of many small bodies (Profile 1, Fig. 18), in the south the bodies are fewer and the basement is deeper (Profile 3, Fig. 18). The magnetic anomalies over the southern part (which were categorized as province 5) may be the result of the pre-granitic basement that is exposed on the Tembelan and Anambas Islands as their nature rules out the possibility that they are caused by a granitic basement. It was stated earlier that the magnetic anomalies of province 5 resemble oceanic magnetic anomalies. The nature of the pre-granitic basement (basic intrusives such as gabbro and diabase) shows some affinity to an oceanic crust, and might cause similar anomalies.

At the south, the small Seribu Platform has a low magnetic field and a gravity high over its western side (Profile 7, Fig. 19). Oil company drill holes (Fig. 37) on this platform penetrate a late Cretaceous granite. Mesozoic granites have not been found on Java (Katili, 1972), implying that the Seribu Platform may be the continuation of the Cretaceous granite belt on southern Sumatra

(Katili, 1962; Fig. 37). The seismic reflection data clearly indicate the Seribu Platform to be a fault-block.

## BASINS

The sedimentary basins can be classified according to their position relative to subduction zones, magmatic arcs and other tectonic features. Where an oceanic plate underthrusts other plates two sedimentary basins usually occur. One is a basin between the trench and the volcanic arc, the "arc-front basin"; the other is behind the volcanic arc, the "foreland basin" (terminology after Hamilton, 1972a).

Starting at the north, the northeast trending portion of the Brunei Basin is part of the Northwest Borneo geosyncline (Fig. 38). The paleogeographic setting of the Northwest Borneo geosyncline has been a subject of controversy ever since the feature was first described by Liechti, et al., (1960). It is now thought (Chung, 1968) that the Northwest Borneo geosyncline started to develop in the late Cretaceous with the deposition of shale, sandstone, and chert associated with ophiolites. The axis of deposition moved northwestward toward the present coastline. The geosyncline was interpreted to be an early and middle Tertiary

melange, formed by subduction to the southeast (Haile, 1972; Hamilton, 1972), that migrated gradually to the northwest. The Palawan Trough (Fig. 8) probably marks the final position of the subduction zone. As the subduction zone migrated, intense folding of the sediments of the arc-front basins took place. The northeast portion of the Brunei Basin is the last arc-front basin situated to the southeast of the Palawan Trough

The northwestern portion of the Brunei Basin is parallel to the Natuna Ridge. If the underthrusting along the Natuna Ridge was from the south, then this basin can be interpreted as a foreland basin. The basement is composed of phyllites and other metamorphic rocks of Cretaceous-Eocene age. This is the same age as that of the granitic intrusions on Natuna Island and other portions of the Northern Sunda Shelf, probably indicating that the metamorphism was somehow associated with the end of spreading in the China Basin.

The Gulf of Thailand Basin is probably at least as old as early Mesozoic, judging from the land geology on its margin (Kobayashi, 1960). No basement ages have been published so far, at least partly because recent oil exploration has revealed more than 7.5 km of sediments in its

center (Haile, 1972). The Gulf of Thailand Basin can be divided into several structural units but its history is probably complicated and the basin is difficult to classify in terms of a single environment of formation.

The western Java Sea contains two types of basins. Graben-like basins that include the Sunda and West Java basins resulted from tensional forces. Between these basins is the horst-like structure of the Seribu Platform. The other basins can be classified as foreland basins. The Tjeribon Trough, the South Sumatra Basin, and the southern part of the West Java Basin are situated behind the present magmatic arc and the Billiton Basin behind the Karimundjawa Arch, which is probably a magmatic arc of late-Cretaceous age (see page 183).

In the eastern Java Sea the only foreland basins are the East Java and Madura basins that are behind the present volcanic arc. The other basins (the Bawean Trough, the Barito Basin, the basin between the Pulau Laut and Meratus ridges, the Kangean Basin and the Kutei and Tarakan basins) (Figs. 38, 39), may have originated as arc-front basins due to the northeast trending subduction zones and volcanic arcs in this area (see page 183). Possibly the Madura Basin also started as an arc-front basin that became separated

from the Kangean Basin by the formation of the Madura Ridge  
in the Plio-Pleistocene.

## CHAPTER VI

## TECTONIC EVOLUTION OF THE SUNDA SHELF

## PREVIOUS THEORIES

Kuenen (1935) summarized the existing "explanation" of the structural features of the Sunda Shelf. At that time he had four so-called "geotectonic" maps by Brouwer, van Es, Staub and Smit Sibigna at his disposal. Since then many others have been added to the list, most of them engendered by the negative gravity anomaly zones of Vening Meinesz. All of them consist of a curved pattern joining islands and ridges. Some draw transcurrent faults; some prefer curves when the lines do not join very well; and in doubtful areas they differ in linking up the different islands.

van Bemmelen (1954) discussed the tectonic evolution of the Sunda Shelf as an example for the process of mountain building. According to his hypothesis which was accepted for many years, the orogenic evolution started from distinct centers of diastrophism along the Anambas geosyncline and spread in parallel belts to both the north and south. The mountain systems which developed from this center were grouped into seven parallel zones of 100-300 km width, all



convex to the southwest. Part of the "success" of the theory was that the major part of the seven zones was above water when nothing was known about the subbottom structure. On land, in order to satisfy his hypothesis, van Bemmelen (1949) had to assume that the migration from one zone to another sometimes reversed its direction and that the various orogenic events along a certain zone did not everywhere occur at the same time or with the same intensity. Recently Katili (1971) reviewed some of the geotectonic theories developed for Indonesia, and following Hamilton (1970), constructed a tectonic map based on a plate tectonic model.

The evolution of the Sunda Land must be connected with the tectonic evolution of the eastern Indian Ocean and the western Pacific Ocean. However, the entire southeast Asia is so complex that little is known from the point of view of plate tectonics (Tarling, 1972). In the various reconstructions of Gondwana, Laurasia and Pangea which appeared after the development of plate tectonics theory there is no agreement about the paleogeography of southeast Asia. Some reconstructors (e.g. Dietz and Holden, 1970) do not show the Indonesian Archipelago during the evolution of the supercontinents; others (e.g. Ridd, 1971) suggest that southeast

Asia was part of Gondwanaland and still others (e.g. Hamilton, 1972) propose that southeast Asia was attached to Eurasia at least since later Jurassic time.

#### PROPOSED EVOLUTION OF THE SUNDA SHELF

The structural elements discussed in the last chapter (V) owe their origin to major tectonic events that occurred in this area during the past. The advantage of the marine survey described above as compared to land surveys is that it revealed a relatively small number of structural elements in a very large area, making the interpretation relatively easy. In the rest of this chapter an evolutionary scheme that can best account for the structural elements on the Sunda Shelf and the major structural elements on the adjacent land area is developed. In reconstructing the evolution of the Sunda Shelf the following points were considered:

(1). In pre-Eocene time the Pacific plate migrated north-northwest until early Eocene (40 my) when the direction changed to west-northwest as evidenced by the bend of the Hawaiian-Emperor and other island chains in the Pacific (Morgan, 1972).

(2). At present we have no good hypothesis for the development of Wharton Basin south of the Sunda Shelf, as no sea-floor spreading magnetic anomalies have been recognized in

the area (McKenzie and Sclater, 1971). According to McElhinny (1970), Australia began to drift northward during the middle Cretaceous, although not until the Eocene (McKenzie and Sclater, 1971) was a significant separation between Australia and Antarctica reached. Recent Deep Sea Drilling Project results of Leg 22 (Scientific Staff, 1972) and Leg 26 (Luyendyk, personal communication) and detailed analysis of magnetic anomalies (Sclater, in preparation) show that both the sea floor and the magnetic anomalies in the Wharton Basin become older to the south. This means that an east-west ridge that formerly existed in the Wharton Basin was submerged in the Java Trench probably during the Eocene when the transform fault along the Ninetyeast Ridge stopped its activity (McKenzie and Sclater, 1971). Stoneley (1967) believed that the crust of the eastern Indian Ocean has been moving continuously to the north since the early Jurassic.

(3). The China Basin apparently originated by a north-south extension during the mid-Mesozoic (Ben-Avraham and Uyeda, in press).

(4). The Andaman Sea formed during the late Miocene by a northwest-southeast extension (Rodolfo, 1969) that is still in progress.

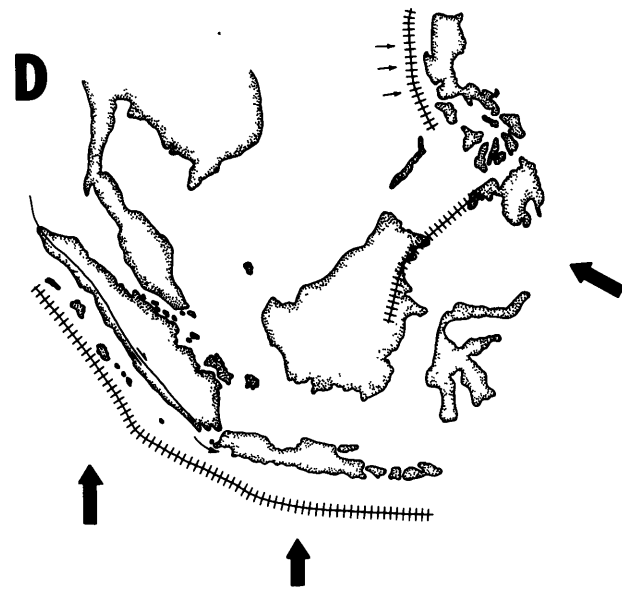
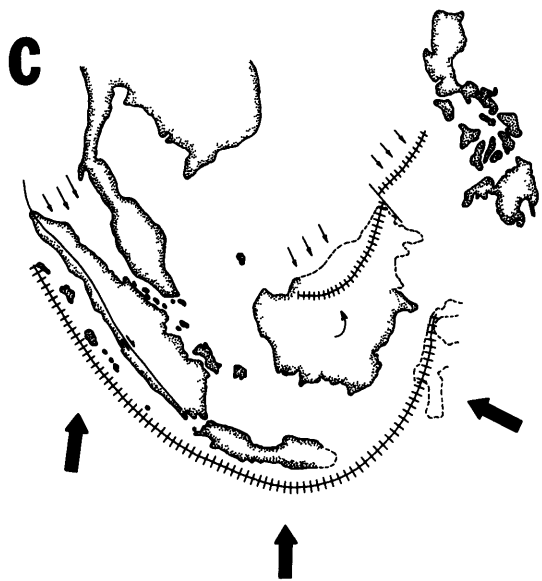
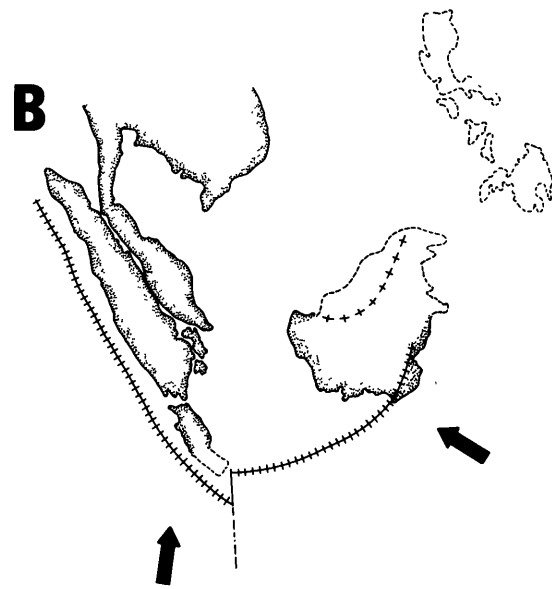
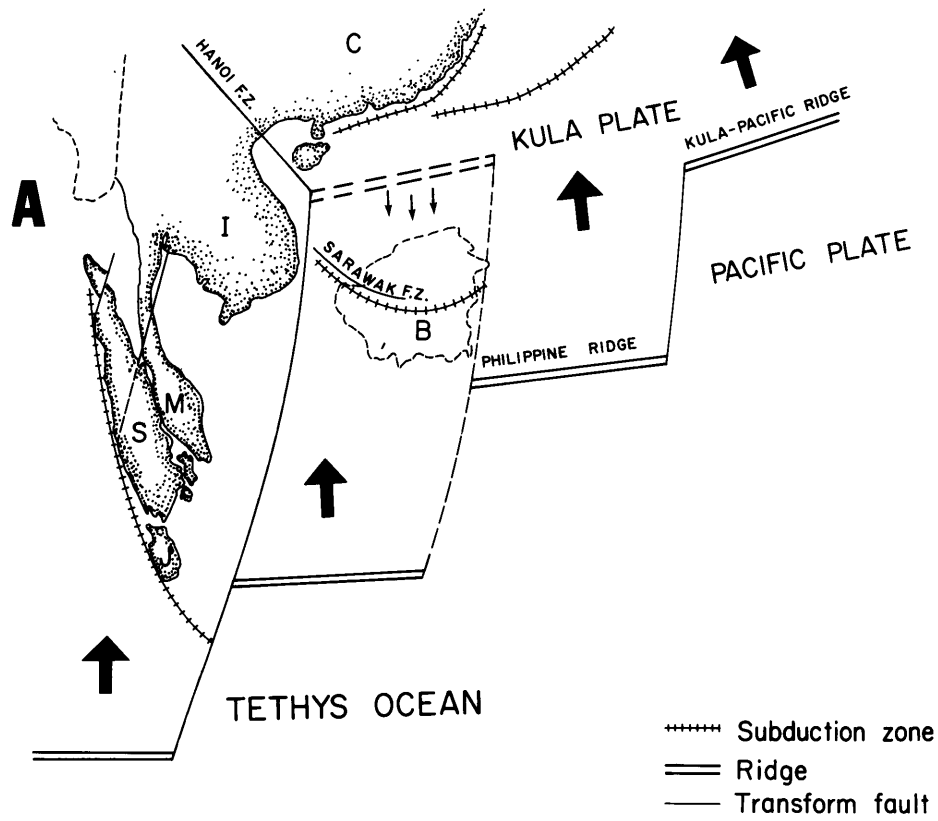
(5). The only paleomagnetic data obtained so far in the entire southeastern Asian region (Haile and McElhinny, 1972) indicate that the Malay Peninsula was at about  $20^{\circ}\text{N}$  in the late Paleozoic and Mesozoic.

All of southeast Asia retains evidence of past subduction zones and other plate-motion features from as long ago as Paleozoic (Hamilton, 1972). One of the most conspicuous examples is the pair of north-south granitic belts in the Malay Peninsula of upper Paleozoic-lower Mesozoic age that probably represent the positions of old magmatic arcs (Katili, 1967; Jones, 1968; Hutchison, 1972). The evolutionary model described in the following section, however, will start in the Cretaceous, since this is the extent of the record from the sea floor in the area.

#### Early-middle Cretaceous.

During early-middle Cretaceous Borneo was next to Mainland China and Hainan; Sumatra and west Java were situated northwest of their present position (Fig. 40a). Bangka and Billiton formed the southward continuation of the eastern granitic belt of Malay Peninsula. A spreading ridge south of Sumatra and Borneo caused a northward motion of the sea floor (of the postulated "Tethys Ocean"), which was absorbed by subduction zones along the Natuna Ridge (Fig. 38).

- Figure 40. A. Schematic sketch of possible arrangement of plates in Cretaceous time. Dashed line indicates less certain position of a spreading ridge and transform fault. Direction of motion indicated by arrows. Letters on land areas from north to south: C, mainland China; I, Indochina; M, Malay Peninsula; S, Sumatra; J, Western Java. B indicates former position of Borneo.
- B. Schematic possible state in late Cretaceous-early Eocene.
- C. Schematic possible state in middle Miocene.
- D. Schematic possible state in late Pliocene.



and along the Andaman-Nicobar Arc, southwest Sumatra, and west Java. The subduction zone along west Sumatra (Hutchison, 1972) and the Andaman-Nicobar Arc (Rodolfo, 1969) is marked by a known ophiolite belt. Structural continuities between southern Sumatra and western Java (van Bemmelen, 1949, p. 633) indicate that during this period the Sunda Strait did not exist and western Java was a direct continuation of Sumatra.

Various tectonic maps (e.g. Yanshin, 1966, Geological Institute, 1970) show a Mesozoic volcanic belt along the southern coast of Mainland China. It is postulated that the volcanic belt together with the granites behind it (Yanshin, 1966) and the subduction zone along the Natuna Ridge once formed the pair of a Pacific-type paired orogeny (Matsuda and Uyeda, 1971). A southward movement of Borneo started at that time.

Two possible configurations of spreading ridges exist (Fig. 40a). One possibility is that of two ridge systems, one of which consists of the Kula-Pacific Ridge and the Philippine Ridge and the other one situated south of Borneo, Sumatra and Java. The other possibility is of one mega ridge, which consisted of four major parts offset by north-south transform faults. It extended from the ridge south of

Sumatra on the west to the Kula-Pacific Ridge on the east. The dashed lines in Figure 40a indicate less certain positions of spreading ridges and transform faults. Three north-south transform faults that are indicated in Figure 40a are consistent with the northward motion of the Indian and Pacific Oceans during this period. The eastern fault was postulated by Uyeda and Ben-Avraham (1972) to extend along the Kyushu Palau Ridge, the middle (less certain) one along the present Philippine Islands (see p. 54) and the western one along the eastern faulted margin of the Indochina Peninsula (Mainguy, 1968; Yanshin, 1966), the Natuna Rift, the Billiton Depression and across central Java to the Wharton Basin (Fig. 38). All describe approximately small circles around a pole of rotation at Latitude  $13.0^{\circ}\text{N}$ , Longitude  $44.0^{\circ}\text{E}$  (Fig. 8). The Mesozoic transform fault along the Ninetyeast Ridge (McKenzie and Sclater, 1971) lying still further west, cannot have had the same pole of rotation.

#### Late Cretaceous-early Eocene

Several major events occurred during the late Cretaceous-early Eocene (Fig. 40b). The spreading ridge south of Sumatra and Borneo probably submerged under these islands



initiating the northward movement of Australia and the eastern Indian Ocean, and the termination of the activity of the transform fault along the Ninetyeast Ridge. Uyeda and Miyashiro (in preparation) show that the Kula-Pacific Ridge became submerged under the Japanese Islands at about 80 mybp. The submergence of the ridges might have caused an acceleration in the opening of the China Basin and the sea of Japan.

A possible consequence of the submergence during this time of spreading ridges along the margins of the Pacific Ocean may have been the change in direction of motion of the Pacific plate, as postulated by Morgan (1972). The Philippine Ridge is the only remnant of the entire ridge system, which formerly extended from the Wharton Basin to the northeast Pacific. The Philippine Ridge was at least 800 kilometers south of its present position when its activity stopped (Ben-Avraham, et al., 1972) probably as a result of the change in direction of motion of the Pacific plate (Uyeda and Ben-Avraham, 1972). The change in direction of motion of the Pacific plate may also explain the isolation of the Philippine Sea, as a new subduction zone initiated along the former transform fault along the Kyushu Palau Ridge (Uyeda and Ben-Avraham, 1972). The emergence of the Philippine Islands (Krause, 1966) and

Taiwan also occurred during this time.

The postulated submergence of a spreading ridge under Sumatra and Borneo may offer an explanation for the widespread emplacement of granite batholites of late Cretaceous-early Eocene ages in the islands on the Singapore Platform, western Borneo, the Khorat-Con Son Platform, Malay Peninsula and Sumatra (Snelling, et al., 1968; Hilde and Engel, 1967; Katili, 1962; Haile, 1970, 1971, and others), none of which form distinct belts. This event also may have uplifted the Singapore Platform, as the oldest sediments on top of the platform's basement probably are of Eocene age (Koesoemodinata and Pulunggono, 1971).

After the subduction of the ridges in the late Cretaceous, the subduction zone south of Borneo shifted to the southeast trending Meratus and Pulau Laut ridges and Bawean Arch, probably as a response to the change in motion of the entire Pacific Plate. The Karimundjawa Arch probably originated as the magmatic arc associated with this new subduction zone. The subduction zone in Sumatra and Andaman-Nicobar arcs shifted to the present position of the Mentawai Islands southwest of Sumatra, as the Indian Ocean-Australian Plate continued to move towards the north. Termination of underthrusting along the Andaman-Nicobar Arc

resulted in an uplift of the arc during this period (Rodolfo, 1969). The magmatic arc that accompanied the new subduction zone along the Mentawai Islands consists of the "old andesites" (van Bemmelen, 1949, p. 117) and the Cretaceous granites on the west coast of Sumatra, and the Seribu Platform in the western Java Sea (Fig. 37). The subduction zone southwest of Sumatra and the one in the eastern Java Sea probably were separated by a transform fault (part of the western fault in Fig. 40a). It seems that this is the time (late Cretaceous-early Eocene) when the separation between the Pacific Ocean Plate and the Indian Ocean Plate occurred, or, in terms of classical geology, when the Tethys Ocean disappeared in this area and the modern Pacific and Indian oceans originated.

#### Middle Miocene

During middle Miocene (Fig. 40c) the subduction zone in the eastern Java Sea migrated southeastward to a position between the western arm of Celebes (Hamilton, 1972) through the ridge in the Flores Sea (Fig. 39) and the submarine ridge south of Java. Subduction was associated with the rifting of Makassar Strait (Hamilton, 1970), as Celebes pulled away from Borneo. At the same period a southeast underthrusting along the Northwest Borneo geosyncline,

which started to evolve in the early Tertiary, reached its full development (Haile, 1968). As a result, Borneo might have rotated counter-clockwise toward Indochina, a movement that may explain the northeast-southwest trending sedimentary ridges in the southern part of the China Basin and also the tensional features in the western Java Sea basinal area. This movement was connected in an unknown manner with the intrusion of basaltic and andesitic dikes in the northern Singapore Platform (Haile, 1970) that gave rise to the sharp magnetic anomalies of province 2 (Fig. 30). The subduction zone along the Mentawai Islands shifted to the trench south of the islands, and resulted in an uplift of the Mentawai Islands as subduction stopped.

By that time the subduction zones south of Sumatra west and east Java were almost continuous and the transform fault between them stopped its activity. This may explain why during this period deposition became continuous throughout the entire Java Sea basinal area as illustrated by the widespread presence of the Batu Radja limestone. It is possible, however, that some differential vertical movement still occurred after the limestone deposition on both sides of the former transform fault, as there is no continuation of sedimentary layers with velocities 2.5-4.2 km/sec

(Fig. 13) from the eastern to western Java Sea. The magmatic arc of this system is composed of a Miocene granitic belt (Umbgrove, 1949) on Sumatra and Java. Termination of the horizontal differential movement on both sides of the transform fault caused the initial formation of the Sumatran fault zone, the southeastward movement of Sumatra and western Java, and the initial opening of the Andaman Basin. The movement of Sumatra might have caused the breaking of Bangka and Billiton away from the Eastern Tin Belt on Malay Peninsula.

#### Late Pliocene

The subduction and magmatic arc system trending southward and eastward from Java had reached its present position (Hamilton, 1972) by the late Pliocene (Fig. 40d). Underthrusting was then well developed south of Java and the Lesser Sunda Islands. During this time the break along the Sunda Strait occurred (van Bemmelen, 1949, p. 633). In fact, it is well documented (van Bemmelen, 1949) that no sea passage was known between Sumatra and Java in older historical times (before 1175 A.D.). The orogenic phase of the late Pliocene gave most of the Sunda Land its present morphology. In-filling of the basinal area had gradually changed the sea floor to a relatively flat plane.

A very important event that occurred during this period is a compressional phase in most of the sedimentary basins. In East Java Basin this compressional event formed the Madura Ridge and the Rembang and Kendeng anticlinoria (see p. 184); in South Sumatra Basin it formed three parallel anticlinoria, the northern one (Palembang) is associated with a strong lineation of the gravity anomalies (see p. 154; Fig. 35); and in the Gulf of Thailand Basin the compression resulted in the broad zone of apparent "diapirs" (Fig. 39). Probably this compressional event had a general north-south direction. It affected the "soft" portions on Sunda Land. It is unknown to me at the present what caused this major compressional event.

By this period the opening of the Andaman Sea and the dextral strike-slip fault on Sumatra reached their full development. Subduction in northwest Borneo that had migrated continuously to the northwest reached the position of the Palawan Trough. Thereafter, the subduction reverted to the east side of Borneo in a zone extending northeastward from northeast Borneo along the Sulu Island Arc (Hamilton, 1971). At the end of the late Pliocene or possibly in the Pleistocene the eastward dipping subduction zone along the Manila Trench (Fig. 40d) originated (Murphy,

1972). At present the Palawan Trough is inactive.

### Recent

The entire Sunda Shelf became more or less stable as this region, the China Basin, eastern Indonesia, and the Sulu and Celebes seas became part of the Asian Plate.

The main type of tectonism of the Sunda Shelf now occurring is small scale uplift (Tjia, 1970a).

### Remarks

The evolutionary steps described above are highly schematic and a more complete tectonic history of this very complex area may be established when more direct information is available. Especially important will be absolute dating of rock units from major tectonic belts and the deep sea floor surrounding the Sunda Shelf. Paleomagnetic studies also are highly desirable, especially for the early Mesozoic period reconstruction.

The model outlined above can explain some of the major structural elements on the Sunda Shelf, particularly the major discontinuity in the gravity, magnetic, and seismic characteristics along the Billiton Depression. It also explains the tensional tectonism in the western Java Sea

basinal area versus the compressional tectonism that dominates the eastern Java Sea basinal area, and the formation of the Singapore Platform. The continuation of the transform fault along the Billiton Depression across Java to the Indian Ocean may have produced the slight offset in the row of volcanoes in central Java (Fig. 10) and the discontinuity in the bathymetric contours in the deep sea floor south of central Java (Fig. 1). It also explains why the island of Java consists of three different structural units: East Java, Central Java and West Java. The evolutionary model also offers an explanation for the magnetic anomalies of province 5. According to the model, some portions of the crust west of the Billiton Depression are pieces of old oceanic crust, perhaps accounting for the magnetic province 5 and some of the deep-refraction data (Table 2 and p. 80). It also suggests that the large north-south faults in the western Java Sea basinal area (Fig. 38), which acted mainly as normal faults during the Tertiary, may have originated as small transform faults during the Mesozoic and were associated with the southward motion of Borneo.



## REFERENCES

- Allen, C.R., 1962, Circum Pacific faulting in the Philippines-Taiwan region: Jour. Geophys. Res., v. 67, p. 4795-4812.
- Alexander, J.B., 1962, A short outline of the geology of Malaya with special reference to Mesozoic orogeny: in G.A. Macdonald and Hisashi Kuno, eds., The crust of the Pacific Basin: Am. Geophys. Union Geophys. Mono. 6, p. 81-86.
- Audley-Charles, M.G., D.J. Crater, and J.S. Milsom, 1972, Tectonic development of eastern Indonesia in relation to Gondwanaland dispersal: Nature Phys. Sci., v. 239, p. 35-39.
- Bancroft, A.M., 1960, Gravity anomalies over a buried step: Jour. Geophys. Res., v. 65, p. 1630-1631.
- Bartholomew, J., (ed.), 1958, The Times atlas of the world; v. 1: Houghton Mifflin Company, Boston.
- Belousov, V.V., 1968, Some problems of development of the earth's crust and upper mantle in the oceans: in L. Knopoff, C.L. Drake, and P.J. Hart, eds., The crust and upper mantle of the Pacific area: Am. Geophys. Union, Geophys. Mono., 12, p. 449-459.
- Ben-Avraham, Z., and J.D. Phillips, 1972, The evolution of the China Basin (abstract): Trans. Am. Geophys. Union, v. 53, p. 519.
- Ben-Avraham, Z., and S. Uyeda, in press, The evolution of the China Basin and the Mesozoic Paleogeography of Borneo: Earth and Planetary Sci. Letters.
- Ben-Avraham, Z., J. Segawa and C.O. Bowin, 1972, An extinct spreading center in the Philippine Sea: Nature, v. 240, p. 453-455.
- Birch, F., 1960, The velocity of compressional waves in rocks to 10 kilobars, Part 1: Jour. Geophys. Res., v. 65, p. 1083-1102.

- Boer, J. de, J.C. Schilling, and D.C. Krause, 1969, Magnetic polarity of pillow basalts from Reykjanes Ridge: *Science*, v. 166, p. 996.
- Bosum, W., G.D. Burton, S.H. Hsieh, E.G. Kind, A. Schreiber, and C.H. Tang, 1970, Aeromagnetic survey of offshore Taiwan: *United Nations ECAFE, CCOP Tech. Bull.*, v. 3, p. 1-34.
- Bott, M.H.P., and R.A. Smith, 1958, The estimation of the limiting depth of gravitational bodies: *Geophys. Prosp.*, v. 6, p. 1-10.
- Bowin, C.O., 1972, Does the lithosphere sink at site of underthrusting?: unpublished manuscript.
- Bowin, C.O., T.C. Aldrich, and R.A. Folinsbee, 1972, VSA gravity meter system: tests and recent developments: *Jour. Geophys. Res.*, v. 77, p. 2018-2033.
- Bowin, C.O. and Z. Ben-Avraham, 1972, Ocean floor underthrusting and the Indonesian island arc: (abstract) *Trans. Am. Geophys. Union*, v. 53, p. 518-519.
- Bowin, C.O., and Z. Ben-Avraham, in preparation, Geophysical study of the Indonesian Trench (Approximate title).
- Brouwer, H.A., 1925, *The geology of the Netherlands East Indies*: MacMillan Co., New York, 160 p.
- Bureau of Mines, the Philippines, 1969, Regional gravity survey of Luzon Island, Philippines: *United Nations ECAFE, CCOP Tech. Bull.*, v. 2, p. 1.
- Burns, R.E., 1964, Sea bottom heat-flow measurements in the Andaman Sea: *Jour. Geophys. Res.*, v. 69, p. 4918-4919.
- Burton, C.K., 1965, Wrench faulting in Malaya: *Jour. Geol.* v. 73, p. 781-798.
- Cain, J.C., S. Hendricks, W.E. Daniels and D.C. Jensen, 1968, Computation of the main geomagnetic field from spherical harmonic expressions: Data user's note NSSDC 68-11, NASA Data Center, 46 p.

- Carey, S.W., 1958, A tectonic approach to continental drift: in S.W. Carey, ed., Continental drift — a symposium, Tasmania Univ., Hobart, Australia, p. 177-355.
- Chase, T.E., and H.W. Menard, 1969, Bathymetric atlas of the northwestern Pacific Ocean: U.S. Naval Oceanographic Office, Washington, D. C.
- Chung, S.K., 1968, Annual report: Geol. Surv. of Malaysia, 100 p.
- Coleman, R.G., 1971, Plate tectonic emplacement of upper mantle peridotites along continental edges: Jour. Geophys. Res., v. 76, p. 1212-1222.
- Coney, P.J., 1970, The geotectonic cycle and the new global tectonics: Geol. Soc. Am. Bull., v. 81, no. 3, p. 739-747.
- Cree, A., 1972, Industry looks at Java Sea geology: The Oil and Gas Jour., v. 70, p. 72-74.
- Daly, R.A., 1940, Strength and structure of the earth: Prentice-Hall, Inc., New York, 434 p.
- Dash, B.P., 1970, Preliminary report on basic geologic and geophysical research in the eastern offshore area of West Malaysia: United Nations ECAFE, Report of seventh session of CCOP, p. 85-87.
- Dash, B.P., 1971, Preliminary report on seismic refraction survey southeast of Natuna Islands and seismic profiling in the vicinity of the Natuna and Tioman Islands on the Sunda Shelf: United Nations ECAFE, Report of eighth session of CCOP, p. 168-174.
- Dash, B.P., K.O. Ahmed, and P. Hubral, 1970, Seismic investigation in the region of Poulo Panjang, offshore from southwestern Viet-Nam: United Nations ECAFE, CCOP Tech. Bull., v. 3, p. 37-54.
- Dash, B.P., C.M. Shepstone, S. Dayal, S. Guru, B.L.A. Hains, G.A. King and G.A. Ricketts, 1972, Seismic investigations on the northern part of the Sunda Shelf south and east of great Natuna Island: United Nations ECAFE, CCOP Tech. Bull., v. 6, p. 179-196.

- De Bruyn, J.W., 1951, Isogam maps of Caribbean Sea and surroundings and of southeast Asia: 3rd World Petroleum Congress Proc., The Hague, p. 598-612.
- Dewey, J.F., and J.M. Bird, 1970, Mountain belts and the new global tectonics: Jour. Geophys. Res., v. 75, no. 14, p. 2625-2647.
- Dewey, J.F., and J.M. Bird, 1971, Origin and emplacement of the ophiolite suite: Appalachian ophiolites in Newfoundland: Jour. Geophys. Res., v. 76, p. 3179-3206.
- Dickinson, W.R., 1970, Relations of andesites, granites, and derivative sandstones to arc-trench tectonics: Rev. Geophys. Space Physics, v. 8, p. 813-860.
- Dickinson, W.R., 1971, Plate tectonic models of geosynclines: Earth and Planetary Sci. Letters, v. 10, p. 165-174.
- Dietz, R.S., 1961, Continent and ocean basin evolution by spreading of the sea floor: Nature, v. 190, p. 854.
- Dietz, R.S., and J.C. Holden, 1970, Reconstruction of Pangea: Breakup and dispersion of continents, Permian to present: Jour. Geophys. Res., v. 75, p. 4939-4956.
- Drake, C.L., M. Ewing, and G.H. Sutton, 1959, Continental margins and geosynclines: The east coast of North America north of Cape Hatteras: Phys. and Chem. of the Earth, v. 3, p. 110-198.
- Earle, W., 1845, On the physical structure and arrangement of the islands of the Indian Archipelago: Jour. Royal Geog. Soc. London, v. 15, p. 358-365.
- Edgar, N.T., J.I. Ewing, and J. Hennion, 1971, Seismic refraction and reflection in Caribbean Sea: Am. Assoc. Petroleum Geologists Bull., v. 55, p. 833-870.
- Edwards, G., and W.A. McLaughlin, 1965, Age of granites from the Tin Province of Indonesia: Nature, v. 206, p. 814-816.
- Emery, K.O., 1969, Distribution pattern of sediments on the continental shelves of western Indonesia: United Nations ECAFE, CCOP Tech. Bull., v. 2, p. 79-82.

- Emery, K.O., 1971, Bottom sediments of Malacca Strait: United Nations ECAFE, CCOP Tech. Bull., v. 4, p. 149-152.
- Emery, K.O., and Hiroshi Niino, 1963. Sediments of the Gulf of Thailand and adjacent continental shelf: Geol. Soc. Am. Bull. v. 74, p. 541-554.
- Emery, K.O., Elazar Uchupi, J.D. Phillips, C.O. Bowin, E.T. Bunce, and S.T. Knott, 1970, Continental rise off eastern North America: Am. Assoc. Petroleum Geologists Bull., v. 54, p. 44-108.
- Emery, K.O. and Zvi Ben-Avraham, 1972, Structure and stratigraphy of the China Basin: Am. Assoc. Petroleum Geologists Bull., v. 56, p. 839-859.
- Emery, K.O., Elazar Uchupi, John Sunderland, H.L. Uktolseja and E.M. Young, 1972, Geological structure and some water characteristics of the Java Sea and adjacent continental shelf: United Nations ECAFE, CCOP Tech. Bull., v. 6, p. 197-223.
- Ernst, W.G., 1970, Tectonic contact between the Franciscan melange and the Great Valley sequence—crustal expression of a late Mesozoic Benioff zone: Jour. Geophys. Res., v. 75, p. 886-901.
- Ewing, J., J. Antoine and M. Ewing, 1960, Geophysical measurements in the western Caribbean Sea and in the Gulf of Mexico: Jour. Geophys. Res., v. 65, p. 4087-4126.
- Fisher, R.L. (ed.) 1964, A preliminary report on Expeditions Monsoon and Lusiad, S.I.O., Ref. 64-19, 238 p.
- Fisher, R.L., 1968, Bathymetry of the eastern Indian Ocean: Scripps Inst. Oceanog., scale 1:2,000,000.
- Fitch, F.H., 1961, Annual report: Geol. Surv. Dept., British Territories in Borneo, p. 36-47.
- Fitch, F.H., 1963, Possible role of continental core movement in the geological evolution of British Borneo: Rept. Geol. Surv. Dept., British Borneo, Proc. British Borneo Geol. Conf. p. 31-41.

- Fitch, T.J., 1970, Earthquake mechanisms and island arc tectonics in the Indonesian-Philippines region: *Seism. Soc. Am. Bull.*, v. 60, p. 565-591.
- Fitch, T.J., 1972, Plate convergence, transcurrent faults, and internal deformation adjacent to southeast Asia and western Pacific: *Jour. Geophys. Res.*, v. 77, p. 4432-4460.
- Fitch, T.J., and P. Molnar, 1970, Focal mechanisms along inclined earthquake zones in the Indonesia-Philippine region: *Jour. Geophys. Res.*, v. 75, p. 1431-1444.
- Frerichs, W.E., 1971, Paleobathymetric trends of Neogene foraminiferal assemblages and sea floor tectonism in the Andaman Sea area: *Marine Geol.* v. 11, p. 159-173.
- Garland, G.D., 1965, *The earth's shape and gravity*: Pergamon Press, 183 p.
- Garson, M.S., and A.H.G. Mitchell, 1970, Transform faulting in the Thai Peninsula: *Nature*, v. 228, p. 45-47.
- Geological Institute and Institute of Oceanology of the Academy of Sciences, USSR, 1970, *Tectonic map of the Pacific segment of the earth*: scale 1:10,000,000.
- Gervasio, F.C., 1968, Age and nature of orogenesis of the Philippines: *United Nations ECAFE, CCOP Tech. Bull.*, v. 1, p. 113-128.
- Gervasio, F.C., 1971, Geotectonic development of the Philippines (abstract): *Twelfth Pacific Sci. Congress*, v. 1, p. 380.
- Grant, F.S., and G.F. West, 1965, *Interpretation theory in applied geophysics*: McGraw-Hill Book Co., New York, 584 p.
- Gray, F., 1959-1962, Proton magnetometer surveys in the Solomon Islands and western Pacific Ocean 1958: *British Solomon Islands Geol. Record, Rept.*, no. 65, p. 200-209.

- Grow, J.A., 1972, A geophysical study of the central Aleutian arc: Ph.D. dissertation, University of California, San Diego, 132 p. (unpublished).
- Haile, N.S., 1963, The Cretaceous-Cenozoic Northwest Borneo geosyncline: British Borneo Geol. Surv. Bull., v. 4, p. 1-18.
- Haile, N.S., 1968, Geosynclinal theory and organizational pattern of the Northwest Borneo geosyncline: Q. Jour. Geol. Soc. London, v. 124, p. 171-195.
- Haile, N.S., 1970, Notes on the geology of the Tambelan, Anambas and Bunguran Islands, Sunda Shelf, Indonesia, including radiometric age determinations: United Nations ECAFE, CCOP Tech. Bull., v. 3, p. 55-90.
- Haile, N.S., 1971, Confirmation of a late Cretaceous age for granite from the Bunguran and Anambas Islands, Sunda Shelf, Indonesia: Geol. Soc. Malaysia, Newsletter, no. 30, p. 6-8.
- Haile, N.S., 1972, The Natuna Swell and adjacent Cenozoic basins on the north Sunda Shelf (abstract): Regional Conf. on geol. of southeast Asia, Kuala Lumpur, Malaysia, p. 14-15.
- Haile, N.S., and M.W. McElhinny, 1972, The potential value of paleomagnetic studies in restraining romantic speculation about the geological history of southeast Asia (abstract): Regional Conf. on geol. of southeast Asia, Kuala Lumpur, Malaysia, p. 16.
- Hamilton, Warren, 1969, The volcanic central Andes—a modern model for the Cretaceous batholiths and tectonics of western North America: Oregon Dept. Geol. and Mineral Industries, Bull., v. 65, p. 175-184.
- Hamilton, Warren, 1970, Tectonic map of Indonesia—A progress report: U.S.G.S. Project Rept. (IR) IND-5, 29 p.
- Hamilton, W., 1971, Plate tectonic evolution of Indonesia (abstract): Geol. Soc. Am. Abstracts, v. 3, no. 7, p. 589-590.

- Hamilton, W., 1972, Tectonics of the Indonesian region: U.S.G.S. Project Rept. (IR) IND-20, 13 p.
- Hamilton, W., 1972a, Preliminary tectonic map of the Indonesian region, 1:5,000,000: U.S.G.S. Open File Rept., 3 sheets.
- Harland, W.B., A.G. Smith and B. Wilcock, eds., 1964, The phanerozoic time-scale: Geol. Soc. London.
- Hatherton, T., and W.R. Dickinson, 1969, The relationship between andesitic volcanism and seismicity in Indonesia, the Lesser Antilles, and other island arcs: Jour. Geophys. Res., v. 74, p. 5301-5310.
- Hayes, D.E., and W.J. Ludwig, 1967, The Manila Trench and West Luzon Trough—II. Gravity and magnetic measurements: Deep-Sea Res., v. 14, p. 545-560.
- Heezen, B.C., and M. Tharp, 1971, Physiographic diagram of the western Pacific Ocean: Geol. Soc. Am.
- Hess, H.H., 1962, History of the ocean basins, in Petrological Studies: A volume to honor A.F. Buddington, Geol. Soc. Am., p. 599-620.
- Hilde, T.W.C., and C.G. Engle, 1967, Age, composition and tectonic setting of the granite island, Hon Trung-Long, off the coast of south Vietnam: Geol. Soc. Am. Bull., v. 78, p. 1289-1294.
- Ho, C.S., 1971, Geological evolution of Taiwan: Sino-American Science Cooperation Colloquium on Ocean Resources, v. 1, Marine geol. and geophys., Taipei, Taiwan, p. 25-46.
- Holmes, A., 1959, A revised geological time-scale: Trans. Geol. Soc. Edin., v. 17, p. 183-216.
- Holmes, A., 1965, Principles of physical geology: The Ronald Press Co., New York, 1288 p.
- Hosking, K.F.G., 1972, Primary mineralization of west Malaysia (abstract): Regional Conf. on geol. of south-east Asia, Kuala Lumpur, Malaysia, p. 24-28.



- Houtz, Robert, John Ewing, and Xavier Le Pichon, 1968, Velocity of deep-sea sediments from sonobuoy data: Jour. Geophys. Res., v. 73, p. 2615-2641.
- Humphrey, W., 1970, Petroleum developments in the Far East in 1969: Am. Assoc. Petroleum Geologists Bull., v. 54, p. 1551-1566.
- Humphrey, W., 1971, Petroleum developments in the Far East in 1970: Am. Assoc. Petroleum Geologists Bull., v. 55, p. 1634-1661.
- Hutchison, C.S., 1968, Invalidity of the Billiton Granite, Indonesia, for defining the Jurassic/upper Triassic boundary in the Thai-Malayan orogen: Geol. en Mijnbouw, v. 47, p. 56-60.
- Hutchison, C.S., 1972, Tectonic evolution of the Malay Peninsula and Sumatra-a personal view (abstract): Regional Conf. on geol. of southeast Asia, Kuala Lumpur, Malaysia, p. 29-32.
- Irving, E., J.K. Park, S.E. Haggerty, F. Aumento and B. Loncarevic, 1970, Magnetism and opaque mineralogy of basalts from the Mid-Atlantic Ridge: Nature, v. 228, p. 974.
- Isacks, B., J. Oliver, and L.R. Sykes, 1968, Seismology and the new global tectonics: Jour. Geophys. Res., v. 73, p. 5855-5899.
- Jones, C.R., 1968, Lower Paleozoic rocks of Malay Peninsula: Am. Assoc. Petroleum Geologists Bull., v. 52, p. 1259-1278.
- Kane, M.F., 1970, Geophysical study of the tectonics and crustal structure of the Gulf of Maine: Ph.D. dissertation, Saint Louis University, 100 p. (unpublished).
- Karig, D.E., 1971, Origin and development of marginal basins in the western Pacific: Jour. Geophys. Res., v. 76, p. 2542-2561.
- Karig, D.E., 1972, Remnant arcs: Geol. Soc. Am. Bull., v. 83, p. 1057-1068.

- Katili, J.A., 1962, On the age of the granitic rocks in relation to the structural features of Sumatra: in G.A. Macdonald and Hisachi Kuno, eds., The crust of the Pacific Basin: Am. Geophys. Union, Geophys. Mono. 6, p. 116-121.
- Katili, J.A., 1967, Structure and age of the Indonesian Tin Belt with special reference to Bangka: Tectonophysics, v. 4, p. 403-418.
- Katili, J.A., 1970, Large transcurrent faults in southeast Asia with special reference to Indonesia: Geol. Rundschau, v. 59, p. 581-600.
- Katili, J.A., 1971, A review of the geotectonic theories and tectonic maps of Indonesia: Earth-Science Rev., v. 7, p. 143-163.
- Katili, J.A., 1972, Geochronology of west Indonesia and its implication (abstract): Regional Conf. on geol. of southeast Asia, Kuala Lumpur, Malaysia, p. 33.
- Kaula, W.M., 1966, Tests and combination of satellite determinations of the gravity field with gravimetry: Jour. Geophys. Res., v. 71, p. 5303-5314.
- Keller, G.H., and A.F. Richards, 1967, Sediments of the Malacca Strait, southeast Asia: Jour. Sedimentary Petrology, v. 37, p. 102-127.
- Klompé, Th, H.F., 1954, On the supposed upper Paleozoic unconformity in North Sumatra: Univ. of Indonesia, Contribution from the Dept. of Geol., no. 16, p. 151-165.
- Klompé, Th, H.F., and Sigit Soetarjo, 1965, Geologic map of Indonesia, scale 1:2,000,000, U.S. Geol. Surv., Map I-414.
- Knott, S.T., and E.T. Bunce, 1968, Recent improvement in technique of continuous seismic profiling: Deep-Sea Res., v. 15, p. 633-636.

- Kobayashi, T., 1944, Reciprocal development of radiolarian rocks as between Asiatic and Australian sides: Proc. Imp. Acad. Tokyo, v. 20, p. 234-238.
- Kobayashi, T., 1960, Notes on the geologic history of Thailand and adjacent territories: Japanese Jour. Geol. Geography, v. 13, p. 129-135.
- Koesoemadinata, R.P., 1969, Outline of geologic occurrence of oil in Tertiary basins of West Indonesia: Am. Assoc. Petroleum Geologists Bull., v. 53, p. 2368-2376.
- Koesoemadinata, R.P. and A. Pulunggono, 1971, Offshore Tertiary sedimentary basins in Indonesia: Paper presented at the Twelfth Pacific Sci. Congress, Canberra (unpublished).
- Krause, D.C., 1966, Tectonics, marine geology, and bathymetry of the Celebes Sea — Sulu Sea Region: Geol. Soc. Am. Bull., v. 77, p. 813-832.
- Kuenen, Ph. H., 1935, The Snellius Expedition: v. 5, Geological results, Part 1: Kemink en zoon, Utrecht, 124 p.
- Kuenen, Ph. H., 1950, Marine Geology: New York, John Wiley & Sons, 551 p.
- Le Pichon, X., 1968, Sea-floor spreading and continental drift: Jour. Geophys. Res., v. 73, p. 3661-3705.
- Le Pichon, X., J. Ewing, and R.E. Houtz, 1968, Deep-sea sediment velocity determination made while reflection profiling: Jour. Geophys. Res., v. 73, p. 2596-2614.
- Le Pichon, X.; and M. Talwani, 1969, Regional gravity anomalies in the Indian Ocean: Deep-Sea Res., v. 16, p. 263-274.
- Li, Y.L., and C.Y. Meng, 1970, Geologic map of the Republic of China: Chinese Petroleum Corp., scale 1:4,000,000.

- Liechti, P., F.W. Roe, and N.S. Haila, 1960, Geology of Sarawak, Brunei and the western part of North Borneo: Geol. Surv. Dept., British Territories in Borneo, Bull., 3, v. 1, 360 p.
- Ludwig, W.J., 1970, The Manila Trench and West Luzon Trough - III. Seismic-refraction measurements: Deep-Sea Res., v. 17, p. 533-571.
- Ludwig, W.J., D.E. Hayes, and J.I. Ewing, 1967, The Manila Trench and West Luzon Trough - II. Bathymetry and sediment distribution: Deep-Sea Res., v. 14, p. 533-544.
- Mainguy, M., 1968, Regional geology and prospects for mineral resources on the northern part of the Sunda Shelf: United Nations ECAFE, CCOP Tech. Bull., v. 1, p. 129-142.
- Mainguy, M., 1970, Regional geology and petroleum prospects of the marine shelves of eastern Asia: United Nations ECAFE, CCOP Tech. Bull., v. 3, p. 91-107.
- Mainguy, M., 1971, Tertiary basins of eastern Asia and their offshore extensions: United Nations ECAFE, CCOP Tech. Bull., v. 6, p. 225-227.
- Marova, N.A., 1966, Floor relief of the Indian Ocean in the region of the Java Trench: Okeanologiya, v. 6, p. 3661-3705.
- Matsuda, T., and S. Uyeda, 1970, On the Pacific-type orogeny and its model-extension of the paired belts concept and possible origin of marginal seas: Tectonophysics, v. 11, p. 5-27.
- McElhinny, M.W., 1970, Formation of the Indian Ocean: Nature, v. 228, p. 977-979.
- McKenzie, D., and J.G. Sclater, 1971, The evolution of the Indian Ocean since the late Cretaceous: Geophys. Jour. R.astr.Soc. v. 25, p. 437-528.
- Menard, H.W., 1967, Transitional types of crust under small ocean basins: Jour. Geophys. Res., v. 72, p. 3061-3073.

- Meng, C.Y., and S.S.L. Chang, 1971, The geologic structure of Taiwan: Sino-American Science Cooperation Colloquium on Ocean Resources, v. 1, Marine geol. and geophys. Taipei, Taiwan, p. 189-239.
- Mitchell, A.L., and H.G. Reading, 1971, Evolution of island arcs: *Jour. Geol.*, v. 79, p. 253-284.
- Mohr, E.C.J., 1938, Climate and soil in the Netherlands Indies: *Bull. of the Colonial Inst. of Amsterdam*, v. 1, p. 241-251. Reprinted in *Science and Scientists in the Netherlands Indies*, New York, 1945, p. 250-254.
- Molengraaff, G.A.F., 1913, Folded mountain chains, overthrust sheets and block-faulted mountains in the East Indian Archipelago: *Twelfth Int. Geol. Congr. Toronto*, p. 689-702.
- Molengraaff, G.A.F., 1921, Modern deep-sea research in the East Indian Archipelago: *Geogr. Jour.*, v. 57, p. 95-121.
- Moores, E.M., and F.J. Vine, 1971, The Troodos Massive, Cyprus and other ophiolites as oceanic crust: Evaluation and implications: *Phil. Trans. Royal Soc. A*, v. 268, p. 443-466.
- Morgan, W.J., 1968, Rises, trenches, great faults and crustal blocks: *Jour. Geophys. Res.*, v. 73, p. 1959-1982.
- Morgan, W.J., 1972, Deep mantle convection and plate motions: *Am. Assoc. Petroleum Geologists Bull.*, v. 56, p. 203-213.
- Murphy, R.W., 1972, The Manila Trench-west Taiwan foldbelt: a flipped subduction zone (abstract): *Regional Conf. on geol. of southeast Asia*, Kuala Lumpur, Malaysia, p. 41.
- Nagasaka, K., J. Francheteau, and T. Kishii, 1970, Terrestrial heat flow in the Celebes and Sulu seas: *Marine Geophys. Res.*, v. 1, p. 99-103.
- Nettleton, L.L., 1940, *Geophysical Prospecting for oil*: New York, McGraw-Hill Book Co., 444 p.

- Nur, A., and G. Simmons, 1969, The effect of saturation on velocity in low porosity rocks: *Earth and Planetary Sci. Letters*, v. 7, p. 183-193.
- Packham, G.H., and D.A. Falvey, 1971, An hypothesis for the formation of marginal seas in the western Pacific: *Tectonophysics*, v. 11, p. 79-109.
- Parke, M.L. Jr., K.O. Emery, R. Szymankiewicz, and L.M. Reynolds, 1971, Structural framework of continental margin in South China Sea; *Am. Assoc. Petroleum Geologists Bull.*, v. 55, p. 723-751.
- Peter, G., L.A. Weeks, and R.E. Burns, 1966, A reconnaissance geophysical survey in the Andaman-Nicobar island arc: *Jour. Geophys. Res.*, v. 71, p. 495-509.
- Peters, L.J., 1949, The direct approach to magnetic interpretation and its practical application: *Geophysics*, v. 14, p. 290-320.
- Posavec, M.M., D. Taylor, T.V. Leeuwen, and A. Spector, 1972, Tectonic controls of volcanism and complex movements along the Sumatran fault system (abstract): *Regional Conf. on geol. of southeast Asia*, Kuala Lumpur, Malaysia, p. 47-48.
- Raitt, R.W., 1963, The crustal rocks: *The Sea*, M.N. Hill, ed., v. 3, p. 85-102.
- Raitt, R.W., 1966, Seismic refraction studies of the Indonesian Island arc (abstract 346): *Second Int. Ocean, Cong.*, (Moscow).
- Raitt, R.W., 1967, Marine seismic studies of the Indonesian Island Arc: Paper presented at the Am. Geophys. Union meeting (unpublished).
- Ridd, M. F., 1971, South-east Asia as a part of Gondwanaland: *Nature*, v. 234, p. 531-533.
- Rodolfo, K.S., 1969, Bathymetry and marine geology of the Andaman Basin, and tectonic implications for southeast Asia: *Geol. Soc. Am., Bull.*, v. 80, p. 1203-1230.

- Rodolfo, K.S., 1969a, Sediments of the Andaman basin, northwestern Indian Ocean: *Mar. Geol.* v. 7, p. 371-402.
- Schaub, H.P., and A. Jackson, 1958, The northwestern oil basin of Borneo: *in* Habitat of oil, a symposium: *Am. Assoc. Petroleum Geologists*, p. 1330-1336.
- Schuppli, H.M., 1946, Geology of oil basins of the East Indian Archipelago: *Am. Assoc. Petroleum Geologists Bull.*, v. 30, p. 1-22.
- Scientific Staff, 1972, Deep Sea Drilling Project, Leg 22: *Geotimes*, v. 17, p. 15-17.
- Snelling, N.J., J.D. Bignell, and R.R. Harding, 1968, Ages of Malayan granites: *Geol. en Mijnbouw*, v. 47, p. 358-359.
- Stoneley, R., 1967, A consideration of the northern margin of parts of Gondwanaland leading to a reconstruction of the drift history of the northern Indian Ocean region: Continental drift emphasizing the history of the South Atlantic area: A UNESCO/IUGS Symposium, Montevideo, Uruguay, p. 970-1017.
- Talwani, M., 1970, Gravity: *The Sea*, A.E. Maxwell, ed., v. 4, p. 251-297.
- Talwani, M., J.L. Worzel, and M. Landisman, 1959, Rapid computations for two-dimensional bodies with application to the Mendocino sound submarine fracture zone: *Jour. Geophys. Res.*, v. 64, p. 49-59.
- Talwani, M., and J.R. Heirtzler, 1964, Computation of magnetic anomalies caused by two-dimensional structures of arbitrary shape: *Computers in the Mineral Industries*, Stanford Univ. publication, *Geol. Sci.*, v. 9, pt. 1, p. 464-480.
- Tanner, J.J. and W.E. Kennett, 1972, Petroleum development in the Far East in 1971, v. 56, p. 1823-1845.
- Tarling, D.H., 1972, Drifting over the years: *Nature*, v. 239, p. 38-40.

- Tjia, H.D., 1966, Structural analysis of the pre-Tertiary of the Lukulo area, central Java: Bandung Inst. Technology, Contrib. Dept. Geol., no. 63, 110 p.
- Tjia, H.D., 1970, Transcurrent faulting in the Sarawak-Kiri region, Sarawak, East Malaysia: Geol. Mag., p. 217-224.
- Tjia, H.D., 1970a, Rates of diastrophic movement during the Quaternary in Indonesia: Geologie en Mijnbouw, v. 49, p. 335-338.
- Todd, D.F., and A. Pulunggono, 1971, Wildcatters score in Indonesia: The Oil and Gas Jour., v. 69, p. 105-110.
- Umbgrove, J.H.F., 1938, Geological history of the East Indies: Am. Assoc. Petroleum Geologists Bull., v. 22, p. 1-70.
- Umbgrove, J.H.F., 1947, The pulse of the earth: The Hague, Martinus Nijhoff, 358 p.
- Umbgrove, J.H.F., 1949, Structural history of the East Indies: Cambridge at the University Press, 63 p.
- Untung, M., 1967, Results of a sparker survey for tin ore off Bangka and Belitung islands, Indonesia: United Nations ECAFE, Report of fourth session of CCOP, p. 61-67.
- Uyeda, Seiya and Z. Ben-Avraham, 1972, Origin and development of the Philippine Sea: Nature Physical Sci., v. 240, p. 176-178.
- Vacquier, V., and P.T. Taylor, 1966, Geothermal and magnetic survey off the coast of Sumatra, Part 1: Tokyo Univ. Earthquake Res. Inst., Bull., v. 44, p. 531-540.
- van Baren, F.A. and H. Kiel, 1950, Contribution to the sedimentary petrology of the Sunda Shelf: Jour. Sed. Petrol. v. 20, p. 185-213.
- van Bemmelen, R.W., 1949, The geology of Indonesia: The Hague, Martinus Nijhoff, 1, 732 p., 2, 265 p.



- van Bemmelen, R.W., 1954, Mountain building: The Hague, Martinus Nijhoff, 177 p.
- Vening Meinesz, F.A., 1932 and 1934, Gravity expeditions at sea: v. I, The expeditions, the computations and the results, V. II, The interpretation of the results (with the collaboration of J.H.M. Umbgrove and Ph. H. Kuenen), Ed. Waltman, Delft.
- Vening Meinesz, F.A., 1937, Results of maritime gravity research, 1923-32: in International aspects of oceanography, T.W. Vaughan, ed., National Academy of Sciences, Washington, D. C., p. 61-69.
- Vine, F.J., and D.H. Matthews, 1963, Magnetic anomalies over oceanic ridges: Nature, v. 199, p. 947-949.
- Vogt, P.R., E.D. Schneider, and G.L. Johnson, 1969, The crust and upper mantle beneath the sea: in P.J. Hart, ed., The earth's crust and upper mantle: Am. Geophys. Union, Geophys. Mono. 13, p. 556-617.
- Vogt, P.R., R.H. Higgs, and G.L. Johnson, 1971, Hypotheses on the origin of the Mediterranean Basin: Magnetic data: Jour. Geophys. Res., v. 76, p. 3207-3228.
- Weeda, J., 1958a, Oil basin of east Borneo: in Habitat of oil, a symposium: Am. Assoc. Petroleum Geologists, p. 1337-1346.
- Weeda, J., 1958b, Oil basin of east Java: in Habitat of oil, a symposium: Am. Assoc. Petroleum Geologists, p. 1359-1364.
- Weeks, L.A., R.N. Harbison and G. Peter, 1967, Island arc system in the Andaman Sea: Am. Assoc. Petroleum Geologists Bull., v. 51, p. 1803-1815.
- Wennekers, J.H.L., 1958, South Sumatra basinal area: in Habitat of oil, a symposium: Am. Assoc. Petroleum Geologists, p. 1347-1358.
- Wilford, G.E., 1961, The geology and mineral resources of Brunei and adjacent parts of Sarawak with descriptions of Seria and Miri oilfields: Borneo British Geol. Surv. Rept. Mem. 10, 319 p.

- Wing, C.G., 1969, The MIT vibrating string surface-ship gravimeter: Jour. Geophys. Res., v. 74, p. 5882-5894.
- Woollard, G.P., and W.E. Strange, 1962, Gravity anomalies and the crust of the Earth in the Pacific Basin: in G.A. Macdonald and Hisashi Kuno, eds., The crust of the Pacific Basin: Am. Geophys. Union, Geophys. Mono. 6, p. 60-80).
- Yanshin, A.L., 1966, Tectonic map of Eurasia, Geol. Inst. Acad. Nauk. SSSR and Minist. Geol. SSSR, scale 1:5,000,000.
- Yokoyama, I., and D. Hadikusumo, 1969, Volcanological survey of Indonesian volcanoes, Part 3, A gravity survey on the Krakatau Islands, Indonesia: Tokyo Univ. Earthquake Res. Inst. Bull., v. 47, p. 991-1001.
- Yokoyama, I., and S. Suparto, 1970, Volcanological survey of Indonesian volcanoes, Part 5, A gravity survey on and around Batur Caldera, Bali: Tokyo Univ. Earthquake Res. Inst. Bull., v. 48, p. 317-329.
- Yokoyama, I., I. Surjo, and B. Nazhar, 1970, Volcanological survey of Indonesian volcanoes, Part 4, A gravity survey in central Java: Tokyo Univ. Earthquake Res. Inst. Bull., v. 48, Part 2, p. 303-315.

## APPENDIX I SEISMIC REFRACTION STUDIES

## ANALYSIS OF SONOBUOYS

The sonobuoy oblique angle reflection profiles are typically 10 to 25 km in range. They were obtained during normal incidence reflection profiling, when the range on the sonobuoy opened at a speed of about 7 km/hour. The sonobuoy hydrophone signals were radio transmitted to the ship, where they were recorded on a Precision Graphic Recorder (PGR) and on analog magnetic tape. The technique of using expendable sonobuoys and the velocity and depth calculations using oblique reflection and refraction, has been described by Le Pichon, et al., (1968) and Houtz, et al., (1968).

The data interpretation was started by making several records from the analog magnetic tape using different bandwidth filters. A 10-28 Hz filter passband was found to be the best for data from this area, and was used for laboratory playback of all the buoys. Occasionally, higher filter settings, 25-75 Hz and 100 to 300 Hz, were used in order to distinguish between reflections whose entire transit was in the water column, such as side reflections and reflections from buried interfaces that could not be recognized on the normal incidence profile. The final

profiles were mounted on cardboard, and the refraction and oblique reflection arrivals were traced on clear plastic overlays. Distance-time relations were digitized and the values fed into the computer to plot and compute the velocities within the sedimentary layers and basement, as well as the sediment thickness. All the calculations were done for the refraction arrivals by the slope-intercept method (Houtz, et al., 1968).

The horizontal ranges were determined on the assumption of a surface-sound-channel velocity of 1.50 km/sec. The bottom topography was unusually smooth and no correction for slope is needed. Subbottom topographic relief in some areas, however, is so large that it had to be considered; if the refracting interface appeared in the normal incidence profile, the dip was approximated by fitting an average line through the reflection data. The velocities were then corrected by assuming that the dips in the layers too deep to be seen in the normal incidence profile are parallel to those observed in the shallower sediments or at the sediment/basement interface.

There were no refraction arrivals from the uppermost sedimentary layer except for sonobuoys 7, 17, 21, 32, and 37. At these stations a velocity of 1.60 km/sec was

assumed for the surface layer, in agreement with velocity measurements from wells in the area (Fig. 12).

The shallow water depth and the long (50-75 ms) duration of the outgoing pulse allowed determinations of wide-angle reflection data in only a few instances. Where such data were available they were used to compute the mean velocity between reflection interfaces (interval velocity) (Le Pichon, et al., 1968) for comparison with the horizontal propagation velocities obtained from the refraction data for refraction arrivals from the same interfaces.

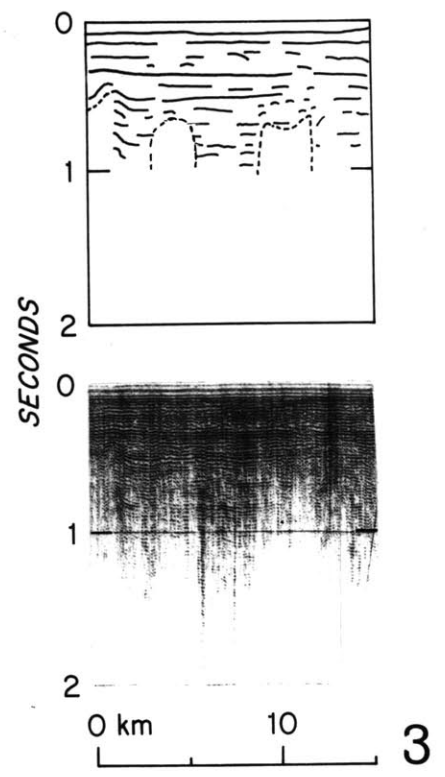
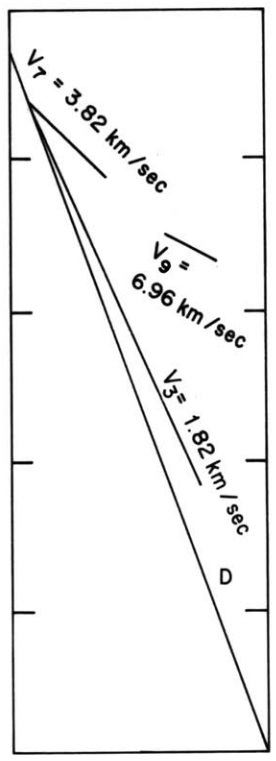
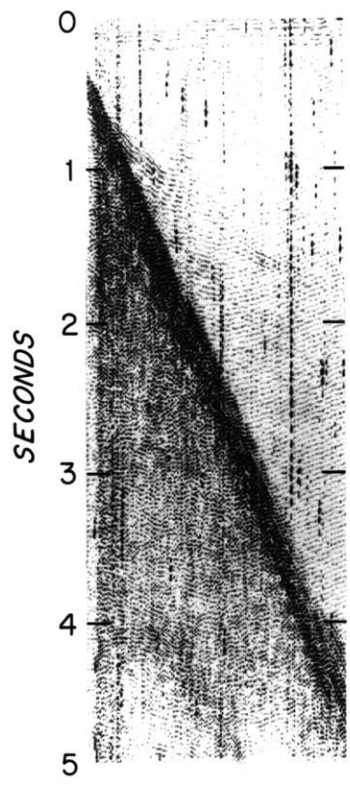
#### SONOBUOY PROFILES

The sonobuoy results served as one of the most important tools for resolution of the subbottom structure. For this reason it is useful to show some of the sonobuoy records and the information determined from them. The fourteen sonobuoy records shown in this appendix were obtained in different structural provinces. These records are about one-third of all those obtained on the shelf, and they cover almost all the circumstances in which the buoys proved helpful in determining basement structure and velocity (sonobuoys 3, 4, 5, 7, 20, and 25), detailed

velocity profile of the sedimentary column inside the basins (sonobuoys 8, 10, 13, 21, 22, 26), and sedimentary structures (sonobuoys 10, 15, 24, and 26). Each of the accompanying figures shows on the left a sonobuoy profile and its tracing, and on the right the concurrent normal incidence reflection profile and its interpretation. The symbols are: D, direct arrival; V, the computed velocity; R, oblique reflection; m, multiple arrival.

Sonobuoy 3 Figure 41.

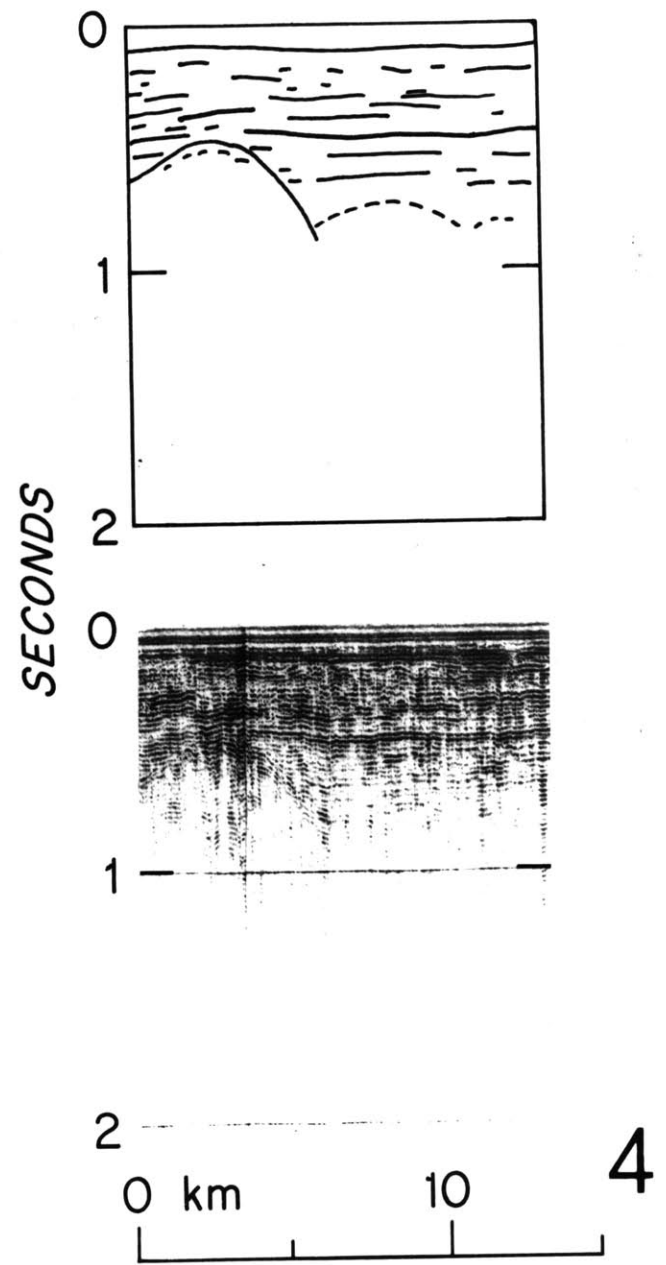
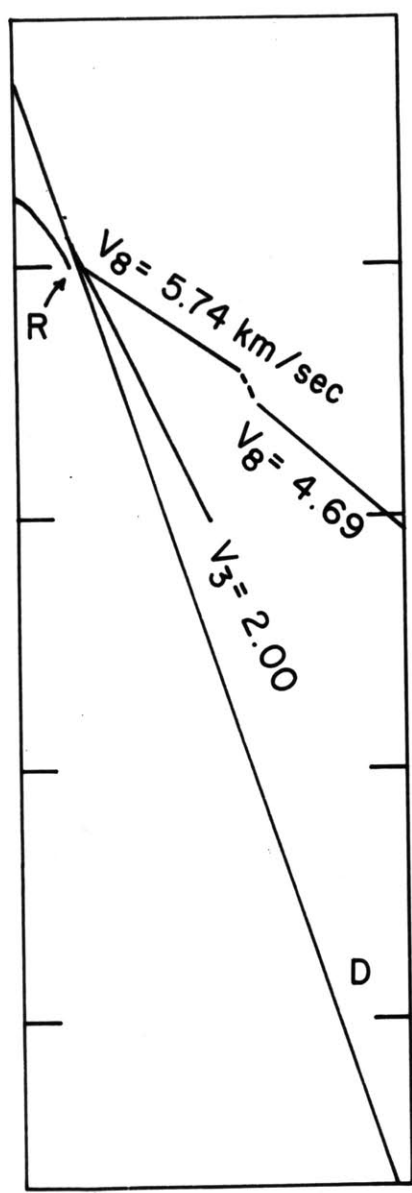
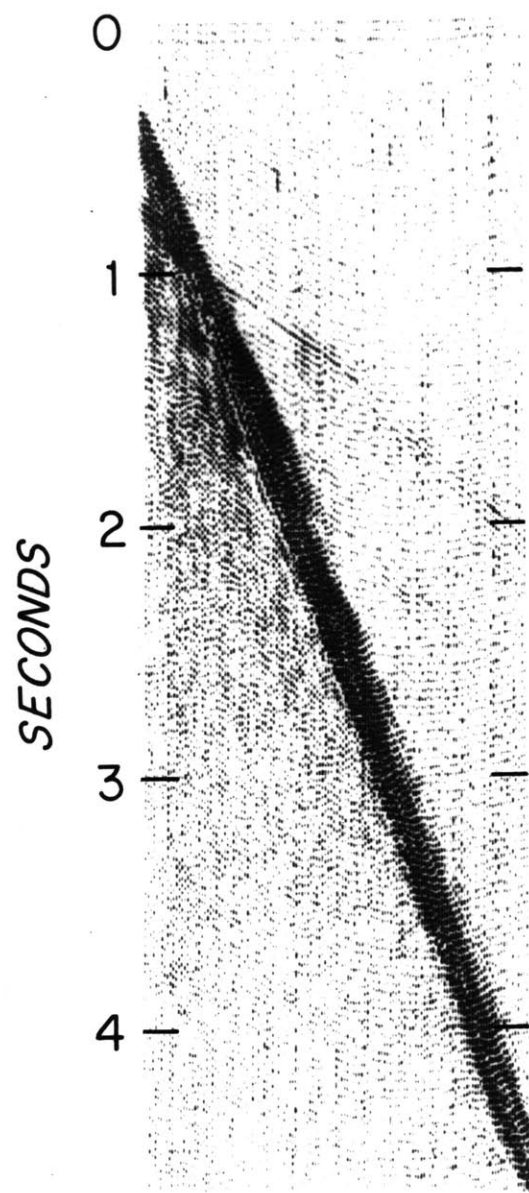
Station 3 is located on line 3 in the area between Sumatra and Borneo. The shape of the basement is difficult to detect on the reflection profile since it is masked by bottom and subbottom multiple reflections. It seems that the basement consists of small isolated massive bodies. The  $V_9$  horizon starts and terminates abruptly and seems to come from a small basement body. The  $V_7$  also terminates abruptly and its depth and horizontal extension indicate that it originated from the body shown on the left hand side of the normal incidence profile. A thin veneer of low velocity sediment ( $V_3$ ) overlies the basement reflectors.





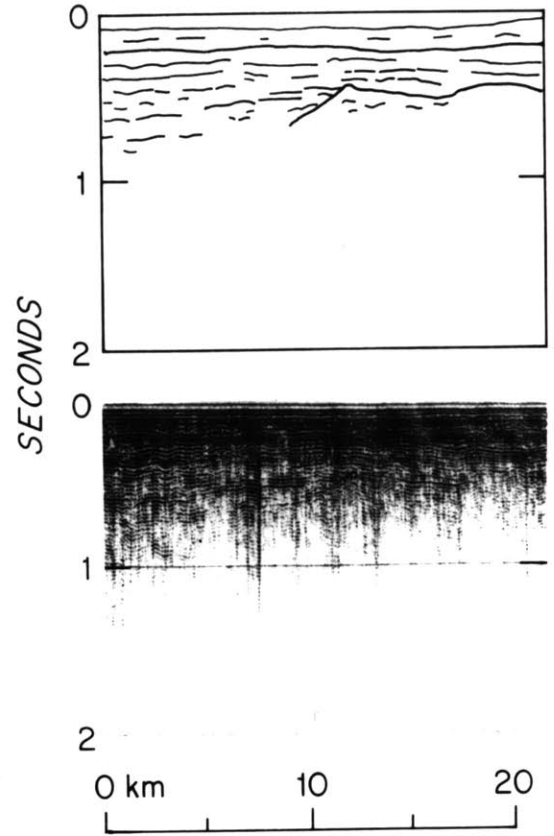
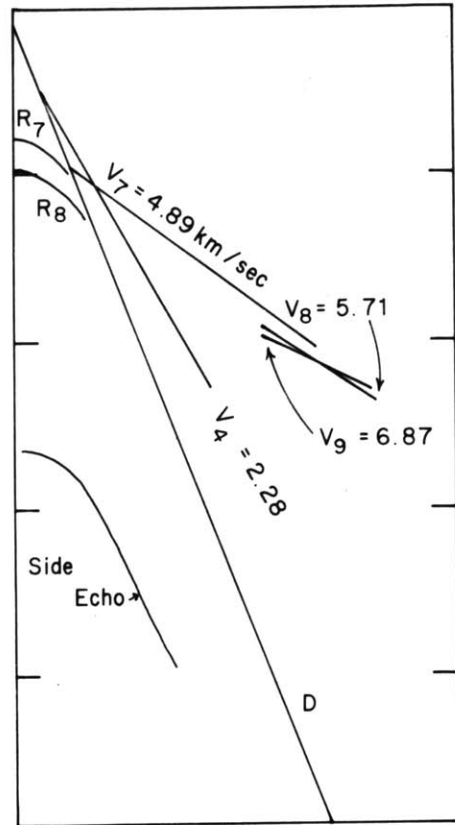
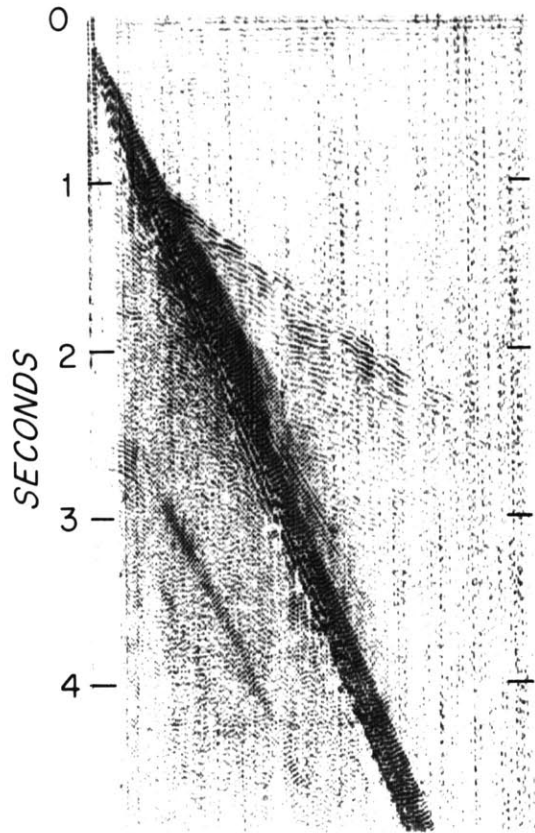
Sonobuoy 4 Figure 42.

Station 4 is located on line 5, about 120 km south of sonobuoy 3 in the same general area. 4.69 and 5.74 obviously originate from the same horizon. 5.74 is the result of propagation upslope and 4.69 downslope. True basement velocity thus lies between these two values. It is indicated as 5.22 km/sec ( $V_g$ ) in Table 1. Note the abrupt change in slope between the 5.74 and the 4.69 lines.



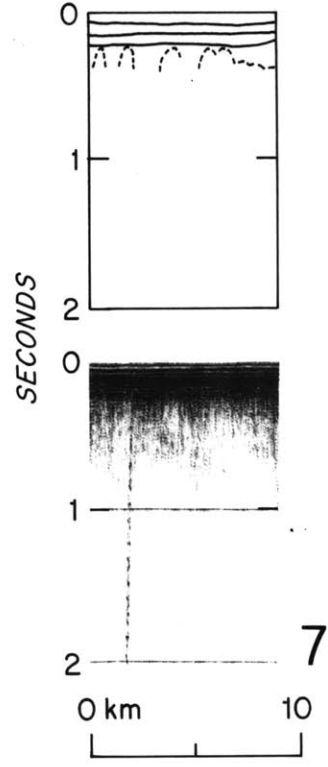
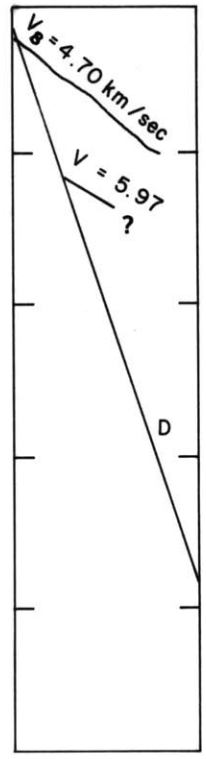
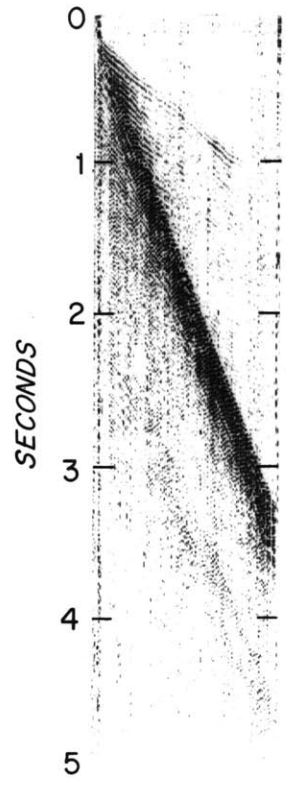
Sonobuoy 5 Figure 43.

Sonobuoy profile 5 was taken southeast of sonobuoy 4 between the Karimata and Billiton Islands. The most dramatic feature here is the sudden appearance of the  $V_8$  and  $V_9$  arrivals while those of  $V_4$  and  $V_7$  are continuous from the beginning.  $V_8$  and  $V_9$  originated from a basement structure of which part may be seen on the normal incidence profile. The positions of these refractions and their slope intercepts suggest that the body starts earlier and deeper than is seen in the normal incidence profile.  $V_7$  probably belongs to consolidated sediment or limestone. The lowest velocity detected ( $V_4$ ) is considerably higher than at any other station in this area except sonobuoy 1 where no low velocity arrivals were detected.



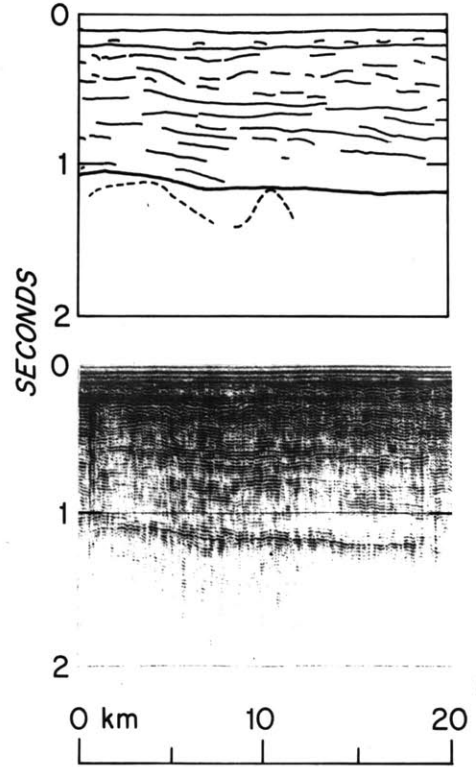
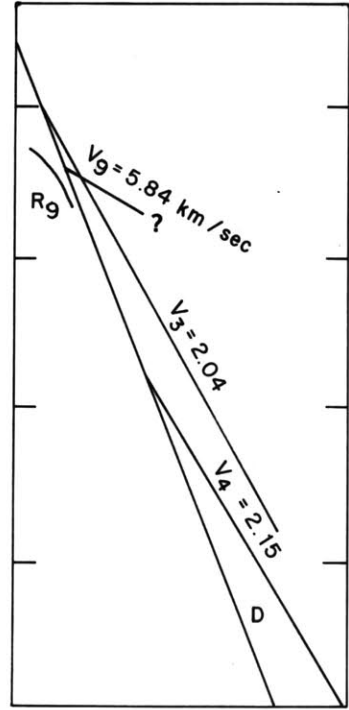
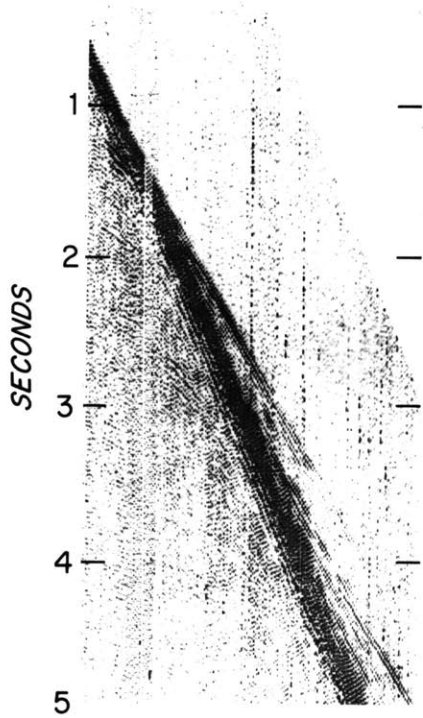
Sonobuoy 7 Figure 44.

Sonobuoy 7 was taken between the two large granitic islands Bangka and Billiton. Other surveys in this area (Untung, 1967) have shown the granitic basement to be very shallow. The  $V_8$  refraction is probably from the top of the granite. The refraction arrival shows some undulations (travel-time differences) that probably reflect the basement topography. The 5.97 refraction arrival appears unreliable, mainly because of the short range over which it was observed. No evidence for such a deeper layer is visible in the normal incidence data.



Sonobuoy 8 Figure 45.

Sonobuoy 8 is located in the Sunda Basin where off-shore drillings show the basin to be the deepest (Banuwati Deep of Todd and Pulunggono, 1971). The refraction with  $V_9$  is very weak, however, the oblique reflection is clear and looks as though it corresponds to the strong reflector on the normal incidence profile. The depth of this reflector is approximately the same as that of the lower Miocene limestone reported by Todd and Pulunggono (1971). The refractors with  $V_3$  and  $V_4$  are very clear and straight and thus seem to belong to well stratified layers. The published stratigraphic sections shows that these layers consist of series of sands and clays of lower Miocene and Mio-Pliocene age.

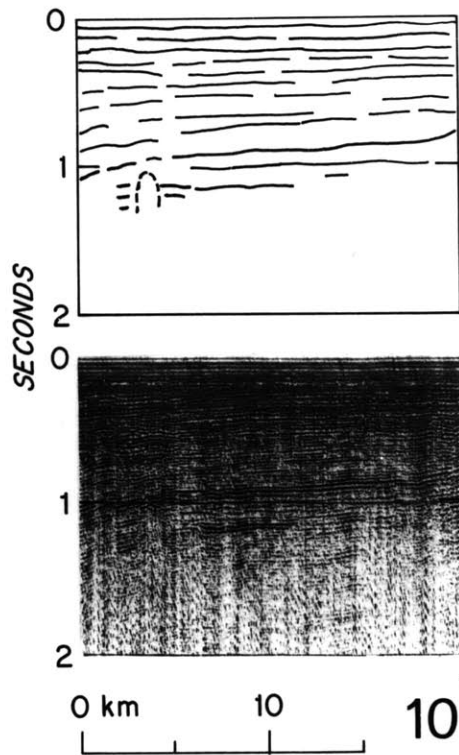
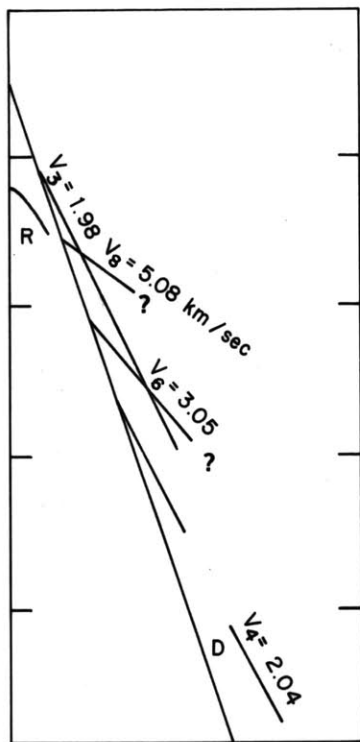
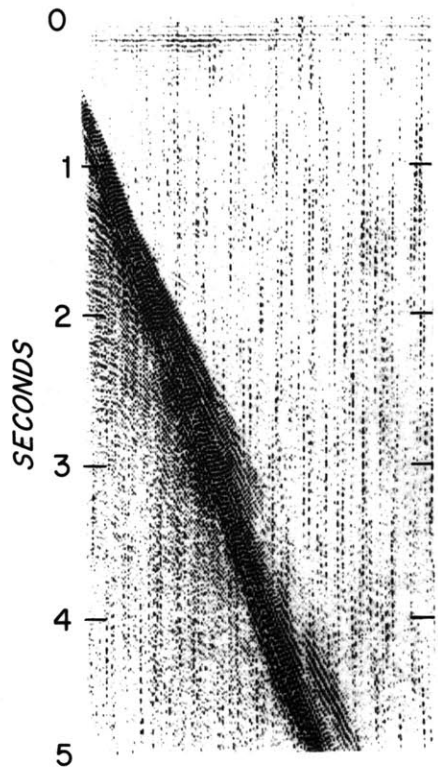


8



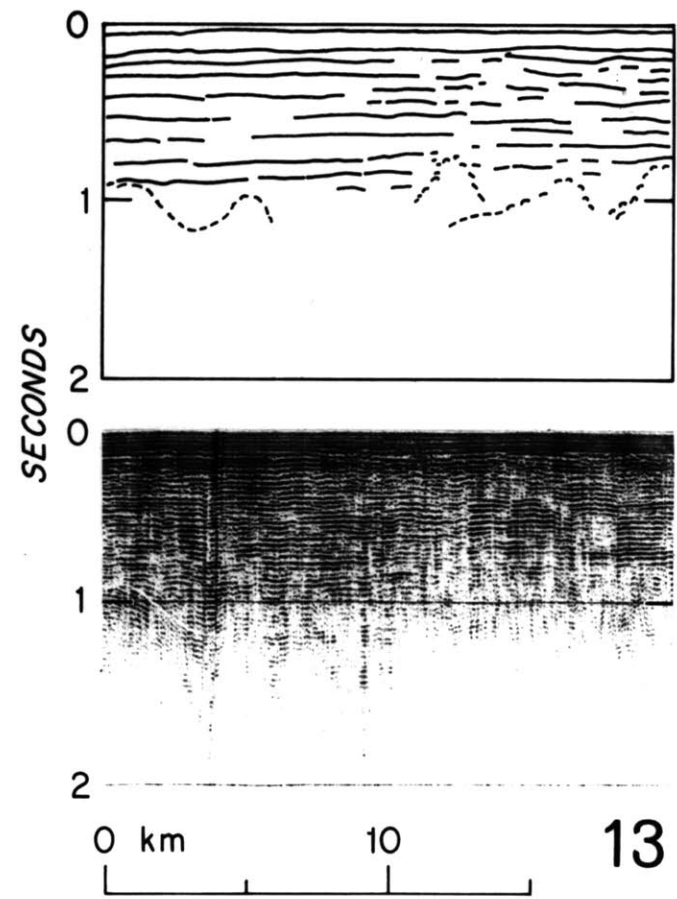
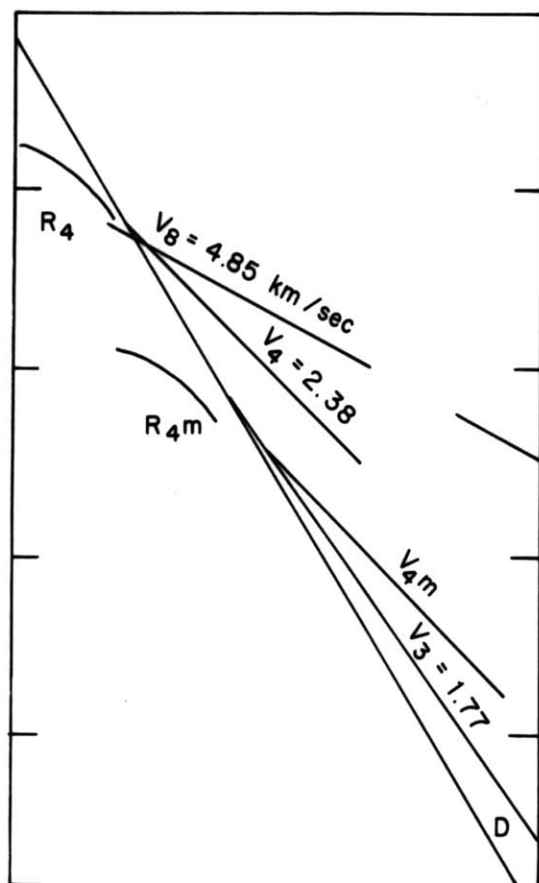
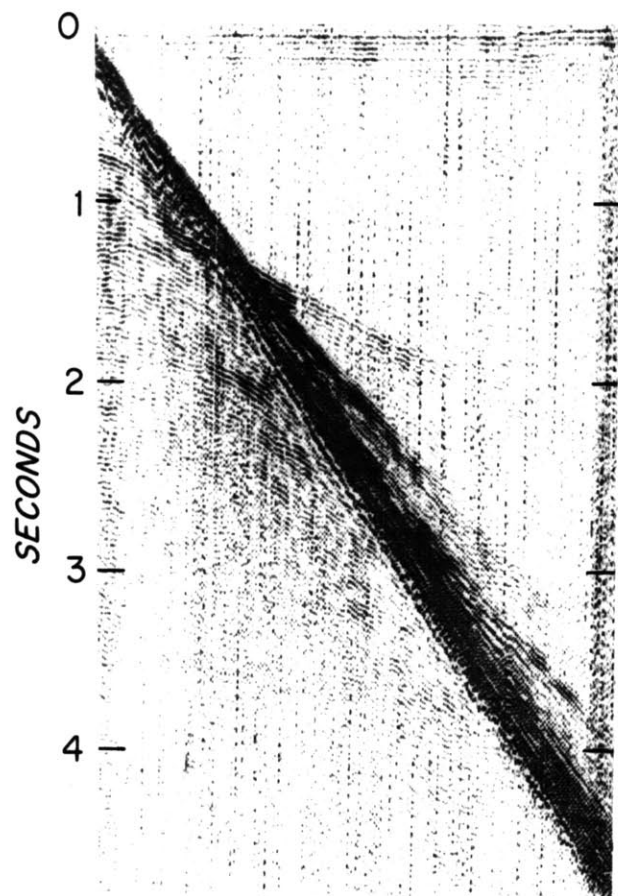
Sonobuoy 10 Figure 46.

Sonobuoy profile 10 in the West Java Basin, is similar in many respects to that of sonobuoy 8; both are in the same type region. The reason for presenting this profile is to show the discontinuities of the arrivals  $V_3$  and  $V_4$ . Although the normal incidence profile shows apparently continuous horizontal reflectors to 1 sec depth, the refraction arrivals suggest that the layers are discontinuous, may be due to faulting or to certain changes in the physical properties of the sediments.



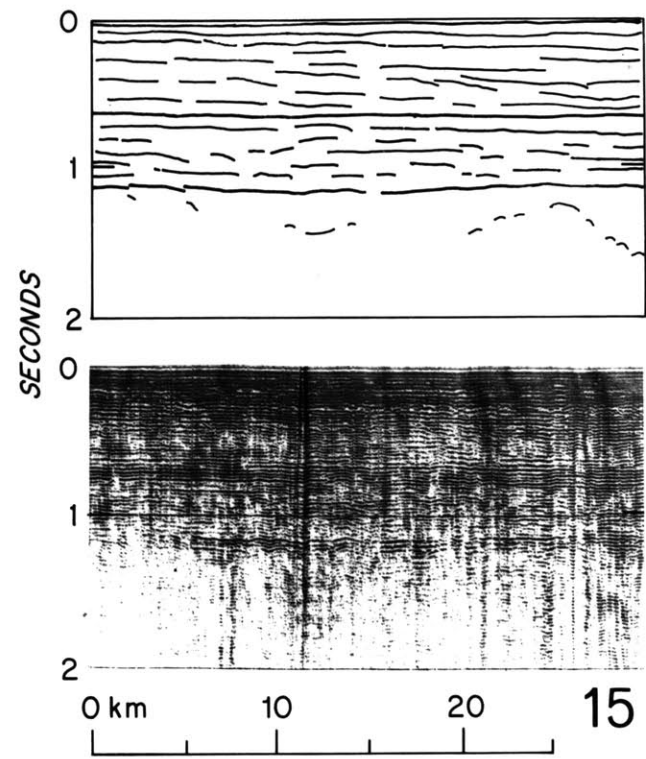
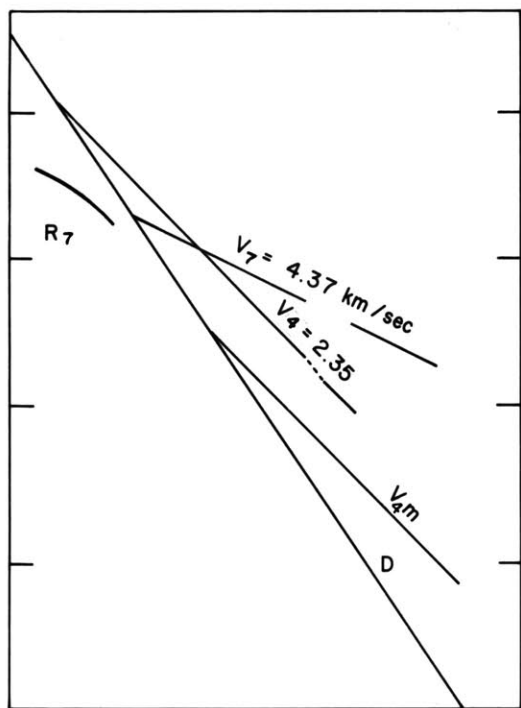
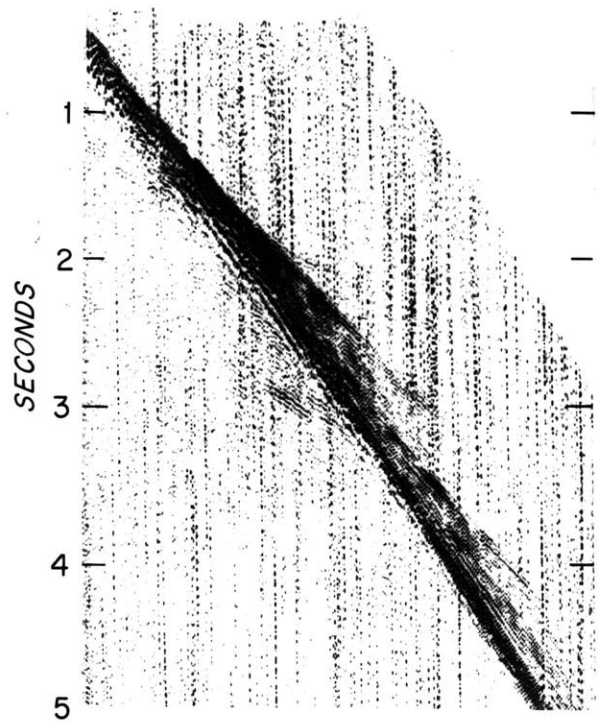
Sonobuoy 13 Figure 47.

Sonobuoy 13 record is one of the best obtained in the Java Sea. It was taken southeast of Billiton Island in an area having no major basement lows or highs. The arrival with  $V_g$  corresponds to a strong reflector which is probably the lower Miocene limestone. A discontinuity in this arrival results from some deeper structures that intrude the limestone horizon. The other arrivals are very clear and continuous, indicating well stratified layers.



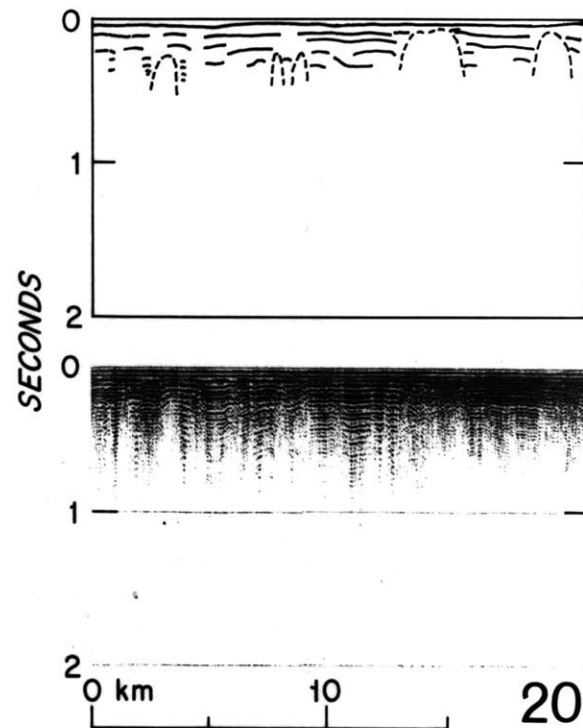
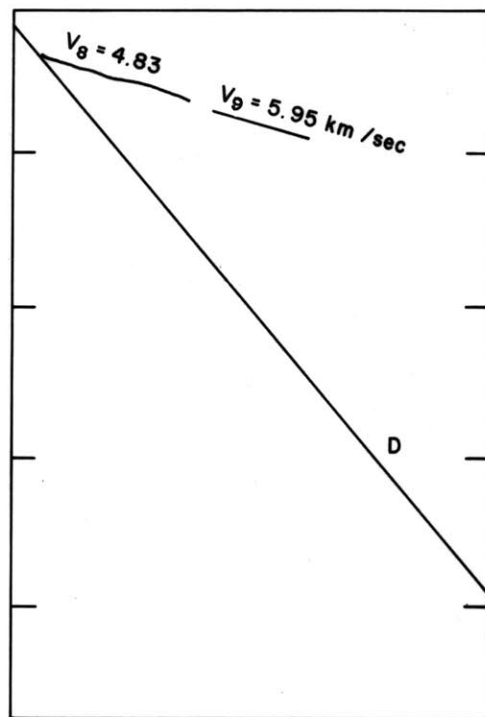
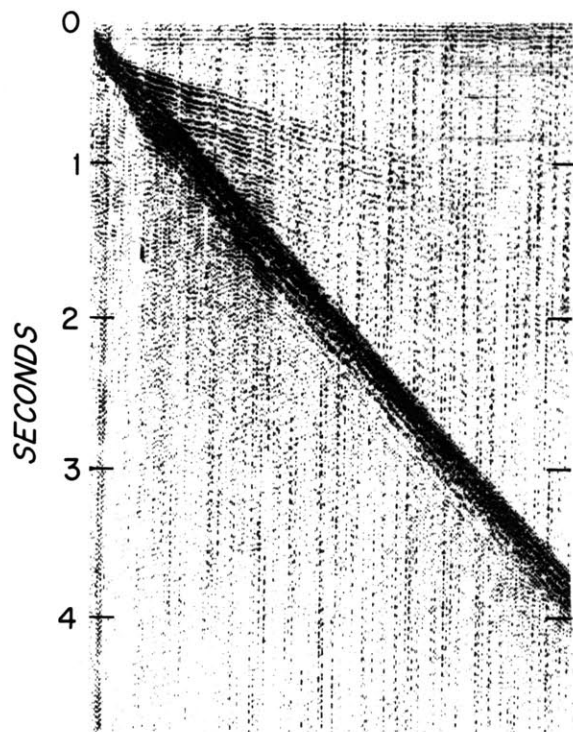
Sonobuoy 15 Figure 48.

Sonobuoy 15 is in the Billiton Basin. The slight curvature of the direct arrival indicates a change of ship's speed during the profile. Since both velocity and depth information are affected, there is some resultant error. The arrival with  $V_7$  comes from a strong reflector that seems to correlate with the lower Miocene limestone.  $V_4$  originates from a much shallower horizon. Both  $V_7$  and  $V_4$  arrivals show discontinuity at the same range, which suggests a vertical discontinuity over most of the sedimentary column. As the normal incidence reflection profile does not reveal this discontinuity, it may have resulted from the change in speed.



Sonobuoy 20 Figure 49.

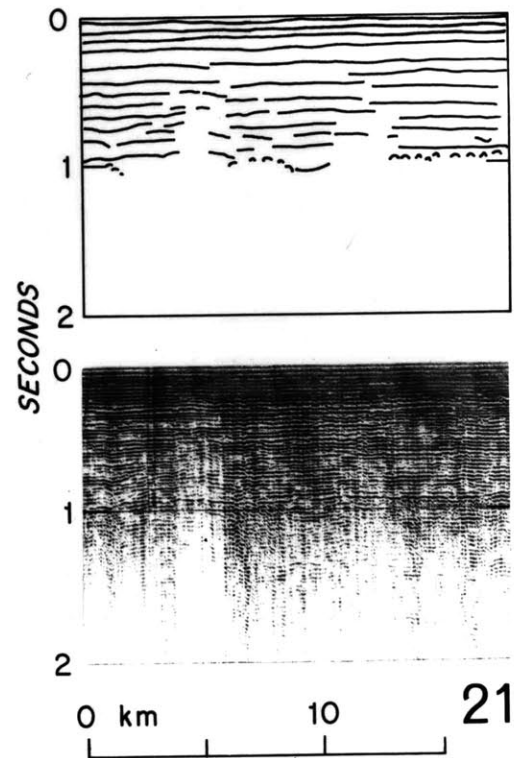
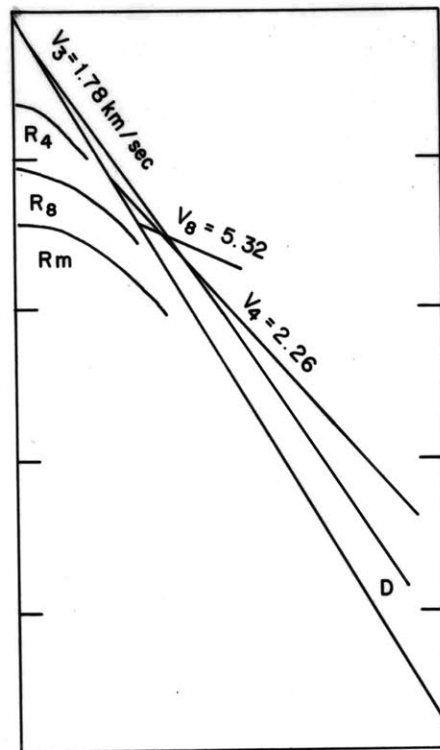
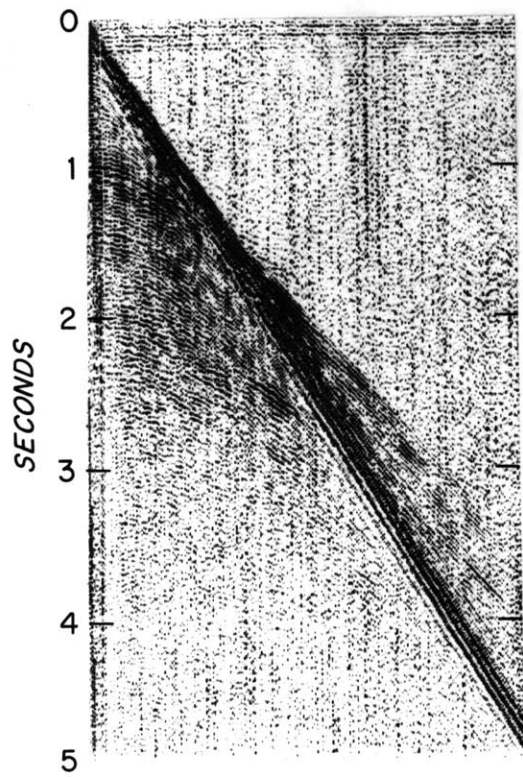
Profile 20 over the Karimunjawa Arch is similar in many respects to that of sonobuoy 7. The basement is shallow and in places almost reaches the seafloor. The arrival with  $V_8$  shows undulations that may reflect the basement topography. The basement velocity ( $V_8$ ) may suggest that it also consists of a granitic body. This conclusion is in accordance with gravity and magnetic data. The high velocity ( $V_9$ ) may be a part of the  $V_8$  arrival.





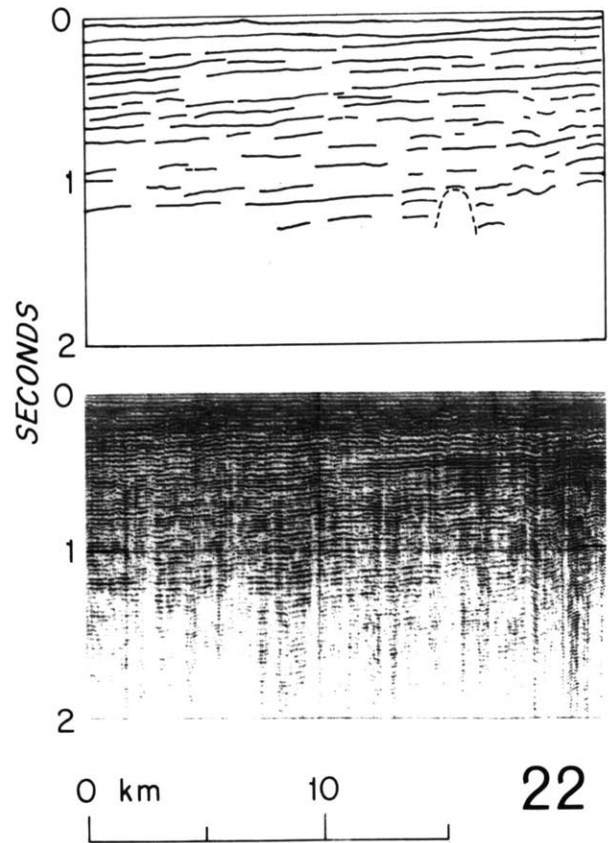
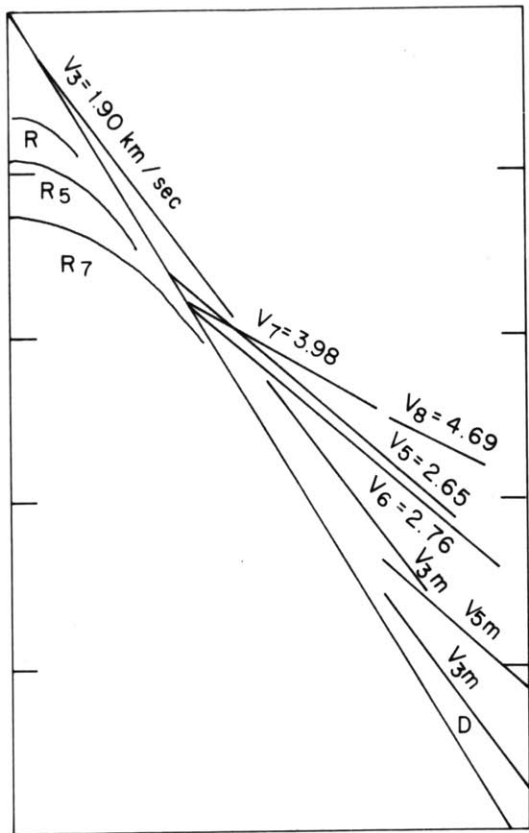
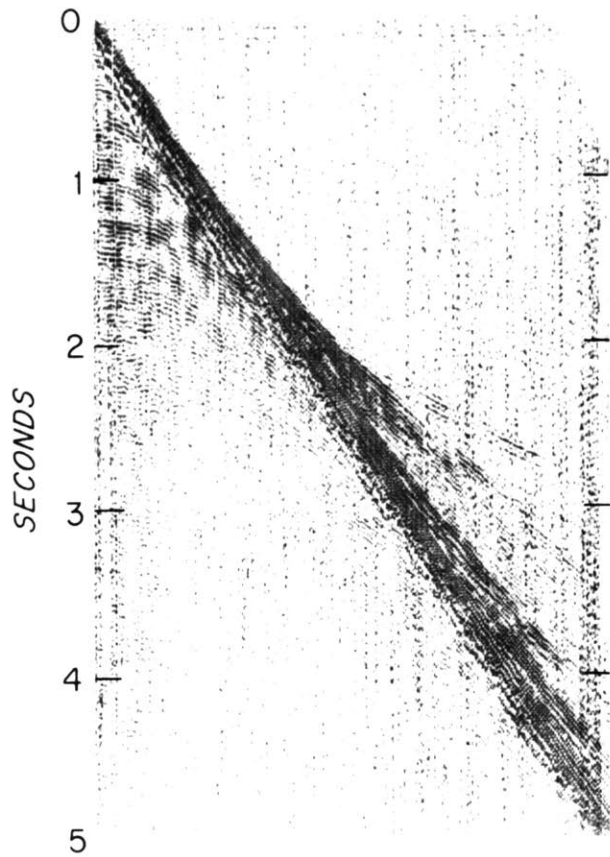
Sonobuoy 21 Figure 50.

Like sonobuoy 15 sonobuoy 21 was also taken over the Billiton Basin. The normal incidence reflection profile is very similar to that of station 15, but the refracted arrivals show different characteristics. Here, sedimentary arrivals are clear and continuous, evidence for continuity of the sedimentary horizons. A difference in acoustic basement material may be indicated by the difference in the velocities: 4.37 for 15 and 5.32 for 21. The basement at station 15 is probably the lower Miocene limestone while in station 21 it may be the granitic flank of the Karimundjawa Arch.



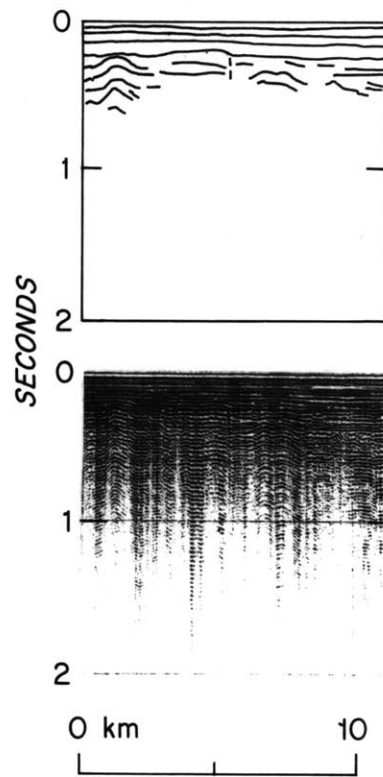
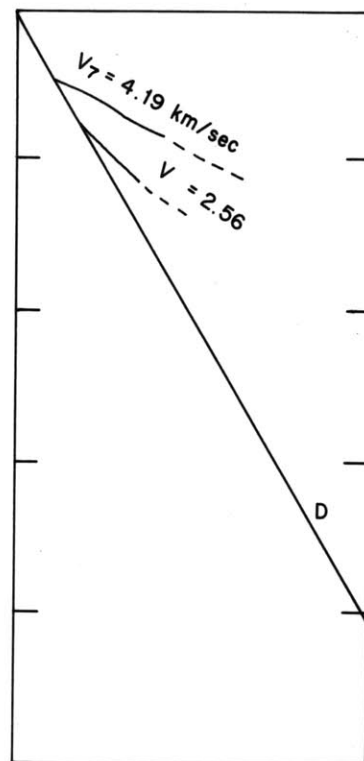
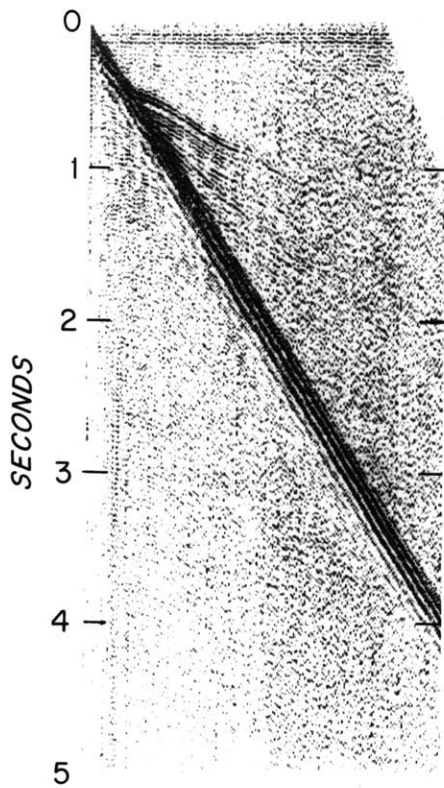
Sonobuoy 22 Figure 51.

Sonobuoy profile 22 is in the Billiton Basin. This is presented as an example of an almost complete velocity sequence from a sedimentary basin.



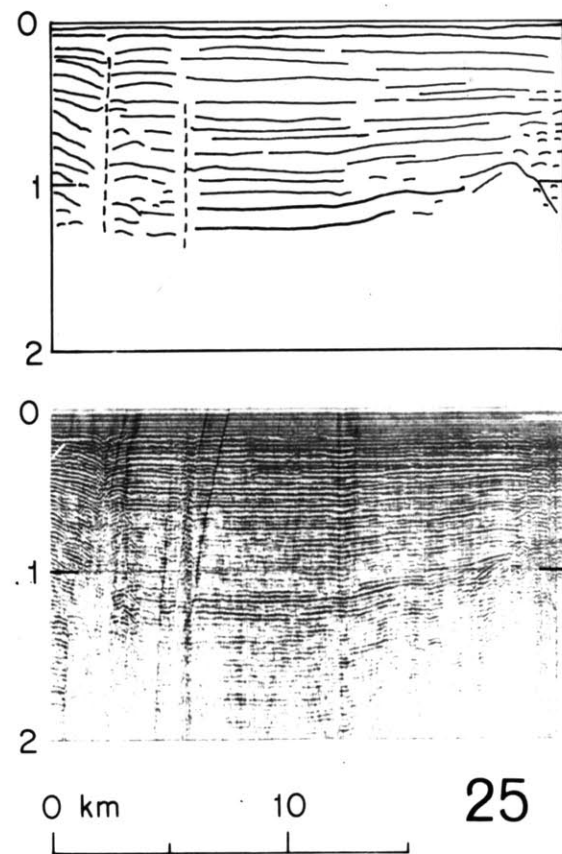
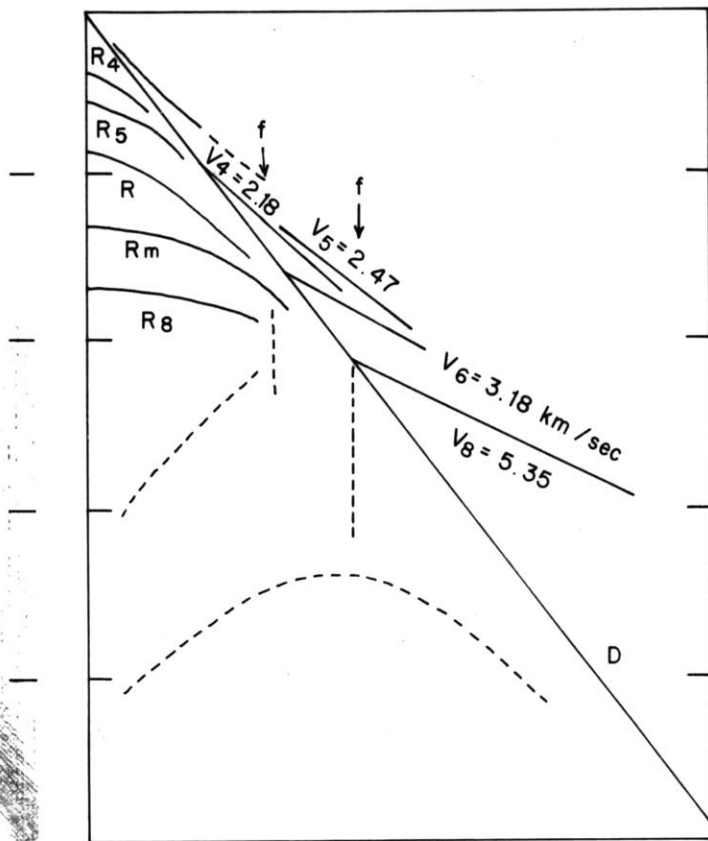
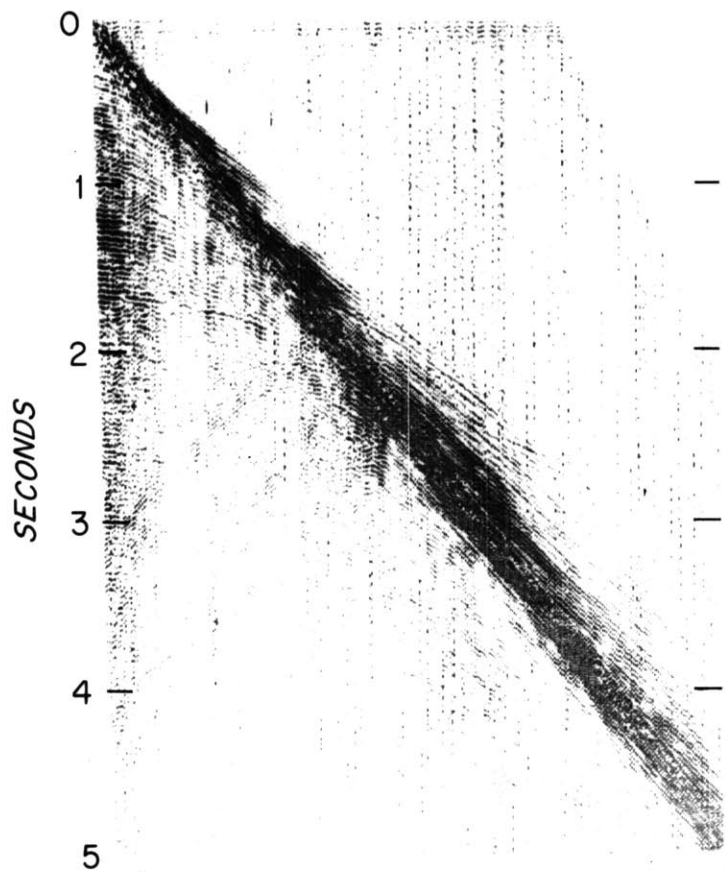
Sonobuoy 24 Figure 52.

Sonobuoy profile 24 was taken over the northern flank of the Karimundjawa Arch. The  $V_7$  shows travel time excursions that reflect the folding in the sediments shown clearly on the normal incidence profile. The 2.56 velocity may be an example of shear wave arrival favored by the fact that layer depth for  $V_7$  and the 2.56 arrival is the same and that the ratio  $4.19/2.56$  is 1.65. Shear waves have been reported previously for continental shelf sediments (Drake, et al., 1959).



Sonobuoy 25 Figure 53.

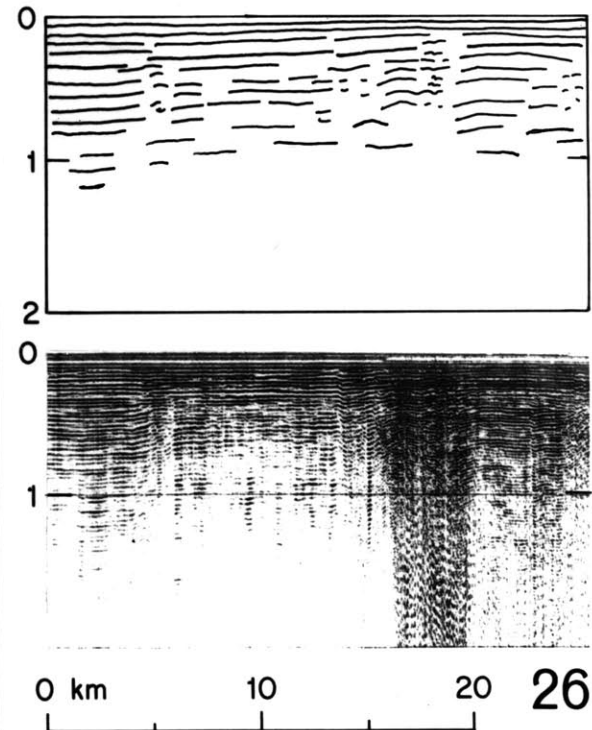
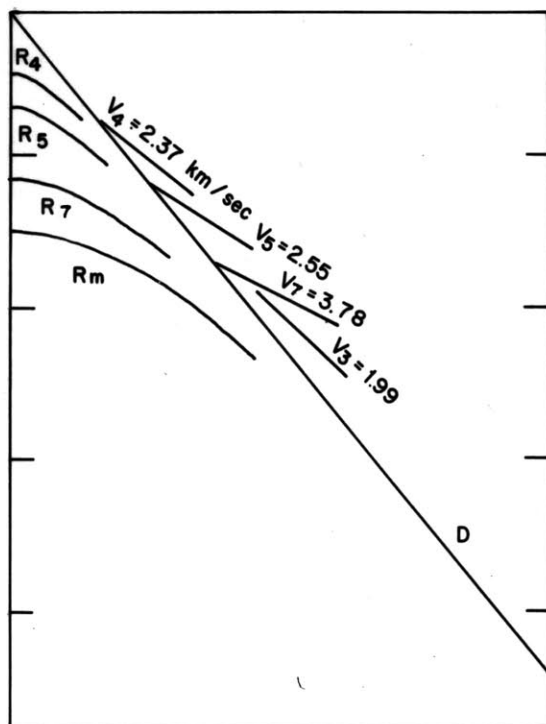
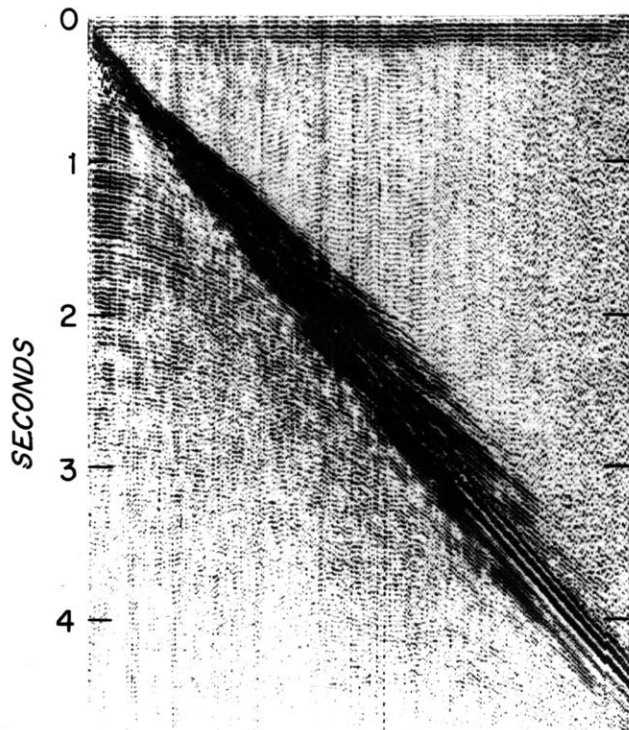
Sonobuoy 25 was taken west of Bawean Island. Both the normal incidence reflections and the refracted arrivals show evidence of crossing a fault zone. The oblique reflection returns from the fault zone are scattered. This may be a deep fault since it intersects the basement as well as the sedimentary column. It may be the one bordering the Bawean arch on its northern side (Cree, 1972 and Fig. 38). The seismic velocities from the sonobuoy should be considered tentative in light of the obvious structural discontinuities since at least some of the arrivals may have been from them.





Sonobuoy 26 Figure 54.

Profile 26 was taken in the area between Bawean Island and East Java. All the arrivals terminate abruptly probably as a result of a fault shown in the reflection profile. This is one of seven sonobuoy records in which oblique reflections were used for interval velocity and depth determinations.



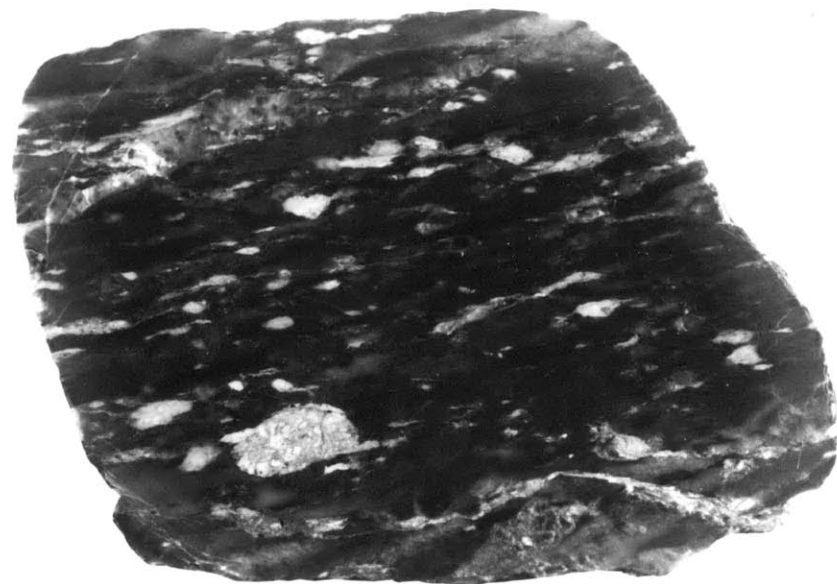
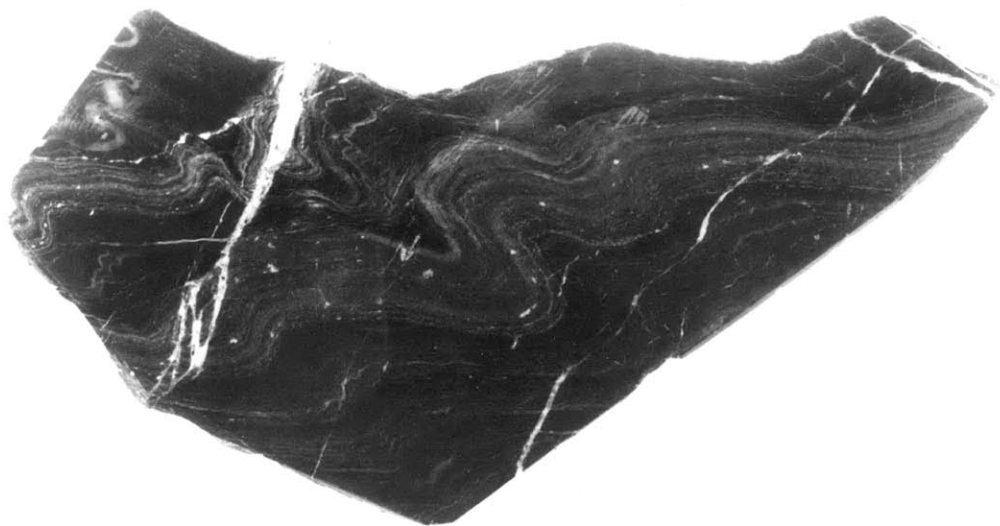
## APPENDIX II PETROLOGY OF BASEMENT ROCK SAMPLES

## THIN SECTION DESCRIPTIONS

Six basement samples whose locations are given in Figure 37 were studied and are described below.

- I Sample I is a fine grained graywacke composed of quartz and feldspar in a very fine clay matrix with mica, chlorite, opaques and many patches of carbonate. It has well developed cleavage and poor sorting.
- II Sample II is a graywacke composed of plagioclase, quartz and calcite with clay matrix. It has abundant veins of carbonate. The texture shows some sedimentary lamination and many fractures. Similar to rock sample I but coarser.
- III Sample III is a laminated phyllite (Figs. 55, 56). The white laminae composed of quartz, calcite and sericite and the dark laminae of organic matter, magnetite and opaques. The rock sample shows apparent mechanical deformation of low temperature. The deformation is probably the result of a directional compression.

Figure 55. Polished-sections of samples III (upper left),  
V (upper right) and VI (bottom).



7 cm

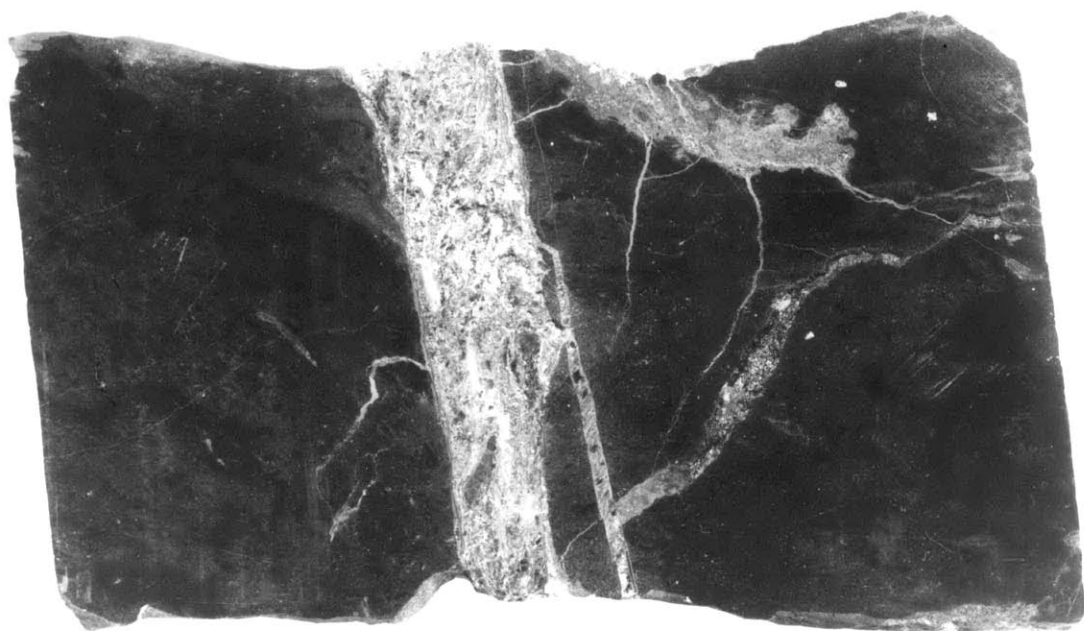
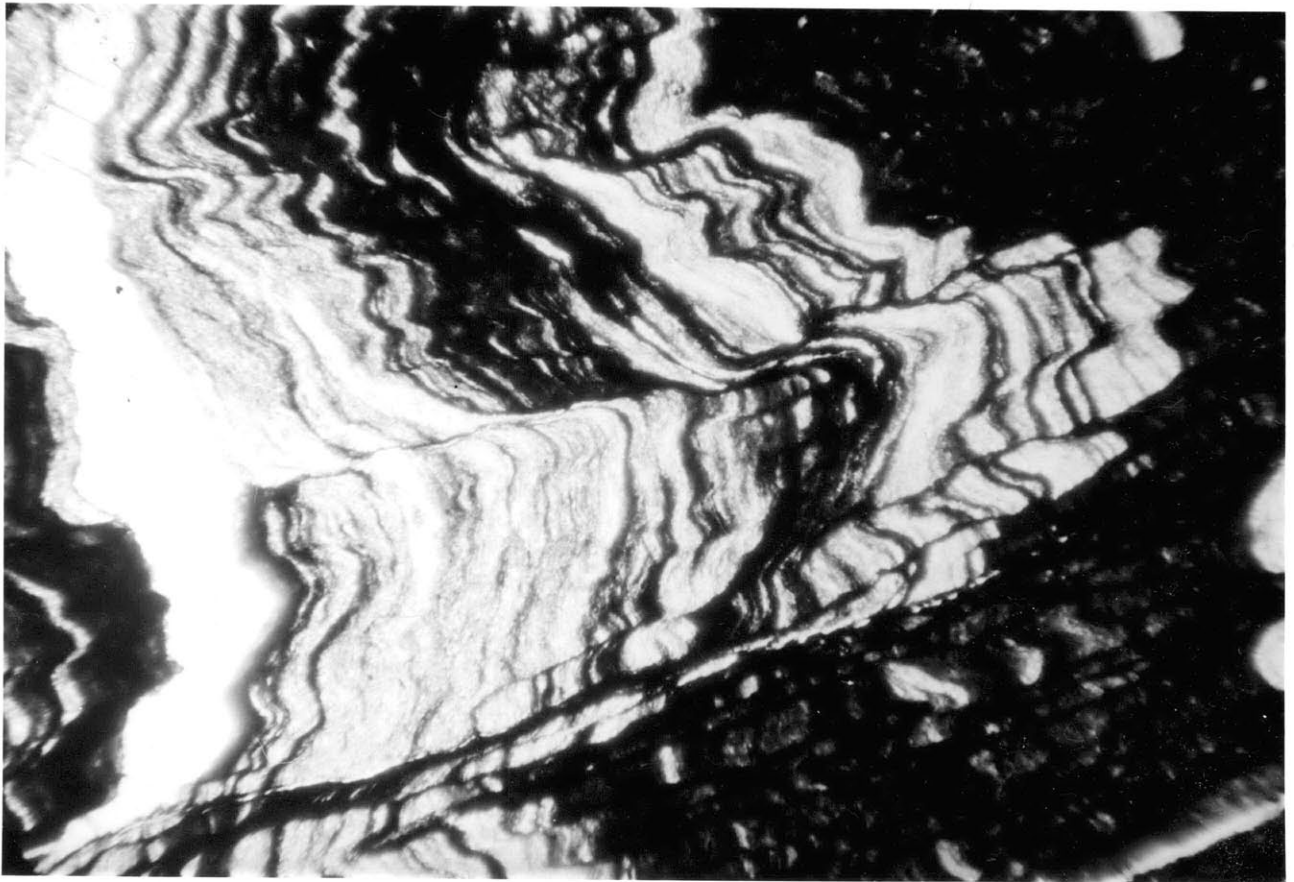
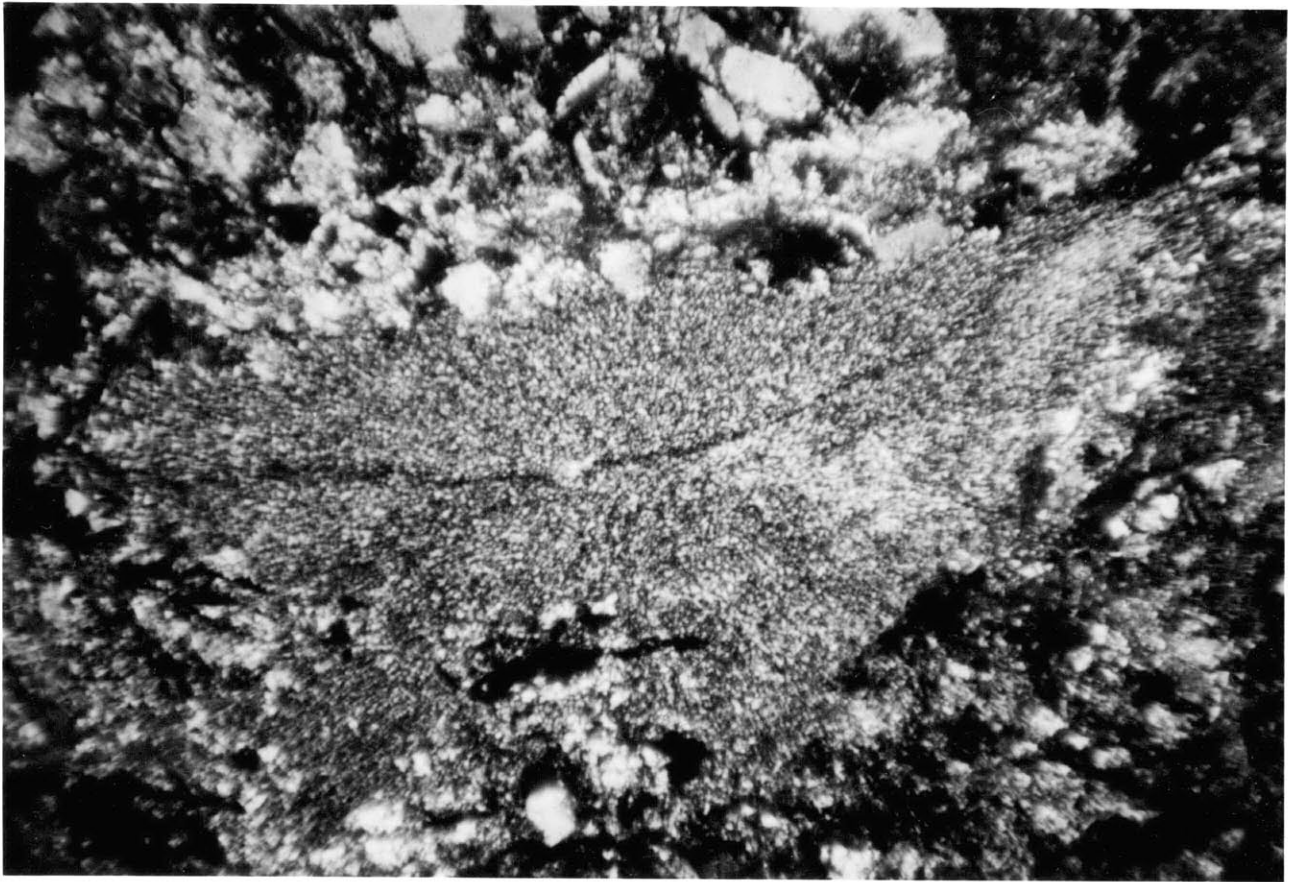


Figure 56. Thin section photographs. Actual width of the sections is 35 mm.

Top: sample III showing black and white laminae highly deformed by folding and faulting.

Bottom: sample IV showing a big vein of chert in the middle. On the periphery are large grains of quartz and feldspar.



- IV Sample IV is a graywacke (Fig. 56) containing abundant clastics of quartz and feldspar. Most of the feldspar has gone to secondary minerals. Veins of chert and much carbonate are abundant throughout the sample. The rock contains some volcanic debris and shows possible graded bedding (turbidites?). Many fractures strike perpendicular to the bedding probably due to compaction. Along the fractures there is secondary chert. Overall the rock sample resembles that of II.
- V Sample V is a sheared limestone and sandstone (Fig. 55) composed of big crystals of limestone and large grains of quartz in a brecciated carbonate matrix. The rock may have originated as a shaley limestone (shelf deposit) that was subsequently sheared.
- VI Sample VI is a serpentized hornblende-hornfels (Fig. 55) containing veins of quartz, calcite, serpentine and chlorite. The metamorphism is one of high temperature and low pressure and may be the result of nearby dike injection. The rock may have originated as a fine grained sedimentary rock in which the original bedding can still be recognized. This interpretation is not unique. It may be that the rock is of igneous source (amphibolite).



## DENSITY MEASUREMENTS

The densities of the six basement samples of Figure 37, were determined (Table 3) in order to help in constructing crustal models based on gravity data. The specimens were weighed dry and then were weighed suspended in fluid of known density (distilled water) to calculate their volume. The densities then were calculated from the mass and volume. The measurements were repeated three times for each sample. Sample IV was cut to a cylindrical shape for velocity measurement and the density for this sample was measured also from the mass and dimension. The results from the two methods agree within 3%.

Table 3. Densities of rock samples.

<u>Sample</u>	<u>Density g/cc</u>
I	2.73 ± 0.10
II	2.63 ± 0.06
III	2.73 ± 0.05
IV	2.73 ± 0.09
V	2.78 ± 0.10
VI	2.71 ± 0.11
Mean	2.72 ± 0.05

## COMPRESSIONAL WAVES VELOCITY MEASUREMENTS

The rock samples offered an opportunity to compare the basement velocities obtained by the sonobuoys to those measured on basement samples from the same area in the laboratory. Unfortunately, except sample IV, all the samples were too small for the measurement technique. Sample IV was saturated with water before the measurements in order to achieve conditions similar to those in nature. The measurements on the water saturated sample were made at zero pore pressure in a technique described by Nur and Simmons (1969). As the sample was obtained from a basin beneath about 3 km of sediment, if one assumes an average density of the overlying sediments to be 2.5 g/cc, then the pressure at the basement is 750 bar. The observed seismic velocity under pressure of 750 bar was 5.38 km/sec. The closest sonobuoy station to this well is number 26 but no basement velocity was detected in this station. Sonobuoys 25 and 27 were taken at about 70-80 km from the well of sample IV and they give basement velocities of 5.35 and 5.30 km/sec respectively, which is in a close agreement with that of sample IV measured at the laboratory.

## BIOGRAPHY

Born: November 16, 1941, Jerusalem, Israel.

1960-1963 Active duty in the Israeli Army

1969 B.Sc. in Geology with honors, The Hebrew University of Jerusalem

1969-1973 Research Fellow, Woods Hole Oceanographic Institution, Woods Hole, Massachusetts

## PUBLICATIONS

Ben-Avraham, Z., 1971, Accumulation of stones by codium

fragile: *Limnology and Oceanography*, v. 16, p. 553-554.

Ben-Avraham, Z., and J. D. Phillips, 1972, The evolution of the China Basin: (abstract), *Trans. Am. Geophys. Union*, v. 53, p. 519.

Ben-Avraham, Z., J. Segawa, and C. O. Bowin, 1972, An extinct spreading center in the Philippine Sea: *Nature*, v. 240, p. 453-455.

Ben-Avraham, Z., and S. Uyeda, in press, The evolution of the China Basin and the Mesozoic paleogeography of Borneo: *Earth and Planetary Science Letters*.

Bowin, C. O., and Z. Ben-Avraham, 1972, Ocean floor underthrusting and the Indonesian island arc: (abstract) *Trans. Am. Geophys. Union*, v. 53, p. 518-519.

Emery, K. O., and Z. Ben-Avraham, 1972, Structure and stratigraphy of the China Basin: Am. Assoc. Petroleum Geologists Bull., v. 56, p. 839-859.

Uyeda, S., and Z. Ben-Avraham, 1972, Origin and development of the Philippine Sea: Nature Physical Sci., v. 240, p. 176-178.